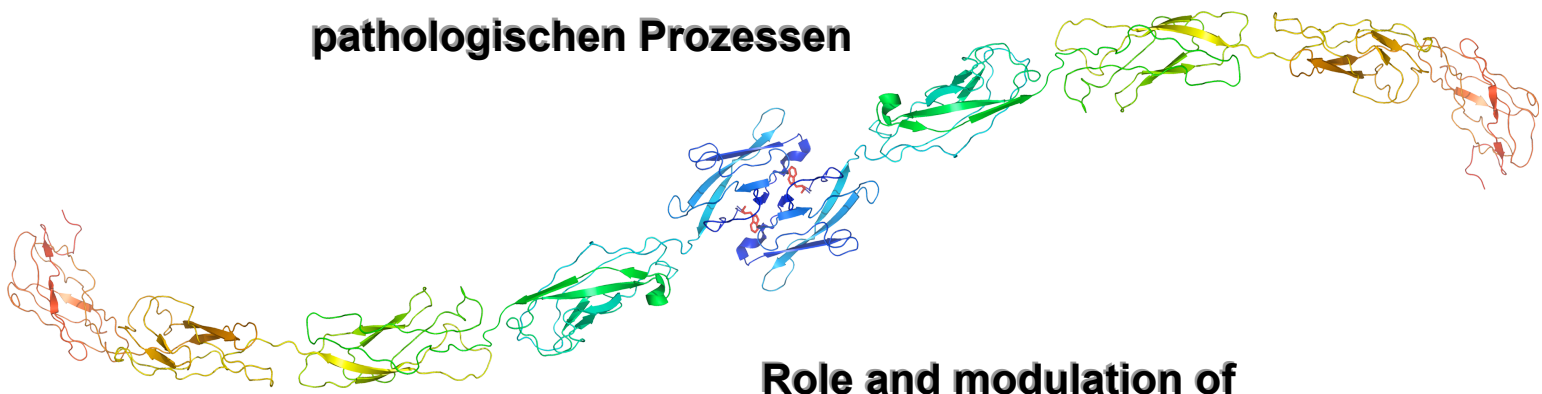


**Rolle und Modulation von Cadherinen in
pathologischen Prozessen**



**Role and modulation of
cadherins in pathologic processes**

Wolfgang-Moritz Felix Heupel

Würzburg, 2010

AUS DEM INSTITUT FÜR ANATOMIE UND ZELLBIOLOGIE
DER JULIUS-MAXIMILIANS-UNIVERSITÄT WÜRZBURG
VORSTAND: PROF. DR. D. DRENCKHAHN

**Rolle und Modulation von Cadherinen in pathologischen
Prozessen**

-

Role and modulation of cadherins in pathologic processes

DISSERTATION ZUR ERLANGUNG DES NATURWISSENSCHAFTLICHEN
DOKTORGRADES DER BAYERISCHEN JULIUS-MAXIMILIANS-UNIVERSITÄT
WÜRZBURG

vorgelegt von

Wolfgang-Moritz Felix Heupel

aus Neuendettelsau

Würzburg, 2010

Eingereicht am:

Mitglieder der Promotionskommission:

Vorsitzender:

Gutachter: Prof. Dr. Detlev Drenckhahn

Gutachter: Prof. Dr. Georg Krohne

Tag des Promotionskolloquiums:

Doktorurkunde ausgehändigt am:

*In Erinnerung an meinen Vater,
für meine Mutter &
für meine Julie.*

„Eine Verbesserung der Bedingungen auf der Welt ist im Wesentlichen nicht von wissenschaftlicher Kenntnis, sondern vielmehr von der Erfüllung humaner Traditionen und Ideale abhängig“

Albert Einstein (1879 – 1955)

1	SUMMARY	4
2	INTRODUCTION	8
2.1	Cell-cell adhesion	8
2.2	Cell contacts	8
2.2.1	Cell-matrix contacts	8
2.2.1.1	Hemidesmosomes	9
2.2.1.2	Focal contacts	9
2.2.2	Cell-cell contacts	10
2.2.2.1	Communication contacts: gap junctions	10
2.2.2.2	Barrier contacts: tight junctions	11
2.2.2.3	Adhesion contacts: desmosomes and adherens junctions	11
2.2.2.3.1	Desmosomes	11
2.2.2.3.2	Adherens junctions	12
2.3	Characterization and classification of cell adhesion molecules	12
2.3.1	Ca ²⁺ -independent cell adhesion molecules	13
2.3.1.1	Immunoglobulin-like cell adhesion molecules	13
2.3.1.2	Integrins	13
2.3.2	Ca ²⁺ -dependent cell adhesion molecules	14
2.3.2.1	Selectins	14
2.3.2.2	Cadherins	15
2.4	Characterization of cadherin interactions	15
2.4.1	Experimental approaches to determine cadherin interactions	15
2.4.2	Cadherin interaction	19
2.4.2.1	First models	19
2.4.2.2	Linear zipper model involving Trp2 swapping	20
2.4.2.3	Trp2 strand swapping in trans-interactions of full length C-cadherin	21
2.4.2.4	Models involving multiple domain interactions	22
2.4.2.5	Interaction via Ca ²⁺ binding linker regions ('X-dimer')	23
2.4.2.6	Insights into cadherin interactions obtained with biophysical force spectroscopy	24
2.4.2.7	VE-cadherin hexamer structures	28
2.4.2.8	Interaction and ultrastructure of desmosomal cadherins	28
2.4.3	Determining cadherin specificity: homophilic vs. heterophilic interactions	29

2.5 Physiological regulation of cadherin function	31
2.5.1 Outside – in signaling	31
2.5.2 Inside – out signaling	32
2.5.3 Cadherin regulation by expression levels and endocytosis	33
2.6 Cadherins in pathological processes	34
2.6.1 Cadherins are pathologically targeted at physiological borders	35
2.6.1.1 Pemphigus family of blistering skin diseases	35
2.6.1.1.1 Induction of pemphigus by pathogenic Dsg autoantibodies	37
2.6.1.1.2 Steric hindrance and desmoglein compensation theory	38
2.6.1.1.3 Cellular signaling in pemphigus	39
2.6.1.2 Vascular inflammation	40
2.7 Aim of this study	41
2.7.1 Characterization of cadherin trans-interactions	41
2.7.2 Investigation of cadherin-mediated signaling	42
2.7.3 Modulation of cadherin function by peptides	42
3 SCIENTIFIC PUBLICATIONS AND ADDITIONAL RESULTS	44
3.1 Scientific publications	44
3.1.1 Publication 1: Pemphigus vulgaris IgG directly inhibit desmoglein 3-mediated transinteraction	44
3.1.2 Publication 2: Pemphigus vulgaris IgG cause loss of desmoglein-mediated adhesion and keratinocyte dissociation in HaCaT cells independent of epidermal growth factor receptor	55
3.1.3 Publication 3: Peptides targeting the desmoglein 3 adhesive interface prevent pemphigus autoantibody-induced acantholysis in pemphigus	67
3.1.4 Publication 4: Endothelial barrier stabilization by a cyclic tandem peptide targeting VE-cadherin transinteraction in vitro and in vivo	75
3.2 Additional experiments and methods	86
3.2.1 Investigating VE-cadherin interactions using site-directed coupling by SNAP-tag technology and AFM force spectroscopy	86
4 DISCUSSION	90
4.1 Integrative summary of results	90

4.2 Direct inhibition vs. desmoglein-mediated signaling in blistering skin disease pemphigus	90
4.3 VE-cadherin as a key component of the endothelial barrier	94
4.4 Peptides modulating cadherin function	95
4.5 Cadherin interaction	98
4.5.1 Future strategies for investigating cadherin interactions	100
5 REFERENCES	103
6 APPENDIX	119
6.1 Addendum	119
6.1.1 Vector construction of VE-cadherin-SNAP-his constructs	119
6.1.2 List of abbreviations	121
6.2 Acknowledgement - Danksagung	122
6.3 Ehrenwörtliche Erklärung	124
6.4 Curriculum vitae	125
6.5 Publikationsverzeichnis	127
6.5.1 Originalarbeiten	127
6.5.2 Kongressbeiträge	129

1 Summary

Ca²⁺ dependent cell adhesion molecules (cadherins) are central for a variety of cell and tissue functions such as morphogenesis, epithelial and endothelial barrier formation, synaptic function and cellular signaling. Of paramount importance for cadherin function is their specific extracellular adhesive trans-interaction. Cadherins are embedded in a cellular environment of intracellular and extracellular regulators that modify cadherin binding in response to various physiological and pathological stimuli. Most experimental approaches used for studying cadherin interaction however lack a physiological proof of principle mostly by not investigating cadherins in their physiological environment. In the present cumulative dissertation, experimental approaches were applied to characterize and modulate vascular endothelial (VE)-cadherin and desmocadherin functions in the (patho-)physiological contexts of endothelial permeability regulation and disturbance of epidermal barrier function, which is typical to the blistering skin disease pemphigus, respectively. Whereas VE-cadherin is a key regulator of the endothelial barrier that separates the blood compartment from the interstitial space of tissues, desmosomal cadherins are crucial for maintenance of epidermal integrity and separation of the external environment from the body's internal milieu. Cadherin functions were both investigated in cell-free and cell-based conditions: by using biophysical single molecule techniques like atomic force microscopy (AFM), cadherin function could be investigated in conditions, where contributions of intracellular signaling were excluded. These experiments were, however, compared and combined with cell-based experiments in which cadherins of epidermal or endothelial cell cultures were probed by laser force microscopy (laser tweezers), fluorescence recovery after photobleaching (FRAP) and other techniques.

The autoimmune blistering skin diseases pemphigus foliaceus (PF) and pemphigus vulgaris (PV) are caused by autoantibodies directed against the extracellular domains of the desmosomal cadherins desmoglein (Dsg) 1 and 3, which are important for epidermal adhesion. The mechanism of autoantibody-induced cell dissociation (acantholysis) in pemphigus, however, is still not fully understood. For the first time, it is shown by AFM force spectroscopy that pemphigus autoantibodies directly inhibit Dsg3 adhesion by steric hindrance but do not inhibit adhesion of Dsg1. However, the full pathogenicity of the autoantibodies depended on cellular signaling processes, since autoantibodies targeting Dsg1 also resulted in loss of cadherin-mediated adhesion in cell-based experiments. However, two other signaling pathways that have been reported to be involved in pemphigus pathogenesis, i.e. epidermal growth factor receptor (EGFR) and c-Src activation, were not found to be important in this context.

Furthermore, peptide-based modulators of cadherin functions were generated for Dsg1/3 and VE-cadherin. By comparing Dsg1, Dsg3 and VE-cadherin sequences to published X-ray

structures of cadherin trans-interactions, specific amino acid sequences of the binding pockets of these cadherins were identified. Peptide versions of these motifs were synthesized and the antagonistic functions of these “single peptides” were validated by AFM force spectroscopy as well as by cell-based assays. By linking two single peptides in tandem, stabilization of cadherin bonds because of by cross-bridge formation between trans-interacting cadherins was demonstrated. Protective effects of tandem peptides were shown by partly preventing pemphigus autoantibody-induced acantholysis, or in the case of VE-cadherin, by stabilizing endothelial barrier properties against barrier disrupting agents like the Ca^{2+} ionophore A23187 and an inhibitory VE-cadherin antibody. Most importantly, VE-cadherin tandem peptides abolished microvascular hyperpermeability induced by the physiologic inflammatory agent tumor necrosis factor- α in the rat mesentery *in vivo*. Both classes of tandem peptides therefore can be considered as a starting point for the generation of potential therapeutic agents that might prevent cell dissociation in pemphigus and breakdown of the endothelial barrier under inflammatory conditions.

Deutsche Zusammenfassung

Die Familie der Ca^{2+} - abhängigen Adhäsionsproteine (Cadherine) spielt eine zentrale Rolle bei elementaren zellulären, geweblichen und Entwicklungsprozessen. Eine in der vorliegenden kumulativen Dissertation untersuchte Funktion von Cadherinen ist ihre zentrale Rolle beim Aufbau und der Aufrechterhaltung der epithelialen (epidermalen) Barriere der Haut und der endothelialen Barriere von Blutgefäßen. Cadherine vermitteln Adhäsion über eine extrazelluläre Bindung (Transinteraktion) mit Cadherinen auf der Zelloberfläche angrenzender Zellen. Die durch Cadherine vermittelte Zelladhäsion und die durch sie kontrollierte Barrierenbildung ist ein dynamischer Prozess, der durch extrazelluläre und intrazelluläre Modulatoren im Zusammenspiel mit vielfältigen physiologischen Prozessen reguliert wird. Verschiedene bedrohliche pathologische Prozesse wie die Blasen-bildende Pemphiguserkrankung der Haut oder die massive Ödembildung durch pathologische Erhöhung der Blutgefäßpermeabilität beruhen in wesentlichen Elementen auf Störungen der Cadherinbindung. Verschiedene *in vitro*-Modellsysteme ermöglichen die Untersuchung von Teilaspekten der Interaktion von Cadherinen. Den meisten dieser Experimentalsysteme fehlt aber der realistische physiologische und gewebliche Bezug zur funktionellen Bedeutung der untersuchten Eigenschaften der Cadherine. In der vorliegenden kumulativen Dissertation wurden verschiedenste Ansätze zur Untersuchung aber auch zur Modulation von Cadherinen im Hinblick zweier (patho-)physiologischer Prozesse durchgeführt. Zum einen befasst sich die Doktorarbeit mit den Blasen-bildenden Hauterkrankungen der Pemphigus-Gruppe, bei welcher die Funktionsstörung desmosomaler Cadherine im Mittelpunkt steht. Zum anderen wurde das vaskuläre endotheliale (VE)-Cadherin und dessen Rolle bei der Regulation und pathologischen

Entgleisung der Gefäßpermeabilität untersucht. Diese Cadherine sind Teil einer epithelialen oder endothelialen Schicht, die das Körperinnere von der Außenwelt bzw. das Interstitium der Gewebe vom Blutkompartiment trennt und abschirmt. Die Funktion dieser Cadherine wurde in der Arbeit sowohl in Zell-freien als auch in Zell-basierten Experimenten analysiert: mittels biophysikalischer Charakterisierung auf Einzelmolekülebene durch Kraftspektroskopie mit dem Atomkraftmikroskop (AFM) konnte die Adhäsion (Transinteraktion) von Cadherinen frei von zellulären Einflüssen isoliert untersucht werden. Diese Einzelmolekülstudien wurden durch Laserkraftmikroskopie (Laserpinzette) und verschiedene zellphysiologische Untersuchungen an epithelialen und endothelialen Zellkulturen und Geweben komplettiert.

Bei der autoimmunen Hauterkrankung Pemphigus foliaceus (PF) und Pemphigus vulgaris (PV) bewirken Autoantikörper, die gegen die desmosomale Cadherine Desmoglein (Dsg) 1 und 3 gerichtet sind, eine Zelldissoziation (Akantholyse), die zu einer charakteristischen Blasenbildung auf der Haut der Patienten teils mit Ablösung der Epidermis führt. Der exakte Mechanismus dieser durch Autoantikörper verursachten Akantholyse ist jedoch in wesentlichen Zügen unverstanden. In der vorliegenden Arbeit wurde mit Hilfe der AFM-Kraftspektroskopie zum ersten Mal gezeigt, dass Pemphigus-Autoantikörper direkt die Dsg3-vermittelte Adhäsion durch sterische Behinderung inhibieren. Zusätzlich wurden auch Unterschiede in der Pathogenität der Autoantikörper in Abhängigkeit von zellulären Signalwegen gefunden. In früheren Studien konnte bereits gezeigt werden, dass neben der vermuteten Hemmung der Cadherinbindung durch die Autoantikörper auch inhibitorische, die Zelladhäsion herabsetzende zytoplasmatische Signalwege für die Pathogenese dieser Krankheit wichtig sind. Daneben belegen Experimente dieser Arbeit, dass die durch Autoantikörper vermittelte Akantholyse in unseren Versuchsbedingungen unabhängig von der in anderen Studien postulierten Beteiligung des epidermalen Wachstumsfaktorrezeptors (EGFR) und von c-Src war.

In weiteren Experimenten wurden spezifische Peptide zur Modulation der Funktion von Dsg1/3 und VE-Cadherin entwickelt. Dazu wurden die Sequenzen von Dsg1, Dsg3 und VE-Cadherin mit den bereits beschriebenen Röntgenkristallstrukturen von anderen Cadherinen verglichen und eigene Strukturmodelle für Dsg1/3 und VE-Cadherin auf der Grundlage einer Analogiemodellierung generiert. Auf diese Weise wurden Sequenzabschnitte identifiziert, die für die Cadherin-Transinteraktion wichtig sind. Aus diesen Sequenzen wurden Peptide abgeleitet, die die Cadherinfunktion entweder in einer agonistischen oder antagonistischen Weise beeinflussen sollten. Die inhibitorische Funktion der Einzelpeptide wurde sowohl durch AFM-Kraftspektroskopie als auch in Zell-basierten Laserpinzetten-Studien validiert. Durch das Zusammenfügen von zwei separaten Einzelpeptidsequenzen wurden Tandempeptide erzeugt. Diese sollten die jeweilige Cadherininteraktion durch das Überbrücken benachbarter adhäsiver

Cadherindomänen stabilisieren. Der stabilisierende, protektive Effekt der Tandempeptide wurde sowohl in Einzelmolekülstudien als auch in Zellkulturstudien bestätigt. So verhinderte das Dsg-spezifische Tandempeptid teilweise die durch Autoantikörper hervorgerufene Akantholyse beim Pemphigus und das VE-Cadherin-spezifische Tandempeptid schützte die Endothelbarriere vor Permeabilitätserhöhung durch das Ca^{2+} - Ionophor A23187 oder durch einen inhibitorischen VE-Cadherin-Antikörper. Dieser schützende Effekt wurde auch in *in-vivo*-Experimenten an perfundierten Mikrogefäßen des Rattenmesenteriums gezeigt, in denen das VE-Cadherin-Tandempeptid den Anstieg der Endothelpermeabilität durch den physiologischen Entzündungsmediator Tumornekrosefaktor- α verhinderte. Durch diese Experimente wurde eine protektive Wirkung beider Tandempeptide gezeigt. Diese Peptide können deshalb als Ausgangspunkt für die Identifikation von spezifischen therapeutischen Agenzien zur Prävention der Akantholyse beim Pemphigus oder Verlust der VE-Cadherin-Bindung bei vaskulärer Hyperpermeabilität angesehen werden.

2 Introduction

2.1 Cell-cell adhesion

During the evolution of higher order organisms on earth the formation of multicellular organisms (*metabionta*; or *metazoa* in the animal kingdom) was an essential step (Hynes and Zhao, 2000). But “sticking” cells together depended on the “invention”¹ of a novel class of proteins: cell adhesion molecules (CAMs) and their molecular compositions, cell contacts (CCs). These are necessary to promote proper cell aggregation and tissue specification but also cellular communication in higher order organisms. The static view of CAMs and CCs as mere mortar for multicellular units, however, has changed in the last years to see them as integrative receptors communicating extracellular signals from the cell’s environment into intracellular compartments. Besides this so-called “outside-in signaling” function, changing structures or function of CAMs/CCs can directly influence the cell’s behavior towards attaching cells or certain stimuli, a range of functions termed as “inside-out signaling”. CAMs/CCs therefore act as both essential structural and signaling components of the cell. Hence, cell-cell adhesion is central to nearly all physiological processes. To account for the complexity of these, consequently several specialized CAMs and CCs have emerged.

2.2 Cell contacts

CCs can both mediate adhesion to the cell’s surrounding extracellular matrix (ECM) or to other cells. The first type of contacts is called cell-matrix contact, whereas the latter is called cell-cell contact (Benninghoff and Drenckhahn, 2008). Ultrastructurally, most contacts consist of three different parts: an extracellular and membrane-spanning part, a so-called intracellular plaque and associated filaments. This structure implies that CCs are directly linked to parts of the cellular cytoskeleton consisting mainly of actin and intermediate filaments and to a minor extend to microtubules. By that, precise positioning and strong anchorage of CCs is achieved.

2.2.1 Cell-matrix contacts

Cell-matrix contacts are asymmetrical in structure and necessary for cells to stick to the ECM. As all epithelial cells depend on basal lamina anchorage, these contacts are very important for the epithelium lining cavities and surfaces of organs and in particular for the epidermis closing the surface of the body and for the endothelium terminating interior surfaces of blood vessels. Moreover, they are essential for most cells to receive survival signals or even to differentiate

¹ Interestingly, the unicellular marine choanoflagellate *Monosiga brevicollis* is known to already express 23 different members of the cadherin family of cell adhesion molecules pointing out the important role of cadherins for metazoan origins. In the choanoflagellate, cadherins are speculated to bind bacterial prey. (Abedin and King, 2008).

into their final cellular fate. Due to their diverse usage of CAMs for adhesion and as cytoskeletal components for anchorage two structural cell-matrix contacts can be distinguished: hemidesmosomes and focal contacts (Benninghoff and Drenckhahn, 2008).

2.2.1.1 Hemidesmosomes

Hemidesmosomes are related to desmosomes (see section 2.2.2.3.1) but anchor keratinocytes of the epidermis via integrin-type CAMs (see section 2.3.1.2) to the ECM (Litjens et al., 2006). Intracellularly, they are linked to the intermediate filament system via plaque proteins BP230 or plectins.

2.2.1.2 Focal contacts

In focal contacts, integrins anchor cells to ECM components and actin filaments inside the cell (Bershadsky et al., 2006). Plaque proteins needed for the anchorage of integrins to the actin

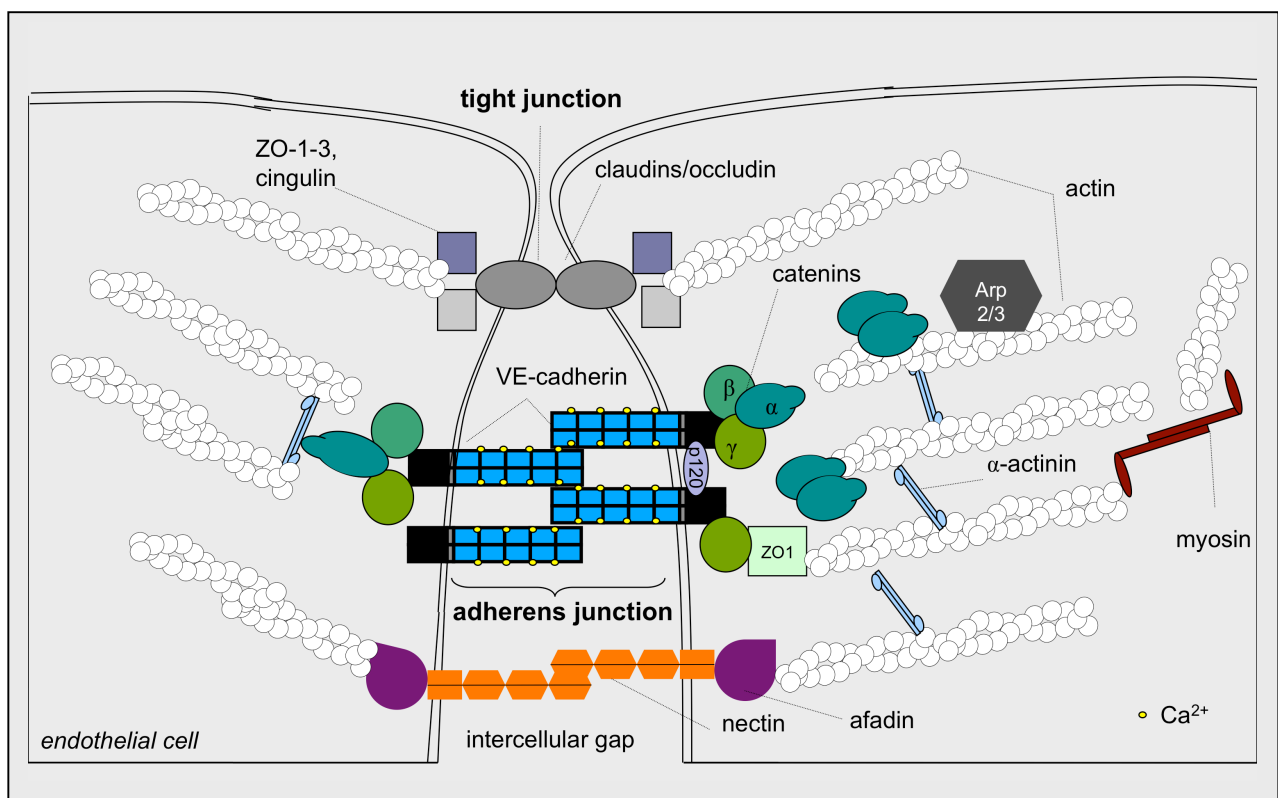


Figure 1: Organization of cell-cell contacts between endothelial cells.

AJs and TJs are the main cellular contacts in endothelial cells. Both contacts consist of (i) intercellular CAMs and (ii) intracellular plaque or adapter proteins for the anchorage to (iii) cytoskeletal components. In AJs, homophilically interacting VE-cadherins are indirectly or directly linked via catenins (α , β , γ , p120) and ZO1 to actin, which in turn is organized by α -actinin or Arp2/3. α -actin preferentially binds to actin as a homodimer and thereby regulates Arp2/3, whereas the binding of α -actin to β -catenin is dependent on a monomeric state. Contractile elements like myosin are able to alter actin organization by inducing constriction. Claudins and occludin are CAMs of TJs and coupled via ZO1-3 and cingulin to actin. As another CAM, nectin mediates homophilic interactions in endothelial cells and is coupled via afadin to the actin cytoskeleton.

system are α -actinin, vinculin or talin. Often, specialized signaling kinases are also associated at cytoplasmic plaques, such as focal adhesion kinase (FAK) and integrin-linked kinase (ILK). These are important regulators for cellular processes like apoptosis and proliferation. Contractile filament bundles (stress fibres) containing actin and myosin motor proteins also anchor to focal contacts and play an important role in cellular migration during which they dynamically change in size and composition. Both hemidesmosomes and focal contacts, accordingly, also communicate positional stimuli inside cells or act as biomechanical sensors.

2.2.2 Cell-cell contacts

Besides adhesion meant for forming multicellular units, cell-cell contacts also serve as intercellular communicators. Hence cell-cell contacts are divided into communication contacts (gap junctions), barrier contacts (tight junctions) and adhesion contacts (TJ).

2.2.2.1 Communication contacts: gap junctions

Gap junctions (Nexus, maculae communicantes) are connections providing metabolic or electrical coupling between neighboring cells or tissues by directly connecting the cytoplasm of two cells. Structurally, a gap junction is composed of two hemichannels (connexons) that connect in the intercellular space resulting in a thin 2-5 nm cleft between cells (Mese et al., 2007). Connexons are built by compositions of connexin (Cx) hexamers. Connexin types account for different electric conductivity or molecule passage, for example. Tissues with

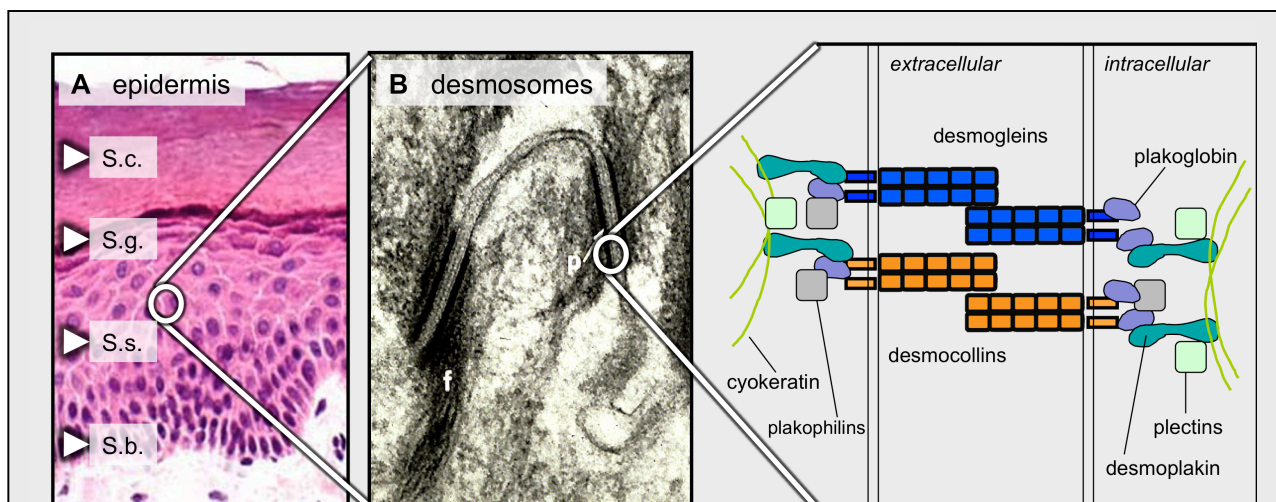


Figure 2: Desmosomes in the human epidermis. In histological slices through the human epidermis several cell layers are visible (A). The lowest monolayer represents the stratum basale (S.b.), followed by multilayered stratum spinosum (S.s.), stratum granulosum (S.g.) and squamous stratum corneum (S.c.). Especially in the S.s., several desmosomes with attached filaments (f) are discernible in electron microscopic images (B). These cell-cell contacts are composed of interacting desmocadherins (desmogleins and desmocollins), which are intracellularly coupled via plakoglobin and plakophilins to desmoplakin. This molecule links the desmocadherins to the cyokeratin filament system. (© A and B: Masayuki Amagai, Keio University, Tokyo).

important functions for gap junctions are cardiac muscle (for synchronization of electric stimulation leading to contraction; Cx43), neurons (as chemical synapses or for axonal structure; Cx32) or the eye lens (Cx50) (Benninghoff and Drenckhahn, 2008).

2.2.2.2 Barrier contacts: tight junctions

With the formation of vertebrate-specific tight junctions (TJs, zonulae occludentes) cells are able to seal the intercellular space, thus providing potentially impermeable barriers that lead to sealing of the intercellular space (Figure 1) (Forster, 2008). However, the permeability of these specialized CCs can be regulated and depends on the composition of the sealing CAMs. These include transmembrane proteins occludin and claudins, which are linked via plaque proteins (ZO1-3 or cingulin) to the actin cytoskeleton. Other CAMs in TJs are junctional adhesion molecules (JAM) A, B and C. Physiologically, TJs also are important for cellular polarity by preventing integral membrane proteins of the apical membrane from intermixing with basal positions. Moreover, TJ-mediated sealing is essential for the blood-tissue-barrier of blood vessels and also for the epithelial barrier of the intestine. In epithelial tissue, TJs form a sealing complex together with adherens contacts and desmosomes (see section 2.2.2.3). In general, TJs are also largely dependent on the proper function of adherens junctions.

2.2.2.3 Adhesion contacts: desmosomes and adherens junctions

Adhesion contacts mediate mechanical intercellular adhesion via specialized CAMs and strong anchorage to the cytoskeleton. In desmosomes, cadherins are linked to the intermediate filament system, whereas in adherens junctions they are anchored to the actin system.

2.2.2.3.1 Desmosomes

The Greek words “desmos” meaning bond and “soma” meaning body are combined in the name of these specialized adhesion contacts. Desmosomes, also known as macula adherens, are spot-like (0.1–0.5 μm) CCs, randomly arranged on lateral membrane sides (Figure 2) and were first described by the Italian pathologist Giulio Bizzozero (1846-1901) (Delva et al., 2009). They promote resistance against shearing forces and are found in most simple and stratified squamous epithelium, but also in muscle tissue of the heart. Desmosomal cadherins of the desmoglein (Dsg1 – Dsg4) or desmocollin (Dsc1 - Dsc3) family are the CAMs of desmosomes and share 30% homology to the classical cadherin of epithelial adherens junctions, E-cadherin, (Garrod et al., 2002). They are linked via the plaque proteins plakoglobin and plakophilins to the structural protein desmoplakin, which in turn promotes anchorage to the intermediate filament system (Delva et al., 2009). The intercellular space between desmosomal contacts is fairly wide (about 30 nm).

2.2.2.3.2 Adherens junctions

Adherens junctions (AJs) are involved in various functions ranging from cell-cell adhesion, tissue homeostasis to control of epithelial and endothelial permeability or cell-cell communications. In AJs, cadherins mediate cell adhesion and are strongly anchored via catenin family proteins to the actin cytoskeleton (Figure 1) (Miyoshi and Takai, 2008; Meng and Takeichi, 2009). Important members of the catenin family include α -catenin, β -catenin, the related plakoglobin (also renamed as γ -catenin) (Ozawa et al., 1989) and p120 catenin (p120^{ctn}) (Ishiyama et al.; Yap et al., 1998). β -catenin, plakoglobin and p120^{ctn} directly bind to the cytoplasmic domain of cadherins. The interaction of β -catenin to E-cadherin is very strong, but can be modulated by phosphorylation (Lickert et al., 2000; Choi et al., 2006). The role of α -catenin in the linkage of cadherins to the actin cytoskeleton has changed in the recent years. α -catenin does not directly bridge actin molecules to β -catenin, but indirectly mediates linkage to actin via a dynamic association with either β -catenin as a α -catenin monomer or with actin as a homodimer (Drees et al., 2005; Yamada et al., 2005). Other linking molecules are EPLIN, α -actinin, vinculin or ZO-1 (Meng and Takeichi, 2009). Recently, linkage to microtubules via adapter proteins Nezha and PLEKHA7, an interaction partner of p120^{ctn}, has been identified as well (Meng et al., 2008). Depending on the microscopic ultrastructure, several AJ forms can be differentiated: punctum adherens, zonula adherens and fascia adherens.

2.3 Characterization and classification of cell adhesion molecules

Crucial to CCs and in particular cell-cell contacts are CAMs. Achieving robust but still dynamic cellular adhesion depends on several and different types of CAMs. Common structural features of CAMs are the extracellular (EC) domain mediating adhesion, a transmembrane part, and the intracellular (IC) domain that is important for intracellular anchorage or signaling functions. CAM-mediated interactions can be characterized by interactions of same (homophilic) or different members (heterophilic) of a certain CAM family. If binding to other CAMs or proteins occurs, the term heterotypic interaction is used. Binding of two opposing CAMs in antiparallel manner is described as a trans-interaction whereas cis-interactions normally involve parallel interactions of CAMs of the same cell. The strength of CAM-mediated intercellular adhesion amongst others depends on two factors: the affinity of CAM-CAM interactions and the avidity, i.e. the combined strength of multiple bond interactions. Avidity is rather more than just the sum of bonds, but combined synergistic strength of bond affinities. An important factor for avidity and intercellular adhesion strength in general is the amount or concentration of molecules present at the cell surface. Affinity is characterized by a dissociation constant that determines the propensity of an intermolecular complex to separate (dissociate) reversibly into its component molecules (equation 1). The dissociation constant is

usually denoted K_D and is the inverse of the association constant K_A . Kinetically, K_D values can be described by the interplay of dissociation (k_{off}) and association (k_{on}) rates (equation 2).



$$K_D = \frac{[A][B]}{[AB]} = \frac{k_{off}}{k_{on}} \quad (\text{equation 2})$$

For classification, CAMs are divided by the need of Ca^{2+} for proper adhesion into Ca^{2+} -independent and Ca^{2+} -dependent molecules.

2.3.1 Ca^{2+} -independent cell adhesion molecules

2.3.1.1 Immunoglobulin-like cell adhesion molecules

The group of Ca^{2+} -independent CAMs consists of immunoglobulin (Ig)-like CAMs (Ig-CAMs) and integrins. Ig-like CAMs owe their name due to the structural similarity of one or more of their EC domains to Ig domains of immunoglobins (Vaughn and Bjorkman, 1996). Ig-CAMs are heterogeneously expressed in different tissues and involved in biological processes such as brain development, building of the vascular network or immunologic interactions (Aplin et al., 1998). Ig-CAM-mediated binding normally involves homophilic trans-interactions. Multiple Ig-CAM domains are believed to bind uncooperatively resulting in a zipper-like assembly (Tsukasaki et al., 2007), but with dissociation rates similar to other CAMs, e.g. cadherins ($k_{off} = 1.5 \text{ s}^{-1}$) (Vedula et al., 2007). Heterophilic interactions to heterophilic Ig-CAMs or other receptors such as growth factor receptors or even cadherins are known (Cavallaro and Christofori, 2004). Information about cytoskeletal anchorage of Ig-CAMs is limited. Important Ig-CAM members are the neural NCAM and netrins, platelet endothelial cell adhesion molecule (PECAM), intercellular adhesion molecules (ICAMs), vascular cell adhesion molecule (VCAM) and nectins. Nectins prefer heterophilic to homophilic partners as the former produce stronger bonds (Martinez-Rico et al., 2005). Furthermore, nectins are important for their role in establishment of AJs via the nectin – afadin system which is believed to prime adhesive interactions for cadherins and therefore can initiate AJ assembly as afadin directly interacts with α -catenin (Takai et al., 2003).

2.3.1.2 Integrins

Integrins form a family of cell-surface glycoproteins that mainly act as receptors for ECM molecules and are predominantly found in focal contacts and hemidesmosomes (Arnaout et al., 2007). They are not only important for ECM attachment but also for physiological processes such as cell motility, platelet activation or the binding of lymphocytes to the

endothelial surface. Integrins consist of obligate heterodimers containing one α - and one β -subunit, which are non-covalently linked. At least 18 different α , and 8 different β proteins are known for mammals, resulting in the formation of numerous different integrins with specific ligand binding. A crystal structure of the extracellular integrin segment in complex with its ligand has been resolved (Xiong et al., 2002). Interestingly, integrins also have a Ca^{2+} binding site in their EC domain, although their binding is largely Ca^{2+} -independent. Often, integrins heterotypically bind to large proteins such as collagens or fibronectin. For some integrins, however, the main adhesive sequence of the ligand consists of a short RGD (arginine-glycine-aspartic acid) tripeptide. Integrin interactions with their ligands are characterized by low affinities ($k_{\text{off}} = 1.3 \text{ s}^{-1}$) (Taubenberger et al., 2007), but usually avidity is increased by high integrin concentrations in the membranes. Moreover, cells can regulate the affinity of their integrins. Intracellular stimuli are known to activate integrins by altering its structural conformation (“inside-out signaling”). This is known to be important for platelet activation during blood clotting. Important integrin - ligand pairs are $\alpha_5\beta_1$ and collagens, $\alpha_L\beta_2$ and ICAM or $\alpha_6\beta_4$ and laminin 5.

2.3.2 Ca^{2+} -dependent cell adhesion molecules

2.3.2.1 Selectins

The second group of CAMs is characterized by its strong dependency for adhesion on divalent cations, mainly Ca^{2+} . Selectins form a small family of single-chain lectin-like glycoproteins (Gonzalez-Amaro and Sanchez-Madrid, 1999). Lectins in turn are polysaccharide-binding proteins. Structurally, selectins consist of an extracellular lectin domain, an epidermal growth factor (EGF)-type domain and several other regulatory EC domains. The IC domain links selectins to the actin cytoskeleton. There are three main members: leukocyte (L)-, endothelial (E)- and platelet (P)-selectin, with its respective ligands GlyCAM-1, E-selectin ligand and P-selectin glycoprotein ligand-1. Selectins bind to sugar moieties on these ligands such as Lewis X-sialylated carbohydrates in a heterotypical manner. Selectins play important physiological roles in leukocyte homing and binding to endothelial cells and are also involved in platelet activation during inflammation. Selectin-mediated adhesion is strongly regulated by spatial and temporal expression of these CAMs. For example, P-selectin as a homing receptor for cells of the immune system is rapidly incorporated into endothelial membranes upon inflammatory stimuli by exocytosis of Weibel-Palade bodies. Selectins are characterized by apparent low affinity of adhesion with rapid associations and subsequent dissociations ($k_{\text{off}} = 0.2 - 0.8 \text{ s}^{-1}$ (Hanley et al., 2004)). However, even lower dissociation rates ($k_{\text{off}} = 0.02 \text{ s}^{-1}$ (Fritz et al., 1998)) have been found when analyzing P-selectin ligand interactions at lower loading rates indicating higher affinity under low forces. Moreover, a mechanism of catch bonds is proposed, where increase of force leads to the locking of the interaction (Marshall et al., 2003). All this is believed to enable the so-called “rolling” of leukocytes on endothelium activated by

inflammation: during high physiological forces, weak selectin interactions slow leukocytes down. After reaching lower “dragging” forces, selectin-mediated adhesion is increased. Involvement of other CAMs then leads to strong adhesion of the cells to the endothelium.

2.3.2.2 Cadherins

Ca^{2+} dependency of adhesion is expressed as part of the name of the largest CAM family found in adhesion contacts, i.e. Ca^{2+} -dependent adhesion molecules, cadherins. These single-span glycoproteins are essential for development, morphogenesis and tissue structure (Stepniak et al., 2009). Since the discovery of cadherins (Grabel et al., 1979; Yoshida and Takeichi, 1982) and the first cadherin molecule, which was termed uvomorulin (Peyrieras et al., 1983) and later renamed to epithelial (E-)cadherin, 113 human cadherin family members have been identified and state for an impressive functional spectrum (Nollet et al., 2000; Hulpiau and van Roy, 2009): reaching from classical cadherins (type I and II) and desmosomal cadherins (desmogleins and desmocollins) to protocadherins, flamingo-cadherins and FAT- or RET-like cadherins (due to its similarities to tumor suppressor FAT or protooncogen RET, respectively). Especially the protocadherins as the largest subclass of cadherins are only poorly understood and it is not clear whether they are adhesion molecules at all. All subclasses have slight to modest structural differences, but most of them contain the characteristic cadherin EC domains. The best-characterized cadherins, classical cadherins, are found in AJs and contain 5 conserved repetitive EC domains (EC1-EC5, each about 110 amino acids long, with dimensions of 45 x 25 x 25 Å), one transmembrane domain and a conserved IC domain. Via this last domain, catenin family proteins tightly anchor cadherins to the actin cytoskeleton. In a historical view, cadherins were believed to mainly interact homophilically by at first forming parallel cis-dimers at the cell surface, which in a second step interact in trans with opposing cis-dimers on the interacting cell surface. This view, however, has changed in recent years (see section 2.4). Moreover, single molecule cadherin binding is a low-affinity interaction ($k_{\text{off}} = 1.8 \text{ s}^{-1}$, $k_{\text{on}} \approx 10^4 \text{ M}^{-1}\text{s}^{-1}$, $K_{\text{D}} \approx 10^{-4} \text{ M}$ as demonstrated for vascular endothelial (VE)-cadherin (Baumgartner et al., 2000; Baumgartner and Drenckhahn, 2002a). Strong adhesion is believed to be mediated by increased avidity by reduction of the lateral mobility through tethering to the actin cytoskeleton and by clusters of cadherins. However, recent biophysical data has questioned some of these views, too.

2.4 Characterization of cadherin interactions

2.4.1 Experimental approaches to determine cadherin interactions

In recent years distinct and manifold strategies have been applied to precisely explore cadherin interactions at the molecular level (Table 1 and Figure 3) (Baumgartner and Drenckhahn, 2002a; Shapiro and Weis, 2009). These investigations closely correlated with the

identification of cadherin atomic structures. In the early years of cadherin research (1980s), mostly biochemical assays (coimmunoprecipitation and bead aggregations) were used. For this, cadherin extracellular domains were recombinantly expressed and tested. Also, mutated or domain-swapped cadherin constructs were used. For studying dimer formation, cadherins were often fused to Ig Fc domains to achieve stable dimers. Other strategies were also applied, including c-Jun/c-Fos- or COMP-, or FKBP-mediated oligomerization systems. Moreover, cadherins were investigated in the cellular context by cell aggregation experiments or artificial bead-cell contacts. Important structural insights stem from crystallization and followed by X-ray scattering or NRM analysis. But also electron microscopic techniques have been applied, ranging from simple imaging to 3D reconstruction techniques. Important progress for the elucidation of cadherin interactions, however, was achieved using biophysical techniques investigating single molecules. Most of these techniques such as atomic force microscopy (AFM) are based on forced cadherin interactions that are studied with single molecule precision. Some alterations of the AFM technique have been applied (surface force apparatus (SFA), biomembrane force probe (BFP), intermolecular force microscopy (IFM))². Individual cadherin molecules on the surface of cells can be tracked by single molecule tracking (SMT). Insights into molecular cadherin dynamics were provided by the transfection of cell with cadherin-GFP fusion proteins and the analysis of these via fluorescence recovery after photobleaching (FRAP). Aside, theoretical models and molecular dynamics simulations have been employed.

² For abbreviations, please refer to table 1.

Table 1. Strategies for investigating cadherin interactions

Biochemical assays	
Mutated or truncated constructs	(Ozawa et al., 1990a; Brieher et al., 1996; Ozawa and Kemler, 1998; Tamura et al., 1998; Yap et al., 1998; Troyanovsky et al., 1999; Chappuis-Flament et al., 2001; Shan et al., 2004; Sivasankar et al., 2009)
EC domain-swapped constructs	(Nose et al., 1990; Shan et al., 2000; Patel et al., 2006)
In-vitro assembly	(Lambert et al., 2005)
Bead aggregation	(Ranheim et al., 1996; Lambert et al., 2000; Chappuis-Flament et al., 2001; Prakasam et al., 2006)
Gel filtration / gradient sedimentation	(Brieher et al., 1996; Chitaev and Troyanovsky, 1998; Legrand et al., 2001; Baumgartner and Drenckhahn, 2002a)
Cross-linking	
Chemical	(Troyanovsky et al., 2003; Troyanovsky et al., 2007)
Ig Fc fusions	(Moll and Vestweber, 1999)
c-Jun/c-Fos fusions	(Ahrens et al., 2002)
FKBP fusions	(Yap et al., 1997)
Cartilage oligomeric matrix protein (COMP) fusions	(Tomschy et al., 1996; Ahrens et al., 2003)
Cell-based experiments	
Cell aggregation	(Nose et al., 1988; Angres et al., 1996; Niessen and Gumbiner, 2002; Shan et al., 2004; Shi et al., 2008; Katsamba et al., 2009)
Flow chamber analysis	(Perret et al., 2002)
Laser tweezers	(Sako et al., 1998; Baumgartner et al., 2003a; Baumgartner et al., 2003b)
Artificial bead – cell contacts	(Levenberg et al., 1998; Lambert et al., 2000; Baumgartner et al., 2003b)
Structural analysis	
Crystallization and X-ray analysis	(Shapiro et al., 1995; Pertz et al., 1999; Boggon et al., 2002; Patel et al., 2006; Parisini et al., 2007)
Nuclear magnetic resonance (NMR)	(Overduin et al., 1995; Haussinger et al., 2002; Miloushev et al., 2008)
Electron microscopy (EM)	(Tomschy et al., 1996; Hewat et al., 2007)
Electron tomography (ET)	(He et al., 2003)
Cryo-electron microscopy of vitreous sections (CEMOVIS)	(Al-Amoudi et al., 2007)
Biophysical techniques	
Atomic force microscopy (AFM)	(Baumgartner et al., 2000; Panorchan et al., 2006b; Shi et al., 2008)
Surface force apparatus (SFA)	(Sivasankar et al., 1999; Zhu et al., 2003; Prakasam et al., 2006)
Biomembrane force probe (BFP)	(Perret et al., 2004; Bayas et al., 2006; Chien et al., 2008)
Intermolecular force microscopy (IFM)	(Tsukasaki et al., 2007)
Single molecule tracking (SMT)	(Sako et al., 1998; Iino et al., 2001; Baumgartner et al., 2003b)
Fluorescence recovery after photobleaching (FRAP)	(Adams et al., 1998; Lambert et al., 2007)
Fluorescence resonance energy transfer (FRET)	(Zhang et al., 2009)
Surface plasmon resonance (SPR)	(Williams et al., 2002; Katsamba et al., 2009)
Theoretical models	(Baumgartner and Drenckhahn, 2002b; Chen et al., 2005; Katsamba et al., 2009)
Molecular dynamics simulations	(Cailliez and Lavery, 2006; Sotomayor and Schulten, 2008)

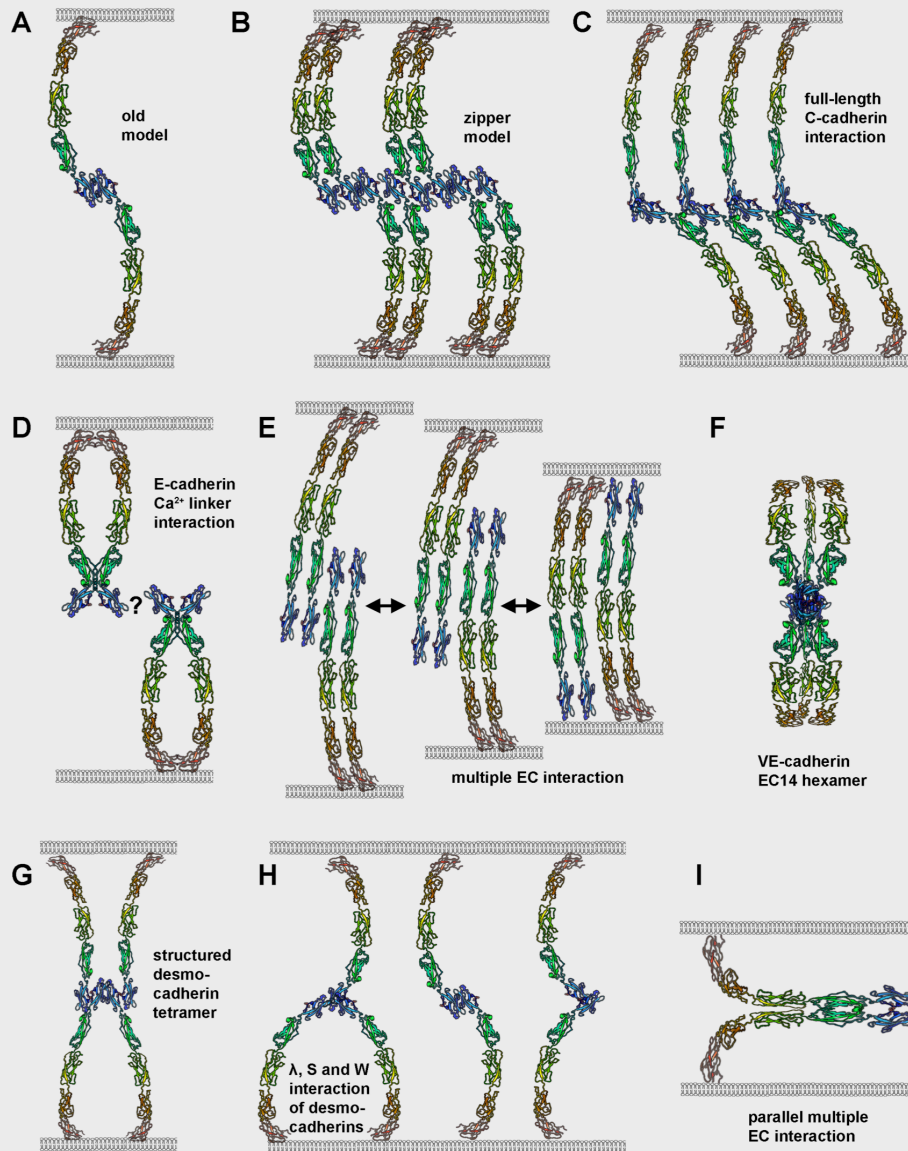


Figure 3. Proposed cadherin interaction schemes. Full-length C-cadherin structures (PDB 1L3W) have been used for illustration of cadherin interaction schemes (*not to scale*). (A) In the first models of cadherin interaction, cadherins were thought to interact as monomers via amino-terminal EC1 domains. (B) N-cadherin EC1 domain crystals revealed both cis-interactions via Trp2 strand swapping and trans-interactions via the opposite, HAV-containing, surface. This was called the zipper model. (C) In C-cadherin full-length EC domain crystals, also both cis- and trans-interactions were resolved. Trans-interactions, however, resulted because of Trp2-mediated strand swapping and cis-interactions involved EC1 and EC2/3 domains of adjacent cadherins. (D) For E-cadherin, T-cadherin and strand swapping cadherin mutants, crystal structures identified cis-interactions involving the Ca^{2+} -binding linker regions between EC1 and EC2 domains ('X-dimer'). (E) Biophysical experiments using the surface force apparatus indicated the presence of cadherin interactions involving multiple EC domains, with an important role for the EC3 domain. (F) In cryo-electron images of VE-cadherin EC14 domain-containing liposomes, VE-cadherin was found to form a hexameric structure and to interact via EC1-mediated interactions. (G) Cryo-electron microscopy of vitreous sections (CEMOVIS) revealed structured interactions of desmocadherins in the native epidermis which involved both cis- and trans-interactions similar to B. (H) In contrast to this, irregular and multiple interaction schemes (λ , S and W) were modeled in electron tomographies of plastic sections from neonatal mouse skin. (I) A parallel, multiple EC domain-involving cadherin trans-interaction was suggested by analyzing biophysical AFM experiments of E-cadherin.

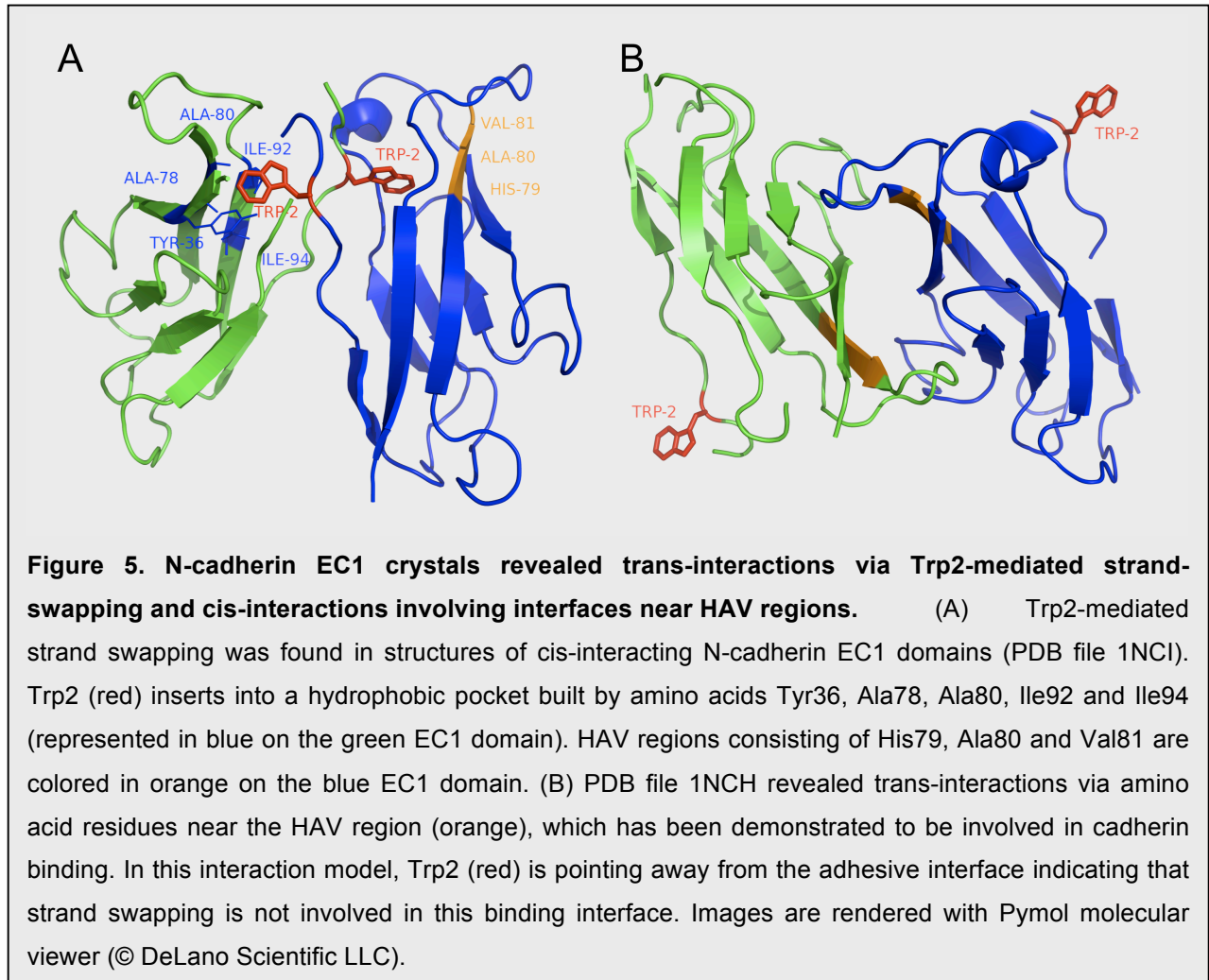
2.4.2 Cadherin interaction

2.4.2.1 First models

As classical and desmosomal cadherins consist of 5 similar EC domains, much energy has been put into identification of the EC domain structure. Finally, this domain was found to be related to the already resolved Ig-fold forming a so-called Greek-key topology and being composed of a seven-stranded β -sandwich topology with Ca^{2+} binding sites located in between adjacent EC domains (Figure 4) (Overduin et al., 1995). Three Ca^{2+} ions are thought to locate in these linker regions and thus are important for proper structural conformation. Moreover, diverse Ca^{2+} binding sites can be differentiated. These are located in linking regions between EC12 and EC23 domains and seem to differently regulate cadherin adhesion (Ozawa et al., 1990c; Cailliez and Lavery, 2005). Also important for structural integrity are correct posttranslational modifications including glycosylations (Liwosz et al., 2006) and proteolytic cleavage. Unprocessed cadherin EC1 domains contain a N-terminal propeptide that needs to be cleaved off for proper adhesion (Haussinger et al., 2004). However, the whole cadherin EC domain consisting of 5 cadherin EC repeats was found to behave differently compared to just a connection of single cadherin EC repeats. Insights into the full-length EC domain structure gained important supramolecular information. Importantly, bended structures have been observed in full-length *Xenopus laevis* C-cadherin crystals (Boggon et al., 2002). With the solving of cadherin EC structures, a plethora of structural data became available to develop models for cadherin-mediated adhesion. During the recent years up to six different principle models for cadherin interactions have been proposed (Figure 3). As already stated, the prevalent first model for cadherin interactions was deduced mainly from biochemical data before high-resolution structures were available. Homophilic trans-Interactions of aminoterminal EC1 domains were believed to promote cadherin-based adhesion, as EC1



Figure 4. X-ray diffraction structure of full-length C-cadherin EC domains. Five different EC domains are visible in the backbone representation of full-length C-cadherin EC domains. β -barrel structural elements are denoted as arrows. In the amino-terminal EC1 domain (blue), Trp2, which is implicated in the interaction mechanism of strand swapping, is colored red and represented with its side chains. The C-cadherin structure is overall bent. Structures are based on information in protein data bank (PDB) file 1L3W and rendered with Pymol molecular viewer (© DeLano Scientific LLC).



domains of different cadherins are extremely well conserved (for example, C-, E- and N-cadherin EC1 domain structures superimpose within 1 Å).

2.4.2.2 Linear zipper model involving Trp2 swapping

After first X-ray structures of interacting N-cadherin domains were resolved by the Shapiro group, the so-called zipper model was proposed (Shapiro et al., 1995). In the first crystals (Figure 5), two different homophilic interactions schemes were observed giving rise to cis-interacting dimers that trans-interact with cis-dimers from an opposing cell surface in a zipper-like structure. Also, as a fundamental principle of cadherin interaction, the twofold-symmetric swapping model was proposed. It states that a conserved tryptophan residue at amino acid position 2 (Trp2) of the cadherin EC1 domain inserts into an also conserved hydrophobic pocket built by residues Tyr36, Ala78, Ala80, Ile92 and ILE94 of the partnering molecule and vice versa. This Trp2 exchange was believed to be the most prominent feature of cadherin interactions. Type II classical cadherins possess two N-terminal Trp, which are also involved in domain swapping: as a result, the angle between dimeric EC1 domains is far more constrained in type II compared to type I cadherins, suggesting extra rigidity in the corresponding type II dimer interface. Desmosomal cadherins lack this 2nd interface providing a more flexible

structure. Interestingly, Trp2 is also believed to confer Ca^{2+} responsiveness of cadherins: only at high Ca^{2+} concentrations Trp2 is free to bind to the hydrophobic pocket of cadherins, but at low Ca^{2+} concentrations it is buried inside its own protomer ("closed monomeric state") and thereby acting as a competitive inhibitor of cadherin interaction (Chen et al., 2005). Confirmation was achieved by characterizing a N-cadherin antibody that specifically binds to Trp2, but only when it is buried in the monomeric cadherin state at low Ca^{2+} conditions (Harrison et al., 2005a). This behavior should also explain why the overall cadherin binding affinities are low even though the dimer interface has the characteristics of a high-affinity protein-protein complex. Various mutational analyses confirmed the importance of Trp2 for cadherin function. Especially, the indole functional group of Trp2 seems to be important for this since indole-3-acetic acid, a synthetic indole moiety, competed with Trp2 in the hydrophobic cadherin acceptor pocket and inhibited cadherin binding (Trojanovsky, 1999). Moreover, during strand swapping, establishment of a salt bridge at the N-terminus involving Glu89 was found to be important for cadherin interaction (Harrison et al., 2005b).

Nevertheless another interaction scheme was discovered in the first N-cadherin crystals. Strand swapping was first found to be important for building cis-dimers, whereas the trans-interaction involved other residues on the opposite interface of the same EC1 domain: these included the so-called HAV (histidine-alanin-valin) motif (Blaschuk et al., 1990; Noe et al., 1999) and had an increased area of buried surface compared to the Trp2 swap-interface. Ala80 as the central part of the HAV sequence is buried in the hydrophobic core accepting Trp2 of the cis-interacting cadherin. Experiments with synthetic peptides representing HAV- or corresponding cell adhesion region (CAR) sequences of desmocadherins confirmed the importance of these amino acids (Tselepis et al., 1998; Noe et al., 1999), although this trans-interaction mechanism was questioned in later studies. In this context, important caveats for the interpretation of crystal structures have to be mentioned. Importantly, recombinant proteins produced in bacteria have been used with the potential of improper conformations via the following issues: i) the presence of unprocessed cadherin propeptides, ii) additional aminoterminal amino acids due to cloning artifacts, iii) lack of full-length EC domains and iv) lack of specific glycosylation. All these modifications have been found to alter cadherin structure and may therefore explain discrepancies between different studies. Finally, crystallization may generate crystal lattice packaging artifacts. Nevertheless, the zipper model seen in the first N-cadherin crystals was able to explain various experimental data on cadherin interaction at the molecular level and therefore was widely accepted as a suitable working model.

2.4.2.3 Trp2 strand swapping in trans-interactions of full length C-cadherin

Upon crystallization of the first full-length EC domain cadherin structure by Boggon et al. (Figure 4), the zipper model was slightly changed (Boggon et al., 2002). In C-cadherin interaction schemes, both cis- and trans-interactions were identified but strand swapping

occurred at the trans-interacting cadherin interface. Lateral cis-interactions were observed between EC1 and neighboring EC23 domains. In this potential cis interface Asp44 contacts the Ca^{2+} binding site. Mutations of Asp44 in R-cadherin indeed diminish adhesiveness (Kitagawa et al., 2000). An intriguing confirmation of Trp2-mediated trans-interactions was provided by biochemical cross-linking experiments by the Troyanovsky group (Troyanovsky et al., 2003). Using E-cadherin mutants with artificial cysteine residues and a cysteine-specific cross-linker, trans-dimers involving Trp2 strand swapping were found to be the predominant form of cadherin interactions in cell culture conditions, but also lateral dimers were present: at micromolar Ca^{2+} conditions, E-cadherin was found to produce cis-dimers via the same adhesive interface. However, both cis- and trans-interactions obviously were mediated by the same adhesive interface (Klingelhofer et al., 2002). Interaction schemes involving HAV-regions, as proposed by the first N-cadherin crystals, were excluded in this setup.

2.4.2.4 Models involving multiple domain interactions

Experiments with the use of the surface force apparatus (SFA) by the group of Leckband produced a strikingly different view on cadherin trans-interaction (Sivasankar et al., 1999; Sivasankar et al., 2001). In the SFA, two small opposing surfaces are brought into contact (Leckband and Sivasankar, 2000). With the help of a leaf spring below the lower surface and light passing through the apparatus resulting in changing interference fringes, forces (resolution 0.1 – 1 nN) and distances (with nm resolution) can be simultaneously measured, respectively. When cadherins were immobilized on two opposing SFA surfaces, multiple unbinding events were detected during retraction, which were believed to represent unbinding of full-length and partial overlapping domains. The EC3 domain was identified as the most important domain for cadherin adhesion. Thus in contrast to other models SFA-derived models describe trans-interactions involving more than two EC domains. These experiments could help to explain the observation, that an antibody targeting the membrane proximal EC domain of E-cadherin is able to disrupt cadherin interaction (Ozawa et al., 1990b). Also, a newer and integrating study on N-cadherin-mediated cellular adhesion demonstrated that the EC12 domain is the minimal adhesive unit that promotes proper cell-mediated adhesion, and larger constructs with EC3 to EC5 enhance adhesion activity (Shan et al., 2004). According to the model of the Leckband group, multiple domain interaction schemes fit well into in-situ intercellular membrane distances (Leckband and Sivasankar, 2000). In AJs of fixed and dehydrated cells, transmission electron microscopy (EM) revealed intercellular gaps of 20-25 nm distance (Farquhar and Palade, 1965). In SFA experiments, the strongest force peak is seen at 25 nm membrane distance, which is explained by fully interdigitated structures. The end-to-end EC1 domain-mediated adhesion of cadherins expects an intercellular space of 40 nm width (Boggon et al., 2002). The discrepancy could, however, be explained by more bent cadherin structures. Moreover, results gained with SFA have been questioned. For example the importance of the

EC3 domain in cadherin interaction could be explained by the fact that mutations in the Ca^{2+} binding site between EC2 and EC3 domains also affect EC1 domain conformation, which is known to mediate strong adhesion (Trojanovsky, 2005). In a recent study, EC1 and EC5 domains of E-cadherin were fluorescently labeled and fluorescence resonance energy transfer (FRET) was measured (Zhang et al., 2009). These results, however, showed that cadherins interact mainly in trans via EC1 domains.

2.4.2.5 Interaction via Ca^{2+} binding linker regions ('X-dimer')

Analysis of EM images of crystals of E-cadherin by the Engel group led to the proposal of a cis-interaction scheme, in which cadherin domains interacted laterally via their Ca^{2+} binding domains in the linker region between EC1 and EC2 (Pertz et al., 1999). This model was called the 'X-dimer' and required the ectodomains to be bent, as seen in EM images in which E-cadherin (EC1-5) was pentamerized via fusion to the cartilage oligomeric matrix protein (COMP). In electron micrographs, dimer formation via cis-interacting aminoterminal EC domains was resolved together with intermittent trans-interactions with other cis-dimers (Tomschy et al., 1996). However, the molecular sites involved in trans-interaction of opposing cadherins were not resolved by this method. With the help of NMR studies, Ca^{2+} -mediated "activation" of E-cadherin EC12 domain monomers was demonstrated by the same group: only in the Ca^{2+} -bound state, monomers became oriented with an accessible adhesive interface (Haussinger et al., 2002). In general, NMR spectroscopy in solution avoids the problem of disturbing crystal forces and is well suited for the study of weak interactions between macromolecules. As a drawback of these E-cadherin interaction studies, Trp2 involvement was not found to be of significance for both cis- and trans-interactions. As an explanation for this discrepancy, it was proposed that an additional false methionine located at position 1, due to the cloning technique used, prevented proper cadherin conformations by disturbing the salt-bridge involving Glu89. New crystal structures of human E-cadherin that lack N-terminal methionine confirm the interaction schemes described by Boggon et al. with the presence of the Glu89 salt bridge and Trp2 swapping in trans-interactions (Parisini et al., 2007). Therefore the interactions schemes involving the Ca^{2+} binding linker regions were considered pure crystallization artifacts for a long time. Two recent studies, however, shed new light on this topic and the complexity of cadherin interaction: the Shapiro group discovered a similar X-dimer interaction scheme in the structure of the non-classical T-cadherin (Ciatto et al., 2010). Mutations in the linker region of T-cadherin disrupted the adhesive activity of T-cadherin. Since non-classical cadherins often lack the necessary strand-swapping sequence signatures, this interaction scheme may also be used by other cadherins besides T-cadherin. Interestingly, strand-swapping mutants of type I and II classical cadherins were also found to interact via linker region-involving X-dimers in crystal structures (Harrison et al., 2010). These findings suggest that X-dimers are existing binding intermediates that facilitate the formation of strand-

swapped dimers, which represent the final interaction state. Interestingly, X-ray structures of the EC domain of cadherin 23, which lacks the strand-swapping interface including Trp2, give rise to speculations on a novel adhesion mechanism involving polar amino acids that bind Ca^{2+} (Elledge et al., 2010).

2.4.2.6 Insights into cadherin interactions obtained with biophysical force spectroscopy

With the development of highly sensitive biophysical techniques, dynamic insights into cadherin interactions have been gained. These techniques are able to describe molecular interactions of single molecules by determining binding affinities, kinetics and unbinding forces. This is based on theoretical calculations describing the weak non-covalent interactions that exist between cadherin interactions (Bell, 1978; Evans and Ritchie, 1997). These bonds will

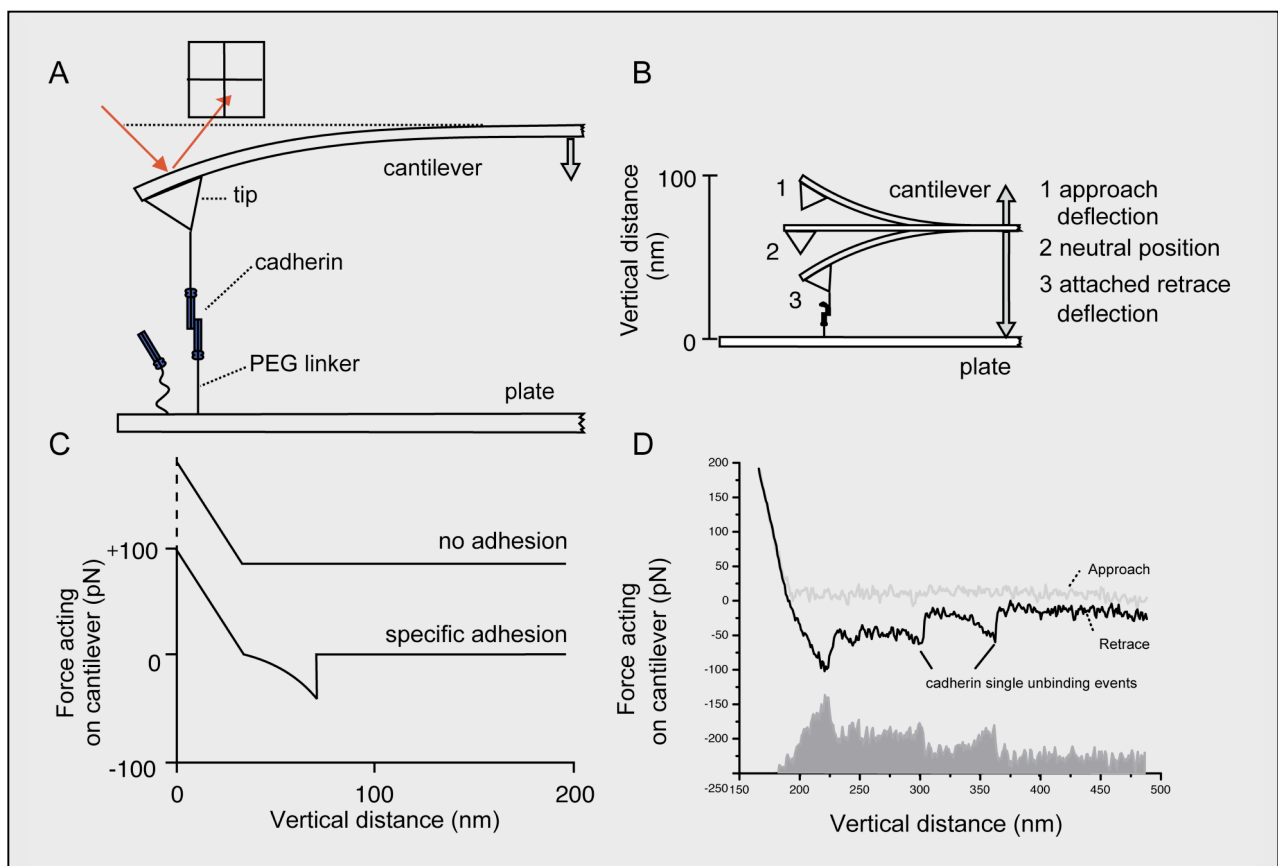


Figure 6. Investigating single molecule binding by atomic force microscopy (AFM) force spectroscopy. Cadherin fusion proteins were covalently coupled to the AFM tip and mica plates via flexible and bifunctional PEG-crosslinker and monitored by force-distance cycles (A). Molecules were brought into contact by repeated downward (approach) and upward movements (retrace) of the AFM tip (B). During upward movement, a downward deflection of the cantilever occurred if plate- and tip- bound cadherin molecules underwent transinteractions (C). After reaching the critical unbinding force, the bond broke and the cantilever jumped back to the neutral position. In a sample force-distance plot, several unbinding events of cadherin molecules are shown (D). By analyzing these curves, binding probability and activities as well as unbinding forces and lengths were determined.

break under any level of external pulling force if held for sufficient time. Thus, when tested with sensitive biophysical techniques, the adhesion strength (i.e. unbinding force) has time- and loading rate-dependent properties.

AFM provides a tool to investigate surfaces at the nanoscale, working similar to a record player with a small tip scanning the surface (Figure 6). In AFM force spectroscopy, this technique is used to measure forces between molecules attached to the AFM setup. For example, recombinant cadherin molecules are attached to the tip of the AFM probe and also a suitable substrate, such as mica plates. This coupling is achieved by sophisticated chemical coupling. Coupling of molecules via flexible polyethylene glycol (PEG) linkers (Ebner et al., 2007) allows the molecules to freely diffuse within the radius of the length of the linker and to undergo unimpaired encounter reactions. During AFM force spectroscopy measurements, the cadherin-coated tip is brought into contact with the cadherin-coated plate by cyclic upward and downward movements. So-called force-distance cycles are consequently recorded. If during the contact phase the cadherin molecules attached to the tip and plate bind to each other, deflection of the AFM cantilever will occur during the following retrace movement until the bond undergoes disruption. Specific single unbinding (disruption) events are then characterized by abrupt jumps of the cantilever toward the neutral position. The shape of the cantilever deflection during retrace allows distinguishing between specific and unspecific interactions, because the flexible PEG linkers undergo characteristic elongation curves during extension. By definition, the unbinding force is the force producing the most frequent failure of bonds in repeated tests of breakage, i.e., the rupture force distribution peak. Consequently, for analysis of AFM experiments (see Figure 6) several theoretical considerations have been made to use experimental AFM data for determination of molecular binding characteristics. As stated above, unbinding forces (f) depend on the loading rate (r). The loading rate is composed of the velocity of unbinding ruptures v (derived from the time - dependent change in displacement (ds/dt)) and the effective spring constant k of the AFM probe, which also includes the elasticity of the linker which is placed in between tip and bound protein (equation 3).

$$\dot{F}(t) = k \frac{ds}{dt} = kv = r \quad (\text{equation 3})$$

By stepwise increasing loading rates, unbinding forces increase in a logarithmic way. This dependence is due to changing lifetimes τ ($= 1 / k_{\text{off}}$) of the adhesion complexes that depend on both intrinsic bond kinetics at zero force (k^0) and response of bond kinetics to external forces f (equation 4). χ_β is the reactive compliance and describes the distance between the maximum of the barrier potential and the minimum of the meta stable state.

$$k_{\text{off}}(f) = k_{\text{off}}^0 e^{\frac{f\chi_\beta}{k_B T}} \quad (\text{equation 4})$$

The lifetime of bonds at zero force ($\tau_0 = 1 / k_{\text{off}}^0$) can be estimated by extrapolation of the force-dependent lifetime of the bonds to zero force, according to Bell's equation and estimation of $k_{\text{off}}(f)$ from the probability of the survival of a given bond and the width of the force distribution via the following equation 5 (Bell, 1978; Evans and Ritchie, 1997) (T = temperature, k_B = Boltzmann constant, f^* = most likely force, i.e. peak of force distribution).

$$f^*(r) = \frac{k_B T}{\chi_\beta} \ln \frac{\chi_\beta r}{k_{\text{off}}^0 k_B T} \quad (\text{equation 5})$$

AFM single molecule force spectroscopy and similar single molecule techniques therefore provide an optimal framework for analyzing cadherin interactions.

In a pioneering approach to characterize cadherin interaction by AFM, short VE-cadherin lifetimes, low unbinding forces and a strong cooperative Ca^{2+} dependency of cadherin interactions were determined (Baumgartner et al., 2000). Moreover, multiple unbinding forces at a given loading rate were observed, which were attributed to different and multimeric interactions similar to the zipper model but contrary to models involving multiple overlapping EC domains. Similar observations were made for other cadherins, including desmocadherins, E-cadherin, LI-cadherin, N-cadherin or cadherin-11 (Baumgartner et al., 2003a; Waschke et al., 2007; Wendeler et al., 2007; Heupel et al., 2008).

Recent AFM-based cadherin experiments interpreted multiple unbinding forces during cadherin interaction in another way: Perret et al. found multiple bonds in E-cadherin interactions by applying a special jump/ramp method (Perret et al., 2004). This led to the identification of several distinct bonds involved in cadherin unbinding that were normally hidden states in Gaussian distributions of unbinding forces. In detail, special jump/ramp modes of force spectroscopy were used to better resolve distributions of unbinding forces, which were fitted to two regression curves yielding two different k_{off}^0 . Similar states were observed in another study with N-, C- and E-cadherin (Shi et al., 2008). Moreover, two different force peaks were resolved during cadherin unbinding: a low force peak (which had been identified in prior studies) and a high force peak. By using these high force peaks in equation 4/5 additionally very long lifetimes of cadherin interaction were identified. Interestingly, long lifetime cadherin interactions were also observed in biochemical studies (Trojanovsky et al., 2007). In another study, full-length cadherins were found to involve two additional longer-lived bonds in cadherin interactions (Bayas et al., 2006). Biphasic unbinding via fast, low probability and slow, high probability binding states were found to be independent of IC domains, but strongly dependent on EC3 domain. It was argued that the fast process required EC1 domain interactions involving Trp2, whereas the other state required at least EC3 or more domains (Chien et al., 2008).

Other biophysical techniques also provided important information about cadherin interactions. In single molecule FRET experiments, cadherins were found to interact via EC1 domains, but no cis dimerizations were detected. It was concluded that lateral aggregation of cadherins for example via fusion to Ig-Fc domains to generate stable dimers, only cooperatively increased probability of cadherin interactions but failed to increase unbinding forces per se (Zhang et al., 2009). Interestingly, cadherin interactions were found to have a memory (Zarnitsyna et al., 2007): Cadherin interactions were negatively “remembered” and consequently led to decreased binding probability after the initial interaction. AFM and FRET experiments have given strong insights for an induced-fit mode of cadherin interaction (Sivasankar et al., 2009). Cadherin mutants lacking Trp2 were found to directly interact via EC1 domains with other cadherins, but only with 25% of the force of wild type (wt) cadherin interactions. Together with results which concluded that Trp2 is normally hidden inside its own β -barrel in monomeric states but extending from it in the hydrophobic pocket of another cadherin after dimerization, this points to the induced-fit model, where multiple interaction schemes lead to an initial complex that in turn is strengthened via strand-swapping.

A biophysical study by Tsukasaki et al. provided interesting explanations for different unbinding states of cadherin interactions (Tsukasaki et al., 2007). Cadherins were found to act cooperatively as a parallel-like multiply-bonded system, consistent with the “fork initiation and zipper” hypothesis. 4 different binding states between paired cadherins were identified to mediate slow stabilization in cell-cell zippering processes. The multiple tandem-aligned domains of cadherins then cooperatively act as a macro-single bond to strengthen adhesion. The EC domains of cadherin pairs were thought to bind in parallel fashion even though the overall orientation of the two cadherins is antiparallel, explaining different outcomes of cadherin crystals.

Nevertheless, although single molecule experiments provided important insights into cadherin interaction, several caveats for these experiments have been mentioned. These include the use of recombinant proteins, in particular when recombinant cadherins from different species are used in the same study. Another critical aspect refers to the analysis of unbinding force distributions in AFM data, because some hidden states are unable to be detected and require special experimental procedures. Data interpretation may become speculative if the discrimination between different EC domain interactions, cooperative cadherin clustering or different energy barriers is not taken into account. Fast cycling rates in AFM force spectroscopy could bias the measurements of cadherin bonds towards weaker bonds with faster kinetics, because stronger bonds involving slow kinetics are unable to form within the cycle (Shi et al., 2008). Partial unfolding events of cadherin domains could contaminate unbinding force distributions (Sotomayor and Schulten, 2008). AFM experiments are sometimes accompanied by chemical problems because of undirected and inflexible cadherin

coupling when not using PEG linkers. Importantly, in AFM experiments artificially enforcing and detaching cadherin interactions could bias cadherin adhesion.

2.4.2.7 VE-cadherin hexamer structures

For VE-cadherin, a type II classical cadherin found in endothelial cells (see section 2.6.1.2), a hexameric interaction scheme has been discussed (Bibert et al., 2002; Hewat et al., 2007). In cryo-electron microscopic images, in-vitro assemblies of VE-cadherins EC1-5 proteins into lipid bilayers resulted in the formation of hexamers, consisting of a trimer of dimers with each aminoterminal EC1 domain producing an antiparallel contact. This should explain why i) in X-ray and electron microscopy EC1 domain are central for adhesion and ii) why SFA measurements or AFM measurements of VE-cadherin resulted in multiple unbinding events, because in the hexameric structure all three bonds should break one each other, with partial unwinding after each breaking event. However, proof of hexameric structures in EC1-5 domain proteins is lacking and recently, in electron microscopic studies using COMP-mediated immobilization, VE-cadherin interactions followed a mechanism similar to classical E-cadherin (Ahrens et al., 2003).

2.4.2.8 Interaction and ultrastructure of desmosomal cadherins

Cell adhesion recognition (CAR) sites were early reported to be important for desmocadherin-mediated adhesion (Runswick et al., 2001). These amino acids are part of the hydrophobic pocket involved in classical cadherin strand dimer formation and are similar to the HAV-sequence of classical type I cadherins. In recent years, application of sophisticated electron microscopic techniques have led to new insights into desmosome structure and bulk desmocadherin interactions. He et al. resolved desmocadherin interactions by fitting C-cadherin crystals into electron densities obtained from electron tomographic reconstructions of sections from freeze-substituted and plastic-embedded samples from neonatal mouse skin (He et al., 2003). Electron tomography is a technique for obtaining 3D images from structures in sections analyzed by transmission EM. Data collection for electron tomography involves collecting images while tilting the specimen around a single axis. Interacting desmocadherins recurred at three shapes of interactions (named W-, I- and S-shapes) and both Trp2 swapping like and independent trans-interactions as well as cis-interactions were observed. This seems feasible because Trp2-mediated swapping as seen in C-cadherin crystals is most likely to apply also for desmocadherins as deduced from structural analyses, although desmocadherin structures are missing (Posy et al., 2008). The overall ultrastructure of the intercellular space of desmosomes appeared flexible but rather unstructured with loosely appearing desmocadherins between opposing cells. In clear contrast to this study, highly structured assemblies of desmocadherins were found with cryo-electron microscopy of vitreous sections (CEMOVIS) and 3D reconstructions (Al-Amoudi et al., 2007; Al-Amoudi and Frangakis, 2008).

This technique allows the observation of biological specimen in their native and hydrated state because of the absence of staining reagents or dehydration steps. In CEMOVIS images, very structured EC1 domain-mediated interactions were seen, potentially involving Trp2 swapping. Also trans W-like interactions and V-like structures between molecules emanating from the same cell membrane were discernible which may represent cis-interactions. The atomic modeling of these interactions was based on first cadherin structures resolved by the Shapiro group (see above). These highly ordered desmocadherin structures seen in CEMOVIS are similar to early electron microscopic images (Rayns et al., 1969). When comparing desmosomal structures of He et al. (2003) and Al-Amoudi et al. (2007), the latter probably represent the native situation because of better structural preservation. However, these studies may also represent different stages of desmosome assembly, with the structured assemblies representing mature desmosomes. An interesting fact which adds to this is the observation by the Garrod group that desmocadherins may interact in a Ca^{2+} -independent, so-called hyper-adhesive state (Garrod et al., 2005). Ca^{2+} irresponsiveness is explained by retention of cadherin-bound Ca^{2+} via cis-interactions of single molecules and appearance of an intercellular midline. It is believed to involve intracellular signaling with PKC α , acting specifically on desmosomes but not on AJs. Structures by Al-Amoudi et al. (2007) may represent such hyper-adhesive desmosomes. Interestingly, highly ordered AJ ultrastructures have not been observed, yet (Miyaguchi, 2000).

2.4.3 Determining cadherin specificity: homophilic vs. heterophilic interactions

Together with the quest for elucidating cadherin interactions, scientists have always aimed to explain the mechanism of cadherin specificity, i. e. the proper sorting of one cell expressing a certain cadherin from other cells expressing different cadherins. In early studies, mainly homophilic cadherin interactions were observed and consequently were thought to be the reason for specificity of tissue separation (Takeichi, 1988).

Newer studies, however, also indicated heterophilic interactions, especially of cadherins of the same family. Identification of a peptide antagonist blocking E- and N-cadherin interaction, both classical type I cadherins, for example demonstrated the homology in binding sequences for classical type I cadherins (Devemy and Blaschuk, 2009). Moreover, recent studies identified cadherin interactions to be quite promiscuous, especially on cell-free single molecule levels. Surface plasmon resonance studies with N- and E-cadherin found heterophilic interactions which were intermediate in strength as compared to both homophilic interactions and, in a theoretical model, this could explain partly intermixed cell aggregation behaviors of these cadherins (Katsamba et al., 2009). But also contradicting results with identical cell-free interactions were found that were unable to describe cell sorting of these cadherins (Shi et al., 2008), and the question remained how molecular specificity is achieved instead.

Structural insights into type II classical cadherins demonstrated that these differ from type I classical cadherins in their EC1 domain interaction, mainly because of the presence of an additional Trp, which is not compatible with EC1 domain swappings seen in type I cadherins (Patel et al., 2006; Miloushev et al., 2008). Nevertheless, both Trps are essential for type II interactions (May et al., 2005). In type II interactions, an extended buried surface (2fold compared to type I) was found in EC1 domain interactions. Moreover, type I classical HAV sequence is altered to QAI in type II cadherins, but obviously not involved in adhesive binding (Shimoyama et al., 1999). All these data suggest that heterophilic interactions between different type I and II classical cadherin subgroups are unlikely on the single molecule level. Interesting experimental data of domain-swapped cadherin constructs demonstrated that EC1 domains directly confer homophilic interactions (Patel et al., 2006), although contradicting results have also been presented (Niessen and Gumbiner, 2002; Shi et al., 2008). As a result of EC1 domain homologies, in bead and cell aggregation assays, very promiscuous interactions of different types of cadherins were reported (Niessen and Gumbiner, 2002). However, it was also concluded that cadherin function was strongly dependent on the experimental conditions used (e.g shaking at low or high rpm, time scale of mixing or cadherin expression levels) indicating kinetic differences underlying cadherin adhesion.

In another study, full-length cadherins were found to involve two additional longer-lived bonds in cadherin interactions (Bayas et al., 2006). Low force peaks were attributed to fast interactions via EC1-2 domains, strong interaction with long life times via EC1-5 domains, and again pointing to an important role for the EC3 domain. Also, low force peaks were found to be similar for different cadherins, whereas strong force peaks were specific for different cadherins. Newer SFA experiments and bead aggregation assays confirmed these findings (Prakasam et al., 2006). In cellular conditions this could lead to establishment of specific cadherin interactions (Panorchan et al., 2006b). Simulations of molecular dynamics looking at buried surfaces of cadherin interactions but not at energy contribution also identified a swapped and a staggered dimer interface, the later being weaker but sequence-dependent, whereas the swapped interfaces were nearly sequence-independent (Cailliez and Lavery, 2006).

Theoretical investigations on the impact of homophilic and heterophilic interactions on cadherin specificity nicely demonstrated that proper cadherin-mediated cell sorting is only possible when cadherins display low affinities (Baumgartner and Drenckhahn, 2002b; Chen et al., 2005). Binding free-energy differences associated with homophilic and heterophilic complexes are quite small resulting in proper and cooperative cell sorting. If interactions were of high affinity, both homo- and heterophilic interactions would lead to strong interactions and consequently no differences between homo- and heterophilic were observable. In this situation, all cadherins would participate in the dimeric interactions and all cells would

immediately stick to each other, leaving no space for cellular specificity. In an analogy, cells expressing different cadherins may act like an intermixing solution of water and oil (Steinberg, 2007).

Another important factor for cadherin specificity is spatially and temporally controlled expression. Cadherin interaction strongly depends on expression levels of cadherins and can lead to binding differences even when expression is changed by 25%. If cadherin concentrations are artificially increased (such as in over-transfection studies) binding specificity is lost because of the occurrence of artificial heterophilic interactions at these expression levels. In physiological cellular situations, local cadherin concentrations in the cellular junction are lower than the K_D of the cadherin interaction and consequently multiple cadherins remain as (competitive) monomers. Nevertheless, besides of these structural aspects several other physiological regulators of cadherin function exist.

2.5 Physiological regulation of cadherin function

Cadherin interaction and consequently cadherin function on cells can be regulated via two physiological approaches. The first one targets the EC domain, whereas the second indirectly alters cadherin function by addressing the IC side.

2.5.1 Outside – in signaling

Inhibiting cadherin interaction effectively blocks cadherin function. Several mechanisms exist to prevent cadherins from forming molecular trans-interactions. These include Ca^{2+} chelation, as Ca^{2+} is needed for proper structural conformation. VE-cadherin interaction has been found to strongly depend on a threshold Ca^{2+} concentration ($K_D = 1.3$ mM). For E-cadherin, several Ca^{2+} -dependent activation steps have been reported: at micromolar concentrations, monomers established correct conformations, whereas cis-interactions only formed in the presence of millimolar Ca^{2+} concentrations (Koch et al., 1999). In another study, Ca^{2+} has been found to be important for adhesive trans- but not for lateral cis-interactions (Chitaev and Troyanovsky, 1998). Spatial lowering of the extracellular Ca^{2+} concentration therefore is an effective mechanism for regulating cadherins, which has been reported for VE-cadherin during inflammation or neural cadherins during synaptic plasticity for example (Baumgartner et al., 2003a; Baumgartner et al., 2003b).

Cleavage of cadherin EC domains by proteases is another mechanism to inhibit its functions. Subtilisin-like proteases, which are important for cleaving prosequences from immature cadherins (Posthaus et al., 2003), γ -secretase (Marambaud et al., 2002), or metalloproteases (Klessner et al., 2009) serve as examples .

For several cadherins, heterotypic interactions were found. Crosstalks with growth factor receptors have been identified for N-, E-, and VE-cadherin. The latter was also found to

interact via EC domains with a special phosphatase, altering intracellular cadherin function (Nawroth et al., 2002). Trans-interacting E-cadherin molecules may recruit epidermal growth factor receptor (EGFR) resulting in phosphatidylinositol-3-kinase and Akt activation, which is thought to finally result in cell contact-mediated inhibition of cell proliferation (Muller et al., 2008). This mechanism is believed to be part of the so-called "contact inhibition". E-cadherin has been found to serve as a receptor for natural killer cell receptor KLRG1 (Li et al., 2009). VE-cadherin has further been shown to interact via their EC domain with fibrinogen (Gorlatov and Medved, 2002).

Surprisingly, extracellular phosphorylation of cadherin domains was reported for drosophila Fat cadherin (Ishikawa et al., 2008). Finally, cadherin interaction itself alters cadherin function and may induce "outside-in signaling". Much information regarding signaling has been concluded from integrins where both inside-out and outside-in signaling is well established. For cadherins extracellular signals can be transduced into the cytoplasm especially via anchorage of cytoplasmic plaque proteins of the catenin family, since these have been found to exhibit various signaling functions (see section 2.5.2).

2.5.2 Inside – out signaling

Because of the overall low affinity of cadherins, intracellular lateral clustering of cadherins via cytoskeletal anchorage has been assumed to promote strong adhesion (Yap et al., 1997). Important functions have been attributed to adapter proteins of the catenin family (Gooding et al., 2004). Theoretical calculations confirmed this hypothesis and predict that numbers of trans-interacting molecules depend on the degree of damping of their lateral mobility by cytoskeletal tethering (Baumgartner and Drenckhahn, 2002b). Some calculations predicted that the actin cytoskeleton is needed for adherent cells to form AJs (Dallon et al., 2009). Special residues in IC cadherin domains have been identified to be important for cadherin interaction. Loss of membrane-proximal IC domains was found to prevent dimerization and weaken adhesion, but this is only partly explained by prevention of p120^{ctn}-mediated clustering (Ozawa and Kemler, 1998; Ozawa, 2003).

However, even some full-length cadherins lack this typical cytoskeletal anchorage: the LI-cadherin IC domain is very short and does not bind catenins (Kreft et al., 1997) and T-cadherin is anchored to membranes via a glycosylphosphatidylinositol link only (Vestal and Ranscht, 1992). Most cadherin constructs lacking IC domains promote basal adhesion, but this adhesion cannot be increased as observed for full-length cadherins (Yap et al., 1998; Shan et al., 2004; Chien et al., 2008). In AFM force spectroscopy experiments with recombinant cadherins on living cells, highly increased unbinding forces were observed which were dependent on the intracellular anchorage to actin or catenins and in contrast to cell-free experiments (Panorchan et al., 2006a; Bajpai et al., 2008; Pittet et al., 2008).

On the other hand, cytoskeletal modulation by actin- or cytokeratin-disrupting agents was found to dramatically reduce AJ- or desmosome-mediated adhesion (Kouklis et al., 1994; Baumgartner et al., 2003b). Increase in intracellular Ca^{2+} has been found to lead to loss of cadherin-mediated adhesion by depolymerizing actin filaments via activation of the Ca^{2+} -dependent protein gelsolin (Yin and Stossel, 1979). Alternatively, $\text{PKC}\alpha$ is activated at high Ca^{2+} conditions leading to cadherin-mediated cell dissociation (Tiruppathi et al., 2002). In endothelial cells, the calmodulin-dependent myosin light chain kinase (MLCK) induces a Ca^{2+} -dependent MLC phosphorylation which leads to cell contraction and loss of AJ-mediated adhesion (Dudek and Garcia, 2001). However, this cytoskeletal anchorage has to be able to dynamically react to different situations (Baumgartner et al., 2003b). Moreover, two actin populations have been found to be important for *Drosophila* E-cadherin: small, stable actin patches for homophilic clusters, in contrast to a rapidly turning contractile actin network governing lateral cadherin clustering (Cavey et al., 2008).

Members of the catenin family act as both structural plaque proteins and dynamical communicators for signaling functions (Hubner et al., 2001). For several members of this family important functions, including regulation of proliferation, gene expression, signaling networks and cross talk to other adhesion contacts were demonstrated. Especially AJ-specific β -catenin and plakoglobin are best characterized in this context (Zhurinsky et al., 2000). Catenin phosphorylation directly alters cadherin adhesion (Lickert et al., 2000). It is still unclear whether this occurs via structural changes of the EC domain or solely via cytoskeletal decoupling. The role of α -catenin in stabilizing cadherin-based adhesion has been strongly revised in recent years: in contrast to previous opinions, α -catenin does not bind to β -catenin and F-actin at the same time. Instead, α -catenin binds to actin as homodimers, and has more affinity to β -catenin in a monomeric than a dimeric form (Nelson, 2008). α -catenin was found to rather stabilize junctions by blocking Arp2/3-mediated dynamic actin remodeling. Small GTPases of the family of Ras homology proteins like RhoA, Rac1 and Cdc42 are also known to directly alter cadherin function by modifying cytoskeletal anchorage, cadherin trafficking and recycling (Fukata et al., 1999; Wojciak-Stothard and Ridley, 2002). However, catenins like p120^{ctn} also directly regulate RhoA and Rac1. As an example of a cadherin-associated kinase, c-Src has been demonstrated to be important in the regulation of cadherin function by interfering with catenin function via their phosphorylation (Wallez et al., 2007).

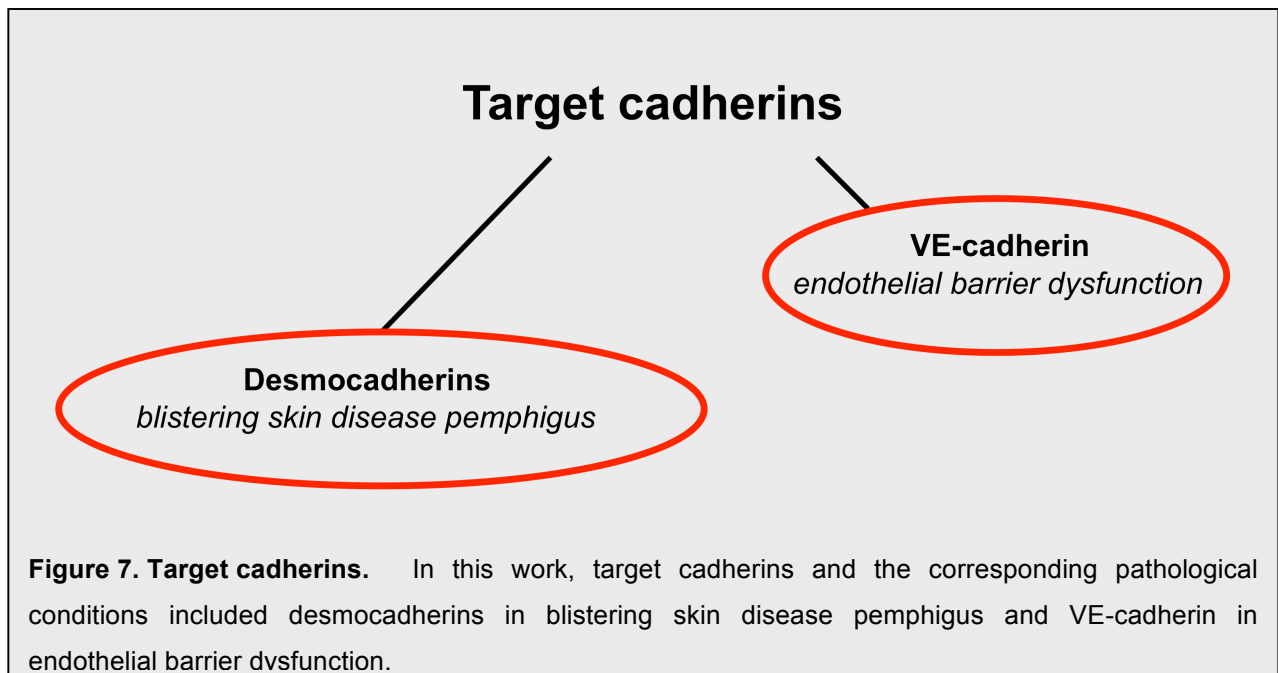
2.5.3 Cadherin regulation by expression levels and endocytosis

As already pointed out when discussing cadherin specificity, expression levels of cadherins are essential for the proper regulation of adhesion. Many zinc finger transcription factors control cadherin expression, for example Slug or Snail, which are considered as repressors of E-cadherin transcription (Cano et al., 2000). Also, microRNAs specific for endogenous cadherin mRNAs have been found, most of them with repressing, but some also with activating function

(Gregory et al., 2008). Interestingly, the catenin-binding region of cadherin consists a “PEST” motif that targets molecules to proteosomal degradation. This domain, however, is normally hidden because of the posttranslational association of cadherins with β -catenin in the endoplasmic reticulum (Hinck et al., 1994; Chen et al., 1999). Beside these aspects, convincing studies provided evidence that levels of adhesion-accessible cadherins are strongly regulated by their dynamic turnover (Trojanovsky et al., 2006). Endocytosis was found to be a strong inducer of loss of cell adhesion. For example, by blocking endocytosis, E-cadherin-mediated interactions were rendered resistant against various adhesion-disturbing signals, including Ca^{2+} chelation. Biochemical studies found long lasting cadherin dimers to increase after inhibition of endocytosis. Various modes of endocytosis, including clathrin-, caveolin- or ubiquitin-mediated pathways, have been found to be involved (Fujita et al., 2002; Yap et al., 2007; Delva and Kowalczyk, 2009). A recent study using different E-cadherin mutants which were tracked by a photoconvertible GFP-variant reported a half-residence time for single cadherins in AJ of 2 min and proposed an alternate ATP-dependent but endocytosis-independent release of cadherins from the cell membranes (Hong et al.). An interesting hypothesis states, that cadherin endocytosis is actually necessary for proper cadherin function (Trojanovsky et al., 2007): E-cadherin dimers were not found to form spontaneously, but were induced after lowering pH levels. This is explained by decreasing activation energies needed for dimer formation. Low pH levels in late endosomes for example could do a similar job. After recycling of endocytosed cadherin dimers to the cell surface, effective cadherin adhesion is possible. This theory, however, could not be experimentally verified yet.

2.6 Cadherins in pathological processes

Surface expression, junctional recruitment, binding activity, cytoskeletal linkage and other properties of cadherins are regulated at different levels in cells (Stepniak et al., 2009). Several mutations in genes coding for cadherins have been associated with hereditary human diseases (El-Amraoui and Petit, 2009). Also, many pathological conditions directly alter and affect cadherins (Berx and van Roy, 2009; El-Amraoui and Petit, 2009). This work focused on pathological conditions affecting VE-cadherin and desmocadherin function, which represent essential components of epidermal and endothelial barriers. For these cadherins, additional introductory information is provided below (section 2.6.1) and in the introductions of the manuscripts in section 3. But there are also several other examples of cadherins in pathological processes. For example, cadherin modifications are the basis of many malignant cancers. Often, loss of E-cadherin function leads to the migratory and invasive phenotype of the so-called epithelial-mesenchymal transition (EMT), finally leading to metastases (Van Aken et al., 2001; Jeanes et al., 2008). In some cases, however, cadherin overexpression promotes tumor invasiveness, and consequently are markers thereof (Hazan et al., 2004). Several



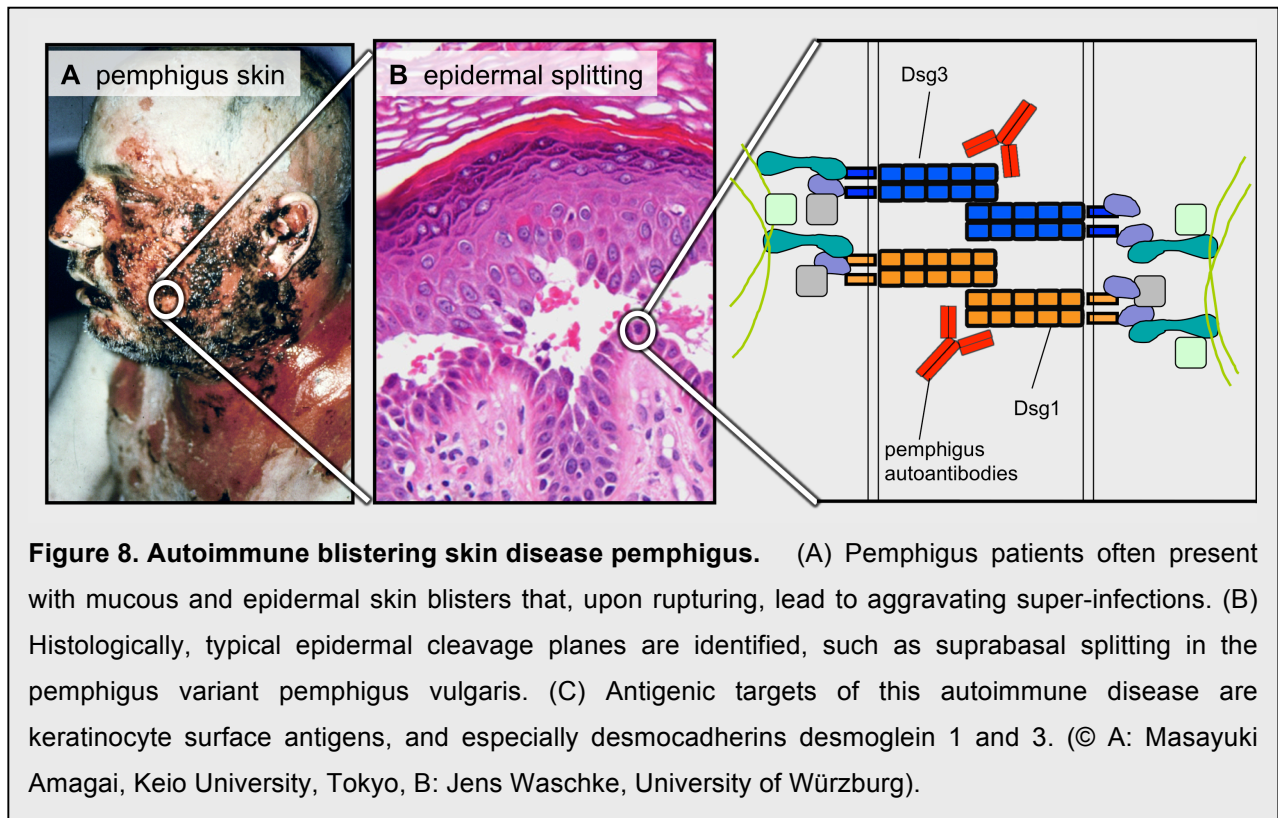
recent studies outlined the role of neural cadherins, namely protocadherins, in the development of psychiatric disorders (Lachman et al., 2008). In some of the patients with mental disorders, M-cadherin mutations affecting cadherin adhesion were found (Bhalla et al., 2008). Several deafness disorders like cases of autosomal recessive Usher syndrome are linked to mutations of cadherins. This can be explained by the fact that cadherin 23 and protocadherin 15 have been found to interact to form tip-links between stereocilia of sensory hair cells (Roux et al., 2006; Kazmierczak et al., 2007; Schwander et al., 2009). In patients with hypotrichosis, i.e. loss of hair growth, and juvenile macula dystrophy of the eye mutations in P-cadherin were reported (Indelman et al., 2002) and in arrhythmogenic right ventricular dysplasia (ARVD), mutations in desmocadherins, mainly Dsg2, inhibit its proper function and lead to cardiomyopathy (Awad et al., 2006; Lai-Cheong et al., 2007).

2.6.1 Cadherins are pathologically targeted at physiological borders

Epithelial cells line the surfaces and cavities throughout the body and are essential for the inside and outside directed body compartmentalization. This work focused on pathological conditions of the epidermal and endothelial barrier, involving desmocadherins and VE-cadherin or blistering skin disease pemphigus and vascular inflammation, respectively (Figure 7).

2.6.1.1 Pemphigus family of blistering skin diseases

Pemphigus is a severe and potentially life-threatening autoimmune blistering skin disease associated with autoantibodies directed to specific keratinocyte surface antigens (Figure 8) (Stanley and Amagai, 2006; Waschke, 2008). Main characteristic of Pemphigus is the appearance of skin blisters. The term pemphigus is derived from the Greek word “pemphix” meaning blister. Microscopically, blisters develop intraepidermally, in contrast to diseases of



the pemphigoid group, which are characterized by sub-epidermal erosions and blisters. There are two main types of pemphigus: pemphigus vulgaris (PV) and pemphigus foliaceus (PF), which differ in the histological localization of blisters: in PV, blisters appear in suprabasal layers of the epidermis and spread from a mucosal infestation (mainly orally) to whole skin involvement. In PF, blisters histologically develop in more superficial layers and involve epidermal skin only. Moreover, drug-induced or tumor-associated (paraneoplastic) forms of pemphigus and an endemic variant of PF (fogo selvagem (Culton et al., 2008)) have been reported. Pemphigus blisters often disrupt upon mechanical stress, which may lead to erythematous blisters and aggravating super-infections. The pemphigus family of blistering skin diseases is not limited to humans and variants of this disease have been shown to occur in dogs, cats and horses. In humans, the incidence of pemphigus is about 0.75 – 5 cases per million, peaking around the 4th to 6th life decade with PV being the predominant form.

Clinical diagnoses mainly rely on the clinical and histological appearance. However, to exclude clinical similar phenotypes like Hailey-Hailey's disease or Impetigo bullosa, autoantibody profiling is essential for a precise diagnosis. Pemphigus autoantibodies normally belong to the IgG₄ subclass (Futei et al., 2001) and are targeted against desmocadherins. PF is usually characterized by an autoantibody profile including IgG directed against Dsg1 but not Dsg3. Autoantibodies against Dsg3, but not to Dsg1, are present in patients with mucosal dominant PV. In PV patients afflicted with both mucous membrane and skin blisters, IgG to both Dsg3 and Dsg1 are mostly detected.

Several decades ago, pemphigus was a life-threatening disease. With the discovery and application of immunomodulatory drugs the situation of pemphigus patients improved. Often, patients are treated with high doses of glucocorticoids or cytostatic drugs to suppress inflammation and immune reactions. Additional treatments include plasmapheresis or injection of high doses of IgG (Jessop and Khumalo, 2008). Recently, monoclonal CD20 antibody rituximab was used to deplete B-cells in otherwise refractory patients. This might turn out to become an effective though expensive therapy (Joly et al., 2007). Nevertheless, pemphigus patients still suffer from high morbidity and social impairments. Specific treatments aimed to the main causes of pemphigus disease are missing. Therefore, specific treatments of the main causes of the disease still need to be developed.

2.6.1.1.1 Induction of pemphigus by pathogenic Dsg autoantibodies

1964, Beutner et al. identified antibodies in pemphigus erosions (Beutner and Jordon, 1964). Some years later, the pathogenicity of these autoantibodies was clearly demonstrated by passively transferring purified IgG fractions of pemphigus patients into neonatal mouse skin (Anhalt et al., 1982). The mice developed skin blisters with identical histology as seen in PV or PF. In the following years, autoantibodies were characterized to bind to a 160 kDa antigen in PF and a 130 kDa antigen in PV, which were later identified as Dsg1 and Dsg3, respectively (Stanley et al., 1986; Amagai et al., 1991). In later follow-up studies, experimental Dsg1 and Dsg3 antibodies were shown to provoke blister formation in mice and blister formation was prevented by antigen absorption of these antibodies (Amagai et al., 1994). In recent years, the group of Amagai provided convincing evidence for pathogenicity of autoantibodies in an active disease model of mice (Amagai et al., 2000b). After injecting recombinant Dsg3 into Dsg3 knockout mice, the animals developed anti-Dsg3 antibodies. Then, B-cells of these mice were isolated and adoptively transferred into immunodeficient but Dsg3-expressing mice. These again produced anti-Dsg3 antibodies, which potently induced pemphigus phenotypes. In contrast to a plethora of studies in which pathogenicity of Dsg autoantibodies was clearly demonstrated there is, however, evidence supporting the hypothesis that in pemphigus patients autoantibodies may occur that are directed to other targets including cholinergic receptors (Nguyen et al., 2000a), pemphaxin (Nguyen et al., 2000b) or E-cadherin (Evangelista et al., 2006; Evangelista et al., 2008). These autoantibodies might also contribute to skin blistering. In addition, pathogenic non-autoantibody factors in pemphigus patients' sera such as Fas ligand are discussed (Puviani et al., 2003). Whether these different autoantibodies or factors are pathogenic or just represent an epiphenomenon secondary to acantholysis is a matter of debate (Nguyen et al., 2000c; Amagai et al., 2006). Genetic variants important for pemphigus pathogenesis have been reported for HLA subtypes (Tron et al., 2005) but not for mutations in Dsg molecules (Capon et al., 2009).

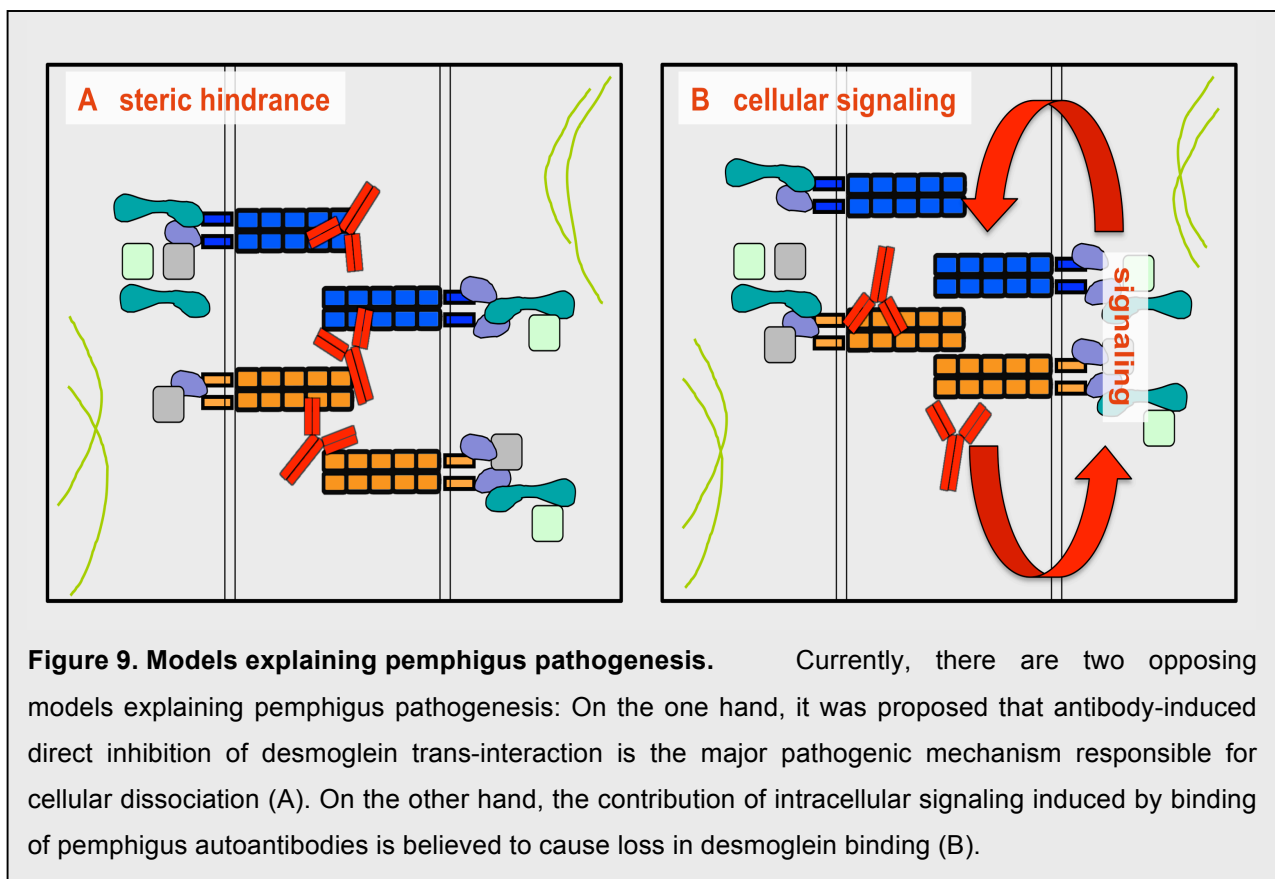


Figure 9. Models explaining pemphigus pathogenesis. Currently, there are two opposing models explaining pemphigus pathogenesis: On the one hand, it was proposed that antibody-induced direct inhibition of desmoglein trans-interaction is the major pathogenic mechanism responsible for cellular dissociation (A). On the other hand, the contribution of intracellular signaling induced by binding of pemphigus autoantibodies is believed to cause loss in desmoglein binding (B).

2.6.1.1.2 Steric hindrance and desmoglein compensation theory

The correlation between clinical phenotypes and the Dsg autoantibody profiles is widely accepted. However, there are also cases where the antibody profile against Dsg1 and 3 in PV does not strictly correlate with clinical phenotypes. Because Dsg3 was found to be the target antigen of PV autoantibodies and to be a cadherin-type adhesion molecule, it was suggestive to believe that Dsg3 antibodies could directly interfere with Dsg3 trans-interaction (Figure 9A). In PV and PF, Dsg autoantibodies are also primarily directed against desmocadherin EC1 domains (Amagai et al., 1992; Sekiguchi et al., 2001; Yokouchi et al., 2009), which are known to be essential for cadherin interaction (as discussed above). Also, it has been reported that AK 23, a monoclonal antibody generated in the active pemphigus mouse model and binding to the aminoterminal EC1 domain, is pathogenic (Tsunoda et al., 2003). In contrast, antibodies against the middle portion or the juxtamembrane part of the Dsg3 EC domain had no pathogenic effect. These data supported the view that pathogenic PV-IgG could interrupt Dsg3 trans-interaction. Together with this concept of steric hindrance, the desmoglein compensation theory was proposed trying to explain clinical and histological phenotypes of certain pemphigus subtypes. It states that Dsg1 and Dsg3 can functionally compensate each other in epidermal adhesion. In the non cornified multilayered epithelium of mucosal layers, Dsg3 is the predominant form whereas Dsg1 is only poorly expressed. Therefore Dsg3 autoantibodies are often found associated with oral blisters. Since Dsg3 is mainly expressed in basal layers of

both the epidermis and mucosal layers, blisters develop preferentially suprabasally. In mucocutaneous PV forms, typically both Dsg3 and Dsg1 autoantibodies are present in affected patients, which in addition to mucosal blistering also have epidermal blisters because both Dsg1 and Dsg3 are targeted and no longer can compensate each other. In PF, which is characterized by the presence of Dsg1 antibodies, epidermal adhesion is selectively disturbed in superficial layers, where Dsg1 is predominantly expressed and Dsg3 is mainly lacking. This is true for apical layers like stratum superficiale. Here, low Dsg3 expression is not able to compensate for the loss of Dsg1 function so that the blisters mainly appear superficially. Diseases involving bacterial toxins corroborated the desmoglein compensation theory because in staphylococcus scaled skin syndrome, where exfoliative toxin A/B extracellularly cleave Dsg1, superficial skin splitting occurs (Amagai et al., 2000a). In pregnant women with PF, neonates usually do not develop the disease although autoantibodies are crossing the placental borders. This phenomenon was explained by compensation with strong expression of Dsg3 in all layers in neonatal epidermis (Wu et al., 2000). Targeted disruption of Dsg3 in mice also caused a similar but not identical PV phenotype (Koch et al., 1997). Nevertheless, due to some inaccurate assumptions of Dsg expression profiles in humans, the compensation theory cannot explain all features of pemphigus histologies (Mahoney et al., 1999; Spindler et al., 2007). Moreover, involvement of other desmocadherin molecules like desmocollin 3 in pemphigus pathogenesis may be relevant (Chen et al., 2008; Spindler et al., 2009). The compensation theory therefore represents a simplified but straightforward explanation for pemphigus pathogenesis but lacks to include recent molecular findings, which also involve cellular signaling in pemphigus.

2.6.1.1.3 Cellular signaling in pemphigus

There is an ongoing debate whether acantholysis - the cellular hallmark of pemphigus pathogenicity, i.e. cell-cell dissociation – can be induced by other mechanism than steric hindrance (Figure 9B). The involvement of other mechanisms such as cellular signaling or Dsg endocytosis triggered by Dsg or non-Dsg autoantibodies has been reported. At least for PF, cellular signaling seems to be important because it was demonstrated that PF-IgG caused keratinocyte dissociation and loss of Dsg1 trans-interaction without directly blocking Dsg1 trans-interaction (Waschke et al., 2005), indicating that direct inhibition of Dsg trans-interaction may not be relevant for PF pathogenesis.

Over the past several years, the contribution of certain signaling pathways to the pemphigus pathogenesis has been studied: since the first discovery of PV-IgG-induced signaling by the group of Kitajima in the mid 90s, the involvement of other molecules is known, ranging from proteases [urokinase-type plasminogen activator (Morioka et al., 1987; Esaki et al., 1995) and matrix metalloproteinase 9 (Cirillo et al., 2007)], receptors [epidermal growth factor receptor (EGFR) (Frusic-Zlotkin et al., 2006; Chernyavsky et al., 2007), Fas ligand (Puviani et al.,

2003)], proteins involved in apoptosis [caspases (Frusic-Zlotkin et al., 2006; Schmidt and Waschke, 2009)] or desmosomal adapter proteins [plakoglobin (Caldelari et al., 2001; de Bruin et al., 2007), RhoA (Waschke et al., 2006) and p120^{ctn} (Kawasaki et al., 2006; Chernyavsky et al., 2008)] to kinases [protein kinase C (PKC) (Kitajima et al., 1999), p38 mitogen-activated protein kinase (p38MAPK) (Berkowitz et al., 2005; Berkowitz et al., 2006; Berkowitz et al., 2008a; Berkowitz et al., 2008b; Lee et al., 2009), c-Src (Chernyavsky et al., 2007) and cyclin-dependent kinase 2 (Cdk2) (Lanza et al., 2008)] and transcription factors [c-Myc (Williamson et al., 2006)] or other enzymes [nitric oxide synthase (NOS) (Marquina et al., 2008)]. However, although blocking of single signaling steps seems to be effective in preventing PV-IgG-mediated acantholysis in vitro and in vivo (Sanchez-Carpintero et al., 2004), the mechanisms involved in desmocadherin-mediated outside-in signaling as well as the interplay of various pemphigus signaling pathways leading to acantholysis remain unclear.

Other important hallmarks in pemphigus are disruption of desmosome assembly (Mao et al., 2009) and loss of desmosomal contacts, which is accompanied with endocytosis of Dsg molecules (Aoyama and Kitajima, 1999; Calkins et al., 2006; Delva et al., 2008) and “cytokeratin retraction” (Wilgram et al., 1961; Wilgram et al., 1964). The latter describes the phenomenon that cytokeratin filaments disappear from cell borders in acantholytic keratinocytes and accumulate perinuclearly.

Obviously, it could be stated that pemphigus is a simple disease with the pathogenic mechanism clearly identified. Nevertheless, explanations for pathogenic cell dissociation, which could finally lead to the identification of specific therapeutic interventions are difficult. Furthermore, pathologic processes in pemphigus are hard to identify because of the partly unknown physiological functions of desmocadherins and desmosomes in general.

2.6.1.2 Vascular inflammation

Endothelial cells form a single cell sheet lining the inner surface of blood vessels. VE-cadherin is the predominant cadherin expressed in these cells and essential for stabilizing endothelial cell-cell contacts. In contrast to VE-cadherin, N-cadherin is diffusely distributed in the plasma membrane of endothelial cells. VE-cadherin is only weakly or not at all expressed in other cells (Boda-Heggemann et al., 2009). With its adhesive functions it is an essential component of the barrier between blood and surrounding tissues, termed endothelial barrier (Figure 1) (Dejana et al., 2008; Vandenbroucke et al., 2008). Together with sealing functions of TJs and nectin-based connections, VE-cadherin-specific AJs are important for both maintenance and regulation of endothelial permeability.

In several pathological processes, loss of VE-cadherin function has been demonstrated (Corada et al., 1999; Hordijk et al., 1999; Alexander and Elrod, 2002). In septic conditions, when bacteria invade the bloodstream, infections cause inflammatory processes that involve

leakage of the blood vessel lining and consequently lead to life-threatening organ swellings or tissue bleedings. VE-cadherin was found to be one of the molecules targeted by several inflammatory mediators such as vascular endothelial growth factor (VEGF), histamine, thrombin and tumor necrosis factor- α (TNF- α) (Rabiet et al., 1994; Rabiet et al., 1996; Andriopoulou et al., 1999; Nwariaku et al., 2002; Konstantoulaki et al., 2003; Angelini et al., 2006). The impact of loss of VE-cadherin function was clearly demonstrated in vivo where vascular permeability was increased after application of the VE-cadherin-specific monoclonal antibody (mAb) 11D4.1 (Corada et al., 1999). VE-cadherin is not only extracellularly targeted, but often the intracellular cytoskeletal anchorage or the phosphorylation status regulate its function. Actin depolymerization or MLCK activation quickly result in loss of VE-cadherin-mediated adhesion and endothelial gap formation. More specific knowledge of (VE-)cadherin-mediated interactions might open perspectives for specific pharmacological modulation of VE-cadherin function and consequently be a promising way for the treatment of vascular leakage.

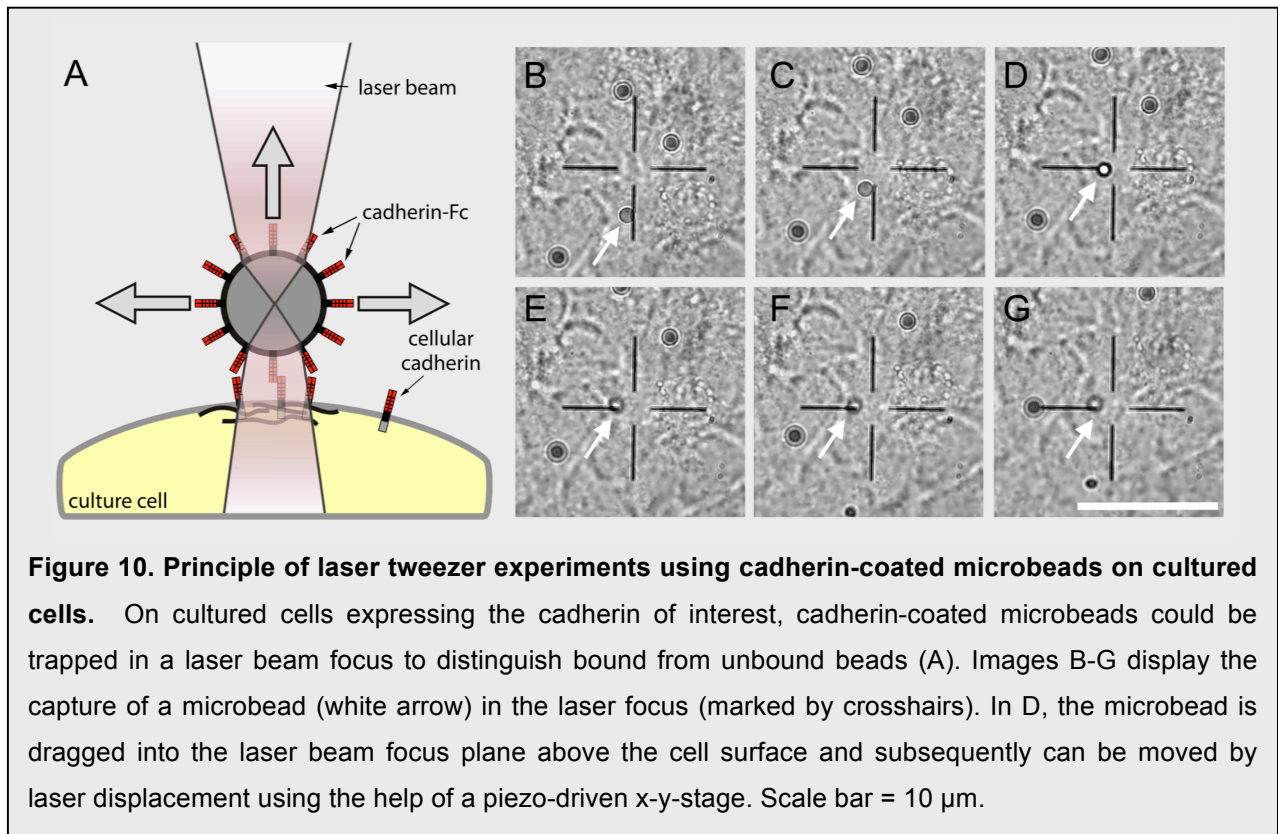
2.7 Aim of this study

The exact mechanism of cadherin trans-interaction is still a matter of debate. Multiple models have been proposed and many experimental approaches exist; however, most of them lack physiological proof of principle, mostly by investigating cadherins outside their physiological environment. In the present cumulative dissertation, experimental approaches to characterize and modulate cadherin functions should be performed in the (patho-) physiological contexts of the epidermal skin blistering disease pemphigus affecting desmocadherins and endothelial dysfunction involving VE-cadherin. The aims of the different studies were as follows:

2.7.1 Characterization of cadherin trans-interactions

Cadherin interaction should be characterized in both cell-free and cell-based conditions. By using AFM force spectroscopy as a biophysical single molecule technique (Figure 6), cadherin function could be investigated in conditions, where contributions of intracellular signaling were excluded. These experiments were compared and combined with cell-based experiments. For example, the adhesion of cadherin-coated beads to the cell surface of epidermal or endothelial should be analyzed by laser tweezer experiments (Figure 10). These experimental approaches allowed us to identify and to differentiate between modulations of cadherin function, which depend on the cellular environment, as compared to mainly biophysical or mechanistic properties of cadherins.

In detail, cell-free AFM experiments using desmocadherin fusion constructs were applied to clarify the mode of trans-interactions of these cadherins. Homophilic and heterophilic Dsg3 interactions were to be characterized and compared to Dsg1 interactions, as both are



important in pemphigus pathogenesis. Moreover, we aimed to investigate the effects of pemphigus autoantibody on these interactions to gain insights into pemphigus pathogenesis. For VE-cadherin, several fusion constructs involving a new protein linkage system (SNAP-tag) for AFM experiments were developed aiming to get insights into the difference between the molecular adhesion of cadherin monomers vs. dimers.

2.7.2 Investigation of cadherin-mediated signaling

Pemphigus is a promising model disease to study consequences of loss of (desmo)cadherin-mediated binding. By using pathogenic pemphigus autoantibodies, cadherin-mediated outside-in signaling should be investigated. Especially, we aimed to investigate the cross-talk of epidermal growth factor receptor (EGFR) with Dsgs and its contribution to pemphigus pathogenesis. However, although blocking of single signaling steps seems to be effective in preventing PV-IgG-mediated acantholysis *in vitro* (Sanchez-Carpintero et al., 2004) and *in vivo*, integrative studies investigating the interplay of these pathways are lacking. With the help of those studies, however, the identification of upstream key networks should be possible. We therefore also sought to further clarify the role of cellular signaling in pemphigus in this study.

2.7.3 Modulation of cadherin function by peptides

Based on the insights gained in the first part of the study, an approach to modulate cadherin function was developed: we aimed to identify peptides targeting cadherin adhesive sequences, which should either inhibit or promote cadherin interactions. Since crystal structures of the

target cadherins Dsg3/1 and VE-cadherin were missing, cadherin monomeric structures had to be rendered by modeling the sequences into already resolved cadherin structures (i.e. E-cadherin). Cadherin interactions of the resulting structures then had to be modeled based on known schemes found in N-cadherin crystals (see section 2.4.2.2). By determining amino acid sequences that apparently were important for these interactions we aimed to identify antagonistic peptides (“single peptides”) that could be used as specific inhibitors of the respective cadherin’s interaction. In a further step, we sought to generate agonistic peptides (“tandem peptides”) that promote cadherin interaction by combining two of these single peptides via a flexible linker. Based on our hypothesis these tandem peptides should stabilize cadherin interactions by simultaneously binding to adhesive sequences of two neighboring cadherin molecules. We aimed to use such peptides as specific modulators of cadherin interactions.

As the main focus of this study laid on the pathological conditions pemphigus and vascular leakage, such peptides should be developed for desmocadherins Dsg1 / Dsg3 and VE-cadherin. The functions of these peptides had to be tested in cell-free single molecule experiments as well as in several in-vitro and also in-vivo systems. Ultimately, the different types of tandem peptides were intended to act as potential therapeutic reagents preventing desmocadherin-mediated cell dissociation in pemphigus and loss of VE-cadherin-based adhesion in vascular dysfunction.

3 Scientific publications and additional results

3.1 Scientific publications

3.1.1 Publication 1: Pemphigus vulgaris IgG directly inhibit desmoglein 3-mediated transinteraction

Heupel WM, Zillikens D, Drenckhahn D, Waschke J

Pemphigus vulgaris IgG directly inhibit desmoglein 3-mediated trans-interaction

J Immunol. 2008;181:1825-1834.

Reproduced / adapted with permission by the Journal of Immunology. Copyright 2008. The American Association of Immunologists, Inc.

URL: <http://www.jimmunol.org/cgi/content/full/181/3/1825>

Pemphigus Vulgaris IgG Directly Inhibit Desmoglein 3-Mediated Transinteraction¹

Wolfgang-Moritz Heupel,* Detlef Zillikens,[†] Detlev Drenckhahn,^{2*} and Jens Waschke^{2*}

The autoimmune blistering skin disease pemphigus is caused by autoantibodies against keratinocyte surface Ags. In pemphigus vulgaris (PV), autoantibodies are primarily directed against desmosomal cadherins desmoglein (Dsg) 3 and Dsg 1, whereas pemphigus foliaceus (PF) patients only have Abs against Dsg 1. At present, it is unclear whether Dsg autoantibodies contribute to pemphigus pathogenesis by direct inhibition of Dsg transinteraction. Using atomic force microscopy, we provide evidence that PV-IgG directly interfere with homophilic Dsg 3 but, similar to PF-IgG, not with homophilic Dsg 1 transinteraction, indicating that the molecular mechanisms in PV and PF pathogenesis substantially differ. PV-IgG (containing Dsg 3 or Dsg 1 and Dsg 3 autoantibodies) as well as PV-IgG Fab reduced binding activity of Dsg 3 by ~60%, comparable to Ca²⁺ depletion. Similarly, the mouse monoclonal PV Ab AK 23 targeting the N-terminal Dsg 3 domain and AK 23 Fab reduced Dsg 3 transinteraction. In contrast, neither PV-IgG nor PF-IgG blocked Dsg 1 transinteraction. In HaCaT monolayers, however, both PV- and PF-IgG caused keratinocyte dissociation as well as loss of Dsg 1 and Dsg 3 transinteraction as revealed by laser tweezer assay. These data demonstrate that PV-IgG and PF-IgG reduce Dsg transinteraction by cell-dependent mechanisms and suggest that in addition, Abs to Dsg 3 contribute to PV by direct inhibition of Dsg transinteraction. *The Journal of Immunology*, 2008, 181: 1825–1834.

Pemphigus is a severe autoimmune blistering skin disease (1, 2) caused by autoantibodies against keratinocyte surface Ags (3–5). It has been demonstrated that pathogenic pemphigus autoantibodies are directed to the cadherin-type adhesion molecules desmoglein (Dsg)³ 1 and 3 (6–9). However, at present, there is evidence supporting the hypothesis that autoantibodies against other targets including cholinergic receptors or pemphaxin also contribute to skin blistering (10–12). Whether these different autoantibodies are pathogenic or just represent an epiphenomenon secondary to acantholysis is a matter of serious debate (13–15). It is widely accepted that there is a correlation between the clinical phenotype and the profile of Dsg autoantibodies (1, 2). Pemphigus foliaceus (PF) is usually characterized by epidermal blistering without development of mucosal erosions and an autoantibody profile including IgG directed to Dsg 1 but not to Dsg 3 (2, 16). Autoantibodies to Dsg 3, but not to Dsg 1, are usually present in patients with mucosal dominant pemphigus vulgaris (PV) (16, 17). In (PV) patients showing both mucous membrane and skin involvement, Abs to both Dsg 3 and Dsg 1 may be detected (2, 16, 17). However, there are also cases where the Ab

profile against Dsg 1 and 3 in PV does not strictly correlate with these clinical phenotypes (18, 19). At present, direct evidence that the presence of Dsg 3-specific Abs in PV but not in PF may account for the more severe clinical phenotype of PV compared with PF patients is lacking.

Because Dsg 3 was found to be the target Ag of PV autoantibodies and to be a cadherin-type adhesion molecule, it was suggestive to believe that Dsg 3 Abs could directly interfere with Dsg 3 transinteraction (6). To test this hypothesis, some progress has been achieved by establishing mouse monoclonal Dsg 3 Abs, which are well characterized regarding the Dsg 3 extracellular subdomain they are directed to (20). It has been reported that AK 23, targeting the N-terminal extracellular domain 1 (EC 1) of Dsg 3, where the predicted adhesive interface is located (21, 22), is pathogenic. In contrast, Abs against the middle portion or the juxtamembrane part of the extracellular Dsg 3 domain had no effect (20). These data suggested that AK 23 could directly interfere with Dsg 3 transinteraction. This would be relevant because Abs to Dsg 1 and Dsg 3 in PV and PF patients are also primarily directed against the EC 1 subdomain (23). However, we found that PF-IgG caused keratinocyte dissociation and loss of Dsg 1 transinteraction without directly blocking Dsg 1 transinteraction, indicating that direct inhibition of Dsg transinteraction is not essential for PF pathogenesis and that Abs targeting the EC 1 subdomain do not necessarily induce direct inhibition (24). Taken together, evidence that Dsg 3 autoantibodies contribute to PV pathogenesis by directly blocking Dsg 3 transinteraction is lacking.

Therefore, the aim of the present study was to clarify whether Abs to Dsg 1 and Dsg 3 from PV patients reduced Dsg transinteraction by cellular signaling mechanisms or directly interfered with Dsg transinteraction. We used single-molecule atomic force microscopy (AFM) which allowed us to study Dsg transinteraction in a cell-free system and thus to rule out the contribution of any cellular signaling pathways. In contrast, we combined this approach with laser tweezer studies testing the binding of microbeads coated with human Dsg 1 and Dsg 3 to the surface of human HaCaT keratinocytes, thereby evaluating the contribution of cellular mechanisms to the effects of pemphigus IgG.

*Department of Anatomy and Cell Biology, University of Würzburg, Würzburg, Germany; and [†]Department of Dermatology, University of Lübeck, Lübeck, Germany

Received for publication February 20, 2008. Accepted for publication May 28, 2008.

The costs of publication of this article were defrayed in part by the payment of page charges. This article must therefore be hereby marked *advertisement* in accordance with 18 U.S.C. Section 1734 solely to indicate this fact.

¹This work was supported by grants from the Deutsche Forschungsgemeinschaft (SFB 487, TP B5) and the Interdisziplinäres Zentrum für Klinische Forschung Würzburg (TP A-51).

²Address correspondence and reprint requests to Dr. Jens Waschke and Dr. Detlev Drenckhahn, Institute of Anatomy and Cell Biology, Julius-Maximilians-University, Koellikerstrasse 6, D-97070 Würzburg, Germany. E-mail addresses: jens.waschke@mail.uni-wuerzburg.de and anato75@mail.uni-wuerzburg.de

³Abbreviations used in this paper: Dsg, desmoglein; PF, pemphigus foliaceus; PV, pemphigus vulgaris; EC, extracellular domain; AFM, atomic force microscopy; ETA, exfoliative toxin A; RT, room temperature; PEG, polyethylene glycol; Dsc, desmocollin; VE, vascular endothelial.

1826

DIRECT INHIBITION OF Dsg TRANSINTERACTION IN PEMPHIGUS

Table I. Ab profile of pemphigus patients' IgG

ELISA	Dsg 1 (U/ml)	Dsg 3 (U/ml)
PV-IgG 1	535	1098
PV-IgG 2	280	685
PV-IgG 3		1177
PV-IgG 4		699
PF-IgG 1	95	
PF-IgG 2	7041	

Materials and Methods

Cell culture and test reagents

The immortalized human keratinocyte cell line HaCaT was grown in DMEM (Invitrogen Life Technologies) including 1.8 mM Ca^{2+} which was supplemented with 50 U/ml penicillin G, 50 μg of streptomycin, and 10% FCS (Biocrom) in a humidified atmosphere (95% air/5% CO_2) at 37°C. The cultures were used for all experiments when grown to confluent monolayers and Dsg 1 expression was detected by dot-blot analysis as well as immunostaining, which was the case on day 7 after plating. Under these conditions, formation of desmosomes was regularly detected by electron microscopy (24). Monoclonal mouse PV Abs AK 23, AK 18, and AK 9 were purchased from Biozol and used at 75 or 160 $\mu\text{g}/\text{ml}$ for experiments. Monoclonal mouse Ab directed against the extracellular domain of Dsg 1 (aDsg 1) was purchased from Progen Industries (clone p124) and used at a 1/20 dilution.

Purification and preparation of patients' IgG

Purification was performed as described previously (24). Sera from two PF patients, two patients suffering from a mucocutaneous form of PV, and two patients with mucous PV whose diagnoses were confirmed clinically, histologically, and serologically and from a volunteer without any skin disease (control IgG) were used for the present study. Patients' sera were tested by ELISA for reactivity against Dsg 1 and Dsg 3, respectively (Table I). IgG fractions PF-IgG 1 and 2 contained Dsg 1 Abs but no Dsg 3 Abs, whereas PV-IgG 1 and 2 contained both Dsg 1 and Dsg 3 Abs. PV-IgG 3 and 4 contained Dsg 3 but not Dsg 1 autoantibodies. IgG fractions were purified by affinity chromatography using protein A agarose. In preliminary experiments, we determined the concentrations of patients' IgG that had maximal effects on Dsg-binding activities in AFM experiments. Afterward, final concentrations of IgG fractions were adjusted to 150–500 $\mu\text{g}/\text{ml}$ for all experiments. For some experiments, three different PF-IgG from additional PF patients were pooled, all of which were tested positive for Dsg 1 and negative for Dsg 3 (data not shown). Preparation of Fab was performed as described previously (24). PV-IgG Fab were generated by papain digestion of PV-IgG 3, PF-IgG Fab by digestion of PF-IgG 1. PV- and PF-IgG Fab were used at concentrations adjusted to IgG fractions (150–500 $\mu\text{g}/\text{ml}$).

Recombinant Dsg 1-Fc, Dsg 3-Fc, and vascular endothelial (VE)-cadherin-Fc

Expression and purification of rFc constructs of human Dsg 3, Dsg 1, and mouse VE-cadherin were performed as described for Dsg 1 (24) using protein A agarose affinity chromatography. For additional experiments, Dsg 1—also containing a hexahistidine tag (his-tag)—was purified using Ni-NTA agarose chromatography according to the manufacturer's protocol (Roche). The protein was eluted by imidazole buffer (200 mM imidazole, 1 M NaCl, 10 mM NaH_2PO_4 (pH 8)) and was immediately subjected to buffer exchange against HBSS via PD-10 desalting columns (GE Healthcare). Dsg 1 was cleaved by exfoliative toxin A (ETA; provided by M. Amagai, Keio Medical School, Tokyo, Japan). Dsg 3 but not Dsg 1 was precipitated by the Dsg 3-specific mouse mAb AK 23 (data not shown).

Fluorescent detection of Ca^{2+} binding with quin-2

Binding of Ca^{2+} to chimeric Dsg proteins was detected using the fluorescent Ca^{2+} indicator quin-2 (25). Briefly, Dsg 1, Dsg 3, or BSA was transferred to polyvinylidene difluoride membranes using vacuum aspiration. The membranes were washed with solution AQ (60 mM KCl, 5 mM MgCl_2 , and 10 mM imidazole-HCl buffer (pH 6.8)) additionally containing 1 mM CaCl_2 for 20 min at room temperature (RT), followed by a 1-h incubation at RT in solution AQ containing 1 mM quin-2. After washing with buffer AQ for 5 min, membranes were dried, finally illuminated with UV light, and photographed through a green filter.

Depletion of Dsg autoantibodies from pemphigus IgG

Pemphigus IgG were depleted of Dsg autoantibodies by immobilization of chimeric Dsg proteins using Talon dynabeads (Invitrogen) as previously reported for Dsg 1 (24). A total of 50 μg of each Dsg 1 and Dsg 3 were incubated with 5-mg beads in 200 μl of HBSS for 0.5 h at RT and slow overhead rotation. The supernatant was discharged and proteins were bound to beads were washed three times with HBSS (200 μl) using a magnetic tube holder. To absorb Dsg autoantibodies, PV-IgG 3 (200 μl containing 0.6 mg IgG) were applied to the beads and incubated for 0.5 h at RT and slow overhead rotation. The supernatant containing the Dsg IgG-depleted IgG fraction (PV-IgG 3 Abs) was finally collected and used for additional experiments. Generation of PF-IgG 1 Abs depleted of Dsg 1 autoantibodies was achieved similarly by incubation of PF-IgG 1 with Dsg 1 immobilized on Talon beads. PV- and PF-IgG Abs were used at 200 $\mu\text{g}/\text{ml}$.

Cytochemistry

HaCaT cells were grown on coverslips to confluence (7 days) and incubated with pemphigus IgG or mAbs for 24 h at 37°C. After incubation with autoantibodies, culture medium was removed and monolayers were fixed for 10 min at RT with 2% formaldehyde (freshly prepared from paraformaldehyde) in PBS. Afterward, monolayers were treated with 0.1% Triton X-100 in PBS for 5 min at RT. After rinsing with PBS at RT, HaCaT cells were preincubated for 30 min with 10% normal goat serum and 1% BSA in PBS at RT and incubated for 16 h at 4°C with mouse mAb directed to Dsg 3 (Zytomed) (dilution 1/100 in PBS). For experiments using mouse mAbs AK 23, AK 18, AK 9, or aDsg 1, a rabbit polyclonal Dsg 3 Ab was used (dilution 1/100 in PBS; Santa Cruz Biotechnology). After several rinses with PBS (three washes for 5 min each), monolayers were incubated for 60 min at RT with Cy3-labeled goat anti-mouse or goat-anti-rabbit IgG (Dianova). Cells were then rinsed with PBS (three washes for 5 min each). Finally, coverslips were mounted on glass slides with 60% glycerol in PBS, containing 1.5% *N*-propyl gallate (Serva) as antifading compound. Monolayers were examined using a LSM 510 (Zeiss). Images were processed using Adobe Photoshop 7.0 software (Adobe Systems).

AFM measurements

Homophilic transinteractions of Dsg 1 and Dsg 3 were characterized by force-distance measurements of Dsg 1 or Dsg 3 coupled via flexible linkers to the tip and substrate of a Bioscope AFM driven by a Nanoscope III controller (Digital Instruments). Dsg 1 or 3 was linked covalently to the Si_3N_4 tip of the cantilever (Veeco Instruments) and freshly cleaved mica plates (SPI Supplies) using polyethylene glycol (PEG) spacers containing an amino-reactive cross-linker group (*N*-hydroxysuccinimide ester) at one end and a thiol-reactive group (2-[pyridyl]dithio) propionate) at the other end, as described previously in detail (26). The *N*-hydroxysuccinimide group served to link PEG to free amino acid groups at both the Si_3N_4 tip and mica, introduced by treatment of tip and mica with 2-aminoethanol HCl (Sigma-Aldrich). Binding events were measured in buffer A (140 mM NaCl, 10 mM HEPES, 5 mM CaCl_2) by force-distance cycles at amplitudes of 500 nm and at 2 Hz frequency. " Ca^{2+} -free conditions" (no Ca^{2+}) were defined as buffer A without addition of CaCl_2 . Force-distance cycles were performed at constant lateral positions and analyzed as described previously in detail (27). Binding activity was normalized to experiments using a cantilever not labeled with Dsg 1 or Dsg 3 to eliminate the contribution of unspecific interactions. For Dsg 1/3 heterophilic-binding analysis, heterophilic-binding activities of VE-cadherin-Fc with Dsg 1 or 3 were measured. These values were subtracted from heterophilic Dsg-binding activities before the latter were normalized to homophilic-binding activities of Dsg 1 or Dsg 3, respectively. For some experiments, both Dsg 1 and Dsg 3 at equal amounts were coated on mica or AFM tips.

Laser tweezer

Coating of polystyrene beads and the working principle of the laser tweezer set-up were described previously in detail (24). Coated beads (10 μl of stock solution) were suspended in 200 μl of culture medium and allowed to interact with HaCaT monolayers for 30 min at 37°C before measuring the number of bound beads (=control values). Beads were considered tightly bound when resisting laser displacement at 42 mW setting. For every condition, 100 beads were counted. Afterward, PV-IgG or PF-IgG were applied for 30 min. Percentage of beads resisting laser displacement under various experimental conditions was normalized to control values.

Electrophoresis and Western blotting

HaCaT cells grown for 1 or 7 days were dissolved in sample buffer, sonicated, heated at 95°C for 5 min, and finally subjected to SDS 7.5% PAGE

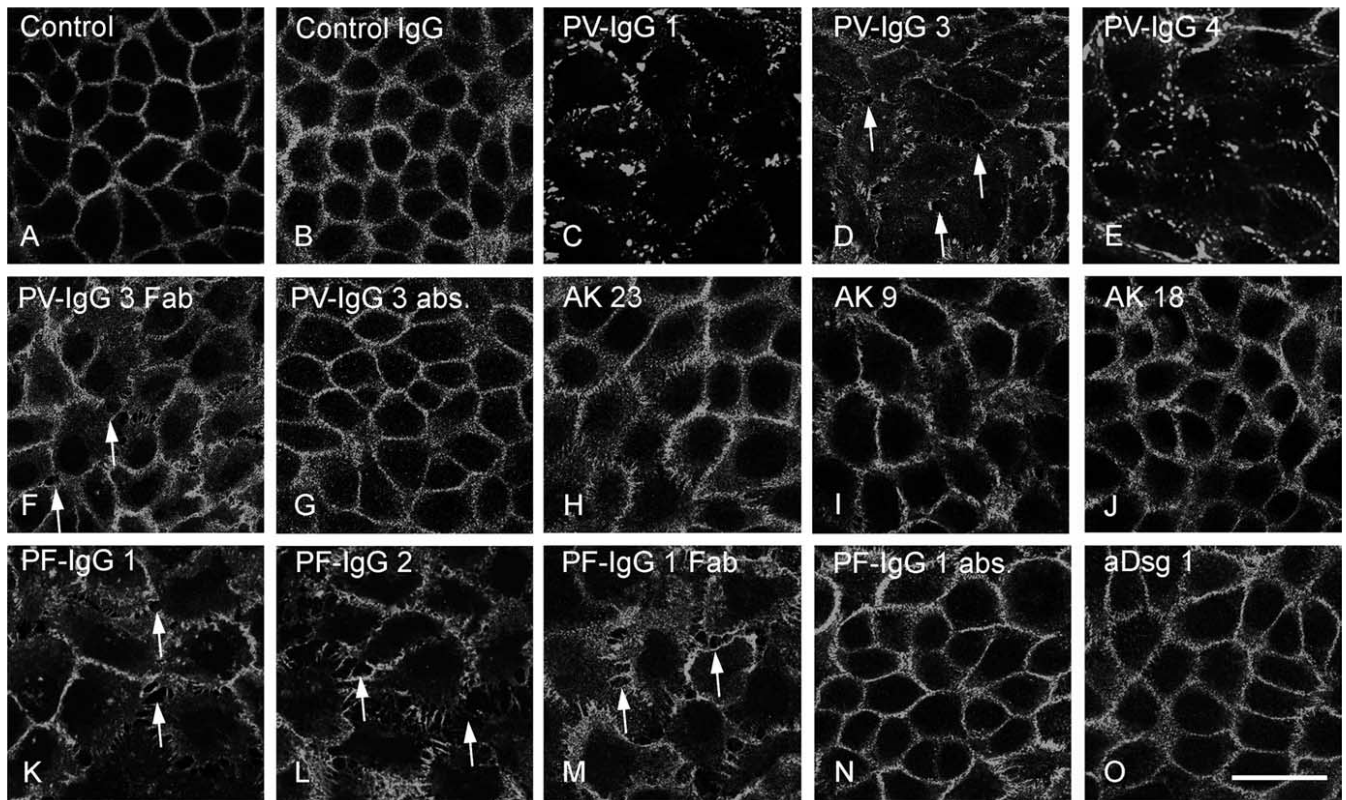


FIGURE 1. PV-IgG as well as PF-IgG induced cell-dissociation in cultured human keratinocytes (HaCaT). When grown to confluence, HaCaT cells were immunostained for Dsg 3. In control monolayers (medium only, *A*) or cells treated with control IgG for 24 h (*B*), Dsg 3 was continuously distributed along cell borders. Incubation with three different PV-IgG fractions (PV-IgG 1, 3, and 4) (*C–E*) resulted in disruption of Dsg 3 staining and intercellular gap formation (arrows in *D*). Fab of PV-IgG 3 were capable of inducing keratinocyte dissociation (arrows in *F*), whereas depletion of Dsg 1 and Dsg 3 Abs from PV-IgG (PV-IgG 3 Abs) abolished the effects of PV-IgG (*G*). Mouse mAb AK 23 disturbed continuous localization of Dsg 3 at cell borders whereas AK 9 and AK 18 had no effect (*H–J*). PF-IgG 1 and 2 as well as PF-IgG Fab caused intercellular gap formation (arrows in *K–M*), which were not seen in PF-IgG depleted of Dsg 1 IgG (PF-IgG 1 Abs, *N*). Note that the mouse mAb against Dsg 1 (aDsg 1) had no effect (*O*). Scale bar, 20 μm for all panels ($n = 5$).

and immunoblotting to Hybond nitrocellulose membranes (Amersham). Membranes were blocked with 5% low fat milk for 1 h at RT in PBS and incubated with anti-Dsg 1 (1/200; Progen) or anti-actin (1/3000; Sigma-Aldrich) primary Ab overnight at 4°C. As secondary Ab, HRP-labeled goat anti-mouse Ab (Dianova) was used. Visualization was achieved using the ECL technique (Amersham).

Statistics

Differences in bead adhesion or single-molecule transinteraction between different protocols have been assessed using the two-tailed Student *t* test. Values throughout are expressed as mean \pm SEM. Statistical significance is assumed for $p < 0.05$.

Results

PV-IgG as well as PF-IgG induced cell dissociation in cultured human keratinocytes (HaCaT)

IgG fractions of six different patients with clinically, histologically, and serologically verified pemphigus were used (Table 1). PV-IgG 1 and 2 contained autoantibodies against Dsg 1 and Dsg 3, whereas PV-IgG 3 and 4 contained Dsg 3-specific autoantibodies only. Abs to Dsg 1 but not to Dsg 3 were present in PF-IgG 1 and 2.

First, we studied the pathogenic effect of pemphigus IgG on cultured human keratinocytes (HaCaT; Fig. 1). Under control conditions or following treatment with IgG from a healthy volunteer (control IgG), Dsg 3 was continuously distributed along cellular junctions (Fig. 1, *A* and *B*). In contrast, PV-IgG treatment resulted in disruption of Dsg 3 staining. Cell dissociation leading to for-

mation of intercellular gaps (indicated by arrows in Fig. 1*D*) was observed and further substantiated using F-actin staining for all PV-IgG fractions used (data not shown)—comparable to our previous studies (28, 29) (Fig. 1, *C–E*). It is noteworthy that the effects of PV-IgG were similar independent of whether Dsg 1 Abs were present (PV-IgG 1) or not (PV-IgG 3 and 4). Gap formation was also observed (arrows) when Fab of PV-IgG were used, whereas the profound disruption of Dsg 3 staining was abolished (Fig. 1*F*). However, all pathogenic effects were eliminated by depletion of autoantibodies against Dsg 1 and 3 from PV-IgG using rDsg for immunoabsorption (Fig. 1*G*).

To further examine the effect of Dsg 3-specific PV Abs, we used three different mouse monoclonal PV Abs directed to well-characterized epitopes on the Dsg 3 extracellular domain (20). It has been shown that AK 23, which is directed against the Dsg 3 N-terminal EC 1, is pathogenic, whereas AK 18 directed against the middle part or AK 9 directed against the juxtamembrane part of the Dsg 3 extracellular domain are not. Consistent with these findings, when applied to HaCaT cells, AK 23 (75 $\mu\text{g}/\text{ml}$) disturbed Dsg 3 localization at cell junctions leading to linear streaks oriented perpendicular to cell borders. However, unlike PV-IgG from patients, AK 23 did not induce formation of large intercellular gaps or a pronounced loss of Dsg 3 staining. Because it has been demonstrated in keratinocyte cultures that AK 23 had dose-dependent effects up to 160 $\mu\text{g}/\text{ml}$ but not at higher concentrations (30), we used 160 $\mu\text{g}/\text{ml}$ AK 23 as well but with similar results (data not

1828

DIRECT INHIBITION OF Dsg TRANSINTERACTION IN PEMPHIGUS

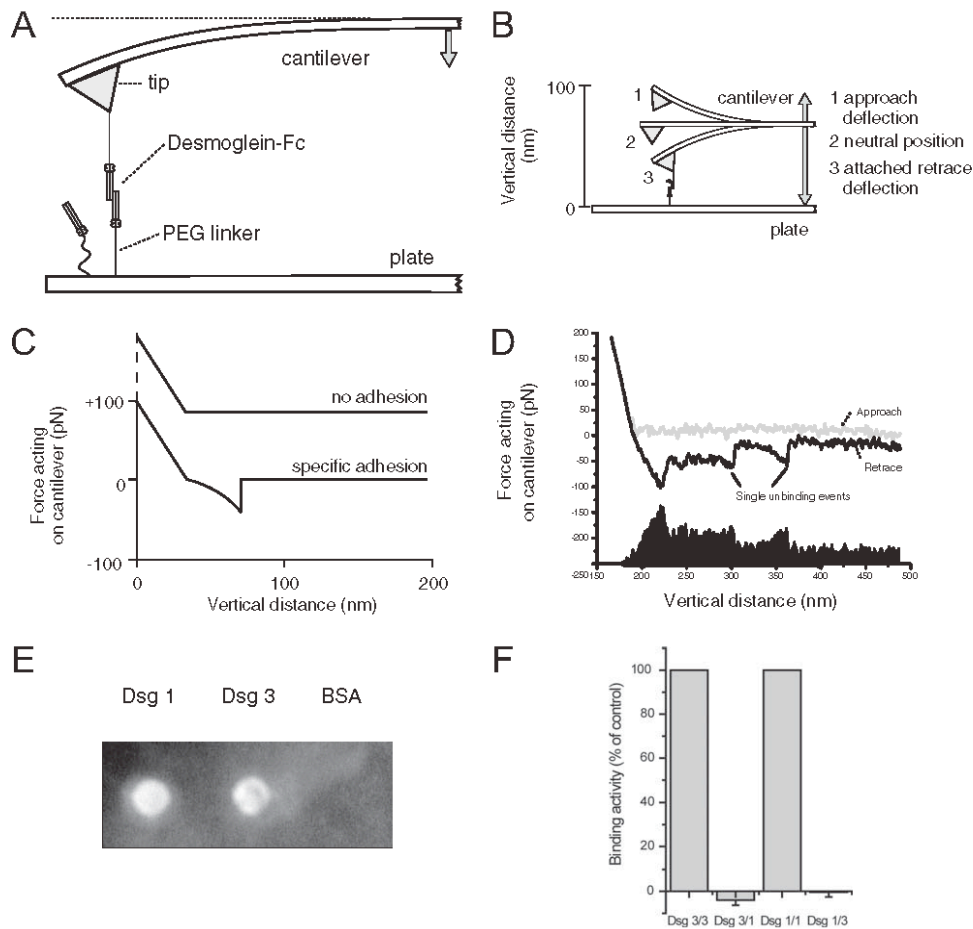


FIGURE 2. Determination of single-molecule binding activities by AFM studies and characterization of chimeric Dsg proteins. Binding activities of Dsg fusion proteins covalently coupled to the tip and plate of the AFM via flexible PEG-linker were monitored by force-distance cycles (A). Molecules were brought into contact by repeated downward (approach) and upward movement (retrace) of the AFM tip (B). During upward movement, a downward deflection of the cantilever occurred if plate- and tip-bound Dsg molecules underwent specific transinteractions (C). After reaching a critical force, the bond broke and the cantilever jumped back to the neutral position. In a sample force-distance plot, several unbinding events of Dsg-Fc molecules are shown (D). Determination of binding activity was done by subtracting approach from retrace curves and integrating the area between the resulting curves. Chimeric proteins Dsg 1 and Dsg 3 used in this study but not BSA bound Ca^{2+} as demonstrated with fluorescent Ca^{2+} indicator quin-2 (E). Compared with homophilic transinteraction (Dsg 3/3 and Dsg 1/1), no specific binding activity was detected for heterophilic transinteraction of Dsg 3 and Dsg 1 in AFM experiments, no matter if Dsg 3 was coupled to the tip (Dsg 3/1) or the plate (Dsg 1/3) of the setup (F).

shown). AK 9 and AK 18 had no effect (Fig. 1, H–J), even when applied at higher concentrations (data not shown).

PF-IgG 1 and 2 as well as PF-IgG Fab induced keratinocyte dissociation leading to formation of intercellular gaps (arrows in Fig. 1, K–M). However, in contrast to PV-IgG, Dsg 3 staining was only missing at gap margins indicating that Dsg 1 Abs were sufficient to cause keratinocyte dissociation whereas Dsg 3 Abs in PV-IgG were responsible for profound fragmentation of Dsg 3 immunostaining. These effects were abolished by depletion of Dsg 1 Abs from PF-IgG (Fig. 1N). A mouse mAb directed against the extracellular domain of Dsg 1 (aDsg 1) had no effect (Fig. 1O).

Determination of Dsg 3 and Dsg 1 single-molecule-binding activities by AFM

We previously used single-molecule AFM force spectroscopy to demonstrate that PF-IgG did not directly interfere with Dsg 1 transinteraction (24). To investigate whether Dsg autoantibodies in PV are pathogenic and whether these IgG would directly reduce the binding activity of Dsg 3 and Dsg 1 in a cell-free system, AFM force spectroscopy was applied as described in detail elsewhere (27). The general principle of this technique is illustrated in Fig. 2. Recombinant human Dsg 1-Fc or Dsg 3-Fc molecules were at-

tached to the tip and plate of the AFM setup (Fig. 2A). Coupling of Dsg molecules via flexible PEG linker allowed the molecules to freely diffuse within the radius of the length of the linker (~8 nm) and to undergo unimpaired encounter reactions. During measurements, the tip was brought into contact to the plate of the setup by cyclic upward and downward movements at 2 Hz frequency (force-distance cycles, Fig. 2B). During downward movement (approach), Dsg molecules bound to the tip and plate interacted leading to deflection of the cantilever in the following retrace movement. Specific single unbinding events were characterized by abrupt jumps of the cantilever toward the neutral position because of bond rupture (Fig. 2C). Due to coupling of several Dsg molecules to the AFM tip, unbinding events typically appeared successively displaying two to five single unbinding events as shown in Fig. 2D. The total area between approach and retrace curve was taken as a measure for binding activity as described previously (27). Approach-retrace cycles of 2000 nm/s and 0.1-s encounter time were performed in the presence or absence of Abs. As outlined above, PV- and PF-IgG, which were depleted from Dsg 1- and Dsg 3-specific autoantibodies by immunoabsorption against the rDsg 1 and rDsg 3 proteins, had no effect on keratinocyte cultures (Fig. 1, G and N). These data verify that the recombinant

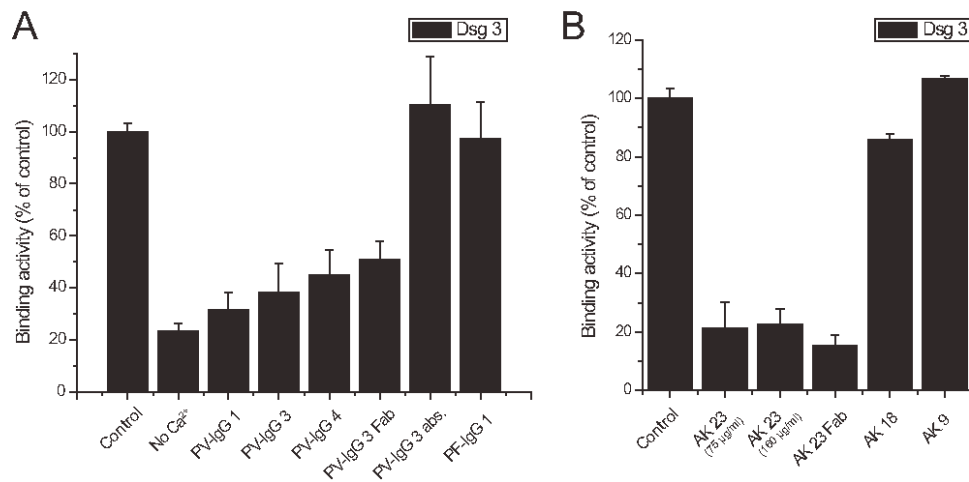


FIGURE 3. PV-IgG and AK 23 blocked Dsg 3 transinteraction in AFM experiments. *A*, Binding activities of Dsg 3 in the presence or absence of different pemphigus IgG were probed by AFM. Depletion of Ca²⁺ by using a Ca²⁺-free buffer (no Ca²⁺) significantly reduced Dsg 3-binding activity to 20%. PV-IgG 1, 3, and 4 reduced binding activity of Dsg 3 to 31, 38, and 44% of control values, respectively. PV-IgG Fab also significantly blocked transinteraction to 51%, whereas Dsg autoantibody-depleted PV-IgG had no effect. Moreover, PF-IgG 1 did not interfere with Dsg 3 transinteraction. ($n = 3-4$ for each condition). *B*, AK 23, directed against the N-terminal domain of Dsg 3, blocked Dsg 3 transinteraction when applied at 75 $\mu\text{g/ml}$, up to 160 $\mu\text{g/ml}$ or as monovalent Fab (21, 22, and 15% of control activity, respectively). AK 18 directed against the middle or AK 9 directed against the C terminus of the Dsg 3 extracellular domain had no effect ($n = 3-4$ for each condition).

proteins, which we used in the following to study Dsg transinteraction, retained the correct conformation during purification procedure (31, 32). This was supported by the ability of AK 23 to immunoprecipitate rDsg 3 (data not shown). In addition, Ca²⁺ binding of rDsg 1 and rDsg 3 was confirmed using the fluorescent Ca²⁺ indicator quin-2 (Fig. 2E).

To investigate whether rDsg 1-Fc and rDsg 3-Fc, in addition to homophilic, also undergo heterophilic transinteraction, we studied the transinteraction of Dsg 3-Fc coupled to the tip of the cantilever to Dsg 1-Fc molecules coupled to the plate (Dsg 3/1) and vice versa (Dsg 1/3) (Fig. 2F). As negative controls, we used experiments where transinteraction of Dsg 1 and Dsg 3 to VE-cadherin was probed. When these values were subtracted and heterophilic-binding activities were normalized to the levels of homophilic Dsg 3 and Dsg 1 transinteraction, heterophilic transinteraction of these two molecules was negligible. Therefore, in the following experiments, we focused on the effect of pemphigus IgG on homophilic Dsg 1 and 3 interactions.

PV-IgG and AK 23 blocked Dsg 3 transinteraction in cell-free AFM experiments

Dsg 3 transinteraction has so far not been probed by AFM single-molecule experiments. As illustrated from the single unbinding events in Fig. 2D, the resulting unit unbinding force of two transinteracting Dsg 3 molecules was in the range of 50 pN, which is comparable to the unbinding force of Dsg 1 (24) and other cadherins probed under same conditions (27). Moreover, we observed higher order unbinding events indicating additional mechanisms of interaction. Dsg 3 transinteractions were strongly Ca²⁺ dependent; Ca²⁺ depletion reduced Dsg 3-binding activity to 23 \pm 3% (Fig. 3A). Interestingly, for all Dsg 3 autoantibody-containing PV-IgG (PV-IgG 1, 3, and 4) a reduction of Dsg 3 transinteraction was detected to 31 \pm 7%, 38 \pm 11%, and 44 \pm 10% of controls, respectively (Fig. 3A). To investigate whether PV-IgG cross-linked Dsg 3 at the tip or the plate of the AFM setup and thereby prevented Dsg 3 transinteraction, PV-IgG Fab were used. However, PV-IgG Fab still reduced Dsg 3 transinteraction to 51 \pm 7%. Together with the finding that PV-IgG depleted of Dsg 3 Abs (PV-IgG 3 Abs) did not reduce Dsg 3 transinteraction (110 \pm 19%,

Fig. 3A), these data indicate that Dsg 3-specific autoantibodies in PV-IgG directly interfered with Dsg 3 transinteraction. Because in previous studies we showed that PF-IgG did not block Dsg 1 transinteraction (24), we further analyzed the effect of PF-IgG on Dsg 3 transinteraction. Not surprisingly, PF-IgG 1, which only included Dsg 1 autoantibodies, did not interfere with Dsg 3 transinteraction (97 \pm 14%, Fig. 3A).

Next, to investigate whether Dsg 3-specific PV Abs directly hinder Dsg 3 transinteraction, mouse monoclonal PV Abs AK 23, AK 18, and AK 9 were tested in Dsg 3 AFM experiments (Fig. 3B). Consistent with the pathogenicity of AK 23 in the mouse model, only AK 23 (75 $\mu\text{g/ml}$) blocked Dsg 3 transinteraction in AFM experiments to a comparable extent like Ca²⁺ depletion (21 \pm 9%). Higher concentrations of AK 23 up to 160 $\mu\text{g/ml}$ did not yield significantly different results (22 \pm 5%). AK 23 Fab were equally effective in blocking Dsg 3 transinteraction (15 \pm 4%, Fig. 3B), whereas AK 18 (86 \pm 2%) and AK 9 (107 \pm 1%) had no effect, even when applied at higher concentrations (data not shown). Taken together, these data demonstrate that both PV-IgG containing Dsg 3 autoantibodies as well as a monoclonal PV Ab binding to the N-terminal EC 1 domain of Dsg 3 directly interfered with Dsg 3 transinteraction.

Dsg 1 transinteraction was not blocked by pemphigus IgG in cell-free AFM experiments

Because PV-IgG 1 also contained Dsg 1 autoantibodies, we next examined the effect of PV-IgG on Dsg 1 transinteraction by AFM force measurements. As illustrated in Fig. 4A, specific reduction of Dsg 1-binding activity could be achieved by Ca²⁺ depletion or addition of a mAb directed against the extracellular domain of Dsg 1 (aDsg 1). In these experiments, Dsg 1-binding activity was reduced to 20 \pm 3% and 29 \pm 7%, respectively. Surprisingly, although including Dsg 1 autoantibodies, treatment with PV-IgG 1 did not change Dsg 1-binding activity (95 \pm 5%). As to be expected, PV-IgG 3, only including Dsg 3 autoantibodies, PV-IgG Fab and AK 23 also did not interfere with Dsg 1 transinteraction (94 \pm 13%, 96 \pm 9%, and 101 \pm 3%, respectively). In line with

1830

DIRECT INHIBITION OF Dsg TRANSINTERACTION IN PEMPHIGUS

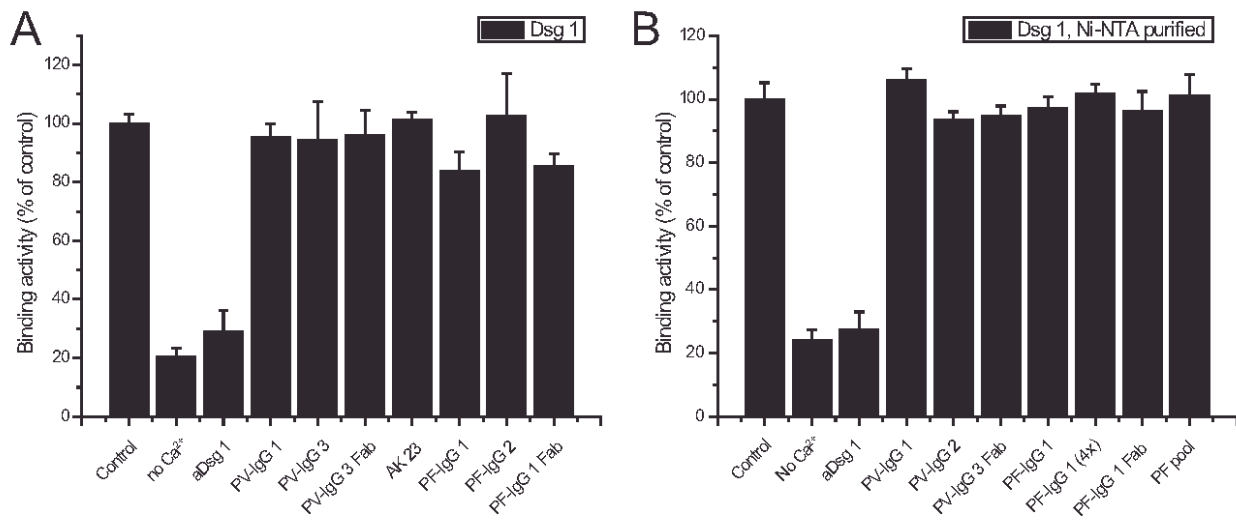


FIGURE 4. PV- and PF-IgG did not block Dsg 1 transinteraction in AFM experiments. *A*, Comparable to Fig. 3, binding activities of Dsg 1 were probed by AFM in the presence or absence of different pemphigus IgG. Depletion of Ca²⁺ by using a Ca²⁺-free buffer (no Ca²⁺) as well as incubation with a mAb directed against the extracellular part of Dsg 1 (aDsg 1) significantly reduced Dsg 1-binding activity to 20 and 29% of controls, respectively. Although containing Dsg 1 autoantibodies, PV-IgG 1 as well as PV-IgG 3 and PV-IgG Fab did not block Dsg 1 transinteraction in this cell-free assay. Similarly, AK 23 directed against Dsg 3 did not affect Dsg 1 transinteraction. PF-IgG 1 and 2 as well as PF-IgG Fab did not interfere with Dsg 1 transinteraction. ($n = 3-4$ for each condition). *B*, Dsg 1 AFM experiments were repeated using rDsg 1 purified by Ni-NTA-column imidazole elution. This protein showed an identical Ca²⁺ dependency of homophilic transinteraction compared with Dsg 1 purified via protein A column. Similarly, mouse monoclonal Dsg 1 Ab (aDsg 1) reduced Dsg 1-binding activity to prove the specificity of Dsg 1 interaction. Neither PV-IgG 1 and 2, both containing Dsg 1 and 3 autoantibodies, nor PV-IgG Fab reduced Dsg 1-binding activity. Moreover, PF autoantibodies also did not interfere with Dsg 1 transinteraction because neither PF-IgG 1 at normal or high (concentrated four times) doses, nor PF-IgG Fab or a pool of three additional PF-IgG fractions blocked Dsg 1 transinteraction ($n = 3-4$ for each condition).

our previous observation (24), Dsg 1-binding activity was not altered by treatment with PF-IgG 1 and 2 as well as PF-IgG Fab ($84 \pm 7\%$, $102 \pm 14\%$, and $85 \pm 5\%$, respectively).

The rDsg 1 used for this study was capable of depleting all pathogenic Dsg 1 Abs from PV- and PF-IgG fractions (Fig. 1, *G* and *N*), which is a strong indication that the correct conformation of Dsg 1 was retained (31). Nevertheless, this does not completely rule out the possibility that the pH shift during purification by protein A affinity chromatography induced minimal conformational changes of the Dsg 1 extracellular domain that inhibited binding of a small fraction of autoantibodies being capable of inducing direct inhibition of Dsg 1 transinteraction. Therefore, essentially all experiments were repeated using Dsg 1 purified via its his-tag by Ni-NTA columns and imidazole elution (Fig. 4*B*). This Dsg 1 protein also proved to be cleaved by ETA (data not shown). ETA cleavage is known to be strictly dependent on the proper conformation of the Dsg 1 extracellular domain (32). In AFM experiments, Ni-NTA column-purified Dsg 1 displayed strong Ca²⁺ dependency of homophilic Dsg 1 transinteraction and was blocked by the monoclonal Dsg 1 Ab (aDsg 1) ($24 \pm 3\%$ and $27 \pm 6\%$ of control binding, respectively), similar to what was detected using Dsg 1 purified by the protein A column. Nevertheless, neither PV-IgG 1 and 2 (both containing Dsg 1 and 3 autoantibodies) nor PV-IgG Fab reduced Dsg 1-binding activity ($106 \pm 4\%$, $93 \pm 3\%$, and $95 \pm 3\%$, respectively). Similar to our previous investigations (24), no direct inhibition of Dsg 1 transinteraction by PF-IgG was observed: neither PF-IgG 1 at normal or higher doses (concentrated four times), PF-IgG Fab, nor a pool of three additional PF-IgG fractions blocked Dsg 1 transinteraction ($97 \pm 4\%$, $102 \pm 3\%$, $96 \pm 6\%$, and $101 \pm 7\%$, respectively). Taken together, the AFM studies revealed that PV-IgG and AK 23 selectively blocked Dsg 3 but not Dsg 1 transinteraction, whereas PF-IgG did not interfere with Dsg-mediated transinteraction in the cell-free system.

Pemphigus IgG caused loss of binding of Dsg 1- and Dsg 3-coated microbeads to the surface of cultured human keratinocytes

To study the role of PV- and PF-IgG in the presence of cellular signaling mechanisms, we used the laser tweezer technique (Fig. 5). For this purpose, microbeads coated with human Dsg 1 or Dsg 3 were allowed to settle on the surface of HaCaT cells for 30 min. Afterward, we counted the number of bound beads resisting the separating forces of the laser beam (Fig. 5*A*). Fig. 5*B* summarizes all laser tweezer experiments using pemphigus IgG. Under control conditions, $77 \pm 5\%$ of Dsg 3 and $82 \pm 2\%$ of Dsg 1 beads could not be displaced by the laser beam focus and were taken as tightly bound (100%). Following incubation with 5 mM EGTA for 30 min to deplete extracellular Ca²⁺, the number of bound Dsg 3- or Dsg 1-coated beads dropped to $22 \pm 5\%$ and $29 \pm 6\%$, respectively, again documenting the strong Ca²⁺ dependency of Dsg adhesion. When HaCaT cells with surface-bound beads were incubated with PV- or PF-IgG fractions for 30 min, the number of both Dsg 3- and Dsg 1-coated beads was significantly reduced. PV-IgG 1, containing Dsg 1 and 3 autoantibodies, reduced the number of Dsg 3 and Dsg 1 beads to $52 \pm 8\%$ and $45 \pm 4\%$, respectively. PV-IgG 4, including Dsg 3 autoantibodies alone, reduced both Dsg 3- and Dsg 1-mediated binding as well ($83 \pm 6\%$ and $71 \pm 14\%$, respectively). Ab-mediated cross-linking was not required for loss of Dsg 3 binding because PV-IgG Fab also blocked Dsg 3 and Dsg 1 binding ($48 \pm 3\%$ and $62 \pm 5\%$, respectively). PV-IgG depleted of Dsg 1 and 3 Abs did not reduce the number of bound Dsg 3- or Dsg 1-coated beads ($97 \pm 3\%$ and $101 \pm 2\%$, respectively) indicating that autoantibodies specific for Dsg 1 and 3 mediate blocking of Dsg transinteraction in this assay.

In addition, following incubation with PF-IgG 1, the number of bound Dsg 3 and Dsg 1 beads dropped to $31 \pm 8\%$ and $50 \pm 7\%$,

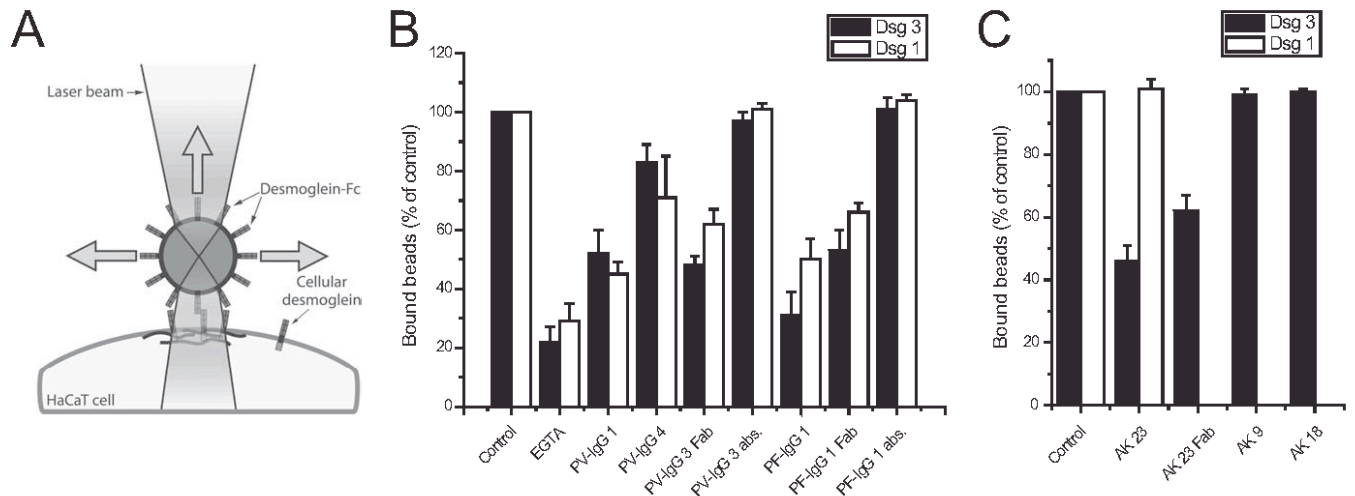


FIGURE 5. Pemphigus IgG blocked Dsg 1 and Dsg 3 bead binding in laser tweezer experiments. *A*, Principle of laser tweezer experiments. On HaCaT cells, Dsg-coated microbeads could be trapped in a laser beam focus to distinguish bound from unbound beads. Dsg 3- (■) and Dsg 1-coated beads (□) were allowed to settle on the surface of HaCaT cells for 30 min (control) and bound beads were counted. *B*, Pemphigus IgG caused loss of binding of Dsg 1- and Dsg 3-coated microbeads to the surface of cultured human keratinocytes. The number of bound beads resisting laser beam displacement at 42 mW was reduced by simultaneous incubation with EGTA (5 mM, 30 min) to 22 and 29% for Dsg 3 and Dsg 1, respectively. Incubation of monolayers with attached beads for 30 min with IgG fractions from PV patients (PV-IgG 1 containing autoantibodies to both Dsg 1 and Dsg 3 and PV-IgG 4, autoantibodies to Dsg 3 only) as well as with PV-IgG Fab significantly reduced the number of bound Dsg 3- and Dsg 1-coated beads. Depletion of Dsg IgG from pemphigus IgG abolished the reduction in Dsg 1- and Dsg 3-mediated bead binding. PF-IgG 1 (only containing autoantibodies to Dsg 1) or PF-IgG Fab also led to a loss in Dsg 1 and Dsg 3 bead binding, whereas Dsg 1 Ab-depleted PF-IgG had no effect ($n = 6$ for each condition). *C*, AK 23 selectively blocked Dsg 3-mediated binding. The monoclonal Dsg 3 Ab AK 23 as well as AK 23 Fab inhibited Dsg 3 but not Dsg 1 transinteraction, whereas AK 18 and AK 9 had no effect ($n = 6$ for each condition).

respectively. PF-IgG Fab had similar effects and reduced Dsg 3- and Dsg 1-mediated binding to $53 \pm 7\%$ and $66 \pm 3\%$, respectively, whereas Dsg 1 autoantibody-depleted PF-IgG had no effects on Dsg 3 and Dsg 1 binding ($101 \pm 4\%$ and $104 \pm 2\%$, respectively). Thus, PF-IgG not containing Dsg 3 autoantibodies and ineffective to block transinteraction of Dsg 1 and Dsg 3 in cell-free AFM experiments, as well as PV-IgG interfering with Dsg 3 but not with Dsg 1 transinteraction, both were effective at

inhibiting binding of Dsg 1- and Dsg 3-coated beads to cultured keratinocytes via Dsg-specific autoantibodies.

We also examined the effect of mouse monoclonal PV Abs on binding of Dsg 3- and Dsg 1-coated beads to HaCaT cells (Fig. 5C). In contrast to pemphigus patients' IgG, monoclonal AK 23 Ab selectively reduced the number of bound Dsg 3 beads to $46 \pm 5\%$ of control, whereas the number of bound Dsg 1 beads was not affected ($101 \pm 3\%$). Moreover, AK 23 Fab also reduced Dsg

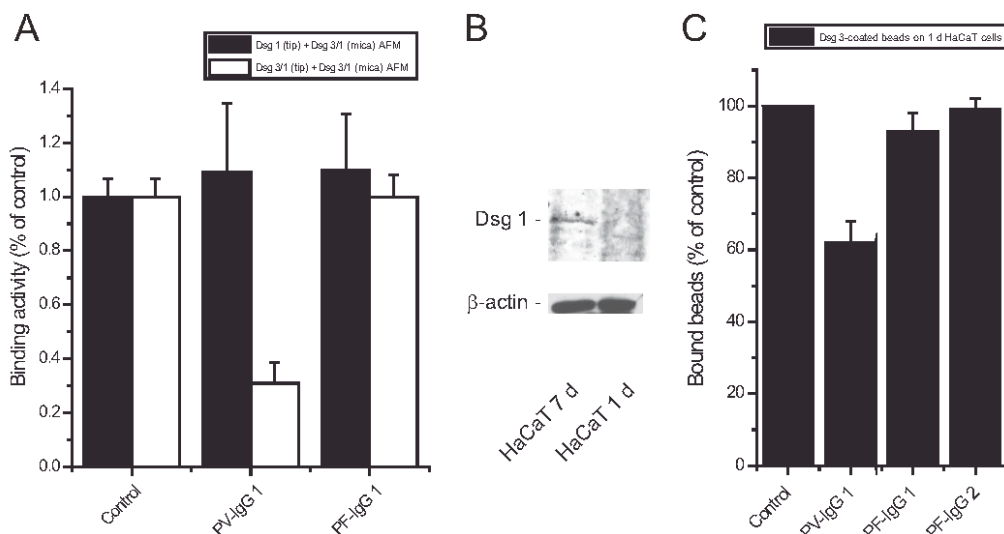


FIGURE 6. Presence of Dsg 3 did not alter PV- or PF-IgG-induced effects on cell-free Dsg 1 transinteraction but absence of Dsg 1 blocked PF-IgG-mediated effects on Dsg 3 bead binding. *A*, AFM tips were either coated with Dsg 1 alone (■) or in combination with Dsg 3 (□) and probed on substrates covered with an equal mixture of Dsg 1 and Dsg 3. PV-IgG 1 did not alter Dsg 1 transinteraction when tips were coated with Dsg 1 alone but was efficient at reducing binding activity when Dsg 3 was also present at AFM tips. In contrast, PF-IgG 1 had no effects under these experimental conditions ($n = 3-4$ for each condition). *B*, Dsg 1 Western blotting of HaCaT cells cultivated for either 1 or 7 days demonstrated that Dsg 1 was not present after 1 but after 7 days. β -actin was used to show equal loading of cell lysates ($n = 3$). *C*, In laser tweezer experiments with HaCaT cells cultivated for 1 day, PV-IgG 1 were effective at reducing the number of bound Dsg 3 beads. In contrast, PF-IgG 1 and 2 had no effect ($n = 6$ for each condition).

1832

DIRECT INHIBITION OF Dsg TRANSINTERACTION IN PEMPHIGUS

3-mediated binding to $62 \pm 5\%$. In contrast, AK 18 and AK 9 did not alter the number of bound Dsg 3-coated beads on HaCaT cells ($99 \pm 2\%$ and $100 \pm 1\%$, respectively).

In other studies it has been shown that presence of Dsg 1 prevents PV-IgG from disrupting intercellular adhesion (33). Similarly, PF-IgG might require the presence of coexpressed Dsg 3 to disrupt homophilic transinteraction of Dsg 1. Therefore, we tested this hypothesis using AFM and laser tweezer experiments (Fig. 6). As a first step, AFM tips were either coated with Dsg 1 alone (Fig. 6A, ■) or in combination with Dsg 3 (Fig. 6A, □) and probed on substrates covered with an equal mixture of Dsg 1 and Dsg 3. PV-IgG 1, though containing Dsg 1 autoantibodies, did not alter Dsg 1 transinteraction when tips were coated with Dsg 1 alone ($109 \pm 26\%$) but was efficient at reducing binding activity when Dsg 3 was also present at AFM tips (reduction to $31 \pm 8\%$ of controls). In contrast, PF-IgG 1 had no effects under the two experimental conditions ($110 \pm 21\%$ and $100 \pm 8\%$, respectively). This indicated that the presence of Dsg 3 did not alter PV- or PF-IgG-induced effects on cell-free Dsg 1 transinteraction. We further tested the effects of PF-IgG on Dsg 3 bead binding on keratinocytes under conditions where Dsg 1 was absent. Western blotting (Fig. 6B) showed that Dsg 1 was not present when HaCaT cells were cultivated for 1 day after passaging but was detected after 7 days – the condition used in previous experiments (Fig. 5). In laser tweezer experiments with HaCaT cells cultivated for 1 day, PV-IgG 1 reduced the number of bound Dsg 3 beads to $62 \pm 6\%$ of controls (Fig. 6C). However, PF-IgG 1 and 2 had no effects (Dsg 3 bead binding $93 \pm 5\%$ and $99 \pm 3\%$, respectively), in contrast to experiments with HaCaT cells cultured for 7 days and expressing Dsg 1 (Fig. 5). These data demonstrated that Dsg 1 is required to mediate the effects of PF-IgG on Dsg 3 binding in keratinocytes.

Discussion

We provide first evidence that Dsg 3 autoantibodies in PV directly inhibit Dsg 3 transinteraction, whereas in contrast Dsg 1 autoantibodies in PV- and PF-IgG reduce Dsg 1 transinteraction not directly but rather indirectly via cellular mechanisms. Using a combined approach of cell-free AFM studies, together with laser tweezer trapping of Dsg-coated microbeads on the surface of human keratinocytes, these conclusions are based on the following observations (Fig. 7): 1) PV-IgG containing Abs to both Dsg 3 and Dsg 1 as well as PV-IgG Fab selectively blocked Dsg 3 but not Dsg 1 transinteraction in single-molecule AFM studies. 2) PF-IgG and PF-IgG Fab did neither interfere with Dsg 1 nor with Dsg 3 transinteraction in AFM studies. 3) PV-IgG and PV-IgG Fab reduced binding of both Dsg 3- and Dsg 1-coated beads to the keratinocyte cell surface. 4) PF-IgG containing Dsg 1 but not Dsg 3 Abs as well as PF-IgG Fab also reduced binding of Dsg 3- and Dsg 1-coated beads. 5) The mouse monoclonal PV Ab AK 23 directed against the putative Dsg 3-binding site and AK 23 Fab specifically blocked Dsg 3 transinteraction in the presence and absence of cells. 6) mAbs against the middle and C-terminal parts of the extracellular Dsg 3 domain did not interfere with Dsg 3 transinteraction.

In a previous study, we showed that PF-IgG reduced transinteraction of Dsg 1 molecules only when assayed in keratinocyte cultures but not in the cell-free AFM setup (24). In the recent study, we confirmed these results and found in addition that autoantibodies to Dsg 1 in PV-IgG also did not directly interfere with Dsg 1 transinteraction. These negative findings seem not to be caused by a loss of proper conformation of Dsg 1, because Dsg 1 was able to bind Ca^{2+} , to deplete all pathogenic Abs from PF-IgG (31) and also was cleaved by ETA (32). However, we cannot completely

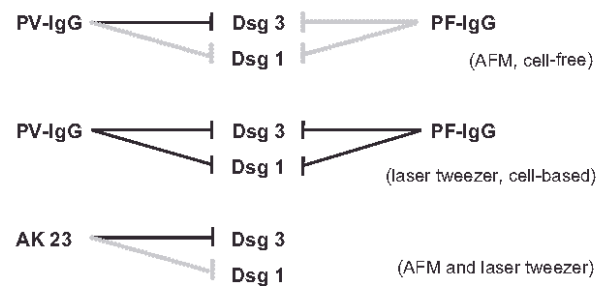


FIGURE 7. Summary of AFM and laser tweezer experiments with pemphigus IgG and AK 23. PV-IgG selectively interfered with Dsg 3 but not with Dsg 1 transinteraction in cell-free AFM studies, whereas PF-IgG had no blocking effect on Dsg 3 and Dsg 1 transadhesion. In contrast, PV- and PF-IgG reduced both Dsg 3 and Dsg 1 transadhesion in cell-based laser tweezer experiments. The pathogenic mouse mAb AK 23, however, only blocked Dsg 3 but not Dsg 1 transinteraction in both experimental set-ups.

rule out that in vivo conformational changes of the Dsg 1 structure occur in response to autoantibody binding which are not equally present in our experiments. Nevertheless, a commercial mouse mAb directed against Dsg 1 blocked Dsg 1 transinteraction demonstrating that this EC 2-directed Ab (manufacturer's specifications and our observations) may cause allosteric conformational changes which impair Dsg 1 adhesion. In clear contrast, we found that PV-IgG and PV-IgG Fab inhibited Dsg 3 transinteraction both in AFM studies and on keratinocytes. The use of Fab allows the conclusion that the loss of binding activity was not due to Ab cross-linking of molecules on the cantilever or the plate of the AFM. Abs to Dsg 3 in PV-IgG were equally effective at inhibiting Dsg 3 transinteraction in AFM studies like the monoclonal Dsg 3 Ab AK 23, which binds to the N-terminal EC 1 domain of Dsg 3 where the predicted binding interface is located and which is targeted by most of Dsg 3 Abs in PV patients (23). These data indicate that direct inhibition of Dsg 3 transinteraction was most likely caused by steric hindrance (34). However, because $\sim 20\%$ of PV Abs have been shown to bind to other parts of the Dsg 3 extracellular domain (23), at this stage we cannot completely rule out the possibility that some autoantibodies in PV-IgG fractions also interfered with Dsg 3 transinteraction by allosteric effects. Nevertheless, we found that AK 9 and AK 18, which target different parts of the extracellular domain, had no effect on Dsg 3 transinteraction. Finally, depletion of Dsg 3-specific Abs by immunoabsorption using rDsg 3 demonstrated that inhibition of Dsg 3 transinteraction was mediated by Dsg 3-specific Abs. Together with the findings that depletion of Dsg-specific Abs from PV-IgG and PF-IgG completely abolished keratinocyte dissociation and loss of Dsg 3 and Dsg 1 bead binding, these data further support the hypothesis that Dsg-specific Abs are required for pemphigus pathogenesis (13). This is also supported by the observation that, in the absence of Dsg 1 in HaCaT cells, PF-IgG-mediated loss of Dsg 3 bead binding was abolished indicating that Dsg 1 is the major autoantigen required for autoantibody-mediated outside-in signaling.

Because heterophilic transinteraction of desmosomal cadherins is thought to be important (35, 36), we also sought to address this issue in our study. However, because we did not observe heterophilic interactions of Dsg 3 and Dsg 1, we were only in the position to probe direct inhibition of homophilic transinteraction. Nevertheless, we can rule out the possibility that the presence of both Dsg 1 and Dsg 3 is needed for PV- or PF-IgG to alter Dsg transinteraction in cell-free single-molecule experiments. It has to be emphasized that this does not exclude the possibility that PV- or PF-IgG also directly interfere with the transinteraction of Dsg 3 or

Dsg 1 with other desmosomal cadherins such as desmocollin (Dsc) 1 or Dsc 3, especially because it has been recently reported that conditional Dsc 3 deficiency in a mouse model led to a severe pemphigus-like phenotype (37). This needs to be clarified in further studies.

In the meantime, several signaling pathways have been shown to participate in pemphigus pathogenesis including protein kinase C, plakoglobin, c-Myc, p38MAPK, Rho A, epidermal growth factor receptor, and Src (29, 38–43). However, except for p38MAPK and Rho A (28, 29, 38, 44), all signaling mechanisms have only been evaluated for their contribution to PV but not to PF pathogenesis. Our results suggest that the pathogenesis of these two pemphigus subtypes may be different because direct inhibition of Dsg-mediated transadhesion may only occur in PV (43). The reduction of Dsg 1 binding to the surface of keratinocytes in response to PV- and PF-IgG which was detected after a 30-min incubation in our laser tweezer studies may be caused by cellular signaling events. This explanation is possible because cellular signaling events have been shown to be triggered by pemphigus IgG within 20 s (45). Moreover, activation of p38MAPK which is now thought to be one of the key signaling mechanisms in pemphigus pathogenesis occurs within the first 30 min (46).

However, it cannot be concluded from our data whether in addition to direct inhibition cellular signaling events were also responsible for PV-IgG-induced loss of Dsg 3 transinteraction in keratinocytes. Because AK 23, which inhibited Dsg 3 transinteraction in AFM experiments, was only effective in reducing binding of Dsg 3- but not of Dsg 1-coated beads in the laser tweezer assay, these data indicate that direct inhibition of Dsg 3 transinteraction is sufficient to reduce binding of Dsg 3 at the keratinocyte surface. However, unlike PV-IgG, AK 23 did not induce a profound disruption of Dsg 3 localization and keratinocyte dissociation in our experiments. Although AK 23 has been shown to effectively induce Dsg 3 depletion in human keratinocyte cultures (30), the effect of AK 23 on cellular signaling events such as p38MAPK signaling was found to be rather weak compared with patients' PV-IgG (47, 48). Therefore, it is likely that AK 23 does not trigger the signaling mechanisms required for reduction of Dsg 1 adhesion and keratinocyte dissociation. This supports the fact that a single mAb does not fully reproduce the effects of polyclonal PV-IgG (30).

Taken together, our data are in line with the hypothesis that direct inhibition of Dsg 3 transinteraction or activation of cell-signaling mechanisms may not be mutually exclusive but rather act in concert in pemphigus pathogenesis (42, 43, 49). Moreover, it is unlikely that direct inhibition of Dsg 3 transinteraction alone accounts for desmosomal splitting and acantholysis in PV. This can be concluded from the finding that complete deficiency of Dsg 3 still allows formation of morphologically intact desmosomes, at least in the absence of mechanical stress (50). For the future, it will be important to determine whether direct inhibition and signaling are completely independent mechanisms or whether cell-signaling events in PV pathogenesis occur in response to direct Ab-mediated loss of cell adhesion (34). Our study suggests that direct inhibition of Dsg 3 transinteraction in PV in addition to cellular signaling events may aggravate the clinical phenotype of PV (43).

Acknowledgments

We are grateful to Masayuki Amagai (School of Medicine, Keio University, Tokyo, Japan) for contribution of ETA as well as for helpful advice and discussion. We thank Hermann Gruber (Johannes Kepler University, Linz, Austria) for generously providing AFM PEG linkers. We thank Stefanie Imhof, Nadja Niedermeier, and Lisa Bergauer for excellent technical assistance.

Disclosures

The authors have no financial conflict of interest.

References

- Bystryn, J. C., and J. L. Rudolph. 2005. Pemphigus. *Lancet* 366: 61–73.
- Stanley, J. R., and M. Amagai. 2006. Pemphigus, bullous impetigo, and the staphylococcal scalded-skin syndrome. *N. Engl. J. Med.* 355: 1800–1810.
- Anhalt, G. J., R. S. Labib, J. J. Voorhees, T. F. Beals, and L. A. Diaz. 1982. Induction of pemphigus in neonatal mice by passive transfer of IgG from patients with the disease. *N. Engl. J. Med.* 306: 1189–1196.
- Beutner, E. H., and R. E. Jordan. 1964. Demonstration of skin antibodies in sera of pemphigus vulgaris patients by indirect immunofluorescent staining. *Proc. Soc. Exp. Biol. Med.* 117: 505–510.
- Schultz, J. R., and B. Michel. 1976. Production of epidermal acantholysis in normal human skin in vitro by the IgG fraction from pemphigus serum. *J. Invest. Dermatol.* 67: 254–260.
- Amagai, M., V. Klaus-Kovtun, and J. R. Stanley. 1991. Autoantibodies against a novel epithelial cadherin in pemphigus vulgaris, a disease of cell adhesion. *Cell* 67: 869–877.
- Eyre, R. W., and J. R. Stanley. 1988. Identification of pemphigus vulgaris antigen extracted from normal human epidermis and comparison with pemphigus foliaceus antigen. *J. Clin. Invest.* 81: 807–812.
- Koch, P. J., M. J. Walsh, M. Schmelz, M. D. Goldschmidt, R. Zimblemann, and W. W. Franke. 1990. Identification of desmoglein, a constitutive desmosomal glycoprotein, as a member of the cadherin family of cell adhesion molecules. *Eur. J. Cell Biol.* 53: 1–12.
- Stanley, J. R., L. Koulu, and C. Thivolet. 1984. Distinction between epidermal antigens binding pemphigus vulgaris and pemphigus foliaceus autoantibodies. *J. Clin. Invest.* 74: 313–320.
- Nguyen, V. T., A. Ndoye, and S. A. Grando. 2000. Novel human $\alpha 9$ acetylcholine receptor regulating keratinocyte adhesion is targeted by pemphigus vulgaris autoimmunity. *Am. J. Pathol.* 157: 1377–1391.
- Nguyen, V. T., A. Ndoye, and S. A. Grando. 2000. Pemphigus vulgaris antibody identifies pemphaxin: a novel keratinocyte annexin-like molecule binding acetylcholine. *J. Biol. Chem.* 275: 29466–29476.
- Nguyen, V. T., A. Ndoye, L. D. Shultz, M. R. Pittelkow, and S. A. Grando. 2000. Antibodies against keratinocyte antigens other than desmogleins 1 and 3 can induce pemphigus vulgaris-like lesions. *J. Clin. Invest.* 106: 1467–1479.
- Amagai, M., A. R. Ahmed, Y. Kitajima, J. C. Bystryn, Y. Milner, R. Gniadecki, M. Hertl, C. Pincelli, M. Fridkis-Hareli, Y. Aoyama, et al. 2006. Are desmoglein autoantibodies essential for the immunopathogenesis of pemphigus vulgaris, or just “witnesses of disease”? *Exp. Dermatol.* 15: 815.
- Grando, S. A., M. R. Pittelkow, L. D. Shultz, M. Dmochowski, and V. T. Nguyen. 2001. Pemphigus: an unfolding story. *J. Invest. Dermatol.* 117: 990–995.
- Payne, A. S., Y. Hanakawa, M. Amagai, and J. R. Stanley. 2004. Desmosomes and disease: pemphigus and bullous impetigo. *Curr. Opin. Cell Biol.* 16: 536–543.
- Amagai, M., K. Tsunoda, D. Zillikens, T. Nagai, and T. Nishikawa. 1999. The clinical phenotype of pemphigus is defined by the anti-desmoglein autoantibody profile. *J. Am. Acad. Dermatol.* 40: 167–170.
- Ding, X., V. Aoki, J. M. Mascaro, Jr., A. Lopez-Swiderski, L. A. Diaz, and J. A. Fairley. 1997. Mucosal and mucocutaneous (generalized) pemphigus vulgaris show distinct autoantibody profiles. *J. Invest. Dermatol.* 109: 592–596.
- Jamora, M. J., D. Jiao, and J. C. Bystryn. 2003. Antibodies to desmoglein 1 and 3, and the clinical phenotype of pemphigus vulgaris. *J. Am. Acad. Dermatol.* 48: 976–977.
- Zagorodniuk, I., S. Weltfriend, L. Shtruminger, E. Sprecher, O. Kogan, S. Pollack, and R. Bergman. 2005. A comparison of anti-desmoglein antibodies and indirect immunofluorescence in the serodiagnosis of pemphigus vulgaris. *Int. J. Dermatol.* 44: 541–544.
- Tsunoda, K., T. Ota, M. Aoki, T. Yamada, T. Nagai, T. Nakagawa, S. Koyasu, T. Nishikawa, and M. Amagai. 2003. Induction of pemphigus phenotype by a mouse monoclonal antibody against the amino-terminal adhesive interface of desmoglein 3. *J. Immunol.* 170: 2170–2178.
- Boggon, T. J., J. Murray, S. Chappuis-Flament, E. Wong, B. M. Gumbiner, and L. Shapiro. 2002. C-cadherin ectodomain structure and implications for cell adhesion mechanisms. *Science* 296: 1308–1313.
- Shapiro, L., A. M. Fannon, P. D. Kwong, A. Thompson, M. S. Lehmann, G. Grubel, J. F. Legrand, J. Als-Nielsen, D. R. Colman, and W. A. Hendrickson. 1995. Structural basis of cell-cell adhesion by cadherins. *Nature* 374: 327–337.
- Sekiguchi, M., Y. Futei, Y. Fujii, T. Iwasaki, T. Nishikawa, and M. Amagai. 2001. Dominant autoimmune epitopes recognized by pemphigus antibodies map to the N-terminal adhesive region of desmogleins. *J. Immunol.* 167: 5439–5448.
- Waschke, J., P. Bruggeman, W. Baumgartner, D. Zillikens, and D. Drenckhahn. 2005. Pemphigus foliaceus IgG causes dissociation of desmoglein 1-containing junctions without blocking desmoglein 1 transinteraction. *J. Clin. Invest.* 115: 3157–3165.
- Tatsumi, R., K. Shimada, and A. Hattori. 1997. Fluorescence detection of calcium-binding proteins with quinoline Ca-indicator quin2. *Anal. Biochem.* 254: 126–131.
- Hinterdorfer, P., W. Baumgartner, H. J. Gruber, K. Schilcher, and H. Schindler. 1996. Detection and localization of individual antibody-antigen recognition events by atomic force microscopy. *Proc. Natl. Acad. Sci. USA* 93: 3477–3481.

27. Baumgartner, W., P. Hinterdorfer, W. Ness, A. Raab, D. Vestweber, H. Schindler, and D. Drenckhahn. 2000. Cadherin interaction probed by atomic force microscopy. *Proc. Natl. Acad. Sci. USA* 97: 4005–4010.
28. Spindler, V., D. Drenckhahn, D. Zillikens, and J. Waschke. 2007. Pemphigus IgG causes skin splitting in the presence of both desmoglein 1 and desmoglein 3. *Am. J. Pathol.* 171: 906–916.
29. Waschke, J., V. Spindler, P. Bruggeman, D. Zillikens, G. Schmidt, and D. Drenckhahn. 2006. Inhibition of Rho A activity causes pemphigus skin blistering. *J. Cell Biol.* 175: 721–727.
30. Yamamoto, Y., Y. Aoyama, E. Shu, K. Tsunoda, M. Amagai, and Y. Kitajima. 2007. Anti-desmoglein 3 (Dsg3) monoclonal antibodies deplete desmosomes of Dsg3 and differ in their Dsg3-depleting activities related to pathogenicity. *J. Biol. Chem.* 282: 17866–17876.
31. Amagai, M., T. Hashimoto, K. J. Green, N. Shimizu, and T. Nishikawa. 1995. Antigen-specific immunoadsorption of pathogenic autoantibodies in pemphigus foliaceus. *J. Invest. Dermatol.* 104: 895–901.
32. Hanakawa, Y., T. Selwood, D. Woo, C. Lin, N. M. Schechter, and J. R. Stanley. 2003. Calcium-dependent conformation of desmoglein 1 is required for its cleavage by exfoliative toxin. *J. Invest. Dermatol.* 121: 383–389.
33. Mahoney, M. G., Z. Wang, K. Rothenberger, P. J. Koch, M. Amagai, and J. R. Stanley. 1999. Explanations for the clinical and microscopic localization of lesions in pemphigus foliaceus and vulgaris. *J. Clin. Invest.* 103: 461–468.
34. Sharma, P., X. Mao, and A. S. Payne. 2007. Beyond steric hindrance: the role of adhesion signaling pathways in the pathogenesis of pemphigus. *J. Dermatol. Sci.* 48: 1–14.
35. Getsios, S., E. V. Amargo, R. L. Dusek, K. Ishii, L. Shen, L. M. Godsel, and K. J. Green. 2004. Coordinated expression of desmoglein 1 and desmocollin 1 regulates intercellular adhesion. *Differentiation* 72: 419–433.
36. Marozzi, C., I. D. Burdett, R. S. Buxton, and A. I. Magee. 1998. Coexpression of both types of desmosomal cadherin and plakoglobin confers strong intercellular adhesion. *J. Cell Sci.* 111(Pt. 4): 495–509.
37. Chen, J., Z. Den, M. Merched-Sauvage, and P. J. Koch. 2007. Loss of desmocollin 3 in the epidermis of mice causes epidermal blistering and telogen hair loss. *J. Invest. Dermatol.* 127: S37 (Abstract).
38. Berkowitz, P., P. Hu, S. Warren, Z. Liu, L. A. Diaz, and D. S. Rubenstein. 2006. p38MAPK inhibition prevents disease in pemphigus vulgaris mice. *Proc. Natl. Acad. Sci. USA* 103: 12855–12860.
39. Caldelari, R., A. de Bruin, D. Baumann, M. M. Suter, C. Bierkamp, V. Balmer, and E. Muller. 2001. A central role for the armadillo protein plakoglobin in the autoimmune disease pemphigus vulgaris. *J. Cell Biol.* 153: 823–834.
40. Chernyavsky, A. I., J. Arredondo, Y. Kitajima, M. Sato-Nagai, and S. A. Grando. 2007. Desmoglein versus non-desmoglein signaling in pemphigus acantholysis: characterization of novel signaling pathways downstream of pemphigus vulgaris antigens. *J. Biol. Chem.* 282: 13804–13812.
41. Kitajima, Y., Y. Aoyama, and M. Seishima. 1999. Transmembrane signaling for adhesive regulation of desmosomes and hemidesmosomes, and for cell-cell detachment induced by pemphigus IgG in cultured keratinocytes: involvement of protein kinase C. *J. Invest. Dermatol. Symp. Proc.* 4: 137–144.
42. Williamson, L., N. A. Raess, R. Caldelari, A. Zakher, A. de Bruin, H. Posthaus, R. Bolli, T. Hunziker, M. M. Suter, and E. J. Muller. 2006. Pemphigus vulgaris identifies plakoglobin as key suppressor of c-Myc in the skin. *EMBO J.* 25: 3298–3309.
43. Waschke, J. 2008. The desmosome and pemphigus. *Histochem. Cell Biol.* 130: 21–54.
44. Berkowitz, P., Z. Liu, L. A. Diaz, and D. D. Rubenstein. 2007. Autoantibodies in the autoimmune disease pemphigus foliaceus induce blistering in vivo via p38MAPK-dependent signaling. *J. Invest. Dermatol.* 127: S34 (Abstract).
45. Seishima, M., C. Esaki, K. Osada, S. Mori, T. Hashimoto, and Y. Kitajima. 1995. Pemphigus IgG, but not bullous pemphigoid IgG, causes a transient increase in intracellular calcium and inositol 1,4,5-triphosphate in DJM-1 cells, a squamous cell carcinoma line. *J. Invest. Dermatol.* 104: 33–37.
46. Berkowitz, P., P. Hu, Z. Liu, L. A. Diaz, J. J. Enghild, M. P. Chua, and D. S. Rubenstein. 2005. Desmosome signaling: inhibition of p38MAPK prevents pemphigus vulgaris IgG-induced cytoskeleton reorganization. *J. Biol. Chem.* 280: 23778–23784.
47. Kawasaki, Y., Y. Aoyama, K. Tsunoda, M. Amagai, and Y. Kitajima. 2006. Pathogenic monoclonal antibody against desmoglein 3 augments desmoglein 3 and p38 MAPK phosphorylation in human squamous carcinoma cell line. *Autoimmunity* 39: 587–590.
48. Nguyen, V. T., J. Arredondo, A. I. Chernyavsky, Y. Kitajima, M. Pittelkow, and S. A. Grando. 2004. Pemphigus vulgaris IgG and methylprednisolone exhibit reciprocal effects on keratinocytes. *J. Biol. Chem.* 279: 2135–2146.
49. Grando, S. A. 2006. Cholinergic control of epidermal cohesion. *Exp. Dermatol.* 15: 265–282.
50. Koch, P. J., M. G. Mahoney, H. Ishikawa, L. Pulkkinen, J. Uitto, L. Shultz, G. F. Murphy, D. Whitaker-Menezes, and J. R. Stanley. 1997. Targeted disruption of the pemphigus vulgaris antigen (desmoglein 3) gene in mice causes loss of keratinocyte cell adhesion with a phenotype similar to pemphigus vulgaris. *J. Cell Biol.* 137: 1091–1102.

3.1.2 Publication 2: Pemphigus vulgaris IgG cause loss of desmoglein-mediated adhesion and keratinocyte dissociation in HaCaT cells independent of epidermal growth factor receptor

Heupel WM [¶], Engerer P [¶], Schmidt E, Waschke J

Pemphigus vulgaris IgG cause loss of desmoglein-mediated adhesion and keratinocyte dissociation in HaCaT cells independent of epidermal growth factor receptor

Am J Pathol. 2009 Feb;174(2):475-85. Epub 2009 Jan 15.

Reprinted from Am J Pathol 2009, 174:475-485 with permission from the American Society for Investigative Pathology.

DOI: 10.2353/ajpath.2009.080392

The American Journal of Pathology, Vol. 174, No. 2, February 2009
Copyright © American Society for Investigative Pathology
DOI: 10.2353/ajpath.2009.080392

Immunopathology and Infectious Diseases

Pemphigus Vulgaris IgG Cause Loss of Desmoglein-Mediated Adhesion and Keratinocyte Dissociation Independent of Epidermal Growth Factor Receptor

Wolfgang-Moritz Heupel,* Peter Engerer,*
Enno Schmidt,[†] and Jens Waschke*

From the Institute of Anatomy and Cell Biology,
and the Department of Dermatology,[†] University of Würzburg,
Würzburg, Germany*

Autoantibody-induced cellular signaling mechanisms contribute to the pathogenesis of autoimmune blistering skin disease pemphigus vulgaris (PV). Recently, it was proposed that epidermal growth factor receptor (EGFR) might be involved in PV signaling pathways. In this study, we investigated the role of EGFR by comparing the effects of epidermal growth factor (EGF) and PV-IgG on the immortalized human keratinocyte cell line HaCaT, and primary normal human keratinocytes. In contrast to EGF treatment, PV-IgG neither caused the canonical activation of EGFR via phosphorylation at tyrosine (Y)1173 followed by internalization of EGFR nor the phosphorylation of the EGFR at the c-Src-dependent site Y845. Nevertheless, both PV-IgG and EGF led to cell dissociation and cytokeratin retraction in keratinocyte monolayers. Moreover, the effects of EGF were blocked by inhibition of EGFR and c-Src whereas the effects of PV-IgG were independent of both signaling pathways. Similarly, laser tweezer experiments revealed that impaired bead binding of epidermal cadherins desmoglein (Dsg) 3 and Dsg 1 in response to PV-IgG was not affected by inhibition of either EGFR or c-Src. In contrast, EGF treatment did not interfere with Dsg bead binding. Taken together, our study indicates that the loss of Dsg-mediated adhesion and keratinocyte dissociation in pemphigus is independent of EGFR. Moreover, the mechanisms by which both EGF and PV-IgG lead to keratinocyte dissociation and cytokeratin retraction appear to be different. (*Am J Pathol* 2009, 174:475–485; DOI: 10.2353/ajpath.2009.080392)

Pemphigus is an autoimmune blistering skin disease caused by antibodies against keratinocyte surface antigens.^{1–3} Particularly, pathogenic autoantibodies are directed against epidermal cadherins desmoglein (Dsg) 3 and Dsg 1.^{4–6} In the mucosal-dominant form of pemphigus vulgaris (PV), antibodies against Dsg 3 are produced, whereas Dsg 1 is an additional target when epidermal involvement occurs. For pemphigus foliaceus (PF) and the Brazilian endemic variant fogo selvagem, Dsg 1 is the major autoantigen. However, non-Dsg targets have also been identified.⁷ Among those, pemphaxin, cholinergic receptors and E-cadherin are the best-studied so far.^{8–10} In addition, pathogenic non-autoantibody factors in pemphigus patients' sera such as Fas ligand are discussed.¹¹ Nevertheless, there is an ongoing debate whether acantholysis—the cellular hallmark of pemphigus pathogenicity—is induced by Dsg antibodies directly interfering with Dsg transinteraction or by cellular signaling mechanisms triggered by Dsg or non-Dsg autoantibodies.¹² At least for PF, cellular signaling seems to be important since no direct inhibition of Dsg 1-mediated binding by PF-IgG was observed by atomic force microscopy under conditions where autoantibodies caused keratinocyte dissociation.¹³ Nevertheless, recently we have demonstrated that PV-IgG directly interfere with Dsg 3 transinteraction.¹⁴

Over the past years, the involvement of several signaling pathways has been studied. However, the mechanisms involved in outside-in signaling as well as the interplay of the several pathways leading to acantholysis remain unclear.¹⁵ *In vitro* and *in vivo* studies have shown activation of p38 mitogen activated protein kinase (MAPK) by pemphigus IgG.^{16,17} Blocking p38 MAPK pre-

Supported by grants from IZKF Würzburg (TP A-51) and SFB 487 (TP B5).

Accepted for publication October 22, 2008.

W.-M.H. and P.E. contributed equally.

Address reprint requests to Dr. Jens Waschke, Institute of Anatomy and Cell Biology, University of Würzburg, Koellikerstr. 6, D-97070 Würzburg/Germany. E-mail: jens.waschke@mail.uni-wuerzburg.de.

476 Heupel et al
AJP February 2009, Vol. 174, No. 2

vented cell dissociation and cytokeratin retraction. In addition, activation of the small GTPase RhoA completely antagonized pemphigus IgG-mediated effects in cultured human epidermis and keratinocyte monolayers.¹⁸ Pemphigus IgG-induced Rho A inactivation was also p38 MAPK-dependent. Furthermore, plakoglobin depletion by pemphigus IgG is supposed to lead to diminished cell adhesion via c-Myc overexpression, which has been shown to result in keratinocyte hyperproliferation.^{19,20} Promotion of cell-cycle progression by PV-IgG-mediated upregulation of cyclin-dependent kinase 2 is another mechanism believed to cause acantholysis via continuing keratinocyte proliferation.²¹

The epidermal growth factor receptor (EGFR) is a receptor tyrosine kinase that activates a complex cellular signaling network involving the classical MAPK cascade (leading to activation of Erk and Akt), signal transducer and activator of transcription, phospholipase C, and RhoA.^{22,23} EGFR can be activated by extracellular ligands like EGF, by intracellular kinases such as c-Src or by G protein coupled receptors.^{24,25} Over a decade ago first work highlighted the interdependence of cell adhesion and EGFR function.²⁶ Stimulation of EGFR resulted in phosphorylation of catenins (cadherin family adapter proteins) and colocalization of EGFR with the cadherin-catenin complex. Moreover, epidermal growth factor (EGF)-mediated phosphorylation of plakoglobin caused depletion of desmoplakin from desmosomes as well as reduced cell adhesion.^{27,28} Activation of EGFR following PV-IgG treatment was speculated to up-regulate Fas receptor signaling resulting in apoptosis and finally in acantholysis.²⁹ Another study explored c-Src-dependent EGFR activation in pemphigus.³⁰ Blocking of c-Src diminished activation of EGFR as well as of p38 MAPK and also reduced pathogenic effects of PV-IgG.

Taken together, EGFR activation could explain various aspects of acantholysis in pemphigus. Therefore, in the present work we aimed to further evaluate the role of EGFR in pemphigus by the following approaches: (i) comparing the effects of EGF and PV-IgG on human keratinocytes, (ii) investigating PV-IgG-mediated EGFR phosphorylation and (iii) examining the requirement of EGFR for PV-IgG-mediated effects by inhibition of EGFR or of c-Src.

Materials and Methods

Cell Culture and Test Reagents

The immortalized human keratinocyte cell line HaCaT³¹ was grown in Dulbecco's modified Eagles medium (Life technologies) that was supplemented with 50 U/ml penicillin-G, 50 µg streptomycin and 10% fetal calf serum (Biocrom) in a humidified atmosphere (95% air/5% CO₂) at 37°C. Normal human epidermal keratinocytes (NHEK) derived from juvenile skin were purchased from PromoCell GmbH (Heidelberg, Germany). Cells were grown in Keratinocyte Growth Medium 2 (PromoCell, Heidelberg, Germany) supplemented with 50 U/ml penicillin-G, 50 µg streptomycin and supplement mix (PromoCell). NHEK

Table 1. Antibody Profile of Pemphigus Patients' IgG

ELISA	Dsg 1 (U/ml)	Dsg 3 (U/ml)
PV-IgG 1	—	1874
PV-IgG 2	60	1000
PV-IgG 3	535	1098
PV-IgG 4	54	1239
PV-IgG 5	—	1177

were grown in low Ca²⁺ (0.15 mmol/L), which was changed to high Ca²⁺ (1.2 mmol/L) one day before experiments were started. For experiments, EGF (Sigma-Aldrich, Taufkirchen, Germany) was used at 20 ng/ml. Pharmacological inhibitor of EGFR (GW2974) (Sigma-Aldrich) at 10 µmol/L and neutralizing antibody against EGFR (LA-1) (Millipore, Schwalbach, Germany) at 1 µg/ml. c-Src inhibitor PP2 (Calbiochem, Darmstadt, Germany) was applied at 10 µmol/L. All inhibitors were pre-incubated for 2 hours. CNF-1 and CNF_γ were used at 300 ng/ml and 900 ng/ml, respectively.

Purification and Preparation of Patients' IgG

Purification was performed as described previously.¹³ Sera from two patients with mucosal-dominant PV and three patients suffering from a mucocutaneous form of PV whose diagnoses were confirmed clinically, histologically, and serologically and from a volunteer without any skin disease (control IgG) were used for the present study. Patients' sera were tested by enzyme-linked immunosorbent assay (ELISA, Medical and Biological Laboratories, Nagoya, Japan) according to the manufacturer's protocols for reactivity against Dsg 1 and Dsg 3, respectively (see Table 1). The cut-off value was 14 U/ml for Dsg 1 and 7 U/ml for Dsg 3. All samples were run in duplicate. PV-IgG 1 and 5 contained Dsg 3 but not Dsg 1 autoantibodies. PV-IgG 2, 3, and 4 contained both Dsg 1 and Dsg 3 antibodies. IgG fractions were purified by affinity chromatography using protein A agarose. Final concentrations of IgG fractions were adjusted to 500 to 1000 µg/ml for all experiments.

Cytochemistry

HaCaT cells were grown on coverslips to confluence and incubated with pemphigus IgG and indicated reagents for 24 hours or the indicated times at 37°C. After incubation, culture medium was removed, monolayers were fixed, permeabilized with ice-cold acetone for 2 minutes and washed with PBS. Afterward, HaCaT cells were incubated for 30 minutes with 10% normal goat serum and 1% bovine serum albumin in PBS at room temperature and incubated for 16 hours at 4°C with mouse monoclonal antibody directed against Dsg 3 (Zytomed, Berlin, Germany; dilution 1:100 in PBS), mouse monoclonal antibody against EGFR (Millipore; 1:100), rabbit polyclonal antibody against Y845 phospho-EGFR (Abcam, Cambridge, USA; 1:50), or mouse monoclonal cytokeratin 5 antibody (Santa Cruz, Heidelberg, Germany; 1:100). After several rinses with PBS (3 × 5 minutes), monolayers

were incubated for 60 minutes at room temperature with Cy3-labeled goat anti-mouse or goat anti-rabbit IgG (Dianova). For visualization of filamentous actin (F-actin) or nuclear staining, ALEXA 488-phalloidin (Molecular Biology, Germany; diluted 1:60 in PBS, incubation for 1 hour at room temperature) and 4,6-diamidino-2-phenylindole (Roche, 1:3000 for 10 minutes at room temperature) were used, respectively. Cells were rinsed with PBS (3 × 5 minutes) and finally mounted on glass slides with 60% glycerol in PBS, containing 1.5% n-propyl gallate (Serva, Heidelberg, Germany). Monolayers were examined using a LSM 510 (Zeiss, Oberkochen, Germany). Images were processed using Adobe Photoshop 7.0 software (Adobe, München, Germany). For evaluation of PV-IgG binding to the surface of keratinocytes, images were quantitatively measured using ImageJ (National Institutes of Health, Bethesda, MD) software analysis. Therefore, after incubation of PV-IgG on HaCaT keratinocytes for the indicated times, cells were fixed and incubated with Cy3-labeled goat anti-human antibody to detect surface-bound PV-IgG. After washing, mean fluorescent intensities were measured in 3 independent areas of each condition with ImageJ. Each condition was repeated three times.

Electrophoresis and Western Blotting

After incubation with pemphigus patients' IgG or reagents for the indicated times, HaCaT cells were dissolved in sample buffer, heated at 95°C for 5 minutes and finally subjected to sodium dodecyl sulfate 7.5% or 10% polyacrylamide gel electrophoresis and immunoblotting to Hybond nitrocellulose membranes (Amersham, Buckinghamshire, UK). Membranes were blocked with 5% low fat milk for 1 hour at room temperature in PBS and incubated with the respective primary antibody overnight at 4°C. The rabbit antibodies against EGFR (Santa Cruz) and Y845 phospho-EGFR (Abcam) as well as the mouse Y1173 phospho-EGFR (Millipore) antibody were used at 1:400. As secondary antibodies HRP-labeled goat anti-mouse or goat anti-rabbit (both from Dianova, Hamburg, Germany) were used. Visualization was achieved using the enhanced chemiluminescence technique (Amersham).

EGFR ELISA

Phosphorylation of EGFR at Y845 was detected using chemiluminescence-based FACE EGFR (Y845) ELISA Kit (Active Motif, Carlsbad, CA) according to the manufacturer's protocol. HaCaT cells were seeded on 96-well plates and grown to confluence before treatment with EGF or pemphigus patients' IgG in the absence or presence of various reagents for 1 hour.

Dispase-Based Keratinocyte Dissociation Assay

The assay was performed as described in the literature with the following modifications.^{19,32} HaCaT cells were seeded on 12-well plates and grown to confluence. After incubation for 24 hours under various conditions, cells

were washed with Hanks' buffered salt solution and treated for 30 minutes with 0.3 ml dispase II (2.4 U/ml, Sigma) at 37°C. Afterward, dispase solution was carefully removed and cells dissolved in 0.5 ml Hank's buffered salt solution (HBSS). Mechanical stress was then applied by pipetting 10 times with a 1 ml pipette. Finally, dissociation was quantified by counting and averaging cell fragments in three defined areas of each condition under a binocular microscope. Every condition was repeated at least four times.

Laser Tweezer

Expression and purification of recombinant Dsg 3 and Dsg 1, coating of polystyrene beads and the laser tweezer set-up were described previously in detail.¹³ Coated beads (10 µl of stock solution) were suspended in 200 µl of culture medium and allowed to interact with HaCaT monolayers for 30 minutes at 37°C before measuring the number of bound beads (= control values). Beads were considered tightly bound when resisting laser displacement at 42 mW setting. For every condition 100 beads were counted. Afterward, EGF or PV-IgG with or without test reagents (pre-incubated for 2 hours) were applied for 30 minutes or the indicated times. Percentage of beads resisting laser displacement under various experimental conditions was normalized to control values.

Statistics

Differences in ELISA values or bead adhesion between different protocols have been assessed using two-tailed Student's *t*-test. Mann-Whitney *U*-test was used for comparison of dispase-based dissociation assay experiments. Values throughout are expressed as mean ± SE. Statistical significance is assumed for *P* < 0.05.

Results

Effects of EGF and PV-IgG Treatment on Human Keratinocytes

In our study, we compared the effects of PV-IgG versus EGF treatment in various experimental setups to gain insight into the role of EGFR in pemphigus. First, we tested the effects of EGF and PV-IgG on desmosomes and the intermediate filament cytoskeleton in cultured human keratinocytes (HaCaT) using immunostaining. In addition, Alexa 488-phalloidin staining of filamentous actin (F-actin) was applied to sensitively detect keratinocyte dissociation, especially under conditions when Dsg 3 staining was altered and thus cell borders were hard to identify. Under control conditions, Dsg 3 was distributed along cell-cell borders together with F-actin (Figure 1, A and B). To examine pathogenic effects on the cytokeratin filament network, we stained the cells for cytokeratin 5 (CK5). In controls, CK5 was detected as a meshwork throughout the cytoplasm except of the cell periphery where staining was weak (Figure 1C). Incubation for 24

478 Heupel et al
AJP February 2009, Vol. 174, No. 2

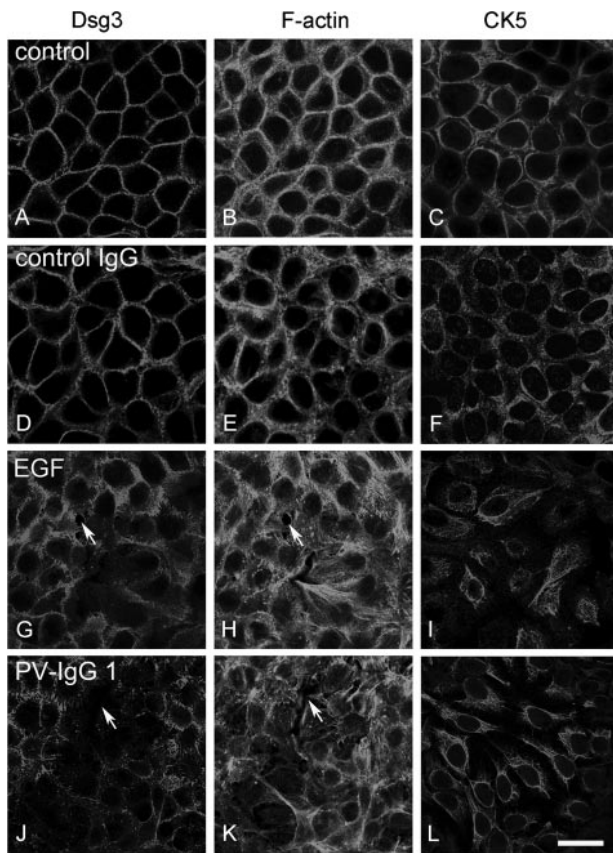


Figure 1. PV-IgG and EGF caused cell dissociation and cytokeratin retraction in keratinocyte monolayers. HaCaT cells were stained for Dsg 3 (A, D, G, J), F-actin (B, E, H, K), or cytokeratin 5 (CK5, C, F, I, L). In control monolayers (A–C) or cells treated with control IgG for 24 hours (D–F), Dsg 3 was distributed along cell borders (A, D) along with F-actin (B, E). Cytokeratin 5 (CK5) immunostaining was detected throughout the cytoplasm except the cell periphery where staining was weak (C, F). EGF treatment caused intracellular gap formation (arrows in G, H) and prominent CK5 retraction (I). Similarly, incubation with PV-IgG 1 (J–L) resulted in intercellular gap formation (arrows in J, K) and CK5 retraction (L) that additionally was accompanied by disruption of Dsg 3 staining (J). Scale bar = 20 μ m for all panels ($n = 4$).

hours with control IgG yielded a similar phenotype (Figure 1, D–F). In contrast, EGF caused formation of intercellular gaps and keratinocyte dissociation after 24 hours, paralleled by disorganization of the actin cytoskeleton including the generation of stress fibers and short F-actin aggregates (Figure 1, G–H). More significantly, CK5 staining revealed a strong retraction of keratin filaments from the cell periphery to the perinuclear area (Figure 1I). These effects already appeared after 2 hours (not shown), but were more prominent after 24 hours EGF treatment. Similarly, PV-IgG incubation caused keratinocyte dissociation, actin reorganization and cytokeratin retraction (Figure 1, J–L). However, in contrast to EGF, Dsg 3 staining shifted from the membrane to the cytoplasm and was fragmented along cell borders in response to PV-IgG indicating loss and aggregation of desmosomes. Experiments were reproduced with PV-IgG 2–4 (data not shown). Thus, prominent cytokeratin retraction and intercellular gap formation were induced by both EGF and PV-IgG. All experiments were repeated with NHEK cells, which yielded similar results

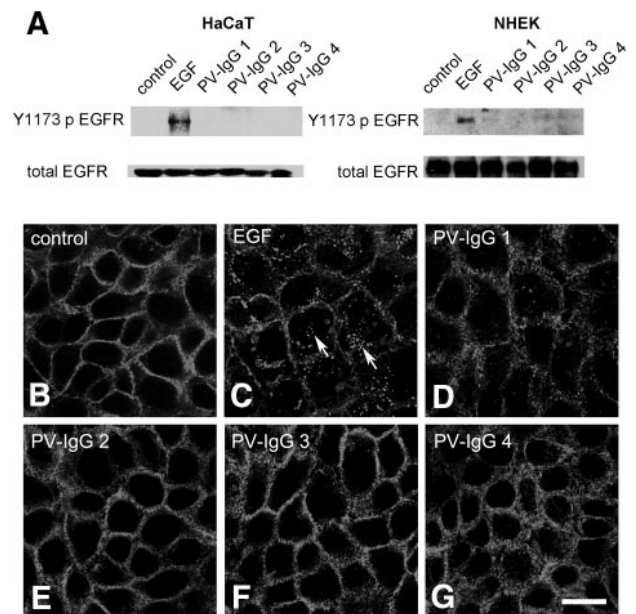


Figure 2. EGF but not PV-IgG caused phosphorylation of EGFR at Y1173 and internalization of EGFR. **A:** In contrast to treatment of HaCaT cells with EGF, PV-IgG 1–4 did not induce phosphorylation of EGFR at Y1173 as revealed by western blotting. Total EGFR amounts were similar under all conditions G. Comparable results were obtained in experiments with NHEK cells. **B–D:** As revealed by immunostaining, EGFR was continuously distributed along HaCaT cell borders (B). EGF treatment (1 hour) resulted in the appearance of intracellular punctuated EGFR staining likely reflecting EGFR internalization (arrows in C). In contrast, no EGFR endocytosis was observed following 1–4 hours PV-IgG treatment (D–G). Scale bar = 20 μ m for all panels. ($n = 4$).

(data not shown). These data suggested that EGFR signaling may account for at least some of the autoantibody-mediated effects, a conclusion that led us to further explore whether EGFR was activated by PV-IgG under these conditions.

EGF but Not PV-IgG Caused Canonical Activation of EGFR

Next we tested if PV-IgG were capable to activate EGFR via the canonical EGF pathway. It is known that EGFR is classically activated via ligand binding leading to dimerization and intracellular EGFR kinase activation.²² This finally results in Y1173 EGFR phosphorylation, subsequent initiation of the MAP kinase cascade as well as in EGFR endocytosis and termination of EGFR signaling.

We incubated EGF or PV-IgG on HaCaT cells for 1 hour and subsequently probed for Y1173 phospho-EGFR in Western blotting studies (Figure 2A) because previous studies from the literature reported significant phosphorylation of EGFR within 1 hour.^{29,30} As expected, EGF treatment resulted in strong phosphorylation of EGFR at Y1173. However, no enhanced signal was seen after PV-IgG 1–4 treatment. Comparable results were obtained when longer incubation periods for up to 24 hours were used. To exclude that EGFR activation is impaired in immortalized HaCaT keratinocytes, experiments were repeated with NHEK cells (Figure 2A). However, Western blotting studies using the Y1173 phospho-EGFR antibody

similarly showed that PV-IgG did not activate EGFR by phosphorylation at Y1173.

Immunostaining revealed EGFR to be localized continuously along cell borders in HaCaT cells (Figure 2B). EGF treatment for 1 hour resulted in punctuated EGFR staining within the cytoplasm of HaCaT cells likely representing endocytosed vesicles containing EGFR (Figure 2C). After PV-IgG treatment, localization of EGFR was not altered (Figure 2, D–G). This was also confirmed in EGFR-over-expressing A431 cells (data not shown). Therefore, canonical activation with phosphorylation of EGFR at Y1173 leading to EGFR endocytosis was not observed in response to PV-IgG, which is in contrast to previous findings from the literature.^{29,30}

EGF but Not PV-IgG Led to Phosphorylation of EGFR at Y845

As a next step, we looked for other modes of EGFR activation by PV-IgG. Y845 is not only an autophosphorylation site in the kinase domain of EGFR but also phosphorylated by c-Src.³³ Since it was recently reported that c-Src is activated after PV-IgG treatment,³⁰ it was important to test if EGFR was phosphorylated at Y845 in response to PV-IgG. We measured phosphorylation of EGFR at Y845 using a commercial ELISA kit (Figure 3A). Control IgG did not lead to an enhanced signal in ELISA experiments. EGF induced a strong phosphorylation (ELISA score 1585% \pm 244% of control). This signal could be efficiently blocked to 42% \pm 5%, 45% \pm 10% and 61% \pm 2% of EGF values using neutralizing EGFR antibody (LA-1), pharmacological inhibitors of EGFR (GW2974) or c-Src kinase (PP2) (Figure 3B). Surprisingly, all PV-IgG tested also resulted in strong and significant EGFR phosphorylation (ELISA scores 590% \pm 16%, 748% \pm 55%, 680% \pm 67%, Figure 3A). These signals, however, were also detected when the respective secondary antibody was applied without Y845 phospho-EGFR primary antibody (ELISA scores 686% \pm 23%, 937% \pm 38%, 476% \pm 66%, respectively). This indicated that the ELISA signals were due to cross-reactivity of the ELISA secondary goat anti-rabbit (garb) antibody with pemphigus IgG bound to the keratinocyte surface. Consistent with this, PV-IgG-induced signals in ELISA experiments were not blocked by LA-1, GW2974, or PP2 (Figure 3B).

We further investigated phosphorylation of EGFR at Y845 by immunostaining. Under control conditions, HaCaT cells did not show any signal using the Y845 phospho-EGFR antibody (Figure 3C) but were positive for total EGFR (Figure 3D). EGF treatment for 1 hour resulted in Y845 phosphorylation of EGFR at the cell membrane as well as in endocytosis of phosphorylated EGFR (arrows in Figure 3E and F). Following treatment with PV-IgG 2, Y845 phospho-EGFR signals were detected at cell borders but no intracellular punctuated staining was observed (Figure 3G and H). However, a similar signal at sites of cell borders was also present following PV-IgG 2-treatment when the secondary garb antibody was used in the absence of the Y845 phospho-EGFR antibody (Fig-

ure 3I). Again, this demonstrated that the secondary garb antibody cross-reacted with PV-IgG bound to the HaCaT surface. Consistent with this interpretation, deposition of PV-IgG on HaCaT cells after 1 hour incubation was confirmed using goat anti-human staining (Figure 3J).

To further substantiate this finding, we performed Western blotting of HaCaT cells treated with EGF or PV-IgG for 1 hour (Figure 3K). Total EGFR amounts were equal in the three experimental conditions. EGF treatment resulted in a strong Y845 phospho-EGFR immunosignal at the expected EGFR size (170 kDa). In controls as well as following incubation with PV-IgG 2, no band was detectable at 170 kDa. However, following incubation with PV-IgG a strong band was visible migrating at 55 kDa. This band was independent of the primary Y845 phospho-EGFR antibody as demonstrated by Western blotting using secondary garb antibody alone (Figure 3L). Similar results were obtained using a goat anti-human secondary antibody and confirmed for 3 additional PV-IgG (not shown). Therefore, this band most likely represented denatured heavy chain fragments of PV-IgG in the cell lysates. We further investigated EGFR phosphorylation at Y845 in NHEK cells (Figure 3M). However, consistent with results from HaCaT cells, only EGF treatment but not incubation with 4 different PV-IgG fractions resulted in Y845 phosphorylation as revealed by Western blotting (Figure 3M).

We then investigated if PV-IgG-induced phosphorylation of EGFR at Y845 occurred at other time points (Figure 4). However, when PV-IgG were incubated on HaCaT for 15, 30, 60 or 120 minutes, EGFR Y845 ELISA signals were indistinguishable to secondary antibody controls (Figure 4A). To investigate whether ELISA values of secondary antibody controls were caused by time-dependent binding characteristics of PV-IgG to the keratinocyte surface, we quantified PV-IgG binding to the surface of HaCaT cells following immunostaining during the same time course. Clearly, a time-dependent binding of PV-IgG to the keratinocyte surface was detected by fluorescence quantification on HaCaT cells, which had been treated with PV-IgG 5 for the indicated times and stained with Cy3-labeled goat anti-human antibody to detect surface-bound PV-IgG (Figure 4B). PV-IgG binding peaked after 1 hour incubation but was reduced after 2 hours. Taken together, ELISA, immunostaining and Western blotting studies showed that PV-IgG did not lead to phosphorylation of EGFR at Y845. Rather, secondary antibody cross-reactivity was observed in all three experimental setups.

Inhibition of EGFR and c-Src Blocked EGF-induced Keratinocyte Dissociation Whereas PV-IgG-induced Effects Were Not Prevented

Since we did not observe activation of EGFR following incubation with PV-IgG in our experiments, we further explored if blocking EGFR or c-Src function was able to prevent EGF- or PV-IgG-induced effects on keratinocytes (Figure 5, compare with Figure 1). EGF-induced intercellular gap formation and keratinocyte dissociation were blocked by pharmacological EGFR inhibition (GW2974,

480 Heupel et al
AJP February 2009, Vol. 174, No. 2

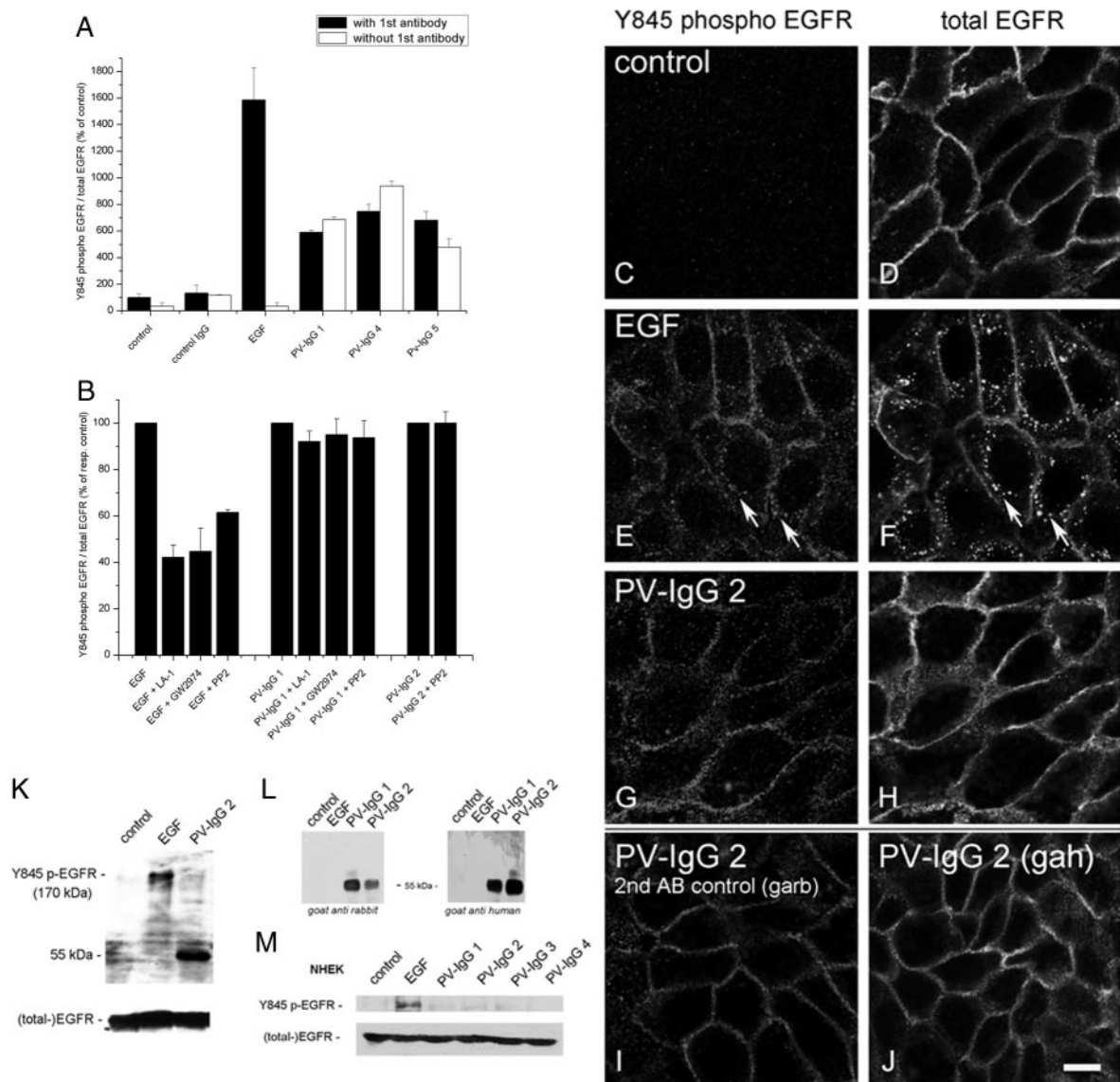


Figure 3. PV-IgG did not induce phosphorylation of EGFR at Y845. **A:** ELISA studies revealed phosphorylation of EGFR at Y845 after EGF but not after control IgG treatment. All three PV-IgG tested also caused an apparent Y845 EGFR phosphorylation. These ELISA signals, however, were also detectable when experiments were performed in the absence of Y845 phospho-EGFR primary antibody indicating cross-reactivity of the secondary goat anti-rabbit (garb) antibody with pemphigus IgG bound to the keratinocyte surface ($n = 4$ to 6). **B:** EGF-induced EGFR phosphorylation at Y845 was reduced by EGFR neutralizing antibody LA-1, inhibition of intrinsic EGFR kinase activity by GW2974 and inhibition of c-Src via PP2. In contrast, these inhibitors did not reduce the PV-IgG 1-induced Y845 EGFR phosphorylation signal ($n = 3$). **C–J:** Moreover, immunostaining using a Y845 phospho-EGFR antibody did not reveal PV-IgG-induced Y845 EGFR phosphorylation. HaCaT cells were immunostained for Y845 phospho-EGFR (**C, E, G, I**) and total EGFR (**D, F, H, J**). Under control conditions, HaCaT cells showed no Y845 phospho-EGFR-specific signal (**C**) but were positive for total EGFR (**D**). EGF treatment (1 hour) resulted in Y845 phospho-EGFR immunostaining at cell borders as well as punctuated staining in the cytoplasm (arrows in **E** and **F**). Following incubation with PV-IgG, Y845 phospho-EGFR staining was detected at cell borders but was absent within the cytoplasm (**G** and **H**). Similar staining patterns were obtained after PV-IgG treatment when secondary garb or goat anti-human (gah) antibodies were applied in the absence of primary antibodies (**I** and **J**). Scale bar = 20 μm for all panels. ($n = 3$). **K:** Western blotting revealed that EGF but not PV-IgG caused Y845 EGFR phosphorylation. In controls and following incubation with PV-IgG, no band was detectable at 170 kDa indicating that EGFR was not phosphorylated at Y845 under these conditions. In contrast, EGF treatment resulted in a strong immunosignal at the expected EGFR size (170 kDa). After treatment with PV-IgG, a strong band was visible migrating at 55 kDa. This band likely represented PV-IgG heavy chains in cell lysates as demonstrated by Western blotting using secondary garb or gah antibodies in the absence of primary antibodies (**L**). ($n = 3$). **M:** Western blotting with NHEK lysates confirmed that treatment with EGF but not with PV-IgG resulted in phosphorylation of EGFR at Y845. Total EGFR bands revealed equal sample loading.

Figure 5A–B) and partially by inhibition of c-Src via PP2 (arrows in Figure 5D–E). EGF-induced cytokeratin retraction was largely abolished by inhibition of both EGFR and c-Src (Figure 5 C and F). In contrast, effects of PV-IgG on HaCaT cells were neither altered by inhibition of EGFR nor of c-Src because intercellular gaps (arrows) and retraction of cytokeratin filaments were discernable under

these conditions (Figure 5G–L). Similar results were obtained using NHEK cells (data not shown).

Next, we quantified cell dissociation in response to EGF and PV-IgG treatment using a standard keratinocyte dissociation assay (Figure 6). Under control conditions, 8 ± 2 cell fragments were counted per cm^2 after applying mechanical stress to dispase-treated monolayers. EGF

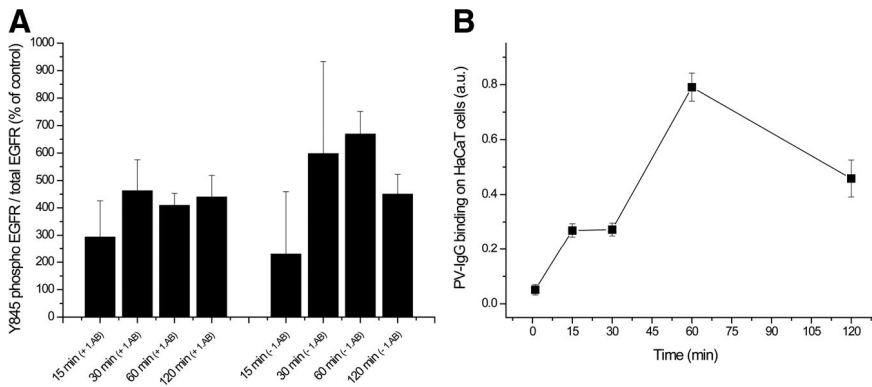


Figure 4. No time-dependent phosphorylation of EGFR at Y845 but binding of PV-IgG to the keratinocyte cell surface. **A:** In time-dependent ELISA studies no specific phosphorylation of EGFR at Y845 after PV-IgG 5 treatment (+1. AB) was observed when directly compared with secondary antibody controls (-1. AB). No statistical differences were detected between different time points and experimental conditions (+1. AB vs. -1. AB). **B:** Binding of PV-IgG 5 to HaCaT cells was determined using quantitative immunostaining of HaCaT cells treated with PV-IgG 5 for the indicated times and stained with Cy3-labeled goat anti-human antibody to detect surface-bound PV-IgG. A clear time-dependent binding of PV-IgG to the keratinocyte surface was detected peaking at 1 hour but declining after 2 hours.

treatment led to a significant increase in fragments (67 ± 6) confirming the findings of the immunofluorescent studies (Figure 1G-I). All 3 PV-IgG tested in the assay (PV-IgG 1, 2, 4) also resulted in strong cell dissociation as marked by increased numbers of cell fragments (203 ± 33 , 177 ± 16 , 66 ± 7 , respectively). Simultaneous incubation of monolayers with EGF in the presence of GW2974 or PP2

partially blocked cell dissociation (15 ± 3 fragments for each condition). In contrast, acantholytic effects of PV-IgG 1, 2 and 4 were independent of EGFR kinase or c-Src because coincubation with GW2974 or PP2 did not significantly alter the number of cell fragments (156 ± 41 and 237 ± 44 for PV-IgG 1, 180 ± 23 and 159 ± 5 for PV-IgG 2 and 77 ± 6 and 78 ± 9 for PV-IgG 4, respectively). These data indicate that inhibition of EGFR signaling was not effective to block PV-IgG-induced cell dissociation. Therefore, to prove that acantholysis caused by PV-IgG can be inhibited by interference with cellular signaling, experiments were performed with Rho A-activating toxins cytotoxic necrotizing factor (CNF) 1 and CNFy. These toxins were shown to block PV-IgG-induced epidermal splitting in skin organ culture as well as autoantibody-mediated intercellular gap formation and loss of Dsg bead binding in laser tweezer assays in HaCaT cells.^{18,34} Consistent with these previous findings, selective activation of Rho A by CNFy was equally effective like activation of all three Rho family GTPases Rho A, Rac 1,

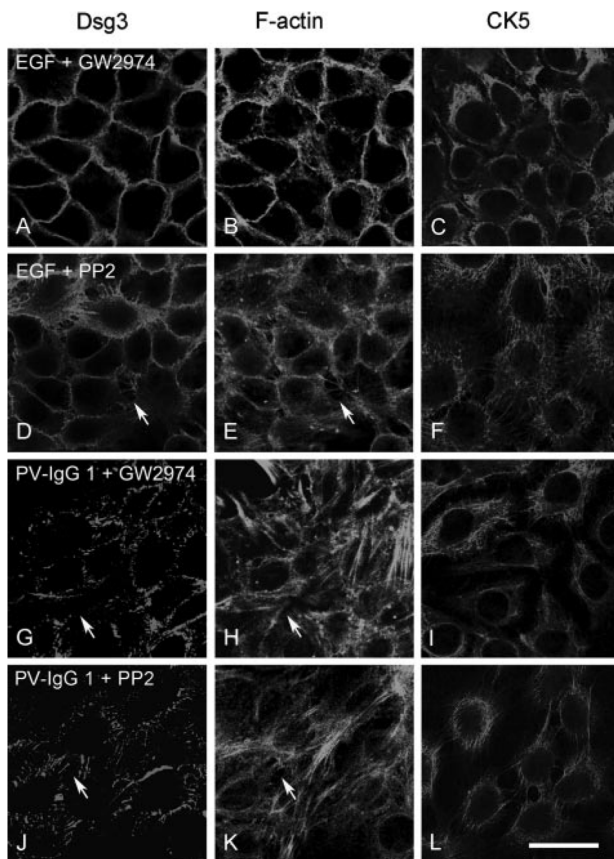


Figure 5. Inhibition of EGFR but not of c-Src blocked EGF-mediated keratinocyte dissociation whereas PV-IgG-induced effects were not affected. HaCaT cells were immunostained for Dsg 3 (A, D, G, J) and for CK5 (C, F, I, L) and F-actin was labeled using Alexa 488-phalloidin (B, E, H, K). **A-C:** EGF-induced effects on keratinocyte monolayers including intercellular gap formation and keratinocyte retraction (compare to Figure 1, G-I) were effectively blocked by pharmacological EGFR inhibition (GW2974). c-Src inhibition via PP2 did partially block EGF-induced intercellular gap formation (arrows in D-E) prevented keratin retraction (F). **G-I:** In contrast, neither inhibition of EGFR (G-I) nor of c-Src (J-L) was effective to reduce PV-IgG-induced keratinocyte dissociation (arrows in G, H, J, K) and cytokeratin retraction (I, L). Scale bar = 20 μ m for all panels. ($n = 4$).

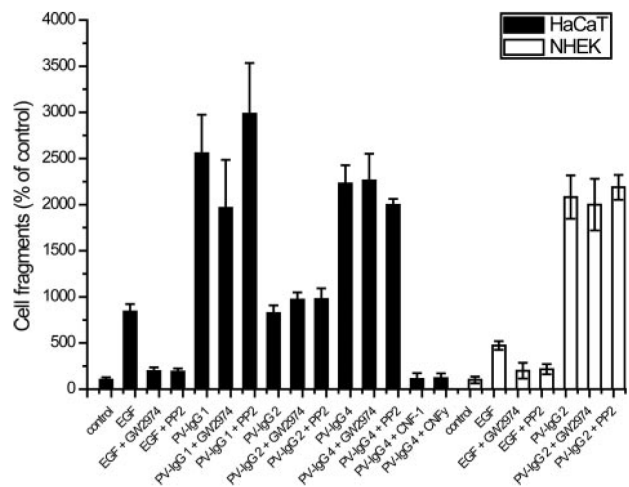


Figure 6. EGF but not PV-IgG caused keratinocyte dissociation dependent on EGFR and c-Src signaling. Keratinocyte dissociation was further quantified using a dispase-base assay. EGF treatment resulted in a strong increase of cell fragments compared with controls. This increase was partially blocked by simultaneous incubation with EGFR kinase inhibitor GW2974 or c-Src inhibitor PP2. In contrast, PV-IgG-mediated acantholysis was independent of EGFR kinase or c-Src because GW2974 and PP2 did not prevent increase in cell fragments. However, cotreatment with CNF1 and CNFy inhibited PV-IgG 4-induced cell dissociation. Similarly, in NHEK cells GW2974 and PP2 application were only sufficient to inhibit EGF- but not PV-IgG-mediated cell layer fragmentation ($n = 6$ for each condition).

482 Heupel et al
AJP February 2009, Vol. 174, No. 2

and Cdc42 by CNF-1 to block pemphigus IgG-induced acantholysis (Figure 6).

We repeated these experiments using NHEK cells (Figure 6). EGF treatment led to cell dissociation ($473\% \pm 46\%$ compared with controls), which was significantly reduced by both GW2974 ($200\% \pm 85\%$) and PP2 treatment ($216\% \pm 55\%$). In contrast, PV-IgG 2 resulted in strong cell sheet fragmentation ($2082\% \pm 234\%$), which was blocked neither by GW2974 ($2000\% \pm 279\%$) nor by treatment with PP2 ($2188\% \pm 135\%$). Taken together, EGFR kinase seemed to be important for EGF-induced keratinocyte dissociation but not to be essential for acantholysis in pemphigus.

PV-IgG Interfered with Dsg-mediated Bead Binding Independent of EGFR or c-Src Whereas EGF Had No Effect

Next, we investigated whether EGFR and c-Src were required for PV-IgG-induced loss of Dsg binding. Previous studies using laser tweezers demonstrated that activation of Rho A by CNF-1 and CNF γ was effective to inhibit PV-IgG-induced loss of Dsg bead binding, consistent with experiments using the cell dissociation assay described above.^{18,34} Therefore, laser tweezers seem to provide an adequate and sensitive approach to evaluate the involvement of different signaling cascades in pemphigus-mediated loss of Dsg binding. In contrast to dissociation assays that quantify keratinocyte cohesion as a result of all of the different intercellular adhesion molecules involved, the laser tweezer assays allows to study the effect of PV-IgG on a single type of adhesion molecule on the microbead surface.

In this assay, binding of Dsg-coated microbeads was probed by laser beam-mediated displacement on the surface of HaCaT cells (Figure 7). Dsg 3- (black bars) and Dsg 1 coated beads (white bars) were allowed to settle on the surface of HaCaT cells for 30 minutes (control) and bound beads were counted. After application of PV-IgG or EGF, the number of bound beads was counted again. The numbers of bound Dsg 3- or Dsg 1-coated beads were not altered following incubation with control IgG but were reduced by incubation with EGTA (5 mmol/L, 30 minutes) to $41\% \pm 6\%$ and $22\% \pm 3\%$ of control levels, respectively. This proved that bead binding was mediated by Ca²⁺-dependent Dsg transinteraction. Neither short term (30 minutes) nor long term (24 hours) treatment with EGF blocked Dsg 3- or Dsg 1-mediated binding. In contrast, incubation of monolayers and attached beads with PV-IgG 2 reduced adhesion of Dsg 3- and Dsg 1-coated beads ($75\% \pm 6\%$ and $54\% \pm 4\%$, respectively), similar to our previous studies.^{13,14,18,34} This reduction, however, was not altered by simultaneous inhibition of EGFR via GW2974 or of c-Src via PP2. In this context, our new data therefore indicate that EGFR and c-Src were not required for PV-IgG-induced loss of Dsg bead binding. Moreover, EGF obviously caused keratinocyte dissociation via mechanisms other than loss of Dsg 3 and Dsg 1 binding.

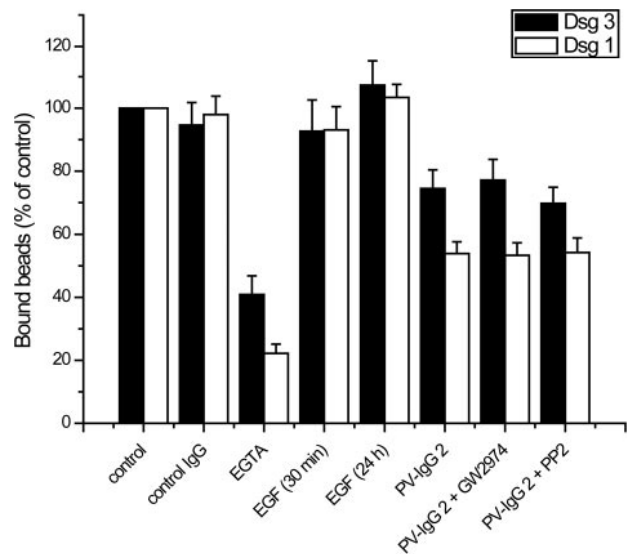


Figure 7. Inhibition of EGFR or c-Src did not prevent PV-IgG-induced loss of Dsg-mediated bead binding in laser tweezer experiments. Dsg 3- (black bars) and Dsg 1 coated beads (white bars) were allowed to settle on the surface of HaCaT cells for 30 minutes before the number of bound beads was counted (control). After application of PV-IgG or EGF, the number of adhering beads was counted again. The number of bound Dsg 3- or Dsg 1-coated beads was not altered after control IgG treatment but reduced by incubation with EGTA (5 mmol/L, 30 minutes) to $41\% \pm 6\%$ and $22\% \pm 3\%$, respectively. EGF did not block Dsg 3- or Dsg 1-mediated binding after incubation for 30 minutes or 24 hours. In contrast, incubation of monolayers and attached beads with PV-IgG 2 for 30 minutes reduced the numbers of Dsg 3 and Dsg 1 beads to $75\% \pm 6\%$ and $54\% \pm 4\%$, respectively. This reduction was unaffected by blocking of EGFR via preincubation with GW2974, or of c-Src via preincubation with PP2. ($n = 6$ for each condition).

Discussion

We investigated the role of EGFR and c-Src in pemphigus pathogenesis by directly comparing EGF- and PV-IgG-mediated effects on cultured human keratinocytes. Although in our experimental setup the effects of EGF and PV-IgG on keratinocyte morphology appeared to be very similar, we did not observe canonical or c-Src-dependent activation of EGFR in response to incubation with PV-IgG. Moreover, inhibition of EGFR or c-Src did not block PV-IgG-induced loss of Dsg binding, cytokeratin retraction and keratinocyte dissociation. Thus, EGFR and c-Src signaling may not be primarily required for PV-IgG-induced acantholysis *in vitro*. Moreover the mechanisms involved in EGF- and PV-IgG-induced keratinocyte dissociation and cytokeratin retraction seem to be different.

Mechanisms by Which EGF Reduces Keratinocyte Cohesion

EGFR activation leads to c-Src activation and plakoglobin phosphorylation, which in turn is known to weaken keratinocyte cohesion and to rearrange the cytokeratin filament network.^{27,28,35} In our experiments, EGF triggered intercellular gap formation and cytokeratin retraction. These effects were blocked by pharmacological inhibitors of EGFR kinase as well as of c-Src, suggesting that EGF-mediated keratinocyte dissociation is at least partly dependent on c-Src.

The mechanisms underlying EGF-induced loss of cell adhesion are only beginning to emerge. Gaudry and colleagues demonstrated that EGF-induced disruption of intercellular cohesion was at least in part mediated by loss of Dsg 2 binding.²⁷ It appeared that EGF caused uncoupling of the Dsg 2-plakoglobin complex from the cytokeratin cytoskeleton because desmoplakin, the primary molecule responsible for cytoskeletal anchorage, was not linked to plakoglobin following EGFR-mediated plakoglobin phosphorylation. However, the effects of EGF signaling on Dsg 3 and Dsg 1, the main targets in pemphigus pathogenesis, have not been characterized so far. Although resulting in intercellular gap formation, EGF failed to reduce Dsg 3- and Dsg 1-mediated bead binding in laser tweezer experiments. Therefore, one could speculate that EGF-mediated loss of cell adhesion is not primarily mediated by inhibition of Dsg 3 and Dsg 1 binding, but rather by other cell adhesion molecules such as Dsg 2 or E-cadherin. This is puzzling since Dsg 3 and Dsg 1 are also anchored to cytokeratin filaments via plakoglobin and desmoplakin and consequently should also be affected by EGFR-mediated plakoglobin phosphorylation. However, other mechanisms in addition to plakoglobin phosphorylation may contribute to EGF-induced cell dissociation because a plakoglobin mutant missing the phosphorylation sites required for EGFR-mediated phosphorylation only partially blocked cell dissociation in response to EGF treatment.²⁸ These mechanisms may involve proteases of the ADAM (a disintegrin and metalloprotease) family. It was demonstrated that EGF increased cellular ADAM10 and ADAM17 levels and thereby caused Dsg 2 and E-cadherin degradation.^{36,37} This is in line with the increased cell dissociation revealed by the keratinocyte dissociation assay in our study. Consistent with our observation that PV-IgG did not activate EGFR and the hypothesis that EGF caused cell dissociation via adhesion molecules others than Dsg 3 and Dsg 1, we did neither find PV-IgG-induced activation of ADAM17 nor shedding of Dsg 3 or Dsg 1 in HaCaT monolayers (unpublished observations). However, it has to be emphasized that in the laser tweezer setup we are only in the position to test binding of non-desmosomal Dsg molecules on the keratinocyte cell surface. Therefore, we cannot completely rule out that EGF-treatment reduces adhesion of Dsg 3 and Dsg 1 molecules within desmosomes.

Role of EGFR and c-Src in Pemphigus

The hypothesis that EGFR signaling plays a significant role in pemphigus pathogenesis is tempting because EGF-induced effects on keratinocytes such as a profound loss of cell cohesion as well cytokeratin retraction are hallmarks of acantholysis in pemphigus. Therefore, Dsg 3 molecules on the cell surface have been proposed to mediate antibody-triggered outside-in signaling at least in part via cross talk with receptor tyrosine kinases such as EGFR.¹⁵ This has already been demonstrated for other cadherins in keratinocytes: transinteracting E-cadherin molecules recruit EGFR resulting in phosphatidylinositol-3-kinase and Akt activation,^{38,39} which is thought

to finally result in cell contact-induced stop of cell proliferation. This mechanism is believed to be part of the so-called "contact inhibition". Because loss of E-cadherin binding should have the opposite effect and therefore lead to increased cell proliferation, it is interesting to note that autoantibodies against Dsg 1 in pemphigus have been shown to cross-react with E-cadherin.¹⁰ However, it remains to be elucidated whether these antibodies interfere with E-cadherin transinteraction. Nevertheless, in our experiments we did neither find canonical activation of EGFR at Y1173 followed by receptor internalization nor phosphorylation at Y845, although in parallel experiments EGF was effective to induce such effects. Accordingly, PV-IgG-induced keratinocyte dissociation, loss of Dsg 3 bead binding in laser tweezer experiments and cytokeratin retraction were not abolished by inhibition of EGFR and c-Src signaling. Thus, the pathogenic effects of PV-IgG under the conditions used in our study were independent of EGFR or c-Src.

It has to be emphasized that our findings contradict previous reports.^{29,30} However, to detect EGFR activation in these studies unspecific phospho-tyrosine antibodies instead of phospho-specific EGFR-antibodies were used.²⁹ In another study, the same ELISA-based measurements of EGFR phosphorylation were used like in our study,³⁰ which, as outlined below, may lead to unspecific signals by interaction of secondary antibodies with keratinocyte-bound PV-IgG. The authors used siRNA to reduce Dsg 3 and Dsg 1 expression and found that PV-IgG-mediated EGFR and c-Src activation was independent of autoantibodies against Dsg 3 and 1.³⁰ From these findings it was concluded that only non-Dsg autoantibodies could activate these signaling mechanisms. In contrast, our previous studies indicate that pathogenic effects of PV-IgG and PF-IgG were dependent on antibodies against Dsg 3 and Dsg 1 because immunoprecipitation using recombinant molecules completely abolished pathogenic effects of autoantibody fractions.^{13,14} Because direct inhibition of Dsg 1 binding by PV-IgG and PF-IgG was not detected in these studies, it is likely that autoantibodies against desmogleins are capable to trigger cellular signaling mechanisms. We characterized autoantibody fractions used in this study only in respect of anti-Dsg autoantibodies whereas identification of all other possible autoantigens was not possible. This is because a plethora of more than 20 different autoantibodies has been found in pemphigus patients' sera of which the pathological significance mostly has not been characterized yet.^{1,6-9} Therefore, it has to be emphasized that we cannot completely rule out that PV-IgG from other patients activate EGFR signaling and that this may be mediated by autoantibodies against autoantigens different from Dsg 3 and Dsg 1. Nevertheless this study demonstrates that PV-IgG-induced acantholysis in human keratinocytes is independent of EGFR signaling.

Cross-Reactivity of Secondary Antibodies with Patients' Autoantibodies in Pemphigus Research

Our data indicate that secondary antibody cross-reactivity with pemphigus autoantibodies bound to the keratinocyte cell surface may result in false-positive signals in several

484 Heupel et al
AJP February 2009, Vol. 174, No. 2

antibody-based detection methods such as immunostaining, Western blotting or ELISA. Working with high concentrations of pemphigus autoantibodies leads to significant deposition of autoantibodies on the keratinocyte cell surface. Especially, when highly sensitive detection methods such as ELISA are used, the cross-reactivity of secondary antibodies with cell-bound autoantibodies may account for positive signals that cannot be reproduced by other methods.

Acknowledgments

We thank Lisa Bergauer and Tanja Reimer for excellent technical assistance and Volker Spindler for technical advice.

References

- Waschke J: The desmosome and pemphigus. *Histochem Cell Biol* 2008, 130:21–54
- Stanley JR, Amagai M: Pemphigus bullous impetigo, and the staphylococcal scalded-skin syndrome. *N Engl J Med* 2006, 355:1800–1810
- Anhalt GJ, Labib RS, Voorhees JJ, Beals TF, Diaz LA: Induction of pemphigus in neonatal mice by passive transfer of IgG from patients with the disease. *N Engl J Med* 1982, 306:1189–1196
- Amagai M, Klaus-Kovtun V, Stanley JR: Autoantibodies against a novel epithelial cadherin in pemphigus vulgaris, a disease of cell adhesion. *Cell* 1991, 67:869–877
- Stanley JR, Koulu L, Thivolet C: Distinction between epidermal antigens binding pemphigus vulgaris and pemphigus foliaceus autoantibodies. *J Clin Invest* 1984, 74:313–320
- Amagai M, Karpati S, Prussick R, Klaus-Kovtun V, Stanley JR: Autoantibodies against the amino-terminal cadherin-like binding domain of pemphigus vulgaris antigen are pathogenic. *J Clin Invest* 1992, 90:919–926
- Nguyen VT, Ndoye A, Shultz LD, Pittelkow MR, Grando SA: Antibodies against keratinocyte antigens other than desmogleins 1 and 3 can induce pemphigus vulgaris-like lesions. *J Clin Invest* 2000, 106:1467–1479
- Nguyen VT, Ndoye A, Grando SA: Pemphigus Vulgaris Antibody Identifies Pemphaxin. A novel keratinocyte annexin-like molecule binding acetylcholine. *J Biol Chem* 2000, 275:29466–29476
- Nguyen VT, Ndoye A, Grando SA: Novel human $\{\alpha\}$ 9 acetylcholine receptor regulating keratinocyte adhesion is targeted by pemphigus vulgaris autoimmunity. *Am J Pathol* 2000, 157:1377–1391
- Evangelista F, Dasher DA, Diaz LA, Prisanth PS, Li N: E-cadherin is an additional immunological target for pemphigus autoantibodies. *J Invest Dermatol* 2008, 128:1710–1718
- Puviani M, Marconi A, Cozzani E, Pincelli C: Fas ligand in pemphigus sera induces keratinocyte apoptosis through the activation of caspase-8. *J Invest Dermatol* 2003, 120:164–167
- Amagai M, Ahmed AR, Kitajima Y, Bystryn JC, Milner Y, Gniadecki R, Hertl M, Pincelli C, Fridkis-Hareli M, Aoyama Y, Frusio-Zlotkin M, Muller E, David M, Mimouni D, Vind-Kezunovic D, Michel B, Mahoney M, Grando S: Are desmoglein autoantibodies essential for the immunopathogenesis of pemphigus vulgaris, or just 'witnesses of disease'? *Exp Dermatol* 2006, 15:815–831
- Waschke J, Bruggeman P, Baumgartner W, Zillikens D, Drenckhahn D: Pemphigus foliaceus IgG causes dissociation of desmoglein 1-containing junctions without blocking desmoglein 1 transinteraction. *J Clin Invest* 2005, 115:3157–3165
- Heupel WM, Zillikens D, Drenckhahn D, Waschke J: Pemphigus vulgaris IgG directly inhibit desmoglein 3-mediated transinteraction. *J Immunol* 2008, 181:1825–1834
- Muller EJ, Williamson L, Kolly C, Suter MM: Outside-in signaling through integrins and cadherins: a central mechanism to control epidermal growth and differentiation? *J Invest Dermatol* 2008, 128:501–516
- Berkowitz P, Hu P, Liu Z, Diaz LA, Enghild JJ, Chua MP, Rubenstein DS: Desmosome signaling. Inhibition of p38MAPK prevents pemphigus vulgaris IgG-induced cytoskeleton reorganization. *J Biol Chem* 2005, 280:23778–23784
- Berkowitz P, Hu P, Warren S, Liu Z, Diaz LA, Rubenstein DS: p38MAPK inhibition prevents disease in pemphigus vulgaris mice. *Proc Natl Acad Sci USA* 2006, 103:12855–12860
- Waschke J, Spindler V, Bruggeman P, Zillikens D, Schmidt G, Drenckhahn D: Inhibition of Rho A activity causes pemphigus skin blistering. *J Cell Biol* 2006, 175:721–727
- Caldeiri R, de Bruin A, Baumann D, Suter MM, Bierkamp C, Balmer V, Muller E: A central role for the armadillo protein plakoglobin in the autoimmune disease pemphigus vulgaris. *J Cell Biol* 2001, 153:823–834
- Williamson L, Raess NA, Caldeiri R, Zakher A, de Bruin A, Posthaus H, Bolli R, Hunziker T, Suter MM, Miller EJ: Pemphigus vulgaris identifies plakoglobin as key suppressor of c-Myc in the skin. *EMBO J* 2006, 25:3298–3309
- Lanza A, Cirillo N, Rossiello R, Rienzo M, Cuttillo L, Casamassimi A, de Nigris F, Schiano C, Rossiello L, Femiano F, Gombos F, Napoli C: Evidence of key role of CDK-2 overexpression in pemphigus vulgaris. *J Biol Chem* 2008, 283:8736–8745
- Schlessinger J: Cell signaling by receptor tyrosine kinases. *Cell* 2000, 103:211–225
- Yarden Y, Slivkowski MX: Untangling the ErbB signalling network. *Nat Rev Mol Cell Biol* 2001, 2:127–137
- Simeonova PP, Wang S, Hulderman T, Luster MI: c-Src-dependent activation of the epidermal growth factor receptor and mitogen-activated protein kinase pathway by arsenic. Role in carcinogenesis. *J Biol Chem* 2002, 277:2945–2950
- Carpenter G: Employment of the epidermal growth factor receptor in growth factor-independent signaling pathways. *J Cell Biol* 2002, 146:697–702
- Hoschuetzky H, Aberle H, Kemler R: Beta-catenin mediates the interaction of the cadherin-catenin complex with epidermal growth factor receptor. *J Cell Biol* 1994, 127:1375–1380
- Gaudry CA, Palka HL, Dusek RL, Huen AC, Kwaidekar MJ, Hudson LG, Green KJ: Tyrosine-phosphorylated plakoglobin is associated with desmogleins but not desmoplakin after epidermal growth factor receptor activation. *J Biol Chem* 2001, 276:24871–24880
- Yin T, Getsios S, Caldeiri R, Godsel LM, Kowalczyk AP, Miller EJ, Green KJ: Mechanisms of plakoglobin-dependent adhesion: desmosome-specific functions in assembly and regulation by epidermal growth factor receptor. *J Biol Chem* 2005, 280:40355–40363
- Frusio-Zlotkin M, Raichenberg D, Wang X, David M, Michel B, Milner Y: Apoptotic mechanism in pemphigus autoimmunoglobulins-induced acantholysis—possible involvement of the EGF receptor. *Autoimmunity* 2006, 39:563–575
- Chernyavsky AI, Arredondo J, Kitajima Y, Sato-Nagai M, Grando SA: Desmoglein VS. non-desmoglein signaling in pemphigus acantholysis: characterization of novel signaling pathways downstream of pemphigus vulgaris antigens. *J Biol Chem* 2007, 282:13804–13812
- Boukamp P, Petrussevska RT, Breitkreutz D, Hornung J, Markham A, Fusenig NE: Normal keratinization in a spontaneously immortalized aneuploid human keratinocyte cell line. *J Cell Biol* 1988, 108:761–771
- Ishii K, Harada R, Matsuo I, Shirakata Y, Hashimoto K, Amagai M: In vitro keratinocyte dissociation assay for evaluation of the pathogenicity of anti-desmoglein 3 IgG autoantibodies in pemphigus vulgaris. *J Invest Dermatol* 2005, 124:939–946
- Biscardi JS, Maa M-C, Tice DA, Cox ME, Leu T-H, Parsons SJ: c-Src-mediated Phosphorylation of the Epidermal Growth Factor Receptor on Tyr845 and Tyr101 Is Associated with Modulation of Receptor Function. *J Biol Chem* 1999, 274:8335–8343
- Spindler V, Drenckhahn D, Zillikens D, Waschke J: Pemphigus IgG causes skin splitting in the presence of both desmoglein 1 and desmoglein 3. *Am J Pathol* 2007, 171:906–916
- Lorch JH, Klessner J, Park JK, Getsios S, Wu YL, Stack MS, Green KJ: Epidermal growth factor receptor inhibition promotes desmosome assembly and strengthens intercellular adhesion in squamous cell carcinoma cells. *J Biol Chem* 2004, 279:37191–37200
- Santiago-Josefat B, Esselens C, Bech-Serra JJ, Arribas J: Post-transcriptional up-regulation of ADAM17 upon epidermal growth factor

- receptor activation and in breast tumors. *J Biol Chem* 2007, 282:8325–8331
37. Bech-Serra JJ, Santiago-Josefat B, Esselens C, Saltig P, Baselga J, Arribas J, Canals F: Proteomic identification of desmoglein 2 and activated leukocyte cell adhesion molecule as substrates of ADAM17 and ADAM10 by difference gel electrophoresis. *Mol Cell Biol* 2006, 26:5086–5095
38. Pece S, Gutkind JS: Signaling from E-cadherins to the MAPK pathway by the recruitment and activation of epidermal growth factor receptors upon cell-cell contact formation. *J Biol Chem* 2000, 275:41227–41233
39. Pece S, Chiariello M, Murga C, Gutkind JS: Activation of the protein kinase Akt/PKB by the formation of E-cadherin-mediated cell-cell junctions. Evidence for the association of phosphatidylinositol 3-kinase with the E-cadherin adhesion complex. *J Biol Chem* 1999, 274:19347–19351

3.1.3 Publication 3: Peptides targeting the desmoglein 3 adhesive interface prevent pemphigus autoantibody-induced acantholysis in pemphigus

Heupel WM[¶], Müller T[¶], Efthymiadis A[¶], Schmidt E, Drenckhahn D, Waschke J

Peptides targeting the desmoglein 3 adhesive interface prevent pemphigus autoantibody-induced acantholysis in pemphigus

J Biol Chem. 2009 Mar 27;284(13):8589-95. Epub 2009 Jan 21

Reproduced / adapted with permission by the Journal of Biological Chemistry.

DOI: 10.1074/jbc.M808813200

Peptides Targeting the Desmoglein 3 Adhesive Interface Prevent Autoantibody-induced Acantholysis in Pemphigus*

Received for publication, November 20, 2008, and in revised form, December 24, 2008. Published, JBC Papers in Press, January 21, 2009, DOI 10.1074/jbc.M808813200

Wolfgang-Moritz Heupel^{†1}, Thomas Müller^{§1}, Athina Efthymiadis[‡], Enno Schmidt[¶], Detlev Drenckhahn^{‡2}, and Jens Waschke^{†3}

From the [†]Department of Anatomy and Cell Biology, University of Würzburg, Koellikerstr. 6, D-97070 Würzburg, the [§]Department of Molecular Plant Physiology and Biophysics, University of Würzburg, Julius-von-Sachs-Platz 2, 97082 Würzburg, and the [‡]Department of Dermatology, University of Würzburg, Josef-Schneider-Str. 2, D-97080 Würzburg, Germany

Pemphigus vulgaris (PV) autoantibodies directly inhibit desmoglein (Dsg) 3-mediated transinteraction. Because cellular signaling also seems to be required for PV pathogenesis, it is important to characterize the role of direct inhibition in pemphigus acantholysis to allow establishment of new therapeutic approaches. Therefore, we modeled the Dsg1 and Dsg3 sequences into resolved cadherin structures and predicted peptides targeting the adhesive interface of both Dsg3 and Dsg1. In atomic force microscopy single molecule experiments, the self-designed cyclic single peptide specifically blocked homophilic Dsg3 and Dsg1 transinteraction, whereas a tandem peptide (TP) consisting of two combined single peptides did not. TP did not directly block binding of pemphigus IgG to their target Dsg antigens but prevented PV-IgG-induced inhibition of Dsg3 transinteraction in cell-free (atomic force microscopy) and cell-based (laser tweezer) experiments, indicating stabilization of Dsg3 bonds. Similarly, PV-IgG-mediated acantholysis and disruption of Dsg3 localization in HaCaT keratinocytes was partially blocked by TP. This is the first evidence that direct inhibition of Dsg3 binding is important for PV pathogenesis and that peptidomimetics stabilizing Dsg transinteraction may provide a novel approach for PV treatment.

Autoantibodies in pemphigus vulgaris (PV)⁴ are mainly directed against the adhesion molecules desmoglein (Dsg) 3 and Dsg1 (1, 2). Recently, we provided direct evidence that PV autoantibodies directly block Dsg3 transinteraction (3). In contrast, Dsg1 autoantibodies in pemphigus foliaceus (PF) were found to disrupt Dsg1 transinteraction most likely via cellular

signaling events rather than by direct inhibition (3, 4). However, it still remained unanswered whether direct inhibition of Dsg3 transinteraction is the sole pathogenic mechanism in mucosal-dominant PV where autoantibodies against Dsg3 but not against Dsg1 are present (1). Alternatively, direct inhibition could act in concert with autoantibody-induced cellular signaling or may just be an epiphenomenon secondary to skin blistering (1, 5–7).

The idea of direct interference with Dsg transinteraction by pemphigus autoantibodies has been proposed when Dsg3 was discovered to be a cadherin-type cell adhesion molecule (8, 9). From structural and mutational analyses, it was concluded that classical cadherins are able to form adhesive dimers through their N-terminal cadherin extracellular domain (EC1) via different interaction schemes (10–13). Investigations of desmosomes using electron tomography from tissue sections also indicated various interaction models for desmosomal cadherins (14). Some of these interaction models resembled the interaction schemes found in the high resolution crystal structure analyses of N- and E-cadherin.

This study was designed to modulate Dsg3 and Dsg1 transinteraction by using peptides fitting the most likely Dsg adhesive interface revealed by three-dimensional modeling. In an earlier study, it was reported that peptides targeting the putative Dsg cell adhesion recognition site blocked desmocadherin-mediated adhesion (15). Homology modeling of Dsg3 and Dsg1 based on the structure of E-cadherin and N-cadherin led to the identification of a peptide sequence expected to block Dsg1 and Dsg3 transinteraction by occupying a predicted binding site. By combining two of these single peptides (SPs) via a flexible linker, a so-called tandem peptide (TP) was generated. This peptide was expected to stabilize Dsg adhesion by cross-linking the binding pockets of two transinteracting Dsg3 or Dsg1 molecules, similar to peptides directed against the adhesive interface of N-cadherin (16). Here we show that TP prevented the effects of PV-IgG on Dsg3 adhesion and attenuated PV-IgG-induced acantholysis in human keratinocytes. These data indicate a significant role of autoantibody-induced direct inhibition of Dsg3 binding in PV pathogenesis and may provide a novel therapeutic approach in PV treatment.

EXPERIMENTAL PROCEDURES

Modeling of the Dsg3 and Dsg1 EC1 and EC2 Domain—The high resolution crystal structure of E-cadherin (Protein Data Bank (PDB) entry 1EDH) was used as a structural template to

* This study was supported by grants from the Deutsche Forschungsgemeinschaft (Grants SFB 487, TP B5, and B2) and the IZKF Würzburg (Grant TP A-51). The costs of publication of this article were defrayed in part by the payment of page charges. This article must therefore be hereby marked "advertisement" in accordance with 18 U.S.C. Section 1734 solely to indicate this fact.

¹ Both authors contributed equally.

² To whom correspondence may be addressed. Tel.: 49-931-31-2384; Fax: 49-931-31-2712; E-mail: drenckhahn@uni-wuerzburg.de.

³ To whom correspondence may be addressed. Tel.: 49-931-31-2384; Fax: 49-931-31-2712; E-mail: jens.waschke@mail.uni-wuerzburg.de.

⁴ The abbreviations used are: PV, pemphigus vulgaris; PF, pemphigus foliaceus; AFM, atomic force microscopy; Dsg, desmoglein; ELISA, enzyme-linked immunosorbent assay; EC, extracellular domain; HaCaT, immortalized human keratinocyte cell line; IgG, immunoglobulins; SP, single peptide; TP, tandem peptide; CP, control peptide; VE-cadherin, vascular endothelial cadherin.

Peptides Targeting the Desmoglein Adhesive Interface

model the EC1 and EC2 of human Dsg1 and Dsg3. Amino acid sequence alignments were produced using CLUSTALW. Amino acid residues of E-cadherin were exchanged for the corresponding amino acids of Dsg1 and Dsg3 using the ProteinDesign tool of Quanta2006 (Accelrys Inc., San Diego, CA). Insertions and deletions were modeled manually. Structure refinement was performed initially by removing steric clashes using side chain rotamer search tools in Xbuilt, Quanta2006. Backbone and side chain conformations were refined subsequently by energy minimization (500 steps steepest gradient energy minimization) and short molecular dynamics simulation (10 ps *in vacuo* simulation) employing only geometrical energy terms and stepwise removing conformational harmonic potentials for the backbone atoms (first round, energy force constant 50 kcal mol⁻¹Å⁻²; second round, 5 kcal mol⁻¹Å⁻²; third round, no harmonic potentials). The final models for Dsg1 and Dsg3 exhibited good backbone and side chain geometry; Ramachandran plot analysis showed that no residues exhibited backbone torsion angles in the disallowed area.

Design and Application of Dsg Antagonistic (SP) and Agonistic (TP) Peptides—To design peptides that possibly antagonize the transinteraction of Dsg1 and Dsg3, we structurally aligned our Dsg models onto the N-cadherin crystal structure, mimicking the putative transinteraction between two cadherin molecules (PDB entry 1NCH). This arrangement was used to form a Dsg1 (or Dsg3) transinteracting pair. One peptide was designed that comprised a fragment of the main binding interface. The amino acid sequence of this SP was LNSMGQD, corresponding to Leu-81–Asp-87 of Dsg1. Because of the homology of this sequence to the corresponding Dsg3 sequence (LNAQLD), SP was also supposed to modulate Dsg3 transinteraction. SP was then cyclized by adding cysteine residues at the N- and C-terminal peptide end. The degree of flexibility of the peptide in its linear and cyclic form was simulated by running molecular dynamics simulation in an explicit water shell (250 ps, 8 Å water layer, CHARMM force field 22) using CHARMM, Quanta2006. The so-called TP was generated by combining two SPs linked via a flexible aminohexan linker coupled to one cysteine of the SP. The sequences of the control peptides CP-1 and CP-2 were RVDAE and N-Ac-CRVDAE-Aminohexan-RVDAEC-NH₂, respectively, and derived from a study targeting VE-cadherin transinteraction with single (CP-1) and tandem (CP-2) peptides. The underlined peptide sequence denotes circularization via a disulfide bond between the given cysteine residues. SP, TP, and CP-2 peptides were obtained from a commercial supplier (PSL GmbH, Heidelberg, Germany). Peptide CP-1 was synthesized according to the Bachem practice of solid-phase peptide synthesis (all chemicals were supplied by Novabiochem (Darmstadt, Germany)). For most experiments, SP and CP-1 were used at 200 μM and TP and CP-2 was used at 20 μM.

Cell Culture and Test Reagents—The immortalized human keratinocyte cell line HaCaT was cultivated as described (3). PV antibody AK 23 was purchased from Biozol (Eching, Germany) and used at 75 μg/ml for experiments.

Purification and Preparation of Pemphigus IgG and Recombinant Dsg-Fc—Purification of the IgG fractions of a patient with a mucocutaneous PV (PV-IgG 1, both Dsg1 and Dsg3 antibodies) and one with mucous PV (PV-IgG 2, only Dsg3 antibody),

was performed as described previously (3). Final IgG concentrations were adjusted to 150–500 μg/ml for experiments. Recombinant human Dsg3 and Dsg1 were expressed and purified as described (3).

Atomic Force Microscopy (AFM) and Laser Tweezer Measurements—Effects of pemphigus IgG, AK 23, and peptides on cell-free homophilic Dsg3 and Dsg1 binding activities in AFM force distance cycles or Dsg3 and Dsg1 bead binding in laser tweezer experiments on HaCaT cells were conducted and analyzed as described recently (3).

Dsg1 and Dsg3 ELISA—For quantification of antibody binding to Dsg1 and Dsg3, ELISA with recombinant Dsg1 and Dsg3 was performed according to the manufacturer's instructions (Medical and Biological Laboratories, Nagoya, Japan). Peptides, AK 23, and pemphigus IgG were incubated with recombinant Dsgs on the ELISA plates in concentrations as described above. For detection of AK 23 binding to Dsg3, peroxidase-coupled mouse anti-human antibody was exchanged by peroxidase-coupled goat anti-mouse antibody. All conditions were run at least in triplicates.

Cytochemistry—HaCaT cells were stained with mouse monoclonal Dsg3 antibody (Zytomed Systems GmbH) as described previously (3).

Dispase-based Keratinocyte Dissociation Assay—The assay was performed as described in the literature with the following modifications (17, 18). HaCaT cells were seeded on 12-well plates and grown to confluence. After incubation for 24 h under various conditions, cells were washed with Hanks' buffered salt solution and treated for 30 min with 0.3 ml of dispase II (2.4 units/ml, Sigma) at 37 °C. Afterward, dispase solution was carefully removed, and cells were dissolved in 0.5 ml of Hanks' buffered salt solution. Mechanical stress was then applied by pipetting 10 times with a 1-ml pipette. Finally, dissociation was quantified by counting and averaging cell fragments in three defined areas of each condition under a binocular microscope. Every condition was repeated at least four times.

RESULTS

Conformational Epitope Modeling for Peptide Design and Function—A model for the EC1-EC2 domain pair of Dsg1 and Dsg3 was built based on the homology to known structures of other cadherins (Fig. 1) (10, 11). First we used the structure of the EC1-EC2 domain of E-cadherin (PDB entry 1EDH, (11)) as a template. Amino acid sequences of Dsg1 and Dsg3 of various species were aligned to that of N- and E-cadherin, and residues that differed between Dsg1 (or Dsg3) and E-cadherin EC1-EC2 were exchanged to finally present the amino acid sequence of human Dsg1 (or human Dsg3). Insertions and deletions between the Dsg1 or Dsg3 and E-cadherin were located only in the loop region within the EC2 domain (β2β3, β3β4, and β6β7 loop) and thus had no effect on the overall fold of the N-terminal EC1 domain of our Dsg1 or Dsg3 model. After refinement by removing steric clashes between side chains, backbone conformation was refined by short molecular dynamics simulations *in vacuo* using only geometrical terms. Analysis of the backbone hydrogen bond network revealed that the secondary structure was well conserved to the structural template, indicating that the amino acid differences between E-cadherin and

Peptides Targeting the Desmoglein Adhesive Interface

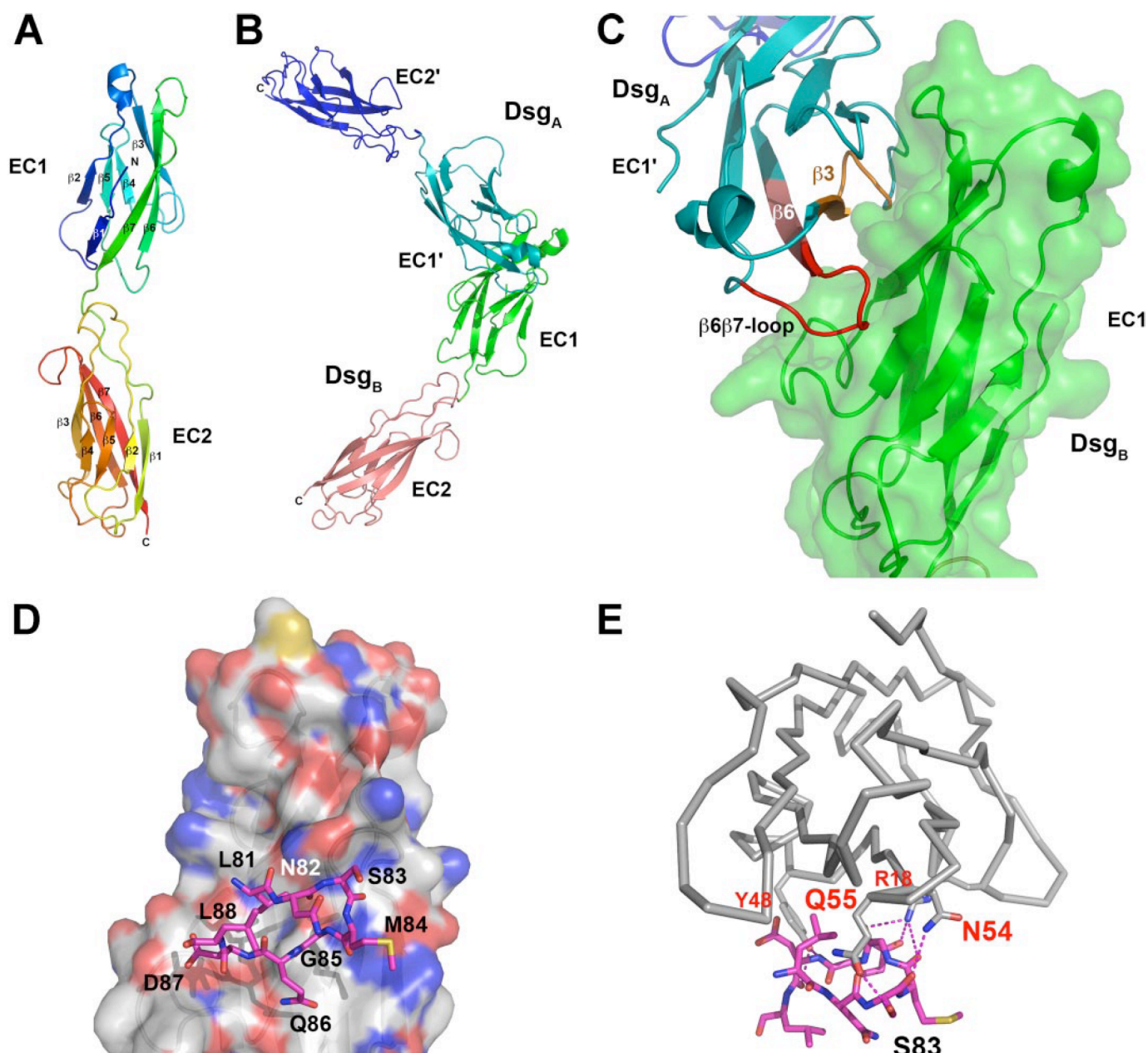


FIGURE 1. Dsg1 EC1 and EC2 modeling and peptide design. *A*, secondary structure elements as well as the N and C termini of the Dsg1 EC1 and EC2 model are indicated. *B*, model of the Dsg1 transinteraction as shaped on the basis of the N-cadherin crystal structure. The two EC1 domains interact via a large interface suggesting an *in vivo* interaction. *C*, blow-up of the interface region with peptide fragments possibly interfering with transinteraction shown in orange and red. A similar model was obtained for Dsg3 (data not shown). *D*, an SP designed to block Dsg transinteraction corresponded to residues Leu-81 to Leu-88 located in the putative binding site on Dsg1, the latter being illustrated by a van der Waals surface representation in atom color code. *E*, in comparison with *D*, the putative polar interactions (hydrogen bonds) are shown as stippled lines in magenta. Note that SP formed numerous H-bonds with residues in the Dsg1 binding site.

Dsg1 or Dsg3 did not lead to major structural rearrangements. The obtained model for Dsg1 (Fig. 1*A*) was compared with the recently determined NMR structure of Dsg2 EC1 (PDB entry 2YQG), revealing a root mean square deviation of only 1.3 Å over 80 C α atoms, thereby confirming that cadherins are structurally well conserved and that our models of Dsg1 or Dsg3 can be used for modeling the transinteraction between Dsgs.

The final model of Dsg1 (or Dsg3) EC1-EC2 was subsequently structurally aligned to a dimer assembly of N-cadherin and its second molecule in the asymmetric unit representing a putative transinteracting cadherin molecule pair (Fig. 1, *B* and

C) (10). This arrangement showed that β -strand 3 (residues Gln-33 to Ser-39 of Dsg1; residues Lys-33 to Ser-39 of Dsg3), the β 3 β 4 loop and part of β -strand 4 (residues Asp-44 to Gln-55 of Dsg1; residues Asp-44 to Lys-55 of Dsg3), and β -strand 6 (residues Tyr-77 to Gln-86 of Dsg1; residues Thr-77 to Leu-86 of Dsg3) would constitute possible peptide fragments that mimic the transinteracting cadherin molecules (Fig. 1*C*). Out of these fragments, the so-called SP (amino acid sequence LNSMGQD, Fig. 1, *D* and *E*) was used, which should target both Dsg1 and Dsg3 because of sequence homologies. Recent structural analyses demonstrated that this sequence is located within

Peptides Targeting the Desmoglein Adhesive Interface

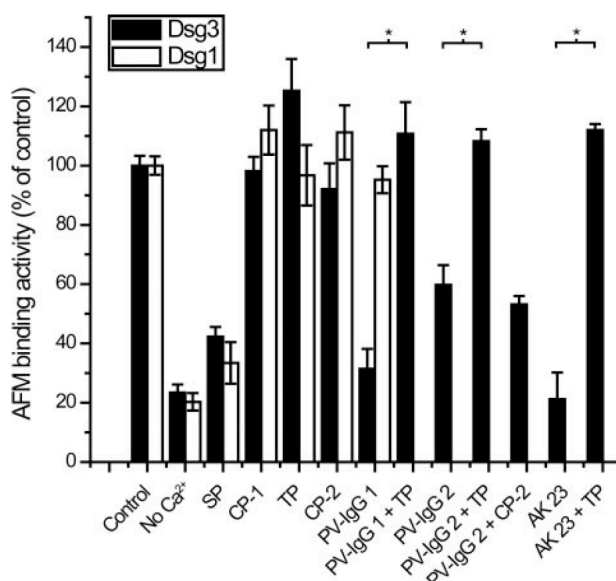


FIGURE 2. SP blocked homophilic Dsg3 or Dsg1 transinteraction and TP prevented PV-IgG- and AK 23-induced blocking of Dsg3 transinteraction in cell-free AFM studies. Binding activities of Dsg3 (black bars) and Dsg1 (white bars) fusion proteins coupled to the tip and plate of the AFM setup were strongly reduced after Ca²⁺ depletion. SP (200 μ M) also blocked Dsg3 and Dsg1 transinteraction, whereas TP (20 μ M) and the corresponding control peptides CP-1 and CP-2 did not. PV-IgG 1 and PV-IgG 2 interfered with Dsg3 transinteraction. Preincubation with TP (20 μ M, $p = 0.00360$ and $p = 0.00036$, respectively) but not CP-2 (20 μ M, $p = 0.4139$) prevented PV-IgG 1- and PV-IgG 2-induced loss of Dsg3 adhesion. Similar results were obtained with mouse PV antibody AK 23 ($p = 0.00275$). PV-IgG 1 did not directly inhibit homophilic Dsg1 transinteraction ($n = 3-4$ for each condition).

an important immunological region of the extracellular Dsg1 and Dsg3 domains (19).

Because linear peptides may exhibit low binding affinity due to conformational flexibility that leads to entropic penalties upon binding, we designed cyclic peptides that should exist in a preformed conformation similar to those also observed in the transinteraction model of Dsg1 or Dsg3. Molecular simulation runs in explicit solvent confirmed that the backbone flexibility of the cyclized peptide was greatly limited when compared with the linear peptides but would not constrain the cyclic peptide into a conformer that deviates from the modeled transinteracting peptide. In this study, the designed SP was used to inhibit the interaction of Dsg1 or Dsg3. To stabilize interactions between two Dsg molecules, the so-called TP was generated by dimerizing two SPs.

SP Blocked Homophilic Dsg3 and Dsg1 Transinteraction, whereas TP Prevented PV-IgG- and AK 23-induced Inhibition of Dsg3 Binding in Cell-free AFM Studies—As a proof of principle, we first studied the effect of the designed peptides in cell-free AFM experiments (Fig. 2). Recombinant Dsg molecules were covalently coupled to the tip and plate of the AFM setup to probe homophilic Dsg transinteraction in force distance cycles. The resulting binding activities revealed the amount and extent of Dsg transinteraction events. As expected, Dsg3 and Dsg1 binding activities (Fig. 2) were strongly reduced after Ca²⁺ depletion, demonstrating Ca²⁺-dependent desmocadherin interaction. For the antagonistic SP, a concentration of 200 μ M was found to efficiently reduce Dsg3 and Dsg1 transinteraction to 42% \pm 3%

and 33% \pm 7% of control levels. Higher SP concentrations were also tested but did not yield different results (data not shown). Specificity of Dsg transinteraction for SP action was demonstrated by the VE-cadherin-targeting control peptide CP-1 (200 μ M), which did not block Dsg3 or Dsg1 transinteraction. In contrast, the TP did not significantly alter Dsg3 and Dsg1 binding activities when applied at 20 μ M and 0.5 h of preincubation, although a slight increase in binding activity was noted for Dsg3 (125% \pm 11%). Higher concentrations were not used because of negative effects on Dsg transinteraction, possibly because occupation of binding sites by single TPs without cross-linking of two Dsg molecules resulted in decreased binding activities. At concentrations below 20 μ M, both SP and TP had diminished effects in inhibiting Dsg transinteraction or preventing PV-IgG-mediated blocking of Dsg3 transinteraction as stated below, respectively (data not shown). Although direct binding of SP to Dsg3 or Dsg1 could not be demonstrated by this approach, our experiments indicate that SP directly inhibited Dsg transinteraction, whereas TP in a concentration of 20 μ M did not. We hypothesized that TP did not increase Dsg binding activities because the measured binding activities already ranged at maximum under control conditions, and unbinding forces of single Dsg bonds were not increased by TP. A control VE-cadherin tandem peptide (CP-2, 20 μ M) did not alter Dsg transinteraction in AFM studies.

Next, we investigated whether TP was effective to block PV-IgG-induced loss of Dsg3 binding. As reported previously, PV-IgG directly interfered with Dsg3 transinteraction (3). This blocking effect was confirmed for two additional PV-IgG fractions, PV-IgG 1 (31% \pm 7%) and PV-IgG 2 (60% \pm 7%), in this study. Interestingly, preincubation with TP (20 μ M) completely prevented PV-IgG-induced loss of transinteraction (binding activities were 111% \pm 11% and 108% \pm 4%, respectively). The control tandem peptide CP-2 (20 μ M), however, did not prevent PV-IgG-mediated reduction in Dsg3 transinteraction (53% \pm 3% Dsg3 binding activity), demonstrating specificity of Dsg3 transinteraction for TP. We performed similar experiments with mouse PV antibody AK 23, which targets the Dsg3 adhesive interface and blocked Dsg3 transinteraction (3, 20). AK 23-induced inhibition of Dsg3 transinteraction (21% \pm 9%) was also prevented by TP (112% \pm 2%). As we have already demonstrated previously (3), PV-IgG did not directly inhibit Dsg1 transinteraction (Fig. 2). Therefore, AFM experiments to study Dsg1 transinteraction with TP preincubation prior to pemphigus IgG treatment were not required. Taken together, AFM experiments demonstrated that TP efficiently prevented PV-IgG-induced loss of Dsg3 transinteraction.

TP Did Not Interfere with Binding of Pemphigus IgG to Dsg1 and Dsg3—It is possible that TP-induced blocking of PV-IgG-mediated loss of Dsg3 transinteraction resulted from interference with binding of pemphigus IgG to Dsg1 and Dsg3. To address this important issue, we analyzed the binding of pemphigus IgG to recombinant Dsg1 and Dsg3 using commercial Dsg ELISA (Fig. 3). ELISA scores for PV-IgG and AK 23 assessed in the absence or presence of TP were not significantly different, indicating that TP did not block binding of pemphigus IgG to Dsg1 and Dsg3. Similarly, Dsg3 binding of AK23,

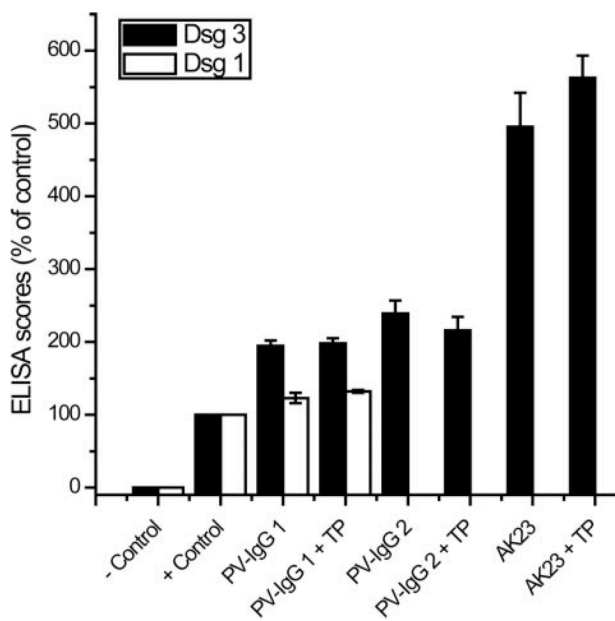


FIGURE 3. TP did not block binding of pemphigus IgG to Dsg1 and Dsg3. ELISA experiments with recombinant Dsg3 (black bars) and Dsg1 (white bars) revealed that autoantibody scores of PV-IgG 1, PV-IgG 2, and AK 23 in the absence or presence of TP (20 μ M) were not significantly different ($p = 0.4040$, $p = 0.751$, $p = 0.2624$, respectively), indicating that TP did not interfere with binding of pemphigus IgG to Dsg1 and Dsg3, respectively. ($n = 3$ for each condition).

which is directed against a putative adhesive domain of Dsg3, was not prevented by simultaneous TP incubation.

TP Prevented PV-IgG- and AK 23-induced Loss of Dsg3 Bead Binding on Keratinocytes—In the following, TP experiments were extended to laser tweezer experiments on cultured human keratinocytes (HaCaT) where binding of microbeads coated with recombinant Dsg3 (black bars) or Dsg1 (white bars) was probed by laser displacement (Fig. 4). The number of surface-bound Dsg3 and Dsg1 beads resisting laser beam displacement was reduced by simultaneous incubation with EGTA (5 mM, 30 min) to $21\% \pm 4\%$ and $28\% \pm 3\%$, which demonstrated Ca^{2+} -dependent bead binding. Similar to preceding studies (3, 4, 21, 22), incubation of monolayers with attached beads for 30 min with PV-IgG 1 and PV-IgG 2 caused significant loss of both Dsg3-coated and Dsg1-coated beads (Dsg3 bead values, $65\% \pm 6\%$ and $72\% \pm 5\%$; Dsg1 bead values, $54\% \pm 4\%$ and $72\% \pm 5\%$, respectively). PV-IgG-induced reduction in Dsg3 bead binding was significantly prevented by a 30-min preincubation of cells with TP at a concentration of 20 μ M ($94\% \pm 2\%$ and $90\% \pm 4\%$ for PV-IgG 1 and PV-IgG 2, respectively), consistent with cell-free Dsg3 AFM experiments. PV-IgG-mediated effects on Dsg bead binding was unaltered by preincubation with 20 μ M CP-2, demonstrating the specificity of Dsg3 bead binding for TP. AK 23 resulted in reduced Dsg3 bead binding ($50\% \pm 4\%$), an effect that was completely blocked by preincubation with TP as well ($105\% \pm 9\%$). On the other hand, TP treatment was unable to prevent PV-IgG-mediated reduction of Dsg1 bead binding (values were $58\% \pm 6\%$ and $83\% \pm 4\%$ for PV-IgG 1 and PV-IgG 2). Because PV-IgG 1 did not directly inhibit Dsg1 transinteraction (Fig. 2), although containing Dsg1 autoantibodies, loss of Dsg1 binding in keratinocytes was likely caused by more indirect mechanisms such as induction of cellular signaling pathways

Peptides Targeting the Desmoglein Adhesive Interface

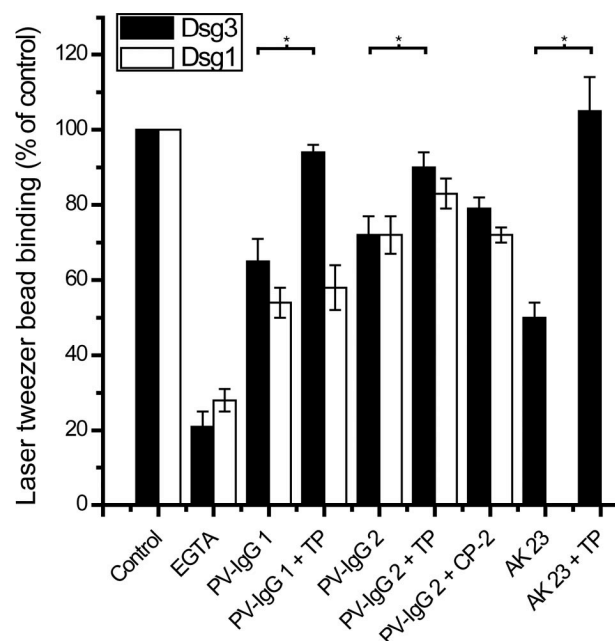


FIGURE 4. In cell-based laser tweezer experiments, TP prevented PV-IgG- or AK 23-induced reduction of Dsg3 bead binding but not PV-IgG-mediated loss of Dsg1 bead binding. The numbers of HaCaT surface-bound Dsg3 (black bars) and Dsg1 beads (white bars) resisting laser beam displacement were reduced by incubation with EGTA (5 mM, 30 min). Incubation of monolayers with attached beads for 30 min with IgG fractions from PV patients significantly reduced the number of bound Dsg3 and Dsg1 beads. However, preincubation with TP (20 μ M) for 30 min prevented AK 23-, PV-IgG 1-, and PV-IgG 2-induced reduction of Dsg3 ($p = 0.00021$, $p = 0.01728$, $p = 0.03142$, respectively) but not reduction of Dsg1 bead binding ($p = 0.5512$, $p = 0.1311$, for PV-IgG 1 and PV-IgG 2, respectively). Preincubation with CP-2 (20 μ M) did not alter PV-IgG-mediated loss in Dsg3 ($p = 0.3522$) and Dsg1 bead binding ($p = 0.9688$) ($n = 6$ for each condition).

that were not blocked by TP-mediated stabilization of Dsg transinteraction.

PV-mediated Acantholysis Was Partially Prevented by TP—Next, we evaluated whether TP would be protective against pemphigus IgG-mediated acantholysis in human keratinocytes using Dsg3 immunostaining to label desmosomes (Fig. 5). Following incubation with medium only (Fig. 5A) or control IgG (Fig. 5B), Dsg3 was detected at cell borders. Incubation with PV-IgG 1 and PV-IgG 2 resulted in gross disruption of Dsg3 staining, often accompanied by intercellular gap formation (Fig. 5, C and F, arrows). Intercellular gap formation was further substantiated by F-actin staining (data not shown) (22). PV-IgG-mediated Dsg3 disorganization was largely prevented by simultaneous incubation of HaCaT cells with TP at a concentration of 20 μ M (Fig. 5, D and G). Under these conditions, Dsg3 was present at all segments of the cell membrane, but localization was discontinuous. Nevertheless, this protocol did not completely suppress intercellular gap formation (Fig. 5, D and G, arrows). Simultaneous incubation with CP-2 did not prevent PV-IgG-induced effects on keratinocytes (Fig. 5, E and H).

We quantified acantholytic effects of pemphigus IgG and peptide treatment using a dispase-based cell dissociation assay (Fig. 6). In these experiments, treatment of HaCaT cells for 24 h with 200 μ M SP resulted in a significantly increased number of cell fragments when compared with controls ($895\% \pm 175\%$), demonstrating that Dsg binding is crucial for keratinocyte adhesion. TP at 20 μ M did not lead to enhanced cell dissociation

Peptides Targeting the Desmoglein Adhesive Interface

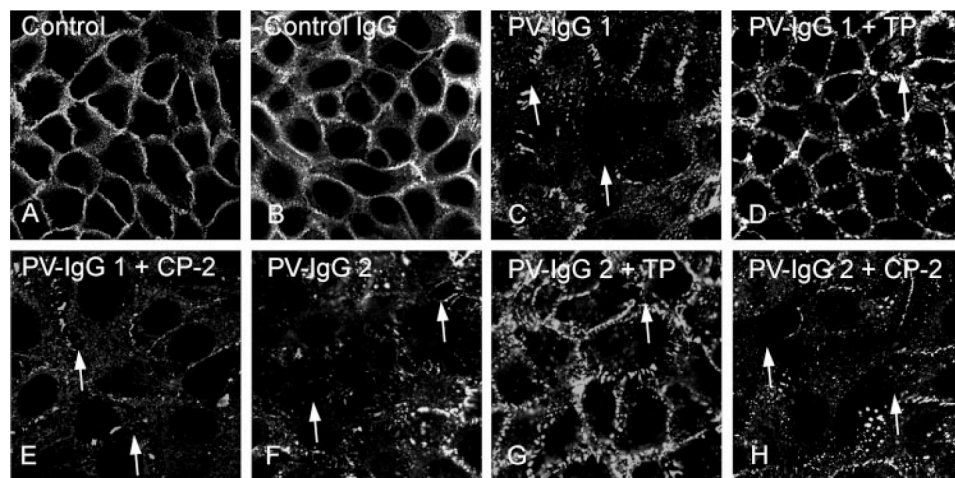


FIGURE 5. TP treatment partially prevented PV-IgG-mediated disruption of Dsg3 localization in human keratinocytes. Dsg3 immunostaining of HaCaT keratinocytes revealed Dsg3 distribution along cell borders following incubation with medium (A) or control IgG (B). Incubation with PV-IgG 1 (C) and IgG 2 (F) resulted in disruption of Dsg3 staining and intercellular gap formation (arrows). PV-IgG-mediated Dsg3 disorganization was largely prevented by incubation of HaCaT cells with TP (20 μM, D and G) but not with CP-2 (20 μM, E and H). Intercellular gap formation was overall reduced but not completely abolished (arrows). Scale bar: 20 μm for all panels. (n = 5).

(100% ± 40%), whereas 20 μM CP-2 treatment resulted in a slight but significant increase (195% ± 24%). PV-IgG 1 caused a strong increase in cell fragments (4000% ± 522%) that was partially blocked by cotreatment with 20 μM of TP (2017% ± 414%). Similar results were obtained with PV-IgG 2; PV-IgG 2 alone dramatically increased cell dissociation (1805% ± 219%), whereas incubation with TP but not CP-2 partially blocked these effects (673% ± 84% and 2494% ± 348%, respectively).

DISCUSSION

The results of the present study demonstrate for the first time that direct inhibition of Dsg3 transinteraction significantly contributes to PV pathogenesis. This was shown

by the use of peptides targeting the adhesive Dsg interface, which were effective to block both PV-IgG-induced direct inhibition of Dsg3 transinteraction and PV-IgG-induced acantholysis in human keratinocytes *in vitro*. This approach is the first to inhibit pathogenic effects of PV-IgG independent of cellular signaling pathways. Similar approaches using peptidomimetics may be applicable for treatment of pemphigus as well as of other autoantibody-mediated diseases where cell adhesion molecule function is impaired.

Modeling of Dsg sequences into structures of resolved classical cadherins identified a peptide sequence that was expected to block Dsg1 and Dsg3 transinteraction by occupying a critical and conserved Dsg binding site. AFM experiments demonstrated that the single peptide reduced homophilic transinteraction of both Dsg1 and Dsg3. This effect was sequence-specific because a comparable peptide from the equivalent region of VE-cadherin had no effect. In a dispase-based cell dissociation assay, SP caused significant acantholysis, indicating that the peptide reduced desmosomal adhesion *in vitro*. In the next step, a tandem peptide was generated that, when applied alone, did not interfere with Dsg1 and Dsg3 transinteraction. Nevertheless, preincubation with TP abolished PV-IgG-induced loss of Dsg3 transinteraction under cell-free conditions as probed by AFM, reduced loss of Dsg3-mediated bead binding measured with laser tweezers, and ameliorated autoantibody-induced acantholysis in keratinocytes. Again, specificity was demonstrated in parallel experiments by the lack of effects of a tandem VE-cadherin peptide. Moreover, although we cannot exclude the possibility that the peptides might bind to other (desmo-) cadherins, SP and TP did not have an effect on another cadherin family member, vascular endothelial cadherin, in comparable experiments.⁵ Taken together, these data provide a first hint that peptidomimetics with stabilizing effects on Dsg3 transin-

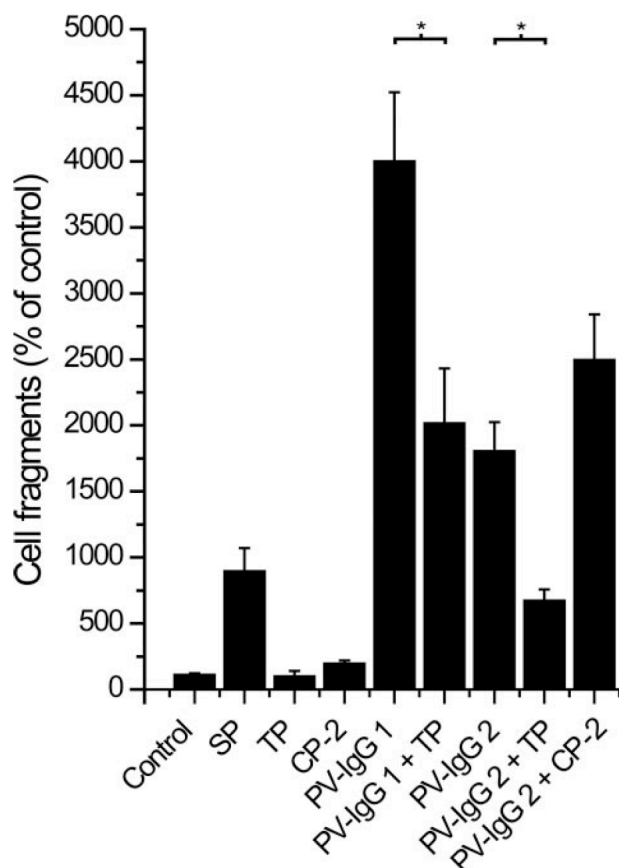


FIGURE 6. TP treatment partially prevented PV-IgG-mediated acantholysis. In dispase-based keratinocyte dissociation assays, SP treatment caused significant cell dissociation. TP (20 μM) had no effect, whereas treatment with CP-2 (20 μM) slightly increased the number of cell fragments. PV-IgG 1 and PV-IgG 2 incubation alone caused strong acantholysis, which was partially blocked by cotreatment with 20 μM TP (p = 0.01515 and p = 0.00018, respectively). CP-2 had no effect on acantholysis caused by PV-IgG 2 (p = 0.1184). (n = 4).

⁵ W.-M. Heupel, T. Müller, A. Efthymiadis, E. Schmidt, D. Drenckhahn, and J. Waschke, unpublished observations.

Peptides Targeting the Desmoglein Adhesive Interface

teraction similar to TP could be a novel therapeutic approach for PV treatment.

It has to be noted that direct interaction of the peptides with the adhesive interface of Dsg1 and Dsg3 was not shown in our study. Biacore studies using surface plasmon resonance were not successful because homophilic binding of Dsg-Fc constructs was too weak to be detected by this approach and specific binding of SP and TP to recombinant desmogleins could not be unequivocally demonstrated, most likely because affinity of peptides to recombinant Dsg molecules was rather low (not shown). This is in line with previous studies from the literature, which used recombinant proteins containing the first two extracellular domains of Dsg2 and Dsc2 only to study homophilic and heterophilic binding (23).

Because TP effectively abolished autoantibody-induced loss of Dsg3 transinteraction but did not significantly increase binding activity under cell-free conditions, these data raised the possibility that TP interfered with autoantibody binding to its target Dsg antigen, especially because recent structural analyses indicate that the SP sequence is located in an important immunological region of the Dsg1 and Dsg3 EC1 domain (19). However, ELISA measurements similar to those used to characterize the autoantibody profiles of the sera of patients demonstrated that TP did not affect binding of autoantibodies to Dsg1 and Dsg3. Similarly, binding of AK 23, which is directed against a putative adhesive domain of Dsg3, also was not prevented by simultaneous TP incubation in ELISA experiments. Therefore, a likely interpretation for the AFM experiments with TP alone is that the binding activities of Dsg1 and Dsg3 seem to be maximal under resting conditions and thus cannot be further enhanced by the peptide.

The second important outcome of the study is that direct inhibition of desmoglein transinteraction significantly contributes to pemphigus vulgaris acantholysis. This can be concluded because blocking of PV-IgG-mediated loss of Dsg3 transinteraction by TP was effective to reduce autoantibody-induced acantholysis *in vitro*. The hypothesis of autoantibody-mediated direct interference with Dsg binding was possible to believe because Dsg3 was discovered to be a cadherin-type cell adhesion molecule (8, 9). Studies using mouse monoclonal Dsg3 antibodies targeting well characterized parts of the Dsg3 extracellular subdomain supported this concept (3, 20). On the other hand, direct inhibitory effects of PV-IgG and PF-IgG on Dsg1 transinteraction were not detectable (3, 4), which led us to propose that direct interference with Dsg binding is specific for PV and may at least in part explain the more severe clinical phenotype of PV when compared with PF (1). Nevertheless, the recent study indicates that other more indirect mechanisms such as cellular signaling pathways or Dsg depletion also seem to be involved because TP did not completely block PV-IgG-induced acantholysis or PV-IgG-induced loss of Dsg1 bead binding. Indeed, accumulating evidence points to a crucial role of signaling mechanisms in pemphigus acantholysis including p38MAPK (24), RhoA (22), plakoglobin (18), c-Myc (25), cdk-2 (26), and tyrosine kinases such as c-Src (27, 28), which seem to be involved in Dsg3 endocytosis and depletion (29, 30). It is possible that some of these cellular pathways are activated as a

consequence of direct Dsg inhibition (5). Moreover, we cannot rule out the possibility that TP also has different effects on heterophilic binding of Dsg1 and Dsg3 to other desmosomal cadherins such as desmocollin 3.

Acknowledgment—We thank Lisa Bergauer for excellent technical assistance.

REFERENCES

1. Waschke, J. (2008) *Histochem. Cell Biol.* **130**, 21–54
2. Stanley, J. R., and Amagai, M. (2006) *N. Engl. J. Med.* **355**, 1800–1810
3. Heupel, W. M., Zillikens, D., Drenckhahn, D., and Waschke, J. (2008) *J. Immunol.* **181**, 1825–1834
4. Waschke, J., Bruggeman, P., Baumgartner, W., Zillikens, D., and Drenckhahn, D. (2005) *J. Clin. Investig.* **115**, 3157–3165
5. Sharma, P., Mao, X., and Payne, A. S. (2007) *J. Dermatol. Sci.* **48**, 1–14
6. Muller, E. J., Williamson, L., Kolly, C., and Suter, M. M. (2008) *J. Invest. Dermatol.* **128**, 501–516
7. Grando, S. A. (2006) *Autoimmunity* **39**, 521–530
8. Amagai, M., Klaus-Kovtun, V., and Stanley, J. R. (1991) *Cell* **67**, 869–877
9. Jones, J. C. R., Arnn, J., Staehelin, L. A., and Goldman, R. D. (1984) *Proc. Natl. Acad. Sci. U. S. A.* **81**, 2781–2785
10. Shapiro, L., Fannon, A. M., Kwong, P. D., Thompson, A., Lehmann, M. S., Grubel, G., Legrand, J. F., Als-Nielsen, J., Colman, D. R., and Hendrickson, W. A. (1995) *Nature* **374**, 327–337
11. Nagar, B., Overduin, M., Ikura, M., and Rini, J. M. (1996) *Nature* **380**, 360–364
12. Posy, S., Shapiro, L., and Honig, B. (2008) *J. Mol. Biol.* **378**, 952–966
13. Tsukasaki, Y., Kitamura, K., Shimizu, K., Iwane, A. H., Takai, Y., and Yanagida, T. (2007) *J. Mol. Biol.* **367**, 996–1006
14. He, W., Cowin, P., and Stokes, D. L. (2003) *Science* **302**, 109–113
15. Tselepis, C., Chidgey, M., North, A., and Garrod, D. (1998) *Proc. Natl. Acad. Sci. U. S. A.* **95**, 8064–8069
16. Williams, G., Williams, E. J., and Doherty, P. (2002) *J. Biol. Chem.* **277**, 4361–4367
17. Ishii, K., Harada, R., Matsuo, I., Shirakata, Y., Hashimoto, K., and Amagai, M. (2005) *J. Invest. Dermatol.* **124**, 939–946
18. Caldelari, R., de Bruin, A., Baumann, D., Suter, M. M., Bierkamp, C., Balmer, V., and Muller, E. (2001) *J. Cell Biol.* **153**, 823–834
19. Tong, J. C., and Sinha, A. A. (2008) *BMC Immunol.* **9**, 30
20. Tsunoda, K., Ota, T., Aoki, M., Yamada, T., Nagai, T., Nakagawa, T., Koyasu, S., Nishikawa, T., and Amagai, M. (2003) *J. Immunol.* **170**, 2170–2178
21. Spindler, V., Drenckhahn, D., Zillikens, D., and Waschke, J. (2007) *Am. J. Pathol.* **171**, 906–916
22. Waschke, J., Spindler, V., Bruggeman, P., Zillikens, D., Schmidt, G., and Drenckhahn, D. (2006) *J. Cell Biol.* **175**, 721–727
23. Syed, S. E., Trinnaman, B., Martin, S., Major, S., Hutchinson, J., and Magee, A. I. (2002) *Biochem. J.* **362**, 317–327
24. Berkowitz, P., Hu, P., Warren, S., Liu, Z., Diaz, L. A., and Rubenstein, D. S. (2006) *Proc. Natl. Acad. Sci. U. S. A.* **103**, 12855–12860
25. Williamson, L., Raess, N. A., Caldelari, R., Zakher, A., de Bruin, A., Posthaus, H., Bolli, R., Hunziker, T., Suter, M. M., and Miller, E. J. (2006) *EMBO J.* **25**, 3298–3309
26. Lanza, A., Cirillo, N., Rossiello, R., Rienzo, M., Cutillo, L., Casamassimi, A., de Nigris, F., Schiano, C., Rossiello, L., Femiano, F., Gombos, F., and Napoli, C. (2008) *J. Biol. Chem.* **283**, 8736–8745
27. Chernyavsky, A. I., Arredondo, J., Kitajima, Y., Sato-Nagai, M., and Grando, S. A. (2007) *J. Biol. Chem.* **282**, 13804–13812
28. Delva, E., Jennings, J. M., Calkins, C. C., Kottke, M. D., Faundez, V., and Kowalczyk, A. P. (2008) *J. Biol. Chem.* **283**, 18303–18313
29. Calkins, C. C., Setzer, S. V., Jennings, J. M., Summers, S., Tsunoda, K., Amagai, M., and Kowalczyk, A. P. (2006) *J. Biol. Chem.* **281**, 7623–7634
30. Yamamoto, Y., Aoyama, Y., Shu, E., Tsunoda, K., Amagai, M., and Kitajima, Y. (2007) *J. Biol. Chem.* **282**, 17866–17876

3.1.4 **Publication 4: Endothelial barrier stabilization by a cyclic tandem peptide targeting VE-cadherin transinteraction in vitro and in vivo**

Heupel WM [¶], Efthymiadis A [¶], Schlegel N, Müller T, Baumer Y, Baumgartner W, Drenckhahn D, Waschke J

Endothelial barrier stabilization by a cyclic tandem peptide targeting VE-cadherin transinteraction in vitro and in vivo

J Cell Sci. 2009 May 15;122(Pt 10):1616-25.

Reproduced / adapted with permission by the Journal of Cell Science.

DOI: 10.1242/10.1242/jcs.040212

Endothelial barrier stabilization by a cyclic tandem peptide targeting VE-cadherin transinteraction in vitro and in vivo

Wolfgang-Moritz Heupel^{1,*}, Athina Efthymiadis^{1,*}, Nicolas Schlegel¹, Thomas Müller², Yvonne Baumer¹, Werner Baumgartner³, Detlev Drenckhahn^{1,‡} and Jens Waschke^{1,‡}

¹University of Würzburg, Institute of Anatomy and Cell Biology, Koellikerstr. 6, D-97070 Würzburg, Germany

²University of Würzburg, Department of Botany I, Julius-von-Sachs-Platz 2, D-97082 Würzburg, Germany

³RWTH Aachen, Institute of Biology II, Kopernikusstr. 16, D-52056 Aachen, Germany

*These authors contributed equally to this work

‡Authors for correspondence: (e-mails: jens.waschke@mail.uni-wuerzburg.de; drenckhahn@uni-wuerzburg.de)

Accepted 28 January 2009

Journal of Cell Science 122, 1616–1625 Published by The Company of Biologists 2009
doi:10.1242/jcs.040212

Summary

Inflammatory stimuli result in vascular leakage with potentially life threatening consequences. As a key barrier component, loss of vascular endothelial (VE-) cadherin-mediated adhesion often precedes endothelial breakdown. This study aimed to stabilize VE-cadherin transinteraction and endothelial barrier function using peptides targeting the VE-cadherin adhesive interface. After modelling the transinteracting VE-cadherin structure, an inhibiting single peptide (SP) against a VE-cadherin binding pocket was selected, which specifically blocked VE-cadherin transinteraction as analyzed by single molecule atomic force microscopy (AFM). The tandem peptide (TP) consisting of two SP sequences in tandem was designed to strengthen VE-cadherin adhesion by simultaneously binding and cross-bridging two interacting cadherin molecules. Indeed, in AFM experiments TP specifically rendered VE-cadherin

transinteraction resistant against an inhibitory monoclonal antibody. Moreover, TP reduced VE-cadherin lateral mobility and enhanced binding of VE-cadherin-coated microbeads to cultured endothelial cells, but acted independently of the actin cytoskeleton. TP also stabilized endothelial barrier properties against the Ca²⁺ ionophore A23187 and the inhibitory antibody. Finally, TP abolished endothelial permeability increase induced by tumour necrosis factor- α in microperfused venules in vivo. Stabilization of VE-cadherin adhesion by cross-bridging peptides may therefore be a novel therapeutic approach for the treatment of vascular hyperpermeability.

Key words: VE-cadherin, Endothelial barrier, TNF- α , Peptide, Inflammation

Introduction

Cadherins are essential for cell adhesion and critically involved in various physiological and pathological processes (Angst et al., 2001; Gumbiner, 2000). The cadherin superfamily comprises Ca²⁺-dependent single-span transmembrane glycoproteins interacting with cadherins of neighbouring cells in homophilic and heterophilic fashion to confer cell adhesion and recognition (Angst et al., 2001; Steinberg and McNutt, 1999; Yap et al., 1997). Crystal structures for C- and N-cadherin revealed a pair of molecules interacting as a symmetric dimer formed through the interaction of the partner extracellular EC1 domains (Boggon et al., 2002; Shapiro et al., 1995). The cytoplasmic domain is responsible for the linkage of cadherins to the actin cytoskeleton via catenins, thereby providing strength and cohesion to adherence junctions (Baumgartner et al., 2003; Navarro et al., 1995).

Vascular endothelial (VE-) cadherin is the predominant cadherin expressed in endothelial cells and has been shown to be essential for stabilizing the endothelial lining of the inner surface of blood vessels and for regulating the barrier between blood and surrounding tissues (Dejana et al., 2008; Vandenbroucke et al., 2008). Loss of VE-cadherin function in pathological processes has been demonstrated (Alexander and Elrod, 2002; Corada et al., 1999; Hordijk et al., 1999) and VE-cadherin was found to be one of the target molecules modulated by signalling of several inflammatory mediators such as histamine, thrombin and tumour necrosis factor- α (TNF- α) (Andriopoulou et

al., 1999; Angelini et al., 2006; Konstantoulaki et al., 2003; Nwariaku et al., 2002; Rabiet et al., 1994; Rabiet et al., 1996). The impact of loss of VE-cadherin function was further demonstrated in vivo where vascular permeability was increased after application of the VE-cadherin-specific monoclonal antibody (mAb) 11D4.1 (Corada et al., 1999). Specific stabilization of VE-cadherin binding could therefore be a promising way to prevent endothelial barrier breakdown. For N-cadherin, it was demonstrated that application of peptides consisting of dimeric N-cadherin binding motifs promoted neurite outgrowth and were therefore considered N-cadherin agonists (Williams et al., 2002). A similar approach that might also be promising would be to modulate VE-cadherin-mediated adhesion: by tandem peptide-mediated cross-bridging of VE-cadherin molecules we sought to strengthen VE-cadherin adhesion and thereby protect endothelial barrier function under conditions where VE-cadherin transinteraction is compromised.

To address this, we modelled the protein sequence of VE-cadherin into the resolved structure of E-cadherin (Nagar et al., 1996) and shaped the transinteracting VE-cadherin surface of the two outermost extracellular domains. By this approach, a single peptide (SP) sequence was selected which fitted into the probable binding interface of VE-cadherin. This peptide was expected to inhibit VE-cadherin transinteraction. A tandem peptide (TP) was then generated by connecting two consecutive SP sequences with a flexible linker. TP was supposed to stabilize VE-cadherin transinteraction by

simultaneously binding to the adhesive interfaces of two interacting VE-cadherin molecules. The proof of function of these peptides was tested by single molecule atomic force microscopy (AFM), fluorescent recovery after photobleaching (FRAP), laser tweezers and measurements of transendothelial resistance (TER). Finally, permeability measurements in individually perfused rat mesenteric venules demonstrated that TP also prevented TNF- α -induced breakdown of endothelial barrier function in vivo.

Results

Model structure of the VE-cadherin-specific peptides

A homology-based model for transinteracting VE-cadherin molecule pairs (Fig. 1A) suggested a small segment of the sequence derived from β 4-strand (residues Arg47 to Glu51; Fig. 1B,C) of the N-terminal VE-cadherin domain 1 as a possible inhibitor because of its involvement in general VE-cadherin transinteraction. This segment exhibited high sequence homology with mouse and rat VE-cadherin. In our interaction model Arg47 of this RVDAAE sequence tightly interacts via hydrogen bonds with the sidechain and mainchain groups of the peptide stretch Thr80 to Glu82 of VE-cadherin (Fig. 1D). Asp49 also forms a putative H-bond with the mainchain amide of Thr80, and the amide group of Ala50 is hydrogen-bonded to the backbone carbonyl group of Asp79. Glu51 can possibly form two salt-bridge interactions with the side-chain amino groups of Lys34 and Lys78. Thus, this short pentapeptide should bind with reasonable affinity to residues in the β 6 β 7-sheet of the complementary transinteracting VE-cadherin molecule. Molecular simulations using the peptide-VE-cadherin complex confirmed a stable interaction between the two molecules, consistent with the experimental interaction studies (see below). Fig. 1E depicts a model of the tandem peptide, which is cyclized via two cysteine residues at the N- and C-terminus and a 6-aminohexanoic acid linker.

Characterization of SP and TP action in cell-free AFM experiments: SP blocked homophilic VE-cadherin transinteraction whereas TP prevented the effects of an inhibitory VE-cadherin antibody

As a proof of principle, we first studied the effect of the designed peptides in cell-free AFM experiments (Fig. 2). Recombinant VE-cadherin molecules were covalently coupled to tip and plate of the AFM setup to probe homophilic VE-cadherin transinteraction via force distance cycles. In order to find optimal peptide concentrations, dose-response experiments investigating the effect of SP and TP on VE-cadherin transinteraction were performed (Fig. 2A). VE-cadherin binding was evaluated via quantification of binding activities revealing the amount and extend of VE-cadherin transinteraction as a combination of single molecule binding probabilities, unbinding forces and multi-bond ruptures (see Materials and Methods section). SP significantly reduced VE-cadherin binding activity at concentrations starting from 20 μ M. At a concentration of 200 μ M, binding activity was reduced to about 30% of control levels, whereas higher doses had no additional effect. Similar reductions were also observed in Ca²⁺-free conditions demonstrating Ca²⁺-dependent binding of VE-cadherin. To achieve maximal inhibitory effects, SP was therefore used at a concentration of 200 μ M in further experiments. In clear contrast, a right-shifted dose-response curve was obtained in TP experiments. TP led to decreased binding activity only at higher concentrations compared with SP. Inhibitory action at high concentrations of TP was expected because saturation of all VE-cadherin binding sites by TP would prevent cross-bridging of adjacent VE-cadherin molecules and thus would result in decreased binding activity. However, significantly increased VE-cadherin binding activity was not observed at any TP concentration investigated. Therefore, to avoid possible inhibitory effects, TP was used at 20 μ M in all further experiments.

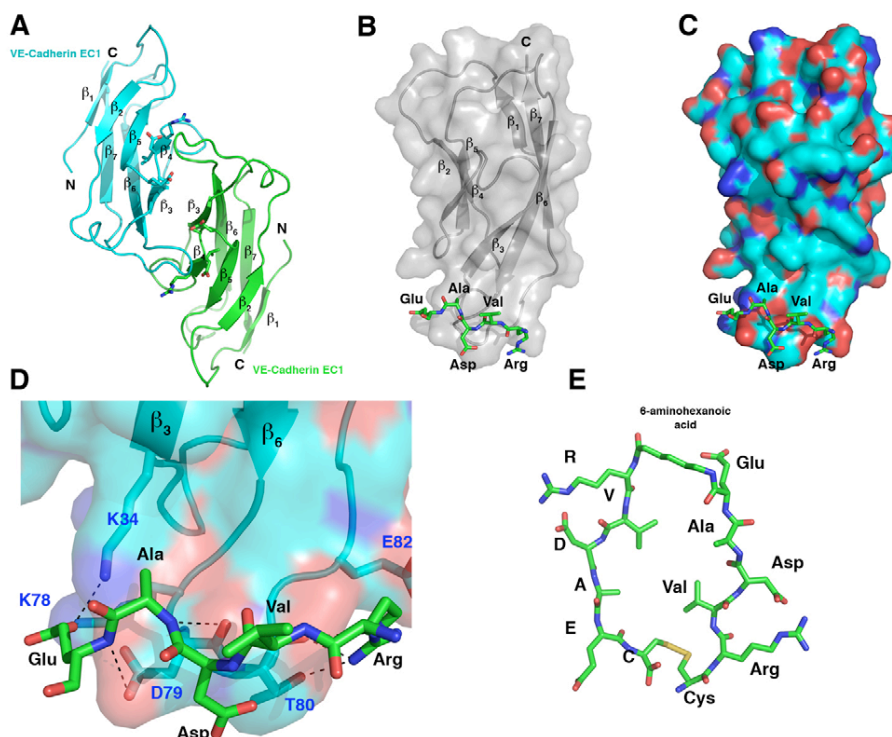


Fig. 1. Structure of VE-cadherin, and peptide design. (A) Model of a *trans*-interacting VE-cadherin EC1 pair. Secondary structure elements and N- and C-termini are indicated. Side chains of the RVDAAE motif are shown in stick format. (B) Docking of the RVDAAE peptide onto the surface of a VE-cadherin EC1 module (grey with transparent surface). (C) Same as in B but with the surface of VE-cadherin EC1 colour-coded according to polarity: blue, nitrogen atoms; cyan, carbon atoms; red, oxygen atoms. (D) Magnification of the peptide binding site. Putative hydrogen bonds between the peptide and the EC1 domain of VE-cadherin are shown as dashed lines. (E) Model of the tandem peptide, which is cyclized by two cysteine residues at the N- and C-terminus and a 6-aminohexanoic acid linker.

Next, VE-cadherin unbinding forces under different peptide conditions were analyzed in force-distance cycles in detail (for representative cycles see Fig. 2B). As shown in Fig. 2C, under control conditions three distinct unbinding force peaks were observed in frequency distribution analyses of >500 unbinding curves at retrace velocities of 600 nm/second ($f_1=35$ pN; $f_2=62$ pN; $f_3=108$ pN). This is consistent with our previous observations and has been explained by lateral oligomerization and cooperative unbinding of cadherin dimers (Baumgartner et al., 2000). The first unbinding peak was further in the range of rupture forces determined for VE-cadherin molecules of opposing cells (Panorchan et al., 2006). When TP was applied at 20 μ M, a shift towards the first unbinding force peak was observed (61% versus 50% of total unbinding events, respectively; see insets in Fig. 2C which show Gaussian multiple peak fittings of

probability density curves for control and TP condition). By contrast, in the presence of SP (200 μ M) VE-cadherin transinteraction revealed distinct but strongly reduced force peaks because probability density curves were corrected by normalization with evaluated interaction frequencies (single molecule interaction frequencies were 52.8%, 54.0% and 20.3% in control, TP and SP condition, respectively). These experiments indicate that TP stabilized VE-cadherin dimers involving two VE-cadherin-Fc molecules but did not result in altered single molecule unbinding forces themselves. Increasing retrace velocities led to a logarithmic increase in unbinding forces as expected but revealed comparable effects of peptides on VE-cadherin unbinding forces (data not shown).

Having characterized peptide effects on VE-cadherin transinteraction, specificity and protective effects were evaluated. Fig.

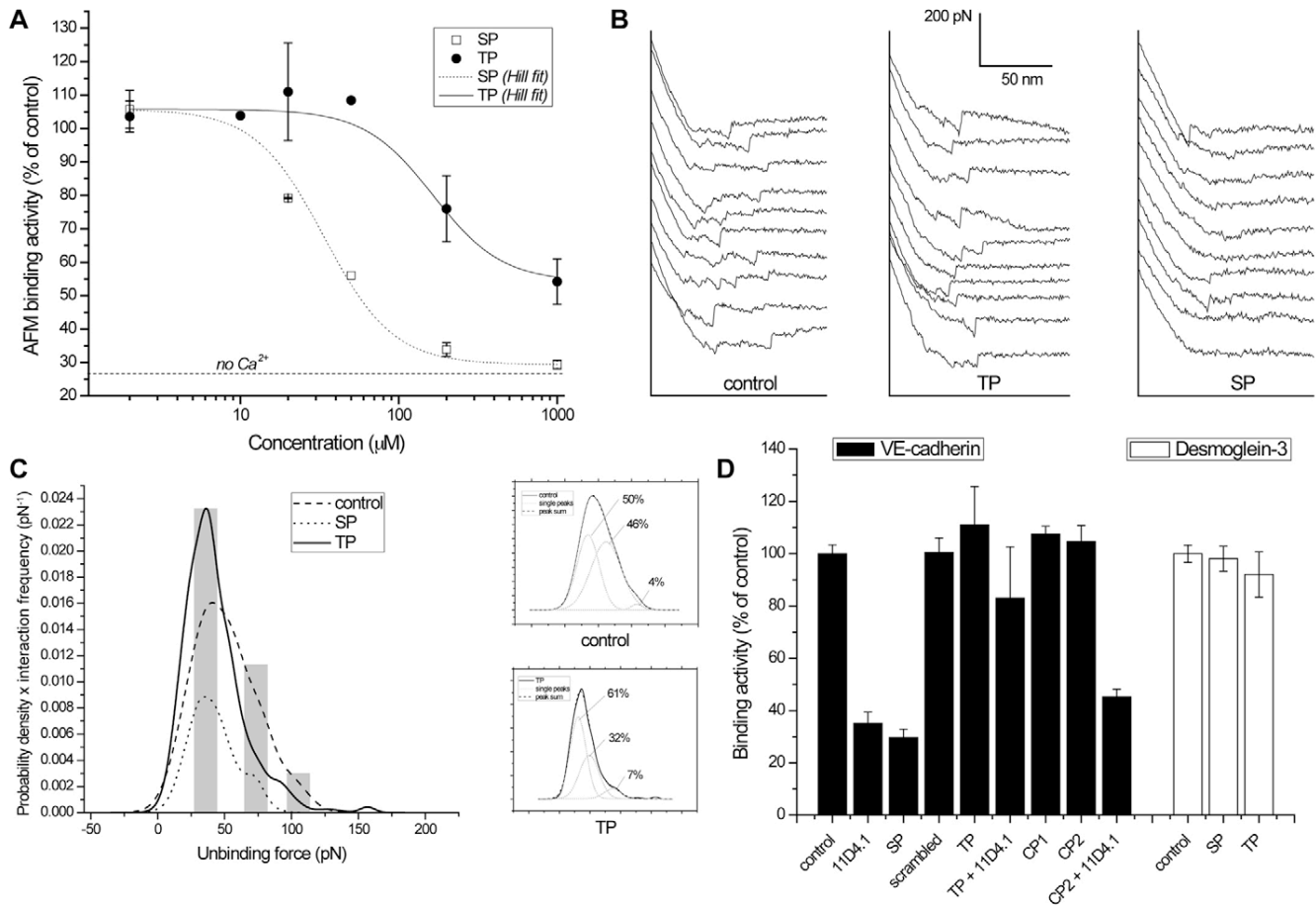


Fig. 2. Effect of SP and TP on single molecule VE-cadherin transinteraction. (A) Dose-response curves show action of SP and TP on VE-cadherin transinteraction as probed by AFM single molecule unbinding studies. SP reduced VE-cadherin binding activity at concentrations of 20 μ M or higher, resulting in a reduction of about 70% at 200 μ M. By contrast, TP displayed a shifted dose-response curve with inhibiting activity starting at 200 μ M. The dashed line indicates VE-cadherin binding activity in Ca^{2+} -free conditions. (B) Sample force-distance cycles in control, 20 μ M TP or 200 μ M SP conditions. Note the similar unbinding events in TP and control conditions but reduced interaction frequency in SP condition. (C) Frequency distribution of single molecule VE-cadherin-Fc unbinding events measured at retrace velocities of 600 nm/second. For each condition, >500 unbinding curves were evaluated and resulting probability densities corrected by interaction frequencies, which were 52.8% for control, 54.0% for TP and 20.3% for SP condition. In control conditions, three different force peaks could be differentiated (marked by grey columns). Note the frequency increase for the first unbinding force peak in TP condition (61% versus 50%; see also insets with Gaussian multiple peak fits of control and TP probability density curves) and reduced interaction frequency after SP treatment. (D) Binding activities of transinteracting VE-cadherin-Fc were strongly reduced after treatment with monoclonal VE-cadherin antibody 11D4.1. As already demonstrated in A, SP at 200 μ M blocked VE-cadherin transinteraction whereas TP at 20 μ M did not. Preincubation with 20 μ M TP, however, prevented 11D4.1-induced loss of VE-cadherin adhesion. Sequence specificity of SP and TP action was demonstrated by a scrambled SP or control peptides CP1 and CP2, which did not have an effect on VE-cadherin binding activity, and by CP2 which was unable to block 11D4.1-mediated inhibition. Moreover, SP and TP at the concentrations used did not influence transinteraction of desmoglein-3-Fc ($n=3-4$ for each condition).

2D summarizes AFM data of VE-cadherin binding activities under conditions using control peptides or TP in the presence or absence of mAb 11D4.1. Treatment with 11D4.1 resulted in significantly reduced binding activity ($35\pm 4\%$ of controls), indicating specificity of VE-cadherin interactions in the AFM setup. SP ($200\ \mu\text{M}$) was found to efficiently reduce VE-cadherin transinteraction to $30\pm 3\%$ of control levels, whereas TP ($20\ \mu\text{M}$) did not significantly alter VE-cadherin binding activities. Next, we investigated whether TP was effective in preventing loss of VE-cadherin binding induced by mAb 11D4.1 because we assumed that TP would stabilize VE-cadherin transinteraction. Interestingly, preincubation with TP blocked mAb 11D4.1-induced loss of transinteraction (binding activities were $83\pm 20\%$ of controls). Sequence specificity of SP and TP action was further demonstrated by a scrambled SP or control peptides CP1 and CP2. CP1 is a SP peptide specific for desmoglein transinteraction and CP2 the tandem version of CP1 (Heupel et al., 2009). All three control peptides did not affect VE-cadherin binding activity, and dimeric CP2 was not effective at blocking mAb 11D4.1-mediated inhibition of VE-cadherin transinteraction. In a parallel set of experiments, SP and TP were shown not to interfere with transinteraction of a member of the desmocadherin family, desmoglein-3-Fc, indicating that the effect on VE-cadherin transinteraction was not due to unspecific effects of the peptides. Taken together, AFM experiments demonstrated that SP efficiently inhibited homophilic VE-cadherin transinteraction demonstrating SP binding to the proposed binding pocket. TP, however, enhanced VE-cadherin-Fc dimer interactions and effectively inhibited antibody-induced loss of VE-cadherin binding.

SP and TP peptides modified lateral diffusion of VE-cadherin-EYFP

To directly investigate effects of SP and TP on VE-cadherin lateral mobility, we used FRAP studies in a cell line stably expressing VE-cadherin-EYFP (CHO-A1; Fig. 3A). In CHO-A1 cells, VE-cadherin-EYFP signals were confined to sites of cell-cell contacts. EYFP signals were specifically bleached at regions of cell-cell contacts and subsequent increases in fluorescence signals were measured over time. In controls, VE-cadherin-EYFP displayed a biphasic, double-exponential recovery after photobleaching with a rapid recovery of the signal within a few seconds followed by a steady increase afterwards (Fig. 3B). Also, a rather slow recovery and high fraction of immobile molecules was noted under all conditions tested, as typically seen for other adhesion molecules (Stehbens et al., 2006). Compared with controls, SP led to a significant increase in fluorescence recovery indicating enhanced lateral diffusion of VE-cadherin-EYFP, probably because of SP-induced interference with VE-cadherin interactions (see Fig. 2D). By contrast, TP treatment resulted in decreased signal recovery. This suggested diminished lateral diffusion of VE-cadherin in response to TP-induced stabilization of VE-cadherin interactions.

TP prevented reduction of VE-cadherin bead binding induced by mAb 11D4.1 and the Ca^{2+} ionophore A23187 but acted independently of cytoskeletal anchorage or signalling

We further investigated whether TP treatment had a protective effect on endogenous VE-cadherin binding using laser tweezer experiments with VE-cadherin-coated microbeads (Fig. 4A). Beads were seeded on the surface of endothelial MyEnd cells to allow formation of cell-to-bead contacts as characterized in detail previously (Baumgartner et al., 2003). After 30 minutes, beads were exposed to a laser beam to test bead binding. The number of beads

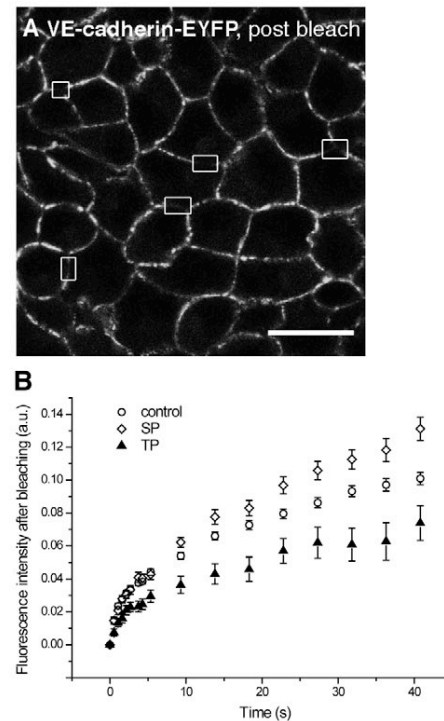


Fig. 3. SP and TP peptides modified lateral diffusion of VE-cadherin-EYFP in FRAP studies. (A) In CHO-A1 cells, VE-cadherin-EYFP signals were continuously seen at sites of cell-cell contacts. In this sample post-bleach image, rectangles indicate region of interests where EYFP fluorescence had just been bleached at sites of cell-cell contacts. Scale bar: $20\ \mu\text{m}$. (B) Measurements of fluorescence intensities in these regions showed a biphasic, double-exponential recovery of EYFP signals after bleaching in all three conditions. After $t\approx 9$ seconds, however, VE-cadherin-EYFP recovery was enhanced in SP-pretreated cells, whereas it was reduced during nearly the whole time series in TP-pretreated cells. Note the overall slow recovery and high fraction of immobile molecules in all conditions.

resisting displacement by the laser beam was counted after 30 minutes ($69\pm 3\%$), taken as tightly bound and set to 100% (Fig. 4B). Preincubation with TP for 30 minutes before bead binding led to a significant increase of bound beads in MyEnd cells ($115\pm 2\%$). Incubation of bound beads with mAb 11D4.1 resulted in a strong reduction of VE-cadherin-mediated bead binding ($63\pm 2\%$). This antibody-mediated weakening of binding was completely prevented by preincubation of MyEnd cells with TP ($10\pm 3\%$). Similar experiments were performed using the Ca^{2+} ionophore A23187, which had been shown to result in dissociation of cell-cell junctions and increased permeability *in vivo* and *in vitro*, at least in part by targeting VE-cadherin cytoskeletal anchorage (Baumgartner et al., 2003; Curry et al., 1990; He and Curry, 1991; Schnittler et al., 1990). A23187 treatment for 45 minutes strongly reduced the number of bound beads ($68\pm 4\%$). However, in the presence of TP, A23187-induced loss of bead binding was completely prevented ($97\pm 2\%$).

We have shown previously that immobilization of VE-cadherin molecules by linkage to the actin cytoskeleton significantly improved VE-cadherin-mediated bead binding (Baumgartner et al., 2003). Addition of the F-actin-disrupting agent cytochalasin D ($10\ \mu\text{M}$) for 30 minutes to endothelial monolayers with surface-bound beads strongly reduced bead binding to $55\pm 4\%$ of controls (Fig. 4B). Importantly, TP largely prevented cytochalasin D-induced

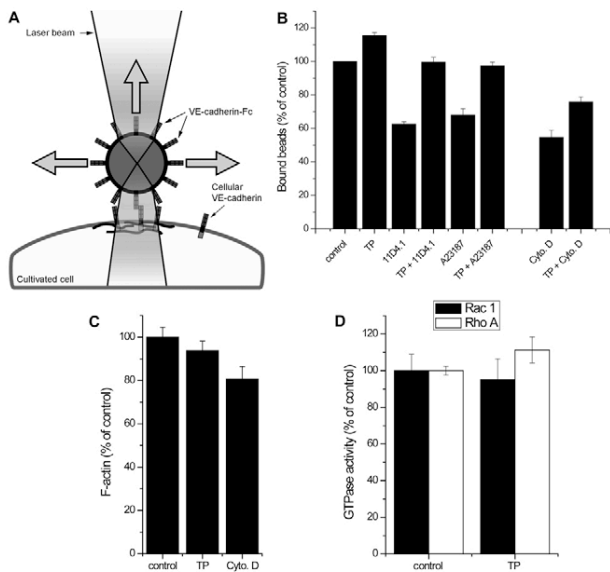


Fig. 4. TP prevented mAb 11D4.1- and A23187-induced loss of VE-cadherin-mediated adhesion but acted independently of F-actin or Rho GTPase function. (A) Principle of laser tweezer experiments. VE-cadherin-coated microbeads were allowed to settle on the surface of MyEnd cells to induce VE-cadherin-mediated homophilic adhesion. Afterwards, beads were trapped in a laser beam focus to discriminate bound from unbound beads. (B) On MyEnd cells, the number of bound beads was significantly increased after incubation with TP for 30 minutes, compared with controls. Incubation with mAb 11D4.1 led to a strong loss of VE-cadherin bead binding. Preincubation with TP (20 μ M), however, completely prevented this reduction. Incubation with the Ca^{2+} ionophore A23187 (10 μ M) for 45 minutes similarly reduced bead binding, whereas preincubation with TP (20 μ M) again completely blocked this effect. Incubation with the F-actin-disrupting agent cytochalasin D (10 μ M) for 30 minutes strongly reduced the number of surface-bound beads. Nevertheless, preincubation with TP in combination with cytochalasin D resulted in increased bead binding compared to cytochalasin D alone ($n=6-8$). (C) Quantification of F-actin demonstrated that only cytochalasin D but not TP treatment significantly decreased the F-actin content. (D) In GTPase activity assays, TP treatment of MyEnd cells did not lead to activation of the small GTPases Rac1 and RhoA.

weakening of bead binding (76 \pm 3%) indicating that TP-mediated improvement of bead binding largely compensated for the loss of anchorage of VE-cadherin to the actin cytoskeleton. We further evaluated effects on the actin cytoskeleton by quantification of F-actin contents in MyEnd cells under the different conditions (Fig.

4C). Cytochalasin D significantly decreased F-actin content (81 \pm 6% of controls) whereas TP had no effect (94 \pm 4% of controls). These experiments indicated that the action of TP did not involve the actin cytoskeleton.

Alternatively, increased VE-cadherin bead binding could also be explained by activation of intracellular signalling cascades as a result of lateral cross-bridging and clustering of VE-cadherin molecules in response to TP treatment. Members of the Rho family of small GTPases have been shown to be critically involved in regulation of endothelial cell junctions (Vandenbroucke et al., 2008). Therefore, we tested the effect of TP on small GTPases Rac1 and RhoA in GTPase activity assays (Fig. 4D). However, TP treatment did not alter the activity of both small GTPases (95 \pm 11% and 111 \pm 7% of controls, respectively). Taken together, stabilization of VE-cadherin bead binding by TP was independent of both the actin cytoskeleton and the GTPases Rac1 and RhoA.

TP prevented A23187-mediated reorganization of endothelial adherens junctions

We visualized the effects of A23187 on endothelial adherens junctions in MyEnd cells by VE-cadherin immunostaining. Under control conditions, immunostaining for VE-cadherin showed continuous linear distribution of VE-cadherin along cell junctions (Fig. 5A). Similar results were obtained in the presence of TP for up to 24 hours (not shown). In the presence of A23187, VE-cadherin immunostaining became strongly frayed and fragmented after 45 minutes of incubation (arrows in Fig. 5C). Similar effects have been described for human umbilical vein endothelial cells after treatment with A23187, histamine, vascular endothelial growth factor or TNF- α (Andriopoulou et al., 1999; Esser et al., 1998; Nwariaku et al., 2002; Schnittler et al., 1990). As shown in Fig. 5D-F, TP partially blocked A23187-induced opening and reorganization of adherens junctions. Quantification of frayed and broadened VE-cadherin immunosignals by image thresholding and area measurements confirmed the protective effects of preincubation with TP against A23187-induced changes (Fig. 5G and Materials and Methods for quantification procedure).

Drop of transendothelial electric resistance (TER) in response to mAb 11D4.1 and A23187 was reduced in the presence of TP

Functional changes of endothelial barrier properties were analyzed by TER measurements in endothelial monolayers. First, we used mAb 11D4.1 to evaluate whether VE-cadherin contributes to endothelial barrier properties. Incubation of MyEnd cells with mAb

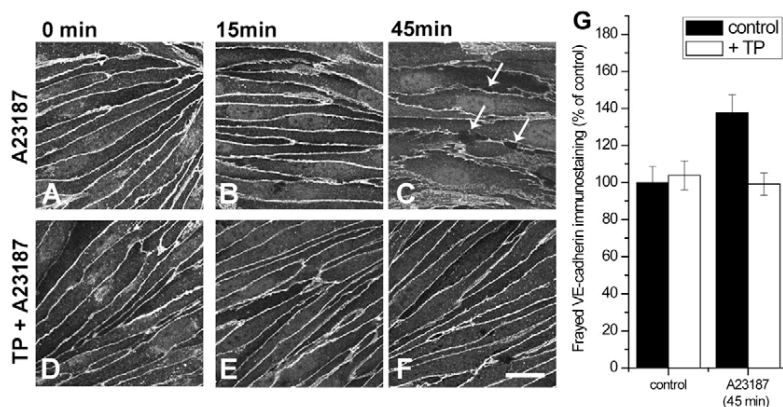


Fig. 5. TP prevented A23187-induced alterations of endothelial adherens junctions. (A-F) Confluent MyEnd monolayers were treated with A23187 (10 μ M) for the indicated times. In parallel experiments (D-F), cells were preincubated for 30 minutes with TP (20 μ M) before addition of A23187. In controls (0 minutes), VE-cadherin immunostaining was regularly distributed along cell borders (A). Incubation with A23187 led to frayed and fragmented immunostainings after 45 minutes (B,C). This effect was prevented by the presence of TP (D-F). (G) Quantification of VE-cadherin-positive immunosignals confirmed frayed and broadened VE-cadherin staining after 45 minutes incubation with A23187 and the protective effects of preincubation with TP. Images shown are representative of six experiments. Scale bar: 20 μ m.

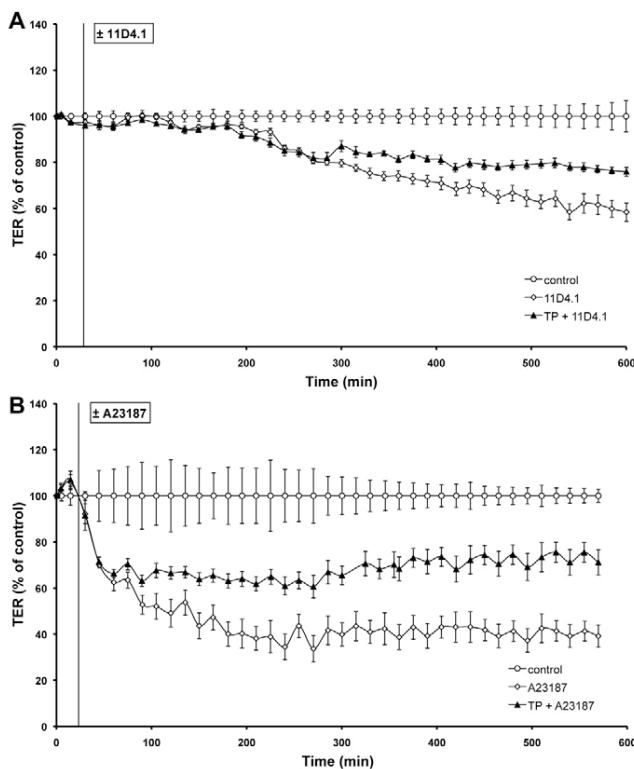


Fig. 6. TP partially prevented loss of TER induced by mAb 11D4.1 and A23187 in endothelial cells. (A) A significant reduction in TER was observed 240 minutes after addition of mAb 11D4.1 (50 µg/ml). Starting after 300 minutes, treatment with TP in addition to mAb 11D4.1 resulted in a significant higher TER compared with mAb 11D4.1 alone ($n=5$). (B) Treatment of endothelial monolayers with A23187 (10 µM) led to a significant reduction in TER within 45 minutes compared with controls, reaching a plateau after 180 minutes. In endothelial cells preincubated for 30 minutes with 20 µM TP, the A23187-induced drop in TER was partially prevented ($n=5$).

11D4.1 led to a significant drop of TER (Fig. 6A). After 4 hours, TER was significantly lower in monolayers incubated with mAb 11D4.1 (86±1%) compared with untreated cells (control) and continued to decrease to 58±4% after 10 hours. Pretreatment with TP partially rescued these effects: cells preincubated with TP and treated with mAb 11D4.1 afterwards displayed a similar short-term antibody-induced decrease in TER after 4 hours (86±2%). However, TP prevented a further drop of TER in the following time course (76±2% after 10 hours) when compared to experiments using mAb 11D4.1 alone.

Next, we investigated whether TP would be effective in preventing endothelial barrier breakdown induced by the Ca^{2+} ionophore A23187. In endothelial monolayers treated with 10 µM A23187, TER began to drop after 45 minutes (70±1%) and reached 40±5% of the control resistance after 10 hours (Fig. 6B). Similar to the response shown in Fig. 6A, monolayers pretreated with TP showed an initial drop of TER comparable to cells exposed to A23187 alone (71±2% of control levels after 45 minutes) but no further reduction in TER was observed during the following time course (71±5% after 10 hours). These experiments demonstrated the capability of TP to partially stabilize barrier functions of cultured endothelial monolayers against direct (mAb 11D4.1) or indirect (A23187) stimuli interfering with VE-cadherin-mediated adhesion.

Several other TP concentrations tested ranging from 10 to 200 µM did not improve protective effects assayed by TER measurements (not shown).

TP treatment prevented TNF- α -induced increase of microvessel permeability *in vivo*

As a final step, we conducted *in vivo* permeability measurements in single perfused venules of the rat mesentery to test whether TP exerted barrier protective effects in the presence of a clinically relevant mediator of inflammation (Fig. 7). TNF- α was chosen because this cytokine has been shown to play a pivotal role in inflammatory endothelial barrier breakdown partially caused by modulation of VE-cadherin binding (Angelini et al., 2006; Nwariaku et al., 2002; Vandembroucke et al., 2008). TNF- α alone resulted in significant increase of hydraulic conductivity (L_p) that became obvious after 120 minutes of treatment. A similar lag phase was observed in previous studies (Brett et al., 1989; Goldblum et al., 1993) (Fig. 7A shows representative experiments; Fig. 7B mean L_p values). Simultaneous application of TNF- α and TP, however, completely blocked TNF- α -induced increase of microvascular permeability. After 150 minutes, L_p values in microvessels perfused with TNF- α and TP [2.35 ± 0.55 (cm/second/cm H_2O) $\times 10^{-7}$] were not statistically different from controls [1.14 ± 0.33 (cm/second/cm H_2O) $\times 10^{-7}$], whereas TNF- α led to strong increase of permeability during this time period [15.13 ± 2.2 (cm/second/cm H_2O) $\times 10^{-7}$]. These experiments demonstrated that TP acted as a VE-cadherin-cross-bridging compound stabilizing the endothelial barrier against a physiologically important inflammatory agent.

Discussion

The present study demonstrates that endothelial barrier function can be stabilized by a short dimeric peptide (tandem peptide, TP) derived from the putative binding interface of the N-terminal portion of the outermost VE-cadherin extracellular domain. Our experiments indicate that TP stabilized VE-cadherin transinteraction by its cross-bridging activity. As expected, the monomeric single peptide (SP) sequence blocked homophilic VE-cadherin transinteraction most probably by occupying the site proposed to be involved in binding. TP-induced stabilization of the endothelial barrier was demonstrated *in vitro* and *in vivo* by its protective effect against various barrier-compromising stimuli.

Stabilization of VE-cadherin-mediated adhesion is important for maintenance of endothelial barrier function *in vitro* and *in vivo*

Our results indirectly indicate that increased intracellular Ca^{2+} , which is known to be a pivotal initial mechanism underlying the effects of most inflammatory mediators (Michel and Curry, 1999; Vandembroucke et al., 2008), destabilizes the endothelial barrier at least in part via loss of VE-cadherin-mediated binding. This conclusion can be drawn from our observation that TP significantly counteracted A23187-mediated reduction of VE-cadherin binding (laser tweezers) and under these conditions attenuated breakdown of TER.

Since it is difficult to extrapolate from *in vitro* studies with endothelial monolayers and non-physiological stimuli (mAb 11D4.1, A23187) to the *in vivo* situation, we tested the barrier stabilizing potency of TP in intact microvessels *in vivo* using TNF- α as a well established physiological inflammatory stimulus playing a key role in organ dysfunction and death (Cinell and Dellinger, 2007; Opal, 2007). TNF- α disrupts endothelial barrier function via

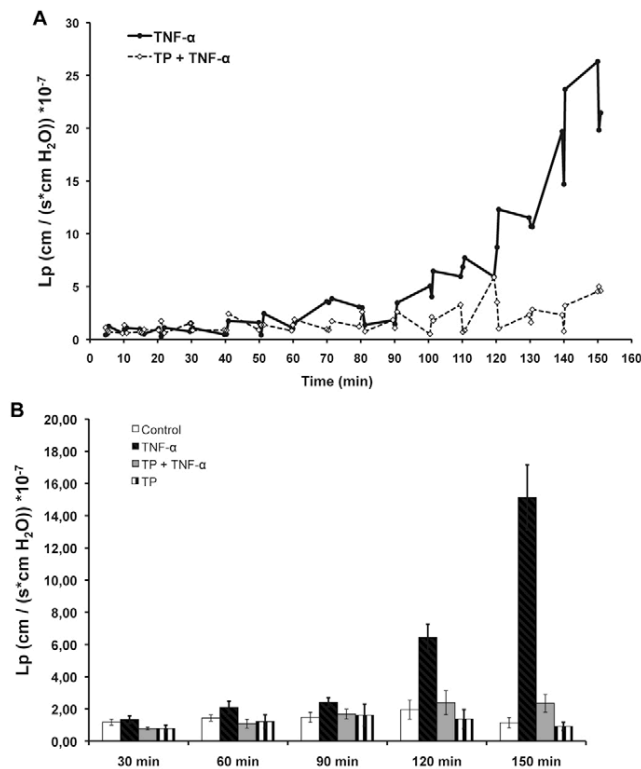


Fig. 7. TP treatment abolished TNF- α -induced increase of microvessel permeability in vivo. (A) Measurements of hydraulic conductivity (L_p) demonstrated that TNF- α strongly increased microvessel permeability, starting after 120 minutes, which was, however, completely prevented by cotreatment with TP. Note that at every time point three independent L_p measurements were made and plotted in this graph. (B) Mean L_p values for each condition show that after 120 minutes TNF- α significantly increased L_p compared with controls. Although having no effect when applied alone, TP completely abolished TNF- α -induced increase of endothelial permeability ($n \geq 5$ for each condition).

several pathways including modulation of VE-cadherin binding (Angelini et al., 2006; Nwariaku et al., 2002). Therefore, we used TNF- α rather than thrombin, which is also known to induce a breakdown of endothelial barrier properties by several pathways in vitro, and is effective in vivo in several vascular beds (Vandenbroucke et al., 2008). However, in microperfused vessels in rat mesentery, thrombin has been reported to have no effect unless venules were previously exposed to inflammatory conditions (Curry et al., 2003). In vivo, simultaneous treatment with TP was effective in blocking TNF- α -induced endothelial hyperpermeability. In view of the crucial role of TNF- α in life-threatening septic inflammation, the present peptide approach to stabilize VE-cadherin transinteraction might be a promising animal model for the treatment of disorders caused by increased vascular leakage.

Tandem peptide mode of action

Single molecule unbinding analysis demonstrated a dose-dependent effect of both TP and SP on VE-cadherin transinteraction. Whereas SP acted as a strong inhibitor of VE-cadherin transinteraction, TP inhibited transinteraction only at high concentrations, at which probably all binding sites of VE-cadherin were occupied by the peptide. Therefore we chose a TP concentration where VE-cadherin

transinteraction was not reduced. At lower concentrations (e.g. 20 μ M) TP did not inhibit, but rather improved, VE-cadherin transinteraction as indicated by increase of the first peak in unbinding force distributions (see also Baumgartner et al., 2000). Moreover, TP rendered VE-cadherin transinteraction partially resistant against destabilization by an inhibitory antibody. The action of SP and TP was specific for VE-cadherin as concluded from AFM experiments using several control peptides and proteins.

It has to be pointed out that the mode of action of TP probably differs from peptides targeting N-cadherin used by the Doherty group (Williams et al., 2002). In their work, it was demonstrated that agonistic N-cadherin peptides promoted axonal outgrowth via clustering and activation of fibroblast growth factor receptor (FGFR), because inhibition of FGFR prevented agonistic effects of their N-cadherin dimeric peptides. Although a similar mode of action is possible for VE-cadherin TP, our results indicate that cross-bridging of transinteracting VE-cadherin molecules itself is effective to strengthen both VE-cadherin binding and endothelial barrier properties. This can be concluded because TP treatment had protective effects on VE-cadherin transinteraction in cell-free single molecule AFM experiments. Because both lateral clustering and transinteraction of cadherin molecules are known to be a prerequisite for enhanced adhesion (Ahrens et al., 2003; Yap et al., 1997) effects of TP on both interaction mechanisms are likely to contribute to endothelial barrier stabilization in vitro and in vivo. However, interaction of VE-cadherin and vascular endothelial growth factor receptor 2 (VEGFR2) or vascular endothelial protein tyrosine phosphatase has been shown (Carmeliet et al., 1999; Nottebaum et al., 2008), the latter interaction also being targeted by TNF- α . Therefore, we cannot rule out that TP-induced signalling mechanisms in addition to enhanced transinteraction may contribute to the protective effects of TP in vivo and in vitro. However, these effects of TP seem to be independent from small GTPases Rac1 and RhoA as well as from reorganization of the actin cytoskeleton. Furthermore, it has been shown that various inflammatory mediators including VEGF lead to VE-cadherin endocytosis (Gavard and Gutkind, 2006). Blocking cadherin endocytosis by stabilizing cadherin interactions enhanced cellular adhesion as demonstrated for E-cadherin (Trojanovsky et al., 2006). A similar mode of action is also conceivable for TP, further strengthening the hypothesis that TP stabilized VE-cadherin interactions. Nevertheless, short term effects of the VE-cadherin inhibiting agents A23187 or cytochalasin D and protective mechanisms of TP against these agents might not rely on modulation of VE-cadherin endocytosis because we have previously shown that a decrease of surface available VE-cadherin is negligible under these conditions (Baumgartner et al., 2003).

Limitations of the approach to stabilize VE-cadherin binding
A reduced concentration range because of competitive equilibria between displacement reactions at higher concentrations, and between stabilization of lateral clustering and transinteractions, may limit the practical effectiveness of tandem peptide action. This may explain some inconsistencies of TP behaviour in laser tweezer and AFM experiments. Different displacement kinetics could account for TP-mediated enhancement of bead binding: with beads held on the cell surface, there is sufficient time for the displacement and subsequent cross-bridging to occur. With the lifetime of transinteracting VE-cadherin bonds being in the range of $\tau_0 \approx 0.55$ seconds (Baumgartner et al., 2000) and $\tau_0 \approx 2.2$ seconds (Panorchan et al., 2006), displacement and subsequent cross-bridging may not fully develop in AFM experiments. Nevertheless, TP stabilized VE-

cadherin transinteraction in AFM experiments, and dose-dependency curves revealed that no concentration other than 20 μM was more effective at protecting endothelial barrier properties. Apparently, this concentration is also applicable *in vivo* because TP completely blocked increased microvessel permeability in response to the inflammatory mediator TNF- α .

Finally, even though systemic *in vivo* application of tandem peptides is most likely to induce severe immune responses, this study is a first step to developing non-peptide drugs that may be useful to protect the endothelial barrier against vascular hyperpermeability.

Materials and Methods

Modelling of the VE-cadherin extracellular domains 1 and 2

A molecular model for the two N-terminal cadherin extracellular domains 1 and 2 (EC1 and 2) of human VE-cadherin was obtained by homology modelling using the crystal structure of E-cadherin [Protein Data Bank (PDB) entry 1EDH] as a template. A multiple sequence alignment was produced using protein sequences of human, mouse and rat VE-cadherin, N-cadherin and E-cadherin with the software CLUSTALW. Amino acid residues differing between VE-cadherin and the structural template were substituted by the corresponding amino acids. Insertions and deletions were modelled manually using the software tool XBUILD in Quanta2006 (Accelrys Inc., San Diego, CA). Close contacts between side chains were first removed by rotamer searches using the XBUILD tool and a subsequent refinement step of the side chain conformer with the lowest starting energy by 100–500 steps of energy minimization using the steepest gradient algorithm and the CHARMM22 force field without electrostatic terms. The resulting final model was further refined by energy minimization and short (50 psec) molecular dynamics simulations *in vacuo* with an all-hydrogen force field CHARMM22 without electrostatic terms. In the first rounds, the protein backbone was kept fixed and only side chain atoms were released. Afterwards, the main chain atoms were released stepwise for minimization by employing a positional harmonic potential (initial force constant 50 kcal/mol/Å²), which was lowered stepwise (at 5 picosecond intervals, the force constant was lowered by 15 kcal/mol/Å²) to maintain the protein architecture. The final structure model exhibited good backbone and side chain geometries with none of the backbone torsion angles occupying disallowed zones in the Ramachandran plot analysis.

Design of the VE-cadherin single and tandem peptides

The N-terminal N-cadherin domain 1 has been crystallized in three different crystal forms suggesting different assemblies for intermolecular cadherin interactions. The crystal structure from the spacegroup P321 (PDB entry INCH) exhibits the largest inter-cadherin interface thus providing the best template for the design of small peptide-based cadherin inhibitors. This assembly is also supported by electron tomography studies on desmosomal knots (He et al., 2003) in which full-length ectodomains are involved in various *trans*- and *cis*-interactions. Another N-cadherin assembly from a N-cadherin EC1-EC2 tandem domain pair suggests a slightly different *trans*-interaction architecture [PDB code INCJ (Tamura et al., 1998)], but similar regions as in structure INCH are in contact. Other cadherin structures propose differing assemblies in which the N-terminal peptide forms intimate contacts via strand-swapping. Although mutagenesis data for N-cadherin propose a similar interaction with the N-terminal residue Trp2 as the central determinant, we have chosen the assembly from the structure INCH because here the interactions are less hydrophobic, possibly yielding peptides with higher solubility. To mimic a putative *cis*-*trans*-interaction between two VE-cadherin molecules, the crystal structure of the N-terminal cadherin domain 1 was used for docking. The two docked VE-cadherin molecules were refined to remove interfering van der Waals contacts using the CHARMM22 force field without electrostatic term and steepest gradient energy minimization. A single peptide (SP) was designed using residues Arg47 to Glu51 of one VE-cadherin moiety. This peptide segment exhibited tight interaction in terms of intermolecular polar bonds and size of buried surface area. The tandem peptide (TP) was generated by combining two SPs using a flexible linker and cyclization by the addition of cysteine residues.

Test reagents

Single peptide RVDAE and scrambled peptide ADVRE were synthesized in our laboratory using Fmoc-based solid-phase peptide synthesis assembling the peptide on Wang resin. All chemicals were supplied by Novabiochem (Darmstadt, Germany). The tandem peptide sequence was N-Ac-CRVDAAE-⁶-amino-hexanoic acid linker²-RVDAEC-NH₂. The sequences of the control peptides CP1 and CP2 were CLNSMGQDC and CLNSMGQDC-⁶-amino-hexanoic acid linker²-CLNSMGQDC, respectively, and derived from a study targeting desmoglein transinteraction with single (CP1) and tandem (CP2) peptides. The underlining of the peptide sequences denotes cyclization via a disulfide bond between the given cysteine residues. TP, CP1 and CP2 peptides were obtained from a commercial supplier (PSL, Heidelberg, Germany). All peptides were purified by reversed-phase HPLC at a purity >95%. After

conducting experiments to construct dose-response curves, peptides were used at 200 μM (SP, scrambled, CP1) and 20 μM (TP, CP2), respectively. The monoclonal antibody against the ectodomain of mouse VE-cadherin (11D4.1) has been described previously (Gotsch et al., 1997), was a gift from D. Vestweber (MPI of Molecular Biomedicine, Münster, Germany) and used at 50 $\mu\text{g/ml}$. A23187 and Cytochalasin D (both from Sigma-Aldrich, Taufkirchen, Germany) were used at 10 μM . Tumor necrosis factor- α (TNF- α ; Sigma-Aldrich) was used at 100 ng/ml.

Cell culture

The immortalized murine microvascular endothelial cell line (MyEnd) was grown in Dulbecco's modified Eagles medium (DMEM, Life Technologies, Karlsruhe, Germany) supplemented with 50 IU/ml penicillin-G, 50 μg streptomycin and 10% fetal calf serum (Biochrom, Berlin, Germany) in a humidified atmosphere (95% air/5% CO₂) at 37°C. VE-cadherin-EYFP-transfected CHO cells (CHO-A1) were cultured as described above with addition of 0.2 g/l geneticin (PAA, C8lbe, Germany). The cultures were used for experiments when grown to confluent monolayers.

Generation of the VE-cadherin-EYFP-expressing cell line CHO-A1

Mouse VE-cadherin full-length cDNA was a kind gift from Dietmar Vestweber (MPI of Molecular Biomedicine), amplified with primers 5'-CCCAAGCTTATGCAGAGGCTCACAGAGC-3' and 5'-GCTCTAGAGATGATGAGTTCCTCC-TGG-3' and cloned in frame with the cDNA encoding EYFP using *Hind*III-*Xba*I-digested plasmid pcDNA3.0-beta2AR-EYFP (a kind gift from Viacheslav Nikolaev, Institute of Pharmacology and Toxicology, University of Würzburg, Germany) to yield pcDNA3.0-VE-cadherin-EYFP. Sequence integrity was confirmed by sequencing. For generation of CHO-A1 cells, the construct was transfected into wild-type Chinese hamster ovary (CHO) cells using Effectene transfection (Qiagen, Hilden, Germany) and a stable-transfected cell line (CHO-A1) was obtained using single cell subsplitting and subsequent characterization for VE-cadherin-EYFP expression.

Atomic force microscopy measurements with recombinant

VE-cadherin-Fc

The AFM setup consisted of a Bioscope AFM driven by a Nanoscope III controller (Veeco Instruments, Mannheim, Germany). Homophilic transinteraction of recombinant VE-cadherin was characterized by force-distance measurements of VE-cadherin coupled to Si₃N₄ tips of the cantilever (Veeco Instruments) and freshly cleaved mica plates (SPI Supplies, West Chester, PA) using flexible polyethylene glycol (PEG) spacers containing an amino-reactive crosslinker group at one end and a thiol-reactive group at the other end, as described previously in detail (Baumgartner et al., 2000). If not otherwise stated, binding events were measured in buffer A (140 mM NaCl, 10 mM Hepes, 5 mM CaCl₂) by force-distance cycles at amplitudes of 300 nm and 1 Hz frequency yielding continuous trace and retrace velocities of 600 nm/second. For every condition, 300–500 force distance cycles were recorded and each condition was repeated with new cantilever and mica preparations three to four times. Analysis of distribution of single molecule unbinding forces was performed as described previously (Baumgartner et al., 2000). Interaction frequency was evaluated by analyzing and counting specific unbinding events in force distance cycles with a VE-cadherin-coated tip under different conditions thereby reflecting both effective concentrations of VE-cadherin molecules on the tip and binding probabilities. For experiments referring to binding activity, the total area between approach and retrace curves was taken as a measure of adhesion. To investigate VE-cadherin specificity of peptides, SP and TP action on recombinant desmoglein 3-Fc was performed as described recently (Heupel et al., 2008).

Measurements of transendothelial resistance (TER)

ECIS 1600R (Applied BioPhysics, New York, NY) was used to measure the transendothelial resistance (TER) of MyEnd monolayers assessing endothelial barrier integrity as described previously (Baumer et al., 2008) with the following modifications: cells were seeded in wells of the electrode array and grown to confluence for 5–7 days. Before experiments, medium was changed (400 μl DMEM) and in some conditions TP was added. The arrays were plugged into the instrument and preincubated for 30 minutes. A measurement of baseline TER was then performed before the addition of mAb 11D4.1 or A23187.

Cytochemistry

Cells on coverslips were fixed for 10 minutes with 2% formaldehyde in PBS and permeabilized with 0.1% Triton X-100 in PBS for 5 minutes. After rinsing with PBS, cells were preincubated for 30 minutes with 3% normal goat serum/1% bovine serum albumin and incubated for 16 hours at 4°C with rat mAb 11D4.1 (undiluted hybridoma supernatant). After several rinses with PBS (3×5 minutes), monolayers were incubated for 60 minutes at room temperature with Cy3-labelled goat anti-rat IgG (Dianova, Hamburg, Germany) diluted 1:600 in PBS. Coverslips were rinsed with PBS (3×5 minutes) and mounted on glass slides with 60% glycerol in PBS, containing 1.5% *n*-propyl gallate (Serva, Heidelberg, Germany) as anti-fading compound. For quantification of frayed VE-cadherin staining, VE-cadherin-positive signals of six images of each condition (out of three independent experiments) were thresholded, resulting areas were measured and normalized to controls using ImageJ (National Institutes of Health, Bethesda, MD).

Laser tweezer experiments

Coating of polystyrene beads, and laser tweezer experiments were done as described previously (Baumgartner et al., 2003). VE-cadherin-Fc-coated beads were suspended in 250 μ l of culture medium and allowed to interact with MyEnd monolayers for 30 minutes at 37°C before initiation of experiments. For some experiments, TP had been preincubated on cells prior to bead incubation or agents (A23187, cytochalasin D or mAb 11D4.1) have been applied to surface-bound beads. Beads were considered tightly bound when resisting laser displacement at 42 mW setting of the home-built laser tweezer setup consisting of a Nd:YAG laser (1064 nm, Laser 2000, Wessling, Germany) and Axiovert 135 microscope (Zeiss, Oberkochen, Germany) equipped with a high NA objective (63 \times 1.2 oil, Zeiss) and a piezo-driven XY position table. For every condition 100 beads were counted and every condition repeated six times. The percentage of beads resisting laser displacement under various experimental conditions was normalized to control values.

Quantification of F-actin

Quantification of F-actin was performed as described previously (Waschke et al., 2004). In brief, MyEnd cells were fixed with formaldehyde and permeabilized with Triton X-100. Then, phalloidin covalently labelled with Alexa Fluor 488 (Molecular Biology, Germany; 1:60) was incubated on cells for 1 hour at 37°C. After washing, phalloidin-Alexa Fluor 488 was extracted from cells by two subsequent 1-hour incubation steps with 1 ml of methanol at 37°C. Methanol supernatants were centrifuged at 100,000 \times g for 20 minutes and quantified with a FITC filter on a Victor plate reader (PerkinElmer, Waltham, MA, USA).

Rac1 and RhoA activation assay

For measurement of Rac1 or RhoA activation in MyEnd cells upon TP treatment, Rac1 or RhoA G-Lisa activation assays (Cytoskeleton, Denver CO, USA) using Rac1-GTP or RhoA-GTP binding domain-coated plates, respectively, were used according to the manufacturer's recommendations (Baumer et al., 2008).

Fluorescence recovery after photobleaching (FRAP) studies

CHO-A1 cells were transferred to live cell imaging chambers, covered with phenol red-free DMEM medium (Sigma-Aldrich) and placed on a 37°C-heated objective. Then, regions of interest at sites of cell-cell contacts were selected and bleaching series were performed using the 514 nm line of an argon laser coupled to a confocal laser scanning microscope (CLSM 5, Zeiss). Region of interest fluorescence intensity measurements of recorded images were analyzed using ImageJ (National Institutes of Health). All values were corrected for background fluorescence and loss in fluorescence due to scanning frequency. For comparison between different conditions, fluorescence intensity values were normalized to pre-bleach values and first post-bleach values set to zero.

In vivo measurements of hydraulic conductivity (L_p)

Preparation and anaesthetizing of Wistar rats were performed as described previously (Waschke et al., 2004). Rats were kept under conditions that conformed to the National Institutes of Health 'Guide for the Care and Use of Laboratory Animals', approved by the Regierung of Unterfranken. All experiments were carried out in straight non-branched segments of venular microvessels (25–35 μ m in diameter) in mesentery of living rats. Measurements were based on the modified Landis technique, which measures the volume flux (J_v/S) per unit surface area across the wall of a microvessel perfused via a glass micropipette following single occlusion of the vessel at usually 50 cm H₂O (Michel and Curry, 1999). All perfusates were mammalian Ringer solutions containing serum albumin at 10 mg/ml (Sigma-Aldrich). Hydraulic conductivity (L_p ; or hydraulic permeability) was estimated for each occlusion as $(J_v/S)/P_{eff}$ and measurements were made at approximately 10-minute intervals for up to 160 minutes. In some conditions, TNF- α and/or TP were added to the perfusate and continuously delivered via the micropipette. In preliminary dose-response experiments, TNF- α was found to consistently increase permeability of mesenteric postcapillary venules at a concentration of 100 ng/ml. For every condition, at least five vessels from different rats were used.

Statistics

Values throughout are expressed as mean \pm s.e.m. Nonparametric Mann-Whitney tests were used to test for differences in L_p groups because baseline L_p distributions are non-Gaussian in rat mesentery venules (Huxley and Rumbaut, 2000; Michel et al., 1974). Otherwise, possible differences were assessed using unpaired Student's *t*-test. Statistical significance was assumed for *P* < 0.05.

We dedicate this paper to the late Rainer Koob, who synthesized the first peptides and provided critical input into this study. We thank Christian Rankl and Peter Hinterdorfer (University of Linz, Austria) for providing AFM analysis software and help with its use, Hermann Gruber (University of Linz, Austria) for providing the AFM PEG linker and Albert Sickmann (Rudolf Virchow Center, Würzburg, Germany) for analyzing peptides by mass spectrometry. We are grateful to Lisa

Bergauer, Tanja Franzeskakis, Nadja Niedermeier, Tanja Reimer and Alexia Witchen for skilful technical assistance. These studies were supported in part by grants from the Deutsche Forschungsgemeinschaft (SFB 487, TP B2 and B5 and SFB 688, TP A4).

References

- Ahrens, T., Lambert, M., Pertz, O., Sasaki, T., Schulthess, T., Mege, R. M., Timpl, R. and Engel, J. (2003). Homoassociation of VE-cadherin follows a mechanism common to "classical" cadherins. *J. Mol. Biol.* **325**, 733–742.
- Alexander, J. S. and Elrod, J. W. (2002). Extracellular matrix, junctional integrity and matrix metalloproteinase interactions in endothelial permeability regulation. *J. Anat.* **200**, 561–574.
- Andriopoulou, P., Navarro, P., Zanetti, A., Lampugnani, M. G. and Dejana, E. (1999). Histamine induces tyrosine phosphorylation of endothelial cell-to-cell adherens junctions. *Arterioscler. Thromb. Vasc. Biol.* **19**, 2286–2297.
- Angelini, D. J., Hyun, S. W., Grigoryev, D. N., Garg, P., Gong, P., Singh, I. S., Passaniti, A., Hasday, J. D. and Goldblum, S. E. (2006). TNF- α increases tyrosine phosphorylation of vascular endothelial cadherin and opens the paracellular pathway through fyn activation in human lung endothelia. *Am. J. Physiol. Lung Cell Mol. Physiol.* **291**, L1232–L1245.
- Angst, B. D., Marcozzi, C. and Magee, A. I. (2001). The cadherin superfamily. *J. Cell Sci.* **114**, 625–626.
- Baumer, Y., Drenckhahn, D. and Waschke, J. (2008). cAMP induced Rac 1-mediated cytoskeletal reorganization in microvascular endothelium. *Histochem. Cell Biol.* **129**, 765–778.
- Baumgartner, W., Hinterdorfer, P., Ness, W., Raab, A., Vestweber, D., Schindler, H. and Drenckhahn, D. (2000). Cadherin interaction probed by atomic force microscopy. *Proc. Natl. Acad. Sci. USA* **97**, 4005–4010.
- Baumgartner, W., Schutz, G. J., Wiegand, J., Golenhofen, N. and Drenckhahn, D. (2003). Cadherin function probed by laser tweezer and single molecule fluorescence in vascular endothelial cells. *J. Cell Sci.* **116**, 1001–1011.
- Boggon, T. J., Murray, J., Chappuis-Flament, S., Wong, E., Gumbiner, B. M. and Shapiro, L. (2002). C-cadherin ectodomain structure and implications for cell adhesion mechanisms. *Science* **296**, 1308–1313.
- Brett, J., Gerlach, H., Nawroth, P., Steinberg, S., Godman, G. and Stern, D. (1989). Tumor necrosis factor/cachectin increases permeability of endothelial cell monolayers by a mechanism involving regulatory G proteins. *J. Exp. Med.* **169**, 1977–1991.
- Carmeliet, P., Lampugnani, M. G., Moons, L., Breviaro, F., Compernelle, V., Bono, F., Balconi, G., Spagnuolo, R., Oostuyse, B., Dewerchin, M. et al. (1999). Targeted deficiency or cytosolic truncation of the VE-cadherin gene in mice impairs VEGF-mediated endothelial survival and angiogenesis. *Cell* **98**, 147–157.
- Cinil, I. and Dellinger, R. P. (2007). Advances in pathogenesis and management of sepsis. *Curr. Opin. Infect. Dis.* **20**, 345–352.
- Corada, M., Mariotti, M., Thurston, G., Smith, K., Kunkel, R., Brockhaus, M., Lampugnani, M. G., Martin-Padura, I., Stoppacciaro, A., Ruco, L. et al. (1999). Vascular endothelial-cadherin is an important determinant of microvascular integrity *in vivo*. *Proc. Natl. Acad. Sci. USA* **96**, 9815–9820.
- Curry, F. E., Joyner, W. L. and Rutledge, J. C. (1990). Graded modulation of frog microvessel permeability to albumin using ionophore A23187. *Am. J. Physiol.* **258**, H587–H598.
- Curry, F. E., Zeng, M. and Adamson, R. H. (2003). Thrombin increases permeability only in venules exposed to inflammatory conditions. *Am. J. Physiol. Heart Circ. Physiol.* **285**, H2446–H2453.
- Dejana, E., Orsenigo, F. and Lampugnani, M. G. (2008). The role of adherens junctions and VE-cadherin in the control of vascular permeability. *J. Cell Sci.* **121**, 2115–2122.
- Esser, S., Lampugnani, M. G., Corada, M., Dejana, E. and Risau, W. (1998). Vascular endothelial growth factor induces VE-cadherin tyrosine phosphorylation in endothelial cells. *J. Cell Sci.* **111**, 1853–1865.
- Gavard, J. and Gutkind, J. S. (2006). VEGF controls endothelial-cell permeability by promoting the beta-arrestin-dependent endocytosis of VE-cadherin. *Nat. Cell Biol.* **8**, 1223–1234.
- Goldblum, S. E., Ding, X. and Campbell-Washington, J. (1993). TNF- α induces endothelial cell F-actin depolymerization, new actin synthesis, and barrier dysfunction. *Am. J. Physiol.* **264**, C894–C905.
- Gotsch, U., Borges, E., Bosse, R., Boggemeyer, E., Simon, M., Mossmann, H. and Vestweber, D. (1997). VE-cadherin antibody accelerates neutrophil recruitment *in vivo*. *J. Cell Sci.* **110**, 583–588.
- Gumbiner, B. M. (2000). Regulation of cadherin adhesive activity. *J. Cell Biol.* **148**, 399–404.
- He, P. and Curry, F. E. (1991). Depolarization modulates endothelial cell calcium influx and microvessel permeability. *Am. J. Physiol.* **261**, H1246–H1254.
- He, W., Cowin, P. and Stokes, D. L. (2003). Untangling desmosomal knots with electron tomography. *Science* **302**, 109–113.
- Heupel, W. M., Zillikens, D., Drenckhahn, D. and Waschke, J. (2008). Pemphigus vulgaris IgG directly inhibit desmoglein 3-mediated transinteraction. *J. Immunol.* **181**, 1825–1834.
- Heupel, W. M., Muller, T., Efthymiadis, A., Schmidt, E., Drenckhahn, D. and Waschke, J. (2009). Peptides targeting the desmoglein 3 adhesive interface prevent autoantibody-induced acantholysis in pemphigus. *J. Biol. Chem.* **284**, 8589–8595.
- Hordijk, P. L., Anthony, E., Mul, F. P., Rientsma, R., Oomen, L. C. and Roos, D. (1999). Vascular-endothelial-cadherin modulates endothelial monolayer permeability. *J. Cell Sci.* **112**, 1915–1923.

- Huxley, V. H. and Rumbaut, R. E. (2000). The microvasculature as a dynamic regulator of volume and solute exchange. *Clin. Exp. Pharmacol. Physiol.* **27**, 847-854.
- Konstantoulaki, M., Kouklis, P. and Malik, A. B. (2003). Protein kinase C modifications of VE-cadherin, p120, and beta-catenin contribute to endothelial barrier dysregulation induced by thrombin. *Am. J. Physiol. Lung Cell Mol. Physiol.* **285**, L434-L442.
- Michel, C. C. and Curry, F. E. (1999). Microvascular permeability. *Physiol. Rev.* **79**, 703-761.
- Michel, C. C., Mason, J. C., Curry, F. E., Tooke, J. E. and Hunter, P. J. (1974). A development of the Landis technique for measuring the filtration coefficient of individual capillaries in the frog mesentery. *Q. J. Exp. Physiol. Cogn. Med. Sci.* **59**, 283-309.
- Nagar, B., Overduin, M., Ikura, M. and Rini, J. M. (1996). Structural basis of calcium-induced E-cadherin rigidification and dimerization. *Nature* **380**, 360-364.
- Navarro, P., Caveda, L., Breviaro, F., Mandoteanu, I., Lampugnani, M. G. and Dejana, E. (1995). Catenin-dependent and -independent functions of vascular endothelial cadherin. *J. Biol. Chem.* **270**, 30965-30972.
- Nottebaum, A. F., Cagna, G., Winderlich, M., Gamp, A. C., Linnepe, R., Polaschegg, C., Filippova, K., Lyck, R., Engelhardt, B., Kamenyeva, O. et al. (2008). VE-PTP maintains the endothelial barrier via plakoglobin and becomes dissociated from VE-cadherin by leukocytes and by VEGF. *J. Exp. Med.* **205**, 2929-2945.
- Nwariaku, F. E., Liu, Z., Zhu, X., Turnage, R. H., Sarosi, G. A. and Terada, L. S. (2002). Tyrosine phosphorylation of vascular endothelial cadherin and the regulation of microvascular permeability. *Surgery* **132**, 180-185.
- Opal, S. M. (2007). The host response to endotoxin, antilipopolysaccharide strategies, and the management of severe sepsis. *Int. J. Med. Microbiol.* **297**, 365-377.
- Panorchan, P., George, J. P. and Wirtz, D. (2006). Probing intercellular interactions between vascular endothelial cadherin pairs at single-molecule resolution and in living cells. *J. Mol. Biol.* **358**, 665-674.
- Rabiet, M. J., Plantier, J. L. and Dejana, E. (1994). Thrombin-induced endothelial cell dysfunction. *Br. Med. Bull.* **50**, 936-945.
- Rabiet, M. J., Plantier, J. L., Rival, Y., Genoux, Y., Lampugnani, M. G. and Dejana, E. (1996). Thrombin-induced increase in endothelial permeability is associated with changes in cell-to-cell junction organization. *Arterioscler. Thromb. Vasc. Biol.* **16**, 488-496.
- Schnittler, H. J., Wilke, A., Gress, T., Suttrop, N. and Drenckhahn, D. (1990). Role of actin and myosin in the control of paracellular permeability in pig, rat and human vascular endothelium. *J. Physiol.* **431**, 379-401.
- Shapiro, L., Fannon, A. M., Kwong, P. D., Thompson, A., Lehmann, M. S., Grubel, G., Legrand, J. F., Als-Nielsen, J., Colman, D. R. and Hendrickson, W. A. (1995). Structural basis of cell-cell adhesion by cadherins. *Nature* **374**, 327-337.
- Stehbens, S. J., Paterson, A. D., Crampton, M. S., Shewan, A. M., Ferguson, C., Akhmanova, A., Parton, R. G. and Yap, A. S. (2006). Dynamic microtubules regulate the local concentration of E-cadherin at cell-cell contacts. *J. Cell Sci.* **119**, 1801-1811.
- Steinberg, M. S. and McNutt, P. M. (1999). Cadherins and their connections: adhesion junctions have broader functions. *Curr. Opin. Cell Biol.* **11**, 554-560.
- Tamura, K., Shan, W. S., Hendrickson, W. A., Colman, D. R. and Shapiro, L. (1998). Structure-function analysis of cell adhesion by neural (N-) cadherin. *Neuron* **20**, 1153-1163.
- Troyanovsky, R. B., Sokolov, E. P. and Troyanovsky, S. M. (2006). Endocytosis of cadherin from intracellular junctions is the driving force for cadherin adhesive dimer disassembly. *Mol. Biol. Cell* **17**, 3484-3493.
- Vandenbroucke, E., Mehta, D., Minshall, R. and Malik, A. B. (2008). Regulation of endothelial junctional permeability. *Ann. NY Acad. Sci.* **1123**, 134-145.
- Waschke, J., Baumgartner, W., Adamson, R. H., Zeng, M., Aktories, K., Barth, H., Wilde, C., Curry, F. E. and Drenckhahn, D. (2004). Requirement of Rac activity for maintenance of capillary endothelial barrier properties. *Am. J. Physiol. Heart Circ. Physiol.* **286**, H394-H401.
- Williams, G., Williams, E. J. and Doherty, P. (2002). Dimeric versions of two short N-cadherin binding motifs (HAVDI and INPISG) function as N-cadherin agonists. *J. Biol. Chem.* **277**, 4361-4367.
- Yap, A. S., Briehar, W. M., Pruschy, M. and Gumbiner, B. M. (1997). Lateral clustering of the adhesive ectodomain: a fundamental determinant of cadherin function. *Curr. Biol.* **7**, 308-315.

3.2 Additional experiments and methods

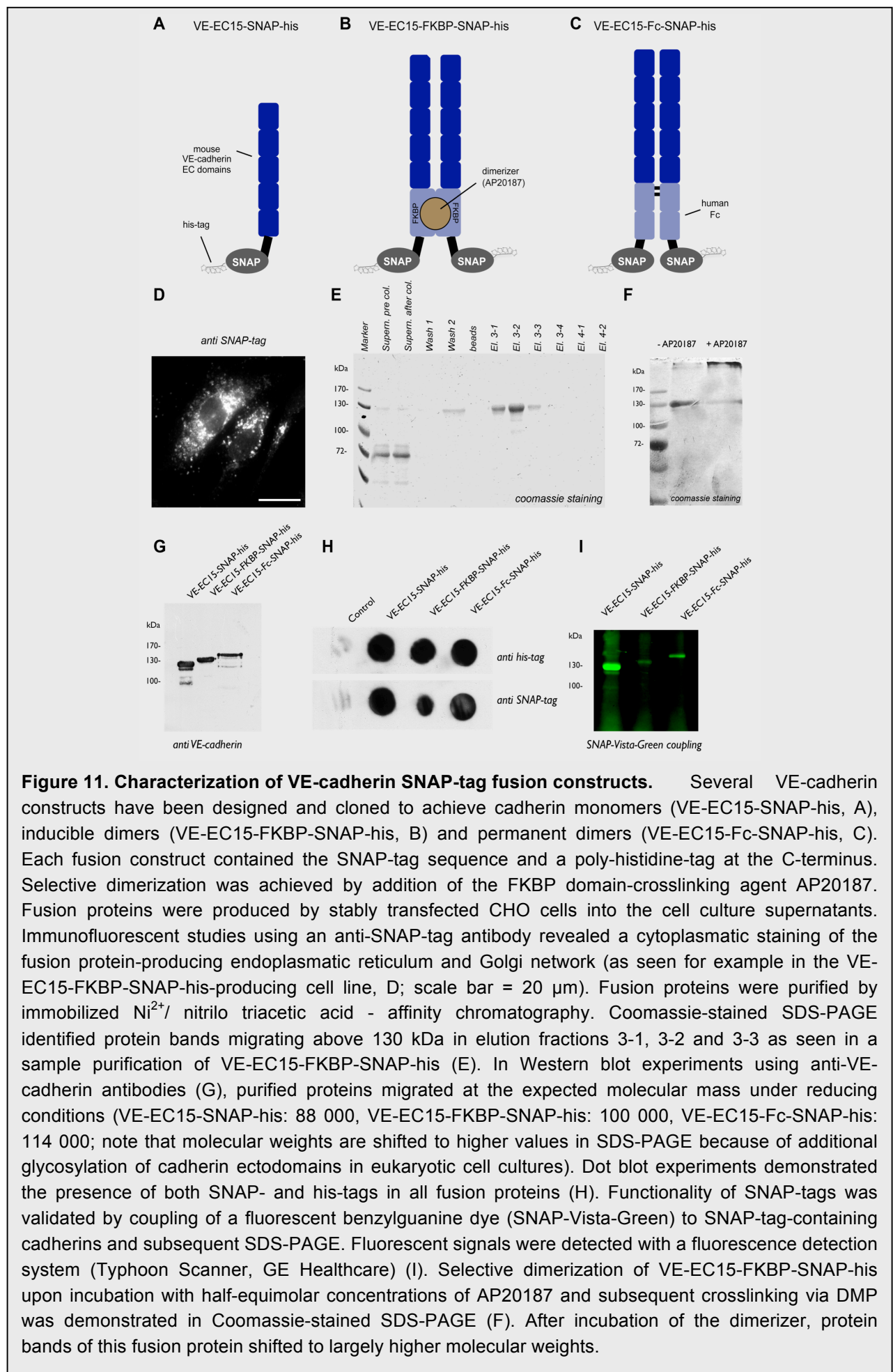
3.2.1 Investigating VE-cadherin interactions using site-directed coupling by SNAP-tag technology and AFM force spectroscopy

Introduction

Cadherins are known to interact in a polar way with specialized EC domains. For the investigation of cadherin interactions in AFM force spectroscopy, site-directed coupling of recombinant molecules to the AFM surfaces is required. Using the SNAP-tag technology such a method was developed. In this technology, modified human DNA repair protein O6-alkylguanine-DNA alkyltransferase is used as a protein tag, which can be fused to the proteins of interest (Keppler et al., 2003). Endogenously, this enzyme irreversibly transfers alkyl groups from its substrate, O6-alkylguanine-DNA, to one of its cysteine residues in the active site. Increasing substrate specificity and abolishing cross-reactivity with endogenous substrates generated the so-called SNAP-tag enzyme. This enzyme shows high specificity for O6-benzylguanine (BG) only. Therefore, SNAP-tag-coupled proteins can be used for direct coupling to BG-containing surfaces.

Methods and Results

Different VE-cadherin-SNAP-tag fusion proteins were cloned, purified and characterized, to be finally used in AFM force spectroscopy experiments (Figure 11). First of all, a monomeric fusion protein consisting of VE-cadherin EC1-5 domains, the SNAP-tag and a carboxyl-terminal poly-histidine-tag (for purification) was cloned (VE-EC15-SNAP-his, see addendum). Secondly, a VE-cadherin fusion protein additionally consisting a modified FKBP homodimerizing domain was generated (VE-EC15-FKBP-SNAP-his). For this, the "ARGENT Regulated Homodimerization Kit" was utilized (ARIAD, Cambridge, MA, USA (Spencer et al., 1993). It is based on the human protein FKBP12 (FK506 binding protein 12) and its small molecule ligands. Endogenously, FKBP is an immunomodulatory protein targeted by the immunosuppressant rapamycin and other ligands. By modifying FKBP ligand specificity, a homologue with high affinity to a synthetic ligand but not cross reacting with endogenous ligands was generated. Chemical compound AP20187 consists of two artificial FKBP ligands and therefore can be used to link two proteins containing a FKBP domain with subnanomolar affinity. VE-EC15-FKBP-SNAP-his could consequently be used as a protein in AFM force spectroscopy that could be selectively dimerized by addition of half-equimolar concentrations of AP20187. A third construct included a fragment coding for the Fc part of human IgG1, including the hinge region and Ig domains CH2 and CH3, and consequently served as a stable



dimer, with the Fc domain being known to induce dimers via disulfide bond formation. Sequence integrities of the cloned constructs were confirmed by sequencing.

Because of the lack of a transmembrane segment, recombinant proteins were supposed to be released into cell culture supernatants due to the presence of a signal peptide. For purification of recombinant proteins, the constructs were transfected into wild-type Chinese hamster ovary (CHO) cells using Effectene transfection reagent (Qiagen, Hilden, Germany) and stable-transfected cell lines were obtained using single cell subsplitting and subsequent characterization of fusion protein production. After collecting cell culture supernatants of serum-free CHO express media (Promocell, Heidelberg, Germany), proteins were purified using Ni-NTA agarose chromatography according to the manufacturer's protocol (Roche, Mannheim, Germany). The proteins were eluted by imidazole buffer (200 mM imidazole, 1 M NaCl, 10 mM NaH₂PO₄ (pH 8)) and immediately subjected to buffer exchange against HBSS via PD-10 desalting columns (GE Healthcare, München, Germany).

In Western blotting experiments of purified proteins, all three mouse VE-cadherin fusion proteins migrated at the expected molecular weights: VE-EC15-SNAP-his (88 000), VE-EC15-FKBP-SNAP-his (100 000), VE-EC15-Fc-SNAP-his (114 000), considering that molecular weights are shifted to higher values in SDS-PAGE due to additional glycosylation of cadherin EC domains. Proteins were all detected by anti VE-cadherin antibodies (Gotsch et al., 1997). Dot blotting with the respective antibodies from abcam (Cambridge, UK) and biocat (Heidelberg, Germany) confirmed the presence of his- and SNAP-tag in fusion proteins. The functionality of the SNAP-tags was validated by coupling of a fluorescent and BG-containing dye (SNAP-Vista-Green) to SNAP-tag-containing cadherin proteins and subsequent SDS-PAGE. Fluorescent signals were detected with a fluorescent gel detection system (Typhoon Scanner, GE Healthcare; FITC filter settings, 488 nm excitation). For dimerizing constructs, stable dimer generation was confirmed in non-reducing SDS-page where VE-EC15-Fc-SNAP-his migrated at twice the molecular weight as the monomer (data not shown). Selective dimerization of VE-EC15-FKBP-SNAP-his upon incubation with half-equimolar concentrations of AP20187 for 1 h and subsequent cross linking by addition of 30x molar excess of dimethyl pimelimidate (DMP; Pierce, Schwerte, Germany) for 1 h at pH 9.0 (the reaction was stopped by addition of 120x molar excess of tris for 15 min) was demonstrated in Coomassie-blue-stained SDS-PAGE (F). Incubation with the dimerizer shifted protein bands of this fusion protein to largely much molecular weights.

SNAP-tag-mediated coupling provides promising features for AFM force spectroscopy. Nevertheless, it also requires efficient and specific chemical coupling steps prior to SNAP-tag-BG linkage. For proper coupling chemistry, commercially available BG-maleimide (Covalys, Witterswil, Switzerland), which was to be coupled to PDP-PEG18 linked to APTES-coated Si₃N₄ plates and AFM tips via NHS-mediated binding (Ebner et al., 2007), did not dissolve in

aqueous solutions. Aqueous solutions, however, were necessary to achieve proper maleimide-mediated reactions with activated PDP groups. As a result, no specific coupling of BG-maleimide to PDP-PEG18 was achieved. Dissolving BG-maleimide in DMP or DMSO-containing solvents did not yield better results. Because of the unavailability of other BG-linkers suitable for our purposes, SNAP-tag-mediated coupling of VE-cadherin constructs failed. Nevertheless, alternatives for these procedures are on the way (see Discussion).

4 Discussion

4.1 Integrative summary of results

In the present manuscripts, roles of desmosomal cadherins and VE-cadherin under pathophysiological conditions of pemphigus and vascular inflammation were investigated and peptide-based modulators of cadherin functions were characterized and applied as potential therapeutic reagents.

4.2 Direct inhibition vs. desmoglein-mediated signaling in blistering skin disease pemphigus

Since the discovery of desmosomal cadherins as key targets in autoimmune blistering skin disease pemphigus, the hypothesis of direct inhibition of cadherin function as the major pathogenic event in this disease has been proposed. Experimental proof, however, had been lacking. By applying cell-free single molecule AFM force spectroscopy we were the first to directly demonstrate the postulated inhibition of Dsg3 transinteraction by PV autoantibodies (Figure 12A, 1). This effect was independent of the autoantibodies' Fc fragments, the dimeric autoantibody structure and the polyclonal character of PV-IgG, as it could be induced by PV-IgG Fab fragments or monoclonal pemphigus antibody AK23, respectively. Recombinant Dsg3 molecules used in these experiments were fully functional as demonstrated by AFM force spectroscopy, binding of Ca^{2+} and immunoprecipitation with AK23, which has been shown to bind conformation-specific to the Ca^{2+} -sensitive adhesive interface of Dsg3.

The importance of Dsg3 for desmocadherin function under mechanical stress has been proposed long ago. Further support for steric hindrance as main cause for PV came from the phenotype of Dsg3 knockout mice, which developed blisters under mechanical stress although establishing functional desmosomes. Interestingly, as another important factor, loss of Dsg molecules on keratinocyte surfaces in response to pemphigus autoantibodies has been shown to be a result of desmocadherin endocytosis. In the physiological context, however, it is difficult to compare inhibition of desmocadherin function by autoantibody-induced steric hindrance with complete loss of desmocadherin molecules from the cell surface of knockout animals. In the case of steric hindrance, intracellular desmocadherin domains are still present and desmocadherin-mediated signaling could continue, probably in an altered way. Transgenic expression of EC domain-truncated desmocadherin constructs in mice adds to these hypotheses with their partly unexpected phenotypes (Holthofer et al., 2007). In future studies, role of heterophilic interactions of Dsg3 molecules with other desmosomal cadherins, such as desmocollins 1-3 in establishment of epidermal barrier function should be investigated. Effects of pemphigus autoantibodies on heterophilic interactions are possible as well. Accordingly, in a recent study involving Dsc3, homophilic interactions and heterophilic interaction with Dsg1 but

not Dsg3 have been identified (Spindler et al., 2009). Nevertheless, pemphigus autoantibodies affected Dsc3-mediated adhesion in cell-based experiments only.

Although this work provided evidence for steric hindrance in pemphigus, pemphigus still emerges as a complex disease and is not just explained by a partial loss of desmocadherin function, since in addition, other relevant aspects have been revealed by our studies. It remains unclear, whether blocking the function of a single desmoglein is sufficient to cause the observed splitting of desmosomes in acantholytic cells. A recent study showed that in the presence of PV-IgG, desmosomes can still be formed, although PV-IgG were detected in the desmosome cores by EM (Aoyama et al.). Moreover, in the case of both PF- and PV-IgG, AFM experiments failed to detect direct autoantibody-mediated inhibition of Dsg1 interactions (Figure 12A, 2). In contrast to this, both PF-IgG and PV-IgG induced overall loss of adhesion of Dsg-coated microbeads to the surface of cultured keratinocytes. We therefore concluded that PV- and PF-IgG-mediated cellular signaling might essentially contribute to pemphigus pathogenesis (Figure 12A, 3). This was corroborated by the use of desmocadherin-stabilizing tandem peptides. In cell-based experiments, these were only effective to partly stabilize Dsg3-mediated binding, which had been shown to be directly inhibited in AFM studies. Loss of Dsg1-based adhesion, however, could not be prevented. Together, these findings strongly indicate that pemphigus autoantibodies induce cellular signaling events that independently result in loss of desmocadherin adhesion. Indeed, activation of a plethora of signaling cascades in pemphigus has been reported in the meantime. Blocking certain signaling cascades has been shown to block acantholysis in vivo (Sanchez-Carpintero et al., 2004; Berkowitz et al., 2006; Lanza et al., 2008). However, the mechanisms involved in desmocadherin-mediated outside-in signaling as well as the temporal and spatial interplay of these pathways has only been partly identified.

In other studies, we therefore focused on the importance of specific signaling pathways in pemphigus by discriminating between primary signaling events that directly lead to acantholysis and secondary events, which are activated in response to acantholysis. In several other studies for example, EGFR or c-Src activation were shown to be involved in pemphigus (Frusic-Zlotkin et al., 2006; Chernyavsky et al., 2007). However, we demonstrated that PV-IgG-induced acantholysis was independent of EGFR and c-Src activation in our model system (Figure 12A, 4). In our experiments pemphigus autoantibodies led to strong keratinocyte dissociation even in the presence of functional inhibitors of EGFR and c-Src. Importantly, this does not exclude the possibility that secondary activation of EGFR worsens the primary effects of PV-IgG and therefore contributes to pemphigus pathogenesis. As a potential mechanism, EGF produced by acantholytic keratinocytes could lead to activation of EGFR signaling in the same and neighboring cells. This has been shown to lead to a migratory

keratinocyte phenotype, which in some aspects is similar to acantholytic keratinocytes. Similar mechanisms could explain the finding of apoptotic phenotypes in pemphigus: Fas ligand has been shown to be increased in pemphigus patients' sera, but could not induce primary events of pemphigus pathogenesis on its own. On the other hand, Fas receptor activation is known to be a potent inducer of caspases, which were reported to be active in late stages of acantholytic keratinocytes (Schmidt and Waschke, 2009).

Since the first discovery of PV-IgG-induced signaling by the group of Kitajima et al. in the mid 90s (Esaki et al., 1995; Aoyama et al., 1999), the involvement of several signaling pathways in pemphigus has been studied. These include receptors, desmosomal adapter proteins, kinases as well as transcription factors. Among the plethora of identified molecules, plakoglobin and p38MAPK appear to have central roles in pemphigus pathogenesis. Plakoglobin not only constitutes a major structural component of desmosomes but also functions as a shuttling signaling molecule, communicating signals from AJs to desmosomes and the nucleus, where it has been demonstrated to inhibit c-Myc function (Williamson et al., 2006). More importantly, PG deficiency has been demonstrated to prevent pemphigus autoantibody-induced acantholysis (Caldelari et al., 2001). On the other hand, p38MAPK activation has been demonstrated for both PF- and PV-IgG, although direct inhibition has only been identified in PV-IgG, yet. Still, this demonstration of desmocadherin-induced signaling takes a key place in pemphigus signaling as several groups have shown p38MAPK to be an upstream signaling molecule (Berkowitz et al., 2005; Berkowitz et al., 2006; Waschke et al., 2006; Berkowitz et al., 2008b). p38MAPK has been linked to perturbation of cytokeleton and actin networks, both directly or via heat shock protein (HSP) 27 or RhoA. The latter links desmocadherin rearrangements to alterations of keratinocyte AJs and its major adhesion molecule E-cadherin. The failure of p38MAPK inhibitors in preliminary and initial clinical studies (D. Rubenstein, University of North Carolina, personal communication) and the hypothesis, that p38MAPK activation is just a salvage pathway of acantholytic keratinocytes, should not impede further strategies involving this molecule.

Integrative studies investigating the interplay of several signaling pathways are lacking. Such studies may help to identify essential upstream signaling molecules which would extend our understanding of both pemphigus pathogenesis and the physiological mechanisms regulating desmosome-mediated adhesion.

By using dimeric peptides that stabilize Dsg trans-interaction, we prevented pemphigus autoantibody-induced cell dissociation, indicating that inhibition of Dsg3 trans-interaction by pemphigus autoantibodies directly contributes to acantholysis. Nevertheless, this approach was unable to block PF-IgG-induced effects, which have been shown to be independent of loss of Dsg1 trans-interaction. Consequently, signaling is also an essential part in pemphigus

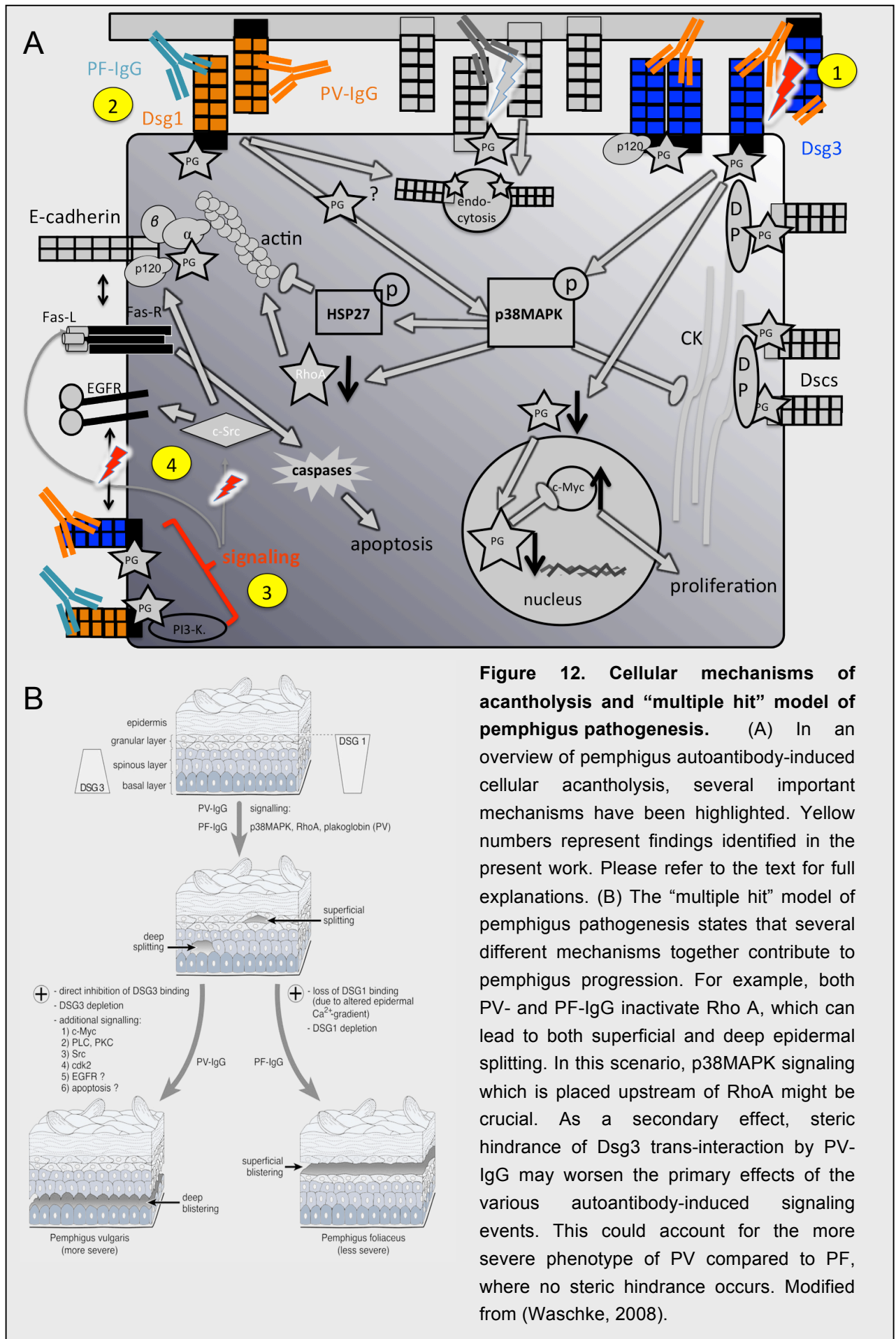


Figure 12. Cellular mechanisms of acantholysis and "multiple hit" model of pemphigus pathogenesis. (A) In an overview of pemphigus autoantibody-induced cellular acantholysis, several important mechanisms have been highlighted. Yellow numbers represent findings identified in the present work. Please refer to the text for full explanations. (B) The "multiple hit" model of pemphigus pathogenesis states that several different mechanisms together contribute to pemphigus progression. For example, both PV- and PF-IgG inactivate Rho A, which can lead to both superficial and deep epidermal splitting. In this scenario, p38MAPK signaling which is placed upstream of RhoA might be crucial. As a secondary effect, steric hindrance of Dsg3 trans-interaction by PV-IgG may worsen the primary effects of the various autoantibody-induced signaling events. This could account for the more severe phenotype of PV compared to PF, where no steric hindrance occurs. Modified from (Waschke, 2008).

pathogenesis. Still, in most cases a discrimination between the following activation mechanisms of acantholytic signaling cascades in pemphigus is difficult: Activation (i) in response to loss of desmocadherin function, (ii) in response to desmocadherin clustering, (iii) in response to allosteric alteration of Dsg structure, (iv) by autoantibody-induced loss of heterotypic interactions and (v) by non-desmocadherin autoantibodies or serum components of pemphigus patients. Based on these considerations, future studies need to address these mechanisms to ultimately gain insights into therapeutic niches for a specific treatment of pemphigus.

Summarizing views on pemphigus pathogenesis support the “multiple hit” hypothesis of pemphigus pathogenesis (Figure 12B). It states, that several and different mechanisms account for the differences in blister formation and clinical progression between PV and PF. Both PV- and PF-IgG might activate major signaling pathways, such as PG-dependent p38MAPK activation, subsequently leading to histological microblisters in many epidermis layers. In a second step, specific mechanisms such as steric hindrance of Dsg3 binding or Dsg3 depletion in the case of PV and Dsg1 depletion in the case of PF may lead to final, pemphigus subtype-specific suprabasal and superficial blisters, respectively.

4.3 VE-cadherin as a key component of the endothelial barrier

Vascular endothelial (VE-) cadherin is the predominant cadherin expressed in endothelial cells and has been shown to be essential for the stabilization of the endothelial lining of the inner surface of blood vessels and for the regulation of the barrier between blood and surrounding tissues (Dejana et al., 2008; Vandenbroucke et al., 2008). Loss of VE-cadherin function in pathological processes has been demonstrated (Corada et al., 1999; Hordijk et al., 1999; Alexander and Elrod, 2002) and VE-cadherin was found to be one of the target molecules modulated by signaling of several inflammatory mediators such as histamine, thrombin and TNF- α . In our study, VE-cadherin has been confirmed to be a core element of the endothelial barrier. Both the modification of VE-cadherin function by extracellular inhibition via an antibody directed against VE-cadherin EC domains or the intracellular increase of Ca²⁺ resulted in loss of VE-cadherin-mediated binding and endothelial barrier breakdown. By the application of extracellular VE-cadherin-cross-bridging tandem peptides designed to stabilize VE-cadherin bonds these effects could be partly reversed. Therefore, VE-cadherin turns out to be an interesting therapeutic target for stabilizing endothelial barrier functions. This has also been confirmed in in-vivo experiments where the increase of microvessel permeability in response to TNF- α treatment was completely prevented by preincubation with the cross-bridging tandem peptide. Interestingly, the inflammatory mediator TNF- α , which has been reported to inhibit VE-cadherin function via inhibition of VE-cadherin anchorage to the actin cytoskeleton, was unable

to exert its barrier-disrupting function when VE-cadherin was extracellularly stabilized by tandem peptides.

4.4 Peptides modulating cadherin function

For both diseased conditions, pemphigus skin blistering and vascular dysfunction, peptides stabilizing trans-interactions of cadherins have been designed to specifically strengthen these adhesion molecules and to inhibit dissociation under pathological processes. At the beginning of this strategy, cadherin structures of the so-far unresolved cadherins VE-cadherin and Dsg1/3 had to be determined. This was accomplished by aligning the respective cadherin amino acid sequences to the resolved E-cadherin structures. On the basis of the postulated structures of VE-cadherin and Dsg3/1, homophilic interactions were modeled by fitting them into the trans-interaction scheme of N-cadherin, which had been resolved as well. In the trans-interacting N-cadherin structure, an adhesive region near to the known “HAV” sequence was identified that displayed a large inter-cadherin interface (see section 2.4.2.2). Consequently, similar adhesive regions could be modeled and peptides corresponding to these adhesive structures were identified for VE-cadherin and Dsg1/3 interactions. The “single peptides”, fulfilled the prediction to inhibit trans-interaction, whereas the tandem constructs of two peptides connected to each other by a flexible linker (“tandem peptides”) acted as cadherin cross-bridging agents.

One example of the various hypothetical modes of tandem peptide action might involve cross-bridging of cadherin molecules in a parallel fashion (Figure 13). Nevertheless, since cadherins are flexible molecules both cis and trans-interactions may be stabilized because of similar adhesive interfaces. More interestingly, by applying this strategy, Trp2 residues, which were identified to be core elements of cadherin interactions, are still freely accessible for interactions in tandem peptide-crossbridged cadherin dimers. The peptides obviously act in a stabilizing way by not directly interfering with the other important adhesive interface including Trp2 and the corresponding hydrophobic binding pockets for Trp2. Peptides mimicking the mode of action of Trp2 for example probably would not lead to enhanced stabilization by competing with natural interaction schemes. TP-mediated mechanisms of cadherin stabilization, however, probably include several effects on the suprastructural organization, which are difficult to separate from each other. Because of entropic reasons, main stabilizing effects of the tandem peptides may involve cooperative effects of several tandem peptides on cadherin clustering, similar to the proposed function of cytoskeletal anchorage. This clustering may rely on several interaction mechanisms. However, competition of mainly hydrophilic peptide-cadherin interactions with aqueous solvents might weaken these interactions.

By comparing cadherin amino acid sequences, it becomes obvious that the identified peptides are highly conserved in the respective cadherins of mammals. In the case of VE-cadherin for

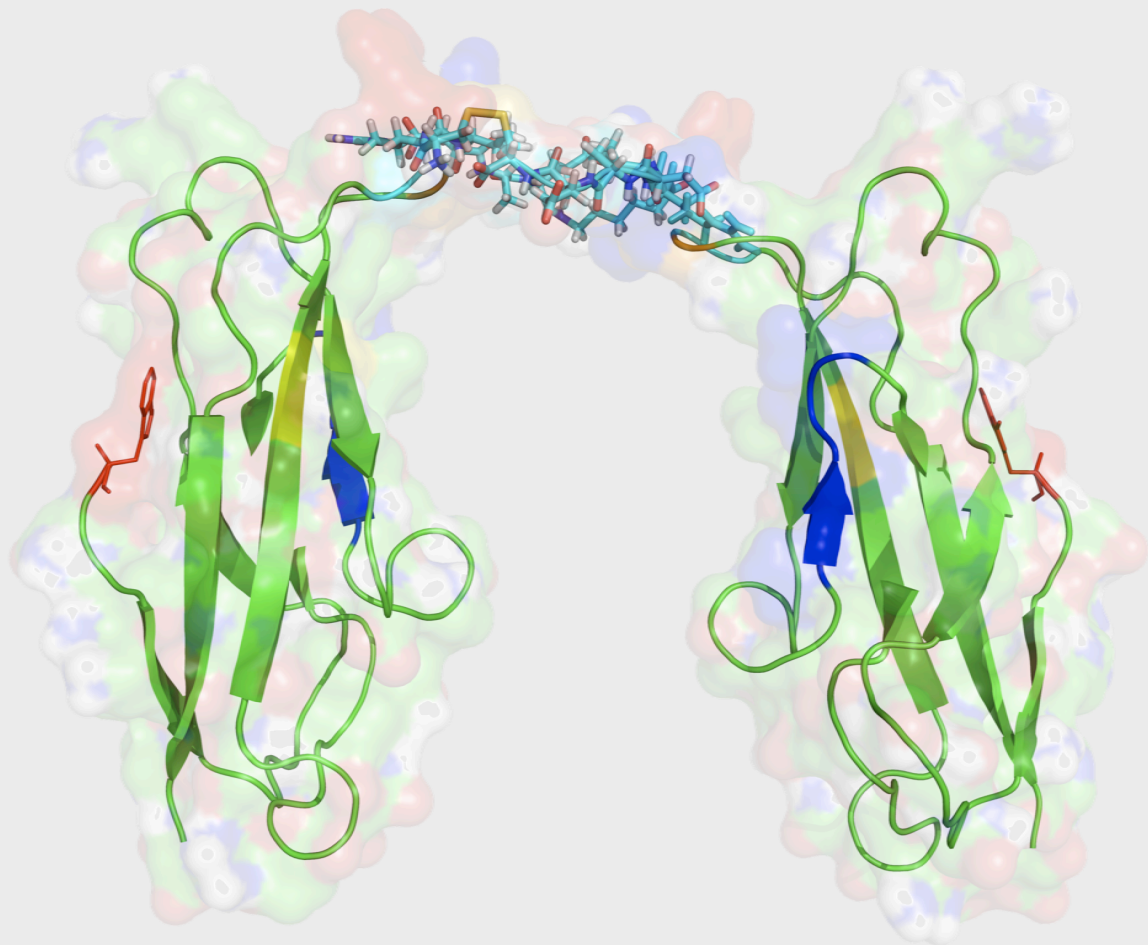
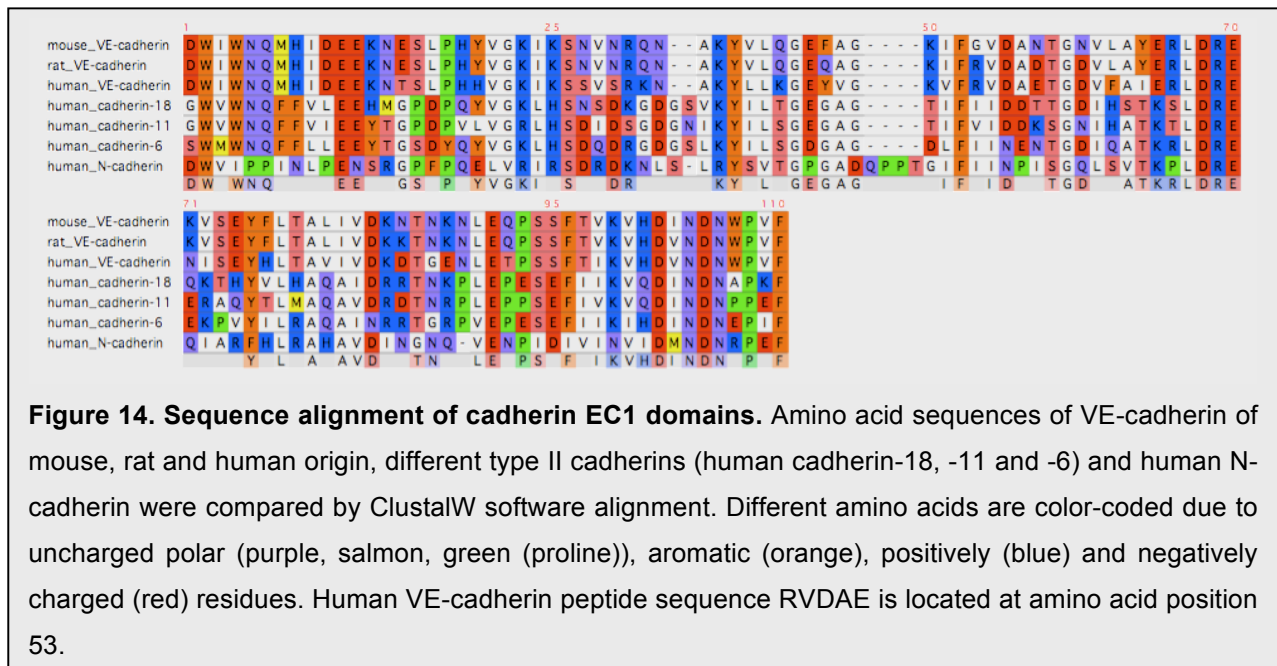


Figure 13. VE-cadherin tandem peptide interaction. By simultaneously binding to the adhesive interfaces of two opposing cadherins, the tandem peptide might mediate stabilization of cadherin interactions. Tandem peptide atoms are represented as cyan sticks and the resulting surface is transparently visible. VE-cadherin EC1 main amino acid structure and transparent surfaces are also depicted. Note, that the two VE-cadherin EC1 domains are oriented in parallel and both Trp2 (red) are freely accessible for additional interactions facilitating cadherin clustering. Structures were rendered with Pymol molecular viewer (© DeLano Scientific LLC).

example, the core amino acids VDA of the sequence RVDAE are identical in VE-cadherin of mouse, rat and human origin. Still, this sequence seems to be very specific for VE-cadherin, since other type II cadherins such as cadherins 6, 11 and 18 do not share this sequence (Figure 14). In addition, the corresponding acceptor sequence of RVDAE peptides involving Tyr80 is conserved in many type II cadherins. Another study using the antagonistic VE-cadherin cyclic peptide CDAEC inhibited retinal neovascularization in-vivo, confirming our results with the antagonistic single RVDAE peptides (Navaratna et al., 2008).



Although agonistic and antagonistic effects of single and tandem peptides were shown in various assays including AFM, laser tweezers, FRAP, TER and microvessel perfusions, direct binding of peptides to cadherin molecules could not be determined, for example in BIAcore studies using surface plasmon resonance. These experiments were not successful because homophilic binding of full-length cadherin-Fc constructs was too weak to be detected and specific binding of SP and TP to recombinant cadherins could not be unequivocally demonstrated most likely because peptide-cadherin affinities were probably too low. Nevertheless, binding of the Dsg1/3 single peptide to Dsg1-Fc was demonstrated in preliminary isothermal titration calorimetry (ITC) experiments. This is a physical technique used to determine thermodynamic parameters of chemical interactions by calorimetrically measuring thermal changes between highly sensitive cells upon injection of a ligand (i.e. peptide) to its receptor (i.e. cadherin). With this technique a dissociation constant of $K_D = 2.5 \mu\text{M} \pm 4.0 \mu\text{M}$ was measured for interaction of single peptides with desmoglein 1-Fc in aqueous solution. Although this affinity may rather seem low, low K_D of cadherin interactions themselves might not necessarily need high affinities of peptides towards cadherin interfaces.

Physiologically and in the cellular context, it has to be pointed out that the mode of action of tandem peptides may also include other mechanisms, as shown for N-cadherin dimeric peptides by the Doherty group (Williams et al., 2002). In their work, it was demonstrated that agonistic N-cadherin peptides promoted axonal outgrowth via activation of fibroblast growth factor receptor (FGFR). Structural changes in N-cadherin clustering consequently influenced heterotypic cadherin interactions. A similar mode of action is possible for our cadherin tandem peptides, although our results indicate that cross-bridging of trans-interacting VE-cadherin molecules itself is effective to mechanically strengthen cadherin interactions and probably represents the primary mechanism.

A definite explanation of the stabilizing effect of tandem peptides remains elusive. Promising strategies involve mutational alterations of cadherin sequences, which have been reported to mediate adhesion either in cis or trans. Moreover, NMR studies could provide insights into exact TP structures. As a caveat, tandem peptides intrinsically have reduced concentration ranges because of competitive equilibria between displacement and dissociations reactions from cadherins at higher concentrations. This might limit the practical effectiveness of tandem peptide action. Despite these uncertainties, protective actions and concentration ranges of these peptides were demonstrated, both in-vitro and in-vivo.

For potential therapeutic use in humans, improvements and modifications of peptide structures have to be made. However, a cyclic pentapeptide containing the HAV-sequence and inhibiting N-cadherin trans-interaction has already been commercially developed and is undergoing clinical trials as a therapy for treating melanomas (ADH-1 / Exherin™ developed by Adherex Technologies, Inc, Durham, USA). It was reported that intravenous doses up to 500 mg/m² body surface were safely tolerated in patients (Kelland, 2007). Small molecule drugs mimicking same effects would minimize risk of immunological reactions in patients and also dramatically decrease the costs of production. As a first step in this direction, full alanine scanning of the parent peptide would be needed to determine the core amino acid sequence that is essential for the observed protective effects. Afterwards, in-silico screenings of suitable small molecules mimicking the structure of the thus identified core sequence could identify target substances for downstream in-vitro and finally in-vivo studies. Recently, this strategy has been successfully applied to identify inhibitory small molecule substitutions for ADH-1 (Burden-Gulley et al., 2009; Burden-Gulley et al., 2010).

4.5 Cadherin interaction

Various models for cadherin interactions have been proposed in the literature. When trying to develop an unifying theory of cadherin interactions several conditions have to be considered and experimental findings both from a structural, biochemical, biophysical and most of all physiological and pathological conditions must be included:

- (i) In various experimental setups, monomeric cadherin constructs have been shown to directly interact on their own. In a recent study, it has been reported that cis dimer formation increased binding probability but did not change adhesion strength (Zhang et al., 2009). An explanation for the failure to detect monomeric interactions in some in-vitro conditions may be the finding that cadherin monomers can exhibit a “closed” monomeric state, which directly competes and hinders interactions. It has been proposed that several in-vivo conditions, such as a pH shift and Ca²⁺ increase reduce

energy barriers needed to open the monomeric cadherin structures for dimer formations. It is becoming obvious that differentiation between cis- and trans-interactions of cadherins is often not possible. It has not only been demonstrated that both ways of interactions share the same adhesive interface but also that supramolecular composition emerges as an essential mechanism in cadherin-mediated adhesion. In crystal structures of C-cadherin full-length EC domain constructs, both cis- and trans-interactions have been resolved to form dense cadherin clusters. In support of this, electron microscopic studies of carefully fixed epidermal sheets revealed desmosomal cadherins to be organized in a similar that is highly structured fashion. Mature cadherin-based contacts obviously exhibit a supramolecular organization that is required or allows strong adhesion.

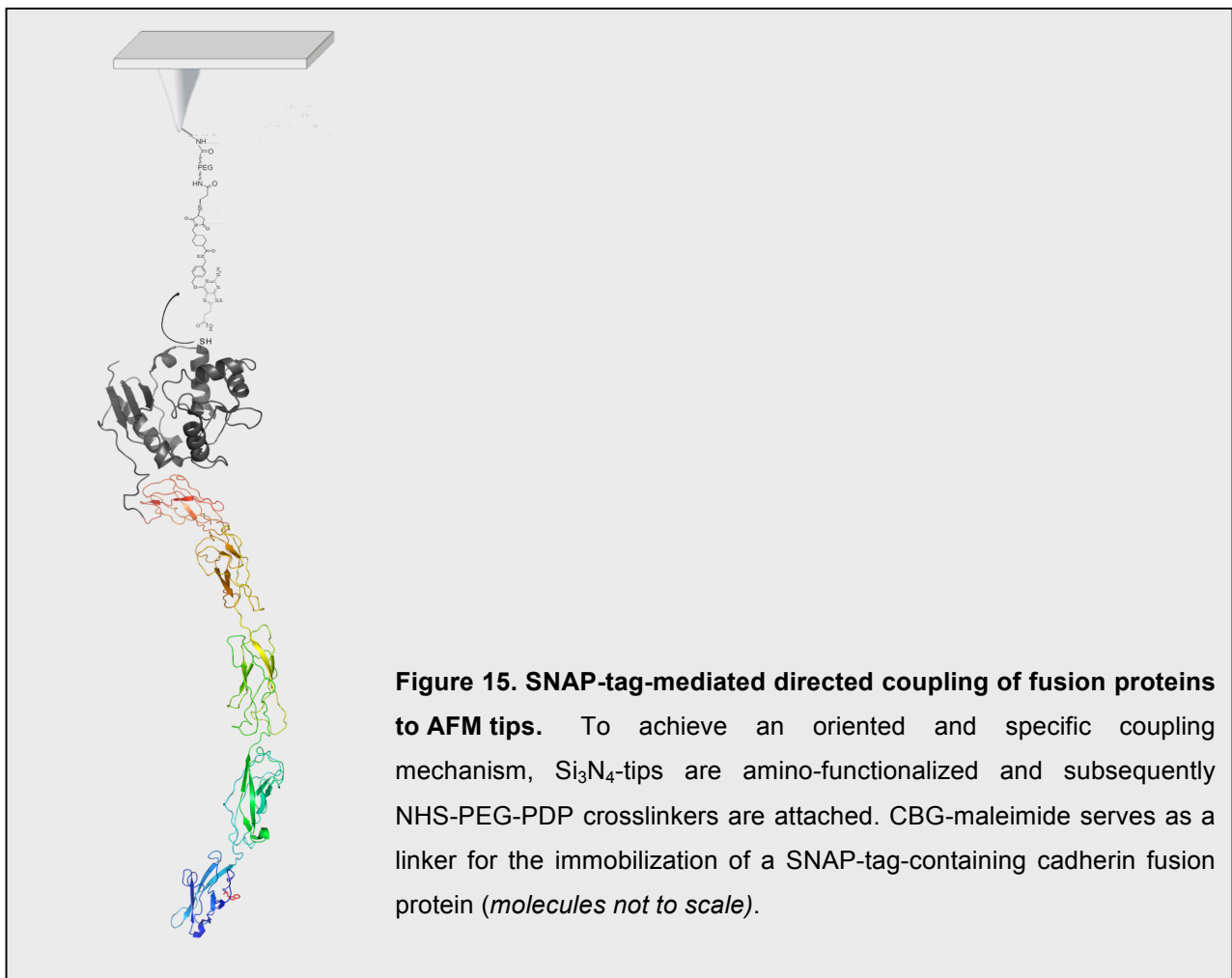
- (ii) The importance of EC1 domains for cadherin interactions has been unequivocally demonstrated. EC1 domains mostly confer specificity for cadherin interactions because they mediate initial encounter reactions. However, some biophysical experiments indicate the presence of multiple EC domain interactions for strengthening of cadherin binding. These may either develop in a direction perpendicular or parallel to cell membranes. Although multiple domain interactions have been questioned, this does not exclude the possibility that these interactions occur and contribute to the dynamic establishment of mature, EC1 domain-based adhesions. The absence of multiple domain structures in cadherin crystals obviously is due to the use of cadherin EC12 domain proteins for crystal generation. The single cadherin EC domain interaction probably may exhibit a hierarchy of cadherin bonds, which are hidden in some experimental conditions.
- (iii) For EC1 domain-based interactions, various atomic models have been described. But still, these different structures may describe different variations of cadherin interactions that all contribute to overall cadherin cluster formation. EC1 domain interactions that involve Trp2-mediated strand swapping seem to be highly conserved for type I and II cadherins as well as for desmocadherins. But also other interfaces such as HAV-related regions contribute to overall adhesion as indicated by cross-bridging cadherin peptides in our studies. High structure flexibility as indicated by the structure of various cadherins opens the possibility that cadherin cis- and trans-interactions may occur between opposing or adjacent cadherins but via the same adhesive interface.
- (iv) Cell-free determinations of heterophilic interactions between different cadherins do not represent physiologic conditions. Theoretical calculations predict that specificity of cadherin interactions relies on low binding constants of single molecules, which are shared among most cadherin subtypes. Cadherin specificity is then achieved via cadherin concentration levels. In this context, the recent findings of fast (but weak) and slow (but strong) binding kinetics of cadherin interactions corroborate this model. Fast,

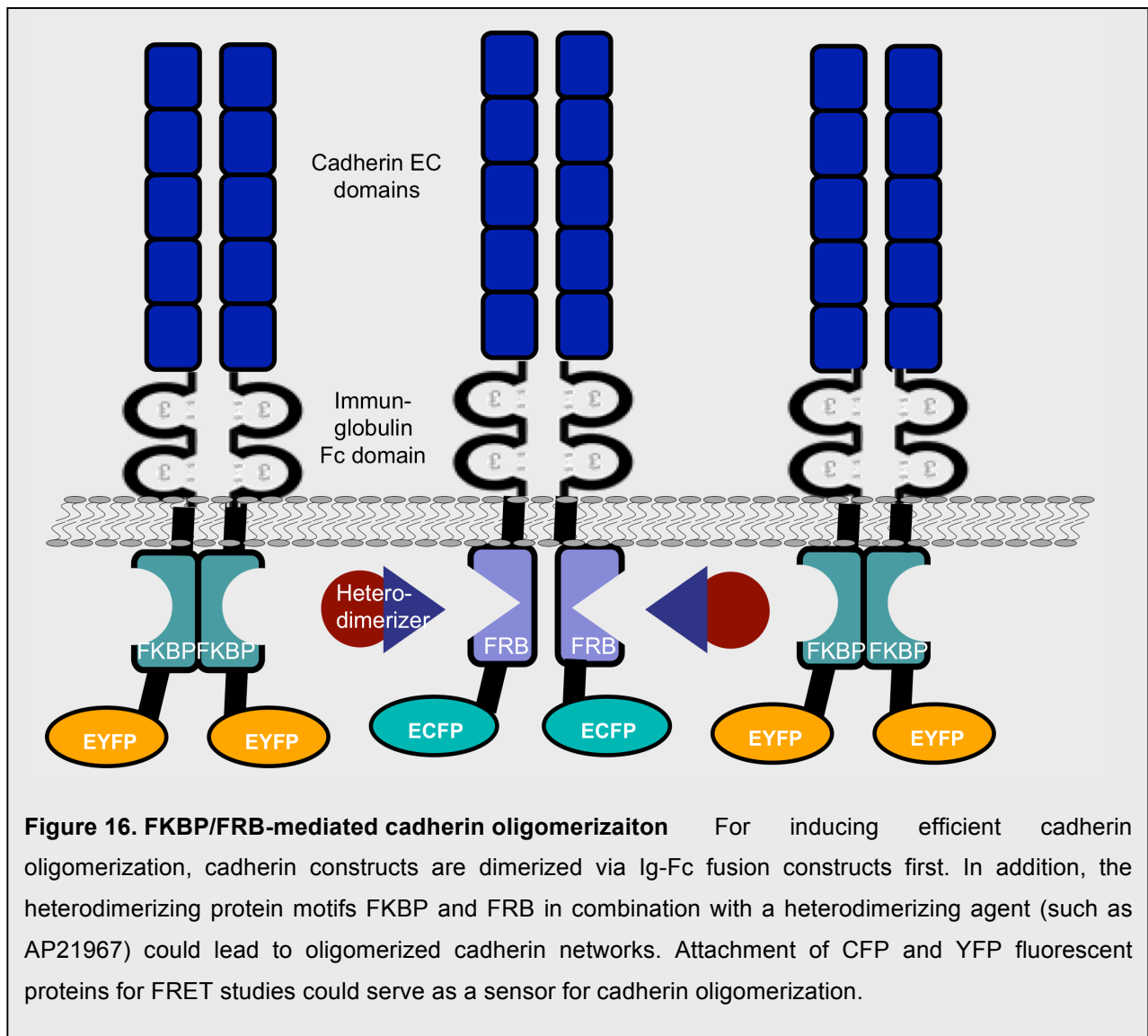
but weak interactions may rely on Trp2-mediated strand swapping, a mechanism that is shared among most cadherins. Slow, but strong interactions then additionally form by using other adhesive interfaces. The final interaction is then characterized by a supramolecular organization that involves multiple three-dimensional cadherin interactions conferring cadherin specificity.

Taken together, cadherins definitely are more than just low-affinity glue (Trojanovsky et al., 2007). They are sophisticated structures containing hidden adhesive sites and are highly regulated under cellular control, which all has to be considered in future investigations.

4.5.1 Future strategies for investigating cadherin interactions

The attempt of SNAP-tag-mediated direct coupling of proteins for AFM force spectroscopy failed due to the hydrophobicity of a cross linking reagent. BG-maleimide, which had been provided by a commercial supplier, was unsuitable for the planned experiments because it did not dissolve in aqueous solutions that were needed for proper coupling reactions. In the meantime, negotiations on the commercial production of an alternative agent, called C8 propanoic acid benzylguanine (CBG)-maleimide, have been started (Figure 15). This reagent has a BG modification that does not hinder binding to SNAP proteins but strongly increases solubility in water. Alternatively, SPDP-treatment of CBG-NH₂, another commercial building block using water-soluble CBG, would yield CBG-NH-PDP, which could be attached to AFM





tips by PEG-maleimide linkers. Using these two linkage steps, specific coupling of CBG substrates to AFM tips and mica plates should be easily achieved by already established linkage protocols (Ebner et al., 2007).

Promising strategies to study adhesion in response to cadherin oligomerization may include chimeric fusion proteins of the FKBP-FRB system (Belshaw et al., 1996; Luik et al., 2008). This system includes two protein-protein binding motifs: (i) the FK506 binding protein (FKBP) and (ii) FRB, a mutated FKBP rapamycin binding domain of FRAP (FKBP and rapamycin-associated protein/mammalian target of rapamycin) (Chen et al., 1995). AP21967, a chemical derivative of the immunosuppressive drug rapamycin, can be used as a heterodimerizing agent connecting the two binding motifs. FKBP and FRB could either be fused to artificial cadherin constructs or endogenous cadherin sequences. In combination with linkage to Ig Fc domains, a network of oligomerized cadherin molecules could be generated (Figure 16). The resulting adhesion of these cadherin-based structures could be easily measured via cell- or bead-binding experiments. Furthermore, attachment of CFP and YFP fluorescent proteins for

FRET studies could serve as a sensor for cadherin oligomerization and visualize oligomerization in live cell experiments.

As already discussed above, determination of heterophilic interactions is strongly dependent on the physiological and cellular background. Future studies should therefore be based on investigations of the *in vivo* situation. So far, CEMOVIS-based structures of desmosomal cadherins gave the best structural predictions to explain both biophysical properties and other structural findings of cadherin interactions. It is therefore essential to combine new ultramicroscopic studies with model systems or organisms that effectively represent physiological conditions, because even studies with transfected cadherin molecules disturb physiological regulation patterns of cadherins for example. Promising AFM experiments investigating heterophilic interactions might include strategies to directly measure cadherin interactions on cells or assess cell-to-cell adhesion by depositing single cells on AFM tips.

5 References

(Please also note the list of references in the respective cumulative publications of section 3)

- Abedin, M. and King, N.** (2008). The premetazoan ancestry of cadherins. *Science* **319**, 946-8.
- Adams, C. L., Chen, Y. T., Smith, S. J. and Nelson, W. J.** (1998). Mechanisms of epithelial cell-cell adhesion and cell compaction revealed by high-resolution tracking of E-cadherin-green fluorescent protein. *J Cell Biol* **142**, 1105-19.
- Ahrens, T., Lambert, M., Pertz, O., Sasaki, T., Schulthess, T., Mege, R. M., Timpl, R. and Engel, J.** (2003). Homoassociation of VE-cadherin follows a mechanism common to "classical" cadherins. *J Mol Biol* **325**, 733-42.
- Ahrens, T., Pertz, O., Haussinger, D., Fauser, C., Schulthess, T. and Engel, J.** (2002). Analysis of heterophilic and homophilic interactions of cadherins using the c-Jun/c-Fos dimerization domains. *J Biol Chem* **277**, 19455-60.
- Al-Amoudi, A., Diez, D. C., Betts, M. J. and Frangakis, A. S.** (2007). The molecular architecture of cadherins in native epidermal desmosomes. *Nature* **450**, 832-7.
- Al-Amoudi, A. and Frangakis, A. S.** (2008). Structural studies on desmosomes. *Biochem Soc Trans* **36**, 181-7.
- Alexander, J. S. and Elrod, J. W.** (2002). Extracellular matrix, junctional integrity and matrix metalloproteinase interactions in endothelial permeability regulation. *J Anat* **200**, 561-74.
- Amagai, M., Ahmed, A. R., Kitajima, Y., Bystry, J. C., Milner, Y., Gniadecki, R., Hertl, M., Pincelli, C., Fridkis-Hareli, M., Aoyama, Y. et al.** (2006). Are desmoglein autoantibodies essential for the immunopathogenesis of pemphigus vulgaris, or just 'witnesses of disease'? *Exp Dermatol* **15**, 815.
- Amagai, M., Hashimoto, T., Shimizu, N. and Nishikawa, T.** (1994). Absorption of pathogenic autoantibodies by the extracellular domain of pemphigus vulgaris antigen (Dsg3) produced by baculovirus. *J Clin Invest* **94**, 59-67.
- Amagai, M., Karpati, S., Prussick, R., Klaus-Kovtun, V. and Stanley, J. R.** (1992). Autoantibodies against the amino-terminal cadherin-like binding domain of pemphigus vulgaris antigen are pathogenic. *J Clin Invest* **90**, 919-26.
- Amagai, M., Klaus-Kovtun, V. and Stanley, J. R.** (1991). Autoantibodies against a novel epithelial cadherin in pemphigus vulgaris, a disease of cell adhesion. *Cell* **67**, 869-877.
- Amagai, M., Matsuyoshi, N., Wang, Z. H., Andl, C. and Stanley, J. R.** (2000a). Toxin in bullous impetigo and staphylococcal scalded-skin syndrome targets desmoglein 1. *Nat Med* **6**, 1275-7.
- Amagai, M., Tsunoda, K., Suzuki, H., Nishifuji, K., Koyasu, S. and Nishikawa, T.** (2000b). Use of autoantigen-knockout mice in developing an active autoimmune disease model for pemphigus. *J Clin Invest* **105**, 625-31.
- Andriopoulou, P., Navarro, P., Zanetti, A., Lampugnani, M. G. and Dejana, E.** (1999). Histamine induces tyrosine phosphorylation of endothelial cell-to-cell adherens junctions. *Arterioscler Thromb Vasc Biol* **19**, 2286-97.
- Angelini, D. J., Hyun, S. W., Grigoryev, D. N., Garg, P., Gong, P., Singh, I. S., Passaniti, A., Hasday, J. D. and Goldblum, S. E.** (2006). TNF-alpha increases tyrosine phosphorylation of vascular endothelial cadherin and opens the paracellular pathway through fyn activation in human lung endothelia. *Am J Physiol Lung Cell Mol Physiol* **291**, L1232-45.

- Angres, B., Barth, A. and Nelson, W. J. (1996).** Mechanism for transition from initial to stable cell-cell adhesion: kinetic analysis of E-cadherin-mediated adhesion using a quantitative adhesion assay. *J Cell Biol* **134**, 549-57.
- Anhalt, G. J., Labib, R. S., Voorhees, J. J., Beals, T. F. and Diaz, L. A. (1982).** Induction of pemphigus in neonatal mice by passive transfer of IgG from patients with the disease. *N Engl J Med* **306**, 1189-96.
- Aoyama, Y. and Kitajima, Y. (1999).** Pemphigus vulgaris-IgG causes a rapid depletion of desmoglein 3 (Dsg3) from the Triton X-100 soluble pools, leading to the formation of Dsg3-depleted desmosomes in a human squamous carcinoma cell line, DJM-1 cells. *J Invest Dermatol* **112**, 67-71.
- Aoyama, Y., Nagai, M. and Kitajima, Y. (1999).** Binding of pemphigus vulgaris IgG to antigens in desmosome core domains excludes immune complexes rather than directly splitting desmosomes. *Br J Dermatol*.
- Aoyama, Y., Owada, M. K. and Kitajima, Y. (1999).** A pathogenic autoantibody, pemphigus vulgaris-IgG, induces phosphorylation of desmoglein 3, and its dissociation from plakoglobin in cultured keratinocytes. *Eur J Immunol* **29**, 2233-40.
- Aplin, A. E., Howe, A., Alahari, S. K. and Juliano, R. L. (1998).** Signal transduction and signal modulation by cell adhesion receptors: the role of integrins, cadherins, immunoglobulin-cell adhesion molecules, and selectins. *Pharmacol Rev* **50**, 197-263.
- Arnaout, M. A., Goodman, S. L. and Xiong, J. P. (2007).** Structure and mechanics of integrin-based cell adhesion. *Curr Opin Cell Biol* **19**, 495-507.
- Awad, M. M., Dalal, D., Cho, E., Amat-Alarcon, N., James, C., Tichnell, C., Tucker, A., Russell, S. D., Bluemke, D. A., Dietz, H. C. et al. (2006).** DSG2 mutations contribute to arrhythmogenic right ventricular dysplasia/cardiomyopathy. *Am J Hum Genet* **79**, 136-42.
- Bajpai, S., Correia, J., Feng, Y., Figueiredo, J., Sun, S. X., Longmore, G. D., Suriano, G. and Wirtz, D. (2008).** α -Catenin mediates initial E-cadherin-dependent cell-cell recognition and subsequent bond strengthening. *Proc Natl Acad Sci U S A* **105**, 18331-6.
- Baumgartner, W. and Drenckhahn, D. (2002a).** Plasmalemmal concentration and affinity of mouse vascular endothelial cadherin, VE-cadherin. *Eur Biophys J* **31**, 532 - 8.
- Baumgartner, W. and Drenckhahn, D. (2002b).** Transmembrane cooperative linkage in cellular adhesion. *Eur J Cell Biol* **81**, 161-8.
- Baumgartner, W., Golenhofen, N., Grundhofer, N., Wiegand, J. and Drenckhahn, D. (2003a).** Ca²⁺ dependency of N-cadherin function probed by laser tweezer and atomic force microscopy. *J Neurosci* **23**, 11008-14.
- Baumgartner, W., Hinterdorfer, P., Ness, W., Raab, A., Vestweber, D., Schindler, H. and Drenckhahn, D. (2000).** Cadherin interaction probed by atomic force microscopy. *Proc Natl Acad Sci U S A* **97**, 4005-10.
- Baumgartner, W., Schutz, G. J., Wiegand, J., Golenhofen, N. and Drenckhahn, D. (2003b).** Cadherin function probed by laser tweezer and single molecule fluorescence in vascular endothelial cells. *J Cell Sci* **116**, 1001-11.
- Bayas, M. V., Leung, A., Evans, E. and Leckband, D. (2006).** Lifetime measurements reveal kinetic differences between homophilic cadherin bonds. *Biophys J* **90**, 1385-95.
- Bell, G. I. (1978).** Models for the specific adhesion of cells to cells. *Science* **200**, 618-27.
- Belshaw, P. J., Ho, S. N., Crabtree, G. R. and Schreiber, S. L. (1996).** Controlling protein association and subcellular localization with a synthetic ligand that induces heterodimerization of proteins. *Proc Natl Acad Sci U S A* **93**, 4604-7.

- Benninghoff, A. and Drenckhahn, D.** (2008). *Anatomie. Makroskopische Anatomie, Histologie, Embryologie, Zellbiologie, Band1* Urban & Fischer Verlag.
- Berkowitz, P., Chua, M., Liu, Z., Diaz, L. A. and Rubenstein, D. S.** (2008a). Autoantibodies in the autoimmune disease pemphigus foliaceus induce blistering via p38 mitogen-activated protein kinase-dependent signaling in the skin. *Am J Pathol* **173**, 1628-36.
- Berkowitz, P., Diaz, L. A., Hall, R. P. and Rubenstein, D. S.** (2008b). Induction of p38MAPK and HSP27 phosphorylation in pemphigus patient skin. *J Invest Dermatol* **128**, 738-40.
- Berkowitz, P., Hu, P., Liu, Z., Diaz, L. A., Enghild, J. J., Chua, M. P. and Rubenstein, D. S.** (2005). Desmosome signaling. Inhibition of p38MAPK prevents pemphigus vulgaris IgG-induced cytoskeleton reorganization. *J Biol Chem* **280**, 23778-84.
- Berkowitz, P., Hu, P., Warren, S., Liu, Z., Diaz, L. A. and Rubenstein, D. S.** (2006). p38MAPK inhibition prevents disease in pemphigus vulgaris mice. *Proc Natl Acad Sci U S A* **103**, 12855-60.
- Bershadsky, A. D., Ballestrem, C., Carramusa, L., Zilberman, Y., Gilquin, B., Khochbin, S., Alexandrova, A. Y., Verkhovsky, A. B., Shemesh, T. and Kozlov, M. M.** (2006). Assembly and mechanosensory function of focal adhesions: experiments and models. *Eur J Cell Biol* **85**, 165-73.
- Berx, G. and van Roy, F.** (2009). Involvement of Members of the Cadherin Superfamily in Cancer. *Cold Spring Harbor Perspectives in Biology*, -.
- Beutner, E. H. and Jordon, R. E.** (1964). Demonstration Of Skin Antibodies In Sera Of Pemphigus Vulgaris Patients By Indirect Immunofluorescent Staining. *Proc Soc Exp Biol Med* **117**, 505-10.
- Bhalla, K., Luo, Y., Buchan, T., Beachem, M. A., Guzauskas, G. F., Ladd, S., Bratcher, S. J., Schroer, R. J., Balsamo, J., DuPont, B. R. et al.** (2008). Alterations in CDH15 and KIRREL3 in patients with mild to severe intellectual disability. *Am J Hum Genet* **83**, 703-13.
- Bibert, S., Jaquinod, M., Concord, E., Ebel, C., Hewat, E., Vanbelle, C., Legrand, P., Weidenhaupt, M., Vernet, T. and Gulino-Debrac, D.** (2002). Synergy between extracellular modules of vascular endothelial cadherin promotes homotypic hexameric interactions. *J Biol Chem* **277**, 12790-801.
- Blaschuk, O. W., Sullivan, R., David, S. and Pouliot, Y.** (1990). Identification of a cadherin cell adhesion recognition sequence. *Dev Biol* **139**, 227-9.
- Boda-Heggemann, J., Regnier-Vigouroux, A. and Franke, W. W.** (2009). Beyond vessels: occurrence and regional clustering of vascular endothelial (VE-)cadherin-containing junctions in non-endothelial cells. *Cell Tissue Res* **335**, 49-65.
- Boggon, T. J., Murray, J., Chappuis-Flament, S., Wong, E., Gumbiner, B. M. and Shapiro, L.** (2002). C-cadherin ectodomain structure and implications for cell adhesion mechanisms. *Science* **296**, 1308-13.
- Brieher, W. M., Yap, A. S. and Gumbiner, B. M.** (1996). Lateral dimerization is required for the homophilic binding activity of C-cadherin. *J Cell Biol* **135**, 487-96.
- Burden-Gulley, S. M., Gates, T. J., Craig, S. E., Gupta, M. and Brady-Kalnay, S. M.** (2010). Stimulation of N-cadherin-dependent neurite outgrowth by small molecule peptide mimetic agonists of the N-cadherin HAV motif. *Peptides*.
- Burden-Gulley, S. M., Gates, T. J., Craig, S. E., Lou, S. F., Oblander, S. A., Howell, S., Gupta, M. and Brady-Kalnay, S. M.** (2009). Novel peptide mimetic small molecules of the HAV motif in N-cadherin inhibit N-cadherin-mediated neurite outgrowth and cell adhesion. *Peptides*.
- Cailliez, F. and Lavery, R.** (2005). Cadherin mechanics and complexation: the importance of calcium binding. *Biophys J* **89**, 3895-903.

- Cailliez, F. and Lavery, R.** (2006). Dynamics and stability of E-cadherin dimers. *Biophys J* **91**, 3964-71.
- Caldelari, R., de Bruin, A., Baumann, D., Suter, M. M., Bierkamp, C., Balmer, V. and Muller, E.** (2001). A Central Role for the Armadillo Protein Plakoglobin in the Autoimmune Disease Pemphigus Vulgaris. *J. Cell Biol.* **153**, 823-834.
- Calkins, C. C., Setzer, S. V., Jennings, J. M., Summers, S., Tsunoda, K., Amagai, M. and Kowalczyk, A. P.** (2006). Desmoglein endocytosis and desmosome disassembly are coordinated responses to pemphigus autoantibodies. *J Biol Chem* **281**, 7623-34.
- Cano, A., Perez-Moreno, M. A., Rodrigo, I., Locascio, A., Blanco, M. J., del Barrio, M. G., Portillo, F. and Nieto, M. A.** (2000). The transcription factor snail controls epithelial-mesenchymal transitions by repressing E-cadherin expression. *Nat Cell Biol* **2**, 76-83.
- Capon, F., Boulding, H., Quaranta, M., Mortimer, N. J., Setterfield, J. F., Black, M. M., Trembath, R. C. and Harman, K. E.** (2009). Genetic analysis of desmoglein 3 (DSG3) sequence variants in patients with pemphigus vulgaris. *Br J Dermatol.*
- Cavallaro, U. and Christofori, G.** (2004). Cell adhesion and signalling by cadherins and Ig-CAMs in cancer. *Nat Rev Cancer* **4**, 118-32.
- Cavey, M., Rauzi, M., Lenne, P. F. and Lecuit, T.** (2008). A two-tiered mechanism for stabilization and immobilization of E-cadherin. *Nature* **453**, 751-6.
- Chappuis-Flament, S., Wong, E., Hicks, L. D., Kay, C. M. and Gumbiner, B. M.** (2001). Multiple cadherin extracellular repeats mediate homophilic binding and adhesion. *J Cell Biol* **154**, 231-43.
- Chen, C. P., Posy, S., Ben-Shaul, A., Shapiro, L. and Honig, B. H.** (2005). Specificity of cell-cell adhesion by classical cadherins: Critical role for low-affinity dimerization through beta-strand swapping. *Proc Natl Acad Sci U S A* **102**, 8531-6.
- Chen, J., Den, Z. and Koch, P. J.** (2008). Loss of desmocollin 3 in mice leads to epidermal blistering. *J Cell Sci* **121**, 2844-9.
- Chen, J., Zheng, X. F., Brown, E. J. and Schreiber, S. L.** (1995). Identification of an 11-kDa FKBP12-rapamycin-binding domain within the 289-kDa FKBP12-rapamycin-associated protein and characterization of a critical serine residue. *Proc Natl Acad Sci U S A* **92**, 4947-51.
- Chen, Y. T., Stewart, D. B. and Nelson, W. J.** (1999). Coupling assembly of the E-cadherin/beta-catenin complex to efficient endoplasmic reticulum exit and basal-lateral membrane targeting of E-cadherin in polarized MDCK cells. *J Cell Biol* **144**, 687-99.
- Chernyavsky, A. I., Arredondo, J., Kitajima, Y., Sato-Nagai, M. and Grando, S. A.** (2007). Desmoglein VS. non-desmoglein signaling in pemphigus acantholysis: Characterization of novel signaling pathways downstream of pemphigus vulgaris antigens. *J Biol Chem.*
- Chernyavsky, A. I., Arredondo, J., Piser, T., Karlsson, E. and Grando, S. A.** (2008). Differential coupling of M1 muscarinic and alpha7 nicotinic receptors to inhibition of pemphigus acantholysis. *J Biol Chem* **283**, 3401-8.
- Chien, Y. H., Jiang, N., Li, F., Zhang, F., Zhu, C. and Leckband, D.** (2008). Two stage cadherin kinetics require multiple extracellular domains but not the cytoplasmic region. *J Biol Chem* **283**, 1848-56.
- Chिताев, N. A. and Troyanovsky, S. M.** (1998). Adhesive but not lateral E-cadherin complexes require calcium and catenins for their formation. *J Cell Biol* **142**, 837-46.

- Choi, H. J., Huber, A. H. and Weis, W. I. (2006).** Thermodynamics of beta-catenin-ligand interactions: the roles of the N- and C-terminal tails in modulating binding affinity. *J Biol Chem* **281**, 1027-38.
- Ciatto, C., Bahna, F., Zampieri, N., Vansteenhout, H. C., Katsamba, P. S., Ahlsen, G., Harrison, O. J., Brasch, J., Jin, X., Posy, S. et al. (2010).** T-cadherin structures reveal a novel adhesive binding mechanism. *Nat Struct Mol Biol*.
- Cirillo, N., Lanza, M., Rossiello, L., Gombos, F. and Lanza, A. (2007).** Defining the involvement of proteinases in pemphigus vulgaris: evidence of matrix metalloproteinase-9 overexpression in experimental models of disease. *J Cell Physiol* **212**, 36-41.
- Corada, M., Mariotti, M., Thurston, G., Smith, K., Kunkel, R., Brockhaus, M., Lampugnani, M. G., Martin-Padura, I., Stoppacciaro, A., Ruco, L. et al. (1999).** Vascular endothelial-cadherin is an important determinant of microvascular integrity in vivo. *Proc Natl Acad Sci U S A* **96**, 9815-20.
- Culton, D. A., Qian, Y., Li, N., Rubenstein, D., Aoki, V., Filho, G. H., Rivitti, E. A. and Diaz, L. A. (2008).** Advances in pemphigus and its endemic pemphigus foliaceus (Fogo Selvagem) phenotype: a paradigm of human autoimmunity. *J Autoimmun* **31**, 311-24.
- Dallon, J. C., Newren, E. and Hansen, M. D. (2009).** Using a mathematical model of cadherin-based adhesion to understand the function of the actin cytoskeleton. *Phys Rev E Stat Nonlin Soft Matter Phys* **79**, 031918.
- de Bruin, A., Caldelari, R., Williamson, L., Suter, M. M., Hunziker, T., Wyder, M. and Muller, E. J. (2007).** Plakoglobin-dependent disruption of the desmosomal plaque in pemphigus vulgaris. *Experimental Dermatology* **16**, 468-475.
- Dejana, E., Orsenigo, F. and Lampugnani, M. G. (2008).** The role of adherens junctions and VE-cadherin in the control of vascular permeability. *J Cell Sci* **121**, 2115-22.
- Delva, E., Jennings, J. M., Calkins, C. C., Kottke, M. D., Faundez, V. and Kowalczyk, A. P. (2008).** Pemphigus vulgaris IgG-induced desmoglein-3 endocytosis and desmosomal disassembly are mediated by a clathrin and dynamin-independent mechanism. *J Biol Chem*.
- Delva, E. and Kowalczyk, A. P. (2009).** Regulation of cadherin trafficking. *Traffic* **10**, 259-67.
- Delva, E., Tucker, D. K. and Kowalczyk, A. P. (2009).** The Desmosome. *Cold Spring Harbor Perspectives in Biology* **1**, -.
- Devemy, E. and Blaschuk, O. W. (2009).** Identification of a novel dual E- and N-cadherin antagonist. *Peptides* **30**, 1539-47.
- Drees, F., Pokutta, S., Yamada, S., Nelson, W. J. and Weis, W. I. (2005).** Alpha-catenin is a molecular switch that binds E-cadherin-beta-catenin and regulates actin-filament assembly. *Cell* **123**, 903-15.
- Dudek, S. M. and Garcia, J. G. (2001).** Cytoskeletal regulation of pulmonary vascular permeability. *J Appl Physiol* **91**, 1487-500.
- Ebner, A., Hinterdorfer, P. and Gruber, H. J. (2007).** Comparison of different aminofunctionalization strategies for attachment of single antibodies to AFM cantilevers. *Ultramicroscopy* **107**, 922-7.
- El-Amraoui, A. and Petit, C. (2009).** Cadherins as Targets for Genetic Diseases. *Cold Spring Harbor Perspectives in Biology*, -.
- Elledge, H. M., Kazmierczak, P., Clark, P., Joseph, J. S., Kolatkar, A., Kuhn, P. and Muller, U. (2010).** Structure of the N terminus of cadherin 23 reveals a new adhesion mechanism for a subset of cadherin superfamily members. *Proc Natl Acad Sci U S A*.

- Esaki, C., Seishima, M., Yamada, T., Osada, K. and Kitajima, Y.** (1995). Pharmacologic evidence for involvement of phospholipase C in pemphigus IgG-induced inositol 1,4,5-trisphosphate generation, intracellular calcium increase, and plasminogen activator secretion in DJM-1 cells, a squamous cell carcinoma line. *J Invest Dermatol* **105**, 329-33.
- Evangelista, F., Dasher, D. A., Diaz, L. A. and Li, N.** (2006). The prevalence of autoantibodies against E-cadherin in pemphigus. *J. Invest. Dermatol.* **126 (Suppl. 1)**, 9 (abstract 51).
- Evangelista, F., Dasher, D. A., Diaz, L. A., Prisanh, P. S. and Li, N.** (2008). E-cadherin Is an Additional Immunological Target for Pemphigus Autoantibodies. *J Invest Dermatol.*
- Evans, E. and Ritchie, K.** (1997). Dynamic strength of molecular adhesion bonds. *Biophys J* **72**, 1541-55.
- Farquhar, M. G. and Palade, G. E.** (1965). Cell junctions in amphibian skin. *J Cell Biol* **26**, 263-91.
- Forster, C.** (2008). Tight junctions and the modulation of barrier function in disease. *Histochem Cell Biol* **130**, 55-70.
- Fritz, J., Katopodis, A. G., Kolbinger, F. and Anselmetti, D.** (1998). Force-mediated kinetics of single P-selectin/ligand complexes observed by atomic force microscopy. *Proc Natl Acad Sci U S A* **95**, 12283-8.
- Frusic-Zlotkin, M., Raichenberg, D., Wang, X., David, M., Michel, B. and Milner, Y.** (2006). Apoptotic mechanism in pemphigus autoimmunoglobulins-induced acantholysis--possible involvement of the EGF receptor. *Autoimmunity* **39**, 563-75.
- Fujita, Y., Krause, G., Scheffner, M., Zechner, D., Leddy, H. E., Behrens, J., Sommer, T. and Birchmeier, W.** (2002). Hakai, a c-Cbl-like protein, ubiquitinates and induces endocytosis of the E-cadherin complex. *Nat Cell Biol* **4**, 222-31.
- Fukata, M., Nakagawa, M., Kuroda, S. and Kaibuchi, K.** (1999). Cell adhesion and Rho small GTPases. *J Cell Sci* **112 (Pt 24)**, 4491-500.
- Futei, Y., Amagai, M., Ishii, K., Kuroda-Kinoshita, K., Ohya, K. and Nishikawa, T.** (2001). Predominant IgG4 subclass in autoantibodies of pemphigus vulgaris and foliaceus. *J Dermatol Sci* **26**, 55-61.
- Garrod, D. R., Berika, M. Y., Bardsley, W. F., Holmes, D. and Taberner, L.** (2005). Hyper-adhesion in desmosomes: its regulation in wound healing and possible relationship to cadherin crystal structure. *J Cell Sci* **118**, 5743-54.
- Garrod, D. R., Merritt, A. J. and Nie, Z.** (2002). Desmosomal cadherins. *Curr Opin Cell Biol* **14**, 537-45.
- Gonzalez-Amaro, R. and Sanchez-Madrid, F.** (1999). Cell adhesion molecules: selectins and integrins. *Crit Rev Immunol* **19**, 389-429.
- Gooding, J. M., Yap, K. L. and Ikura, M.** (2004). The cadherin-catenin complex as a focal point of cell adhesion and signalling: new insights from three-dimensional structures. *Bioessays* **26**, 497-511.
- Gorlatov, S. and Medved, L.** (2002). Interaction of fibrin(ogen) with the endothelial cell receptor VE-cadherin: mapping of the receptor-binding site in the NH2-terminal portions of the fibrin beta chains. *Biochemistry* **41**, 4107-16.
- Gotsch, U., Borges, E., Bosse, R., Boggemeyer, E., Simon, M., Mossmann, H. and Vestweber, D.** (1997). VE-cadherin antibody accelerates neutrophil recruitment in vivo. *J Cell Sci* **110**, 583-8.
- Grabel, L. B., Rosen, S. D. and Martin, G. R.** (1979). Teratocarcinoma stem cells have a cell surface carbohydrate-binding component implicated in cell-cell adhesion. *Cell* **17**, 477-84.
- Gregory, P. A., Bracken, C. P., Bert, A. G. and Goodall, G. J.** (2008). MicroRNAs as regulators of epithelial-mesenchymal transition. *Cell Cycle* **7**, 3112-8.

- Gutberlet, J.** (2006). Untersuchungen zu Wechselwirkungen von VE-Cadherin-Molekülen untereinander und mit TRPC4. In *Institute of Anatomy and Cell Biology*, vol. Dr. rer. nat. Marburg: University of Marburg.
- Hanley, W. D., Wirtz, D. and Konstantopoulos, K.** (2004). Distinct kinetic and mechanical properties govern selectin-leukocyte interactions. *J Cell Sci* **117**, 2503-11.
- Harrison, O. J., Bahna, F., Katsamba, P. S., Jin, X., Brasch, J., Vendome, J., Ahlsen, G., Carroll, K. J., Price, S. R., Honig, B. et al.** (2010). Two-step adhesive binding by classical cadherins. *Nat Struct Mol Biol*.
- Harrison, O. J., Corps, E. M., Berge, T. and Kilshaw, P. J.** (2005a). The mechanism of cell adhesion by classical cadherins: the role of domain 1. *J Cell Sci* **118**, 711-21.
- Harrison, O. J., Corps, E. M. and Kilshaw, P. J.** (2005b). Cadherin adhesion depends on a salt bridge at the N-terminus. *J Cell Sci* **118**, 4123-30.
- Haussinger, D., Ahrens, T., Aberle, T., Engel, J., Stetefeld, J. and Grzesiek, S.** (2004). Proteolytic E-cadherin activation followed by solution NMR and X-ray crystallography. *EMBO J* **23**, 1699-708.
- Haussinger, D., Ahrens, T., Sass, H. J., Pertz, O., Engel, J. and Grzesiek, S.** (2002). Calcium-dependent homoassociation of E-cadherin by NMR spectroscopy: changes in mobility, conformation and mapping of contact regions. *J Mol Biol* **324**, 823-39.
- Hazan, R. B., Qiao, R., Keren, R., Badano, I. and Suyama, K.** (2004). Cadherin switch in tumor progression. *Ann N Y Acad Sci* **1014**, 155-63.
- He, W., Cowin, P. and Stokes, D. L.** (2003). Untangling desmosomal knots with electron tomography. *Science* **302**, 109-13.
- Heupel, W. M., Baumgartner, W., Laymann, B., Drenckhahn, D. and Golenhofen, N.** (2008). Different Ca²⁺ affinities and functional implications of the two synaptic adhesion molecules cadherin-11 and N-cadherin. *Mol Cell Neurosci* **37**, 548-58.
- Hewat, E. A., Durmort, C., Jacquamet, L., Concord, E. and Gulino-Debrac, D.** (2007). Architecture of the VE-cadherin hexamer. *J Mol Biol* **365**, 744-51.
- Hinck, L., Nathke, I. S., Papkoff, J. and Nelson, W. J.** (1994). Dynamics of cadherin/catenin complex formation: novel protein interactions and pathways of complex assembly. *J Cell Biol* **125**, 1327-40.
- Holthofer, B., Windoffer, R., Troyanovsky, S. and Leube, R. E.** (2007). Structure and function of desmosomes. *Int Rev Cytol* **264**, 65-163.
- Hong, S., Troyanovsky, R. B. and Troyanovsky, S. M.** Spontaneous assembly and active disassembly balance adherens junction homeostasis. *Proc Natl Acad Sci U S A* **107**, 3528-33.
- Hordijk, P. L., Anthony, E., Mul, F. P., Rientsma, R., Oomen, L. C. and Roos, D.** (1999). Vascular-endothelial-cadherin modulates endothelial monolayer permeability. *J Cell Sci* **112 (Pt 12)**, 1915-23.
- Hubner, S., Jans, D. A. and Drenckhahn, D.** (2001). Roles of cytoskeletal and junctional plaque proteins in nuclear signaling. *Int Rev Cytol* **208**, 207-65.
- Hulpiau, P. and van Roy, F.** (2009). Molecular evolution of the cadherin superfamily. *Int J Biochem Cell Biol* **41**, 349-69.
- Hynes, R. O. and Zhao, Q.** (2000). The evolution of cell adhesion. *J Cell Biol* **150**, F89-96.
- Iino, R., Koyama, I. and Kusumi, A.** (2001). Single molecule imaging of green fluorescent proteins in living cells: E-cadherin forms oligomers on the free cell surface. *Biophys J* **80**, 2667-77.
- Indelman, M., Bergman, R., Lurie, R., Richard, G., Miller, B., Petronius, D., Ciubutaro, D., Leib, R. and Sprecher, E.** (2002). A missense mutation in CDH3,

encoding P-cadherin, causes hypotrichosis with juvenile macular dystrophy. *J Invest Dermatol* **119**, 1210-3.

Ishikawa, H. O., Takeuchi, H., Haltiwanger, R. S. and Irvine, K. D. (2008). Four-jointed is a Golgi kinase that phosphorylates a subset of cadherin domains. *Science* **321**, 401-4.

Ishiyama, N., Lee, S. H., Liu, S., Li, G. Y., Smith, M. J., Reichardt, L. F. and Ikura, M. Dynamic and static interactions between p120 catenin and E-cadherin regulate the stability of cell-cell adhesion. *Cell* **141**, 117-28.

Jeanes, A., Gottardi, C. J. and Yap, A. S. (2008). Cadherins and cancer: how does cadherin dysfunction promote tumor progression? *Oncogene* **27**, 6920-9.

Jessop, S. and Khumalo, N. P. (2008). Pemphigus: a treatment update. *Am J Clin Dermatol* **9**, 147-54.

Joly, P., Mouquet, H., Roujeau, J. C., D'Incan, M., Gilbert, D., Jacquot, S., Gougeon, M. L., Bedane, C., Muller, R., Dreno, B. et al. (2007). A single cycle of rituximab for the treatment of severe pemphigus. *N Engl J Med* **357**, 545-52.

Katsamba, P., Carroll, K., Ahlsen, G., Bahna, F., Vendome, J., Posy, S., Rajebhosale, M., Price, S., Jessell, T. M., Ben-Shaul, A. et al. (2009). Linking molecular affinity and cellular specificity in cadherin-mediated adhesion. *Proc Natl Acad Sci U S A* **106**, 11594-9.

Kawasaki, Y., Aoyama, Y., Tsunoda, K., Amagai, M. and Kitajima, Y. (2006). Different anti-desmoglein 3 monoclonal antibodies exert epitope-specific regulation of p120-catenin phosphorylation and of p120-catenin binding to desmoglein 3 in human squamous cell line, DJM-1 cell. *J. Invest. Dermatol.* **126 (Suppl. 1)**, 6 (abstract 36).

Kazmierczak, P., Sakaguchi, H., Tokita, J., Wilson-Kubalek, E. M., Milligan, R. A., Muller, U. and Kachar, B. (2007). Cadherin 23 and protocadherin 15 interact to form tip-link filaments in sensory hair cells. *Nature* **449**, 87-91.

Kelland, L. (2007). Drug evaluation: ADH-1, an N-cadherin antagonist targeting cancer vascularization. *Curr Opin Mol Ther* **9**, 86-91.

Keppler, A., Gendreizig, S., Gronemeyer, T., Pick, H., Vogel, H. and Johnsson, K. (2003). A general method for the covalent labeling of fusion proteins with small molecules in vivo. *Nat Biotechnol* **21**, 86-9.

Kitagawa, M., Natori, M., Murase, S., Hirano, S., Taketani, S. and Suzuki, S. T. (2000). Mutation analysis of cadherin-4 reveals amino acid residues of EC1 important for the structure and function. *Biochem Biophys Res Commun* **271**, 358-63.

Kitajima, Y., Aoyama, Y. and Seishima, M. (1999). Transmembrane signaling for adhesive regulation of desmosomes and hemidesmosomes, and for cell-cell detachment induced by pemphigus IgG in cultured keratinocytes: involvement of protein kinase C. *J Invest Dermatol Symp Proc* **4**, 137-44.

Klessner, J. L., Desai, B. V., Amargo, E. V., Getsios, S. and Green, K. J. (2009). EGFR and ADAMs cooperate to regulate shedding and endocytic trafficking of the desmosomal cadherin desmoglein 2. *Mol Biol Cell* **20**, 328-37.

Klingelhofer, J., Laur, O. Y., Troyanovsky, R. B. and Troyanovsky, S. M. (2002). Dynamic interplay between adhesive and lateral E-cadherin dimers. *Mol Cell Biol* **22**, 7449-58.

Koch, A. W., Bozic, D., Pertz, O. and Engel, J. (1999). Homophilic adhesion by cadherins. *Curr Opin Struct Biol* **9**, 275-81.

Koch, P. J., Mahoney, M. G., Ishikawa, H., Pulkkinen, L., Uitto, J., Shultz, L., Murphy, G. F., Whitaker-Menezes, D. and Stanley, J. R. (1997). Targeted Disruption of the Pemphigus Vulgaris Antigen (Desmoglein 3) Gene in Mice Causes Loss of Keratinocyte Cell Adhesion with a Phenotype Similar to Pemphigus Vulgaris. *J. Cell Biol.* **137**, 1091-1102.

- Konstantoulaki, M., Kouklis, P. and Malik, A. B.** (2003). Protein kinase C modifications of VE-cadherin, p120, and beta-catenin contribute to endothelial barrier dysregulation induced by thrombin. *Am J Physiol Lung Cell Mol Physiol* **285**, L434-42.
- Kouklis, P. D., Hutton, E. and Fuchs, E.** (1994). Making a connection: direct binding between keratin intermediate filaments and desmosomal proteins. *J Cell Biol* **127**, 1049-60.
- Kreft, B., Berndorff, D., Bottinger, A., Finnemann, S., Wedlich, D., Hortsch, M., Tauber, R. and Gessner, R.** (1997). LI-cadherin-mediated cell-cell adhesion does not require cytoplasmic interactions. *J Cell Biol* **136**, 1109-21.
- Lachman, H. M., Petruolo, O. A., Pedrosa, E., Novak, T., Nolan, K. and Stopkova, P.** (2008). Analysis of protocadherin alpha gene deletion variant in bipolar disorder and schizophrenia. *Psychiatr Genet* **18**, 110-5.
- Lai-Cheong, J. E., Arita, K. and McGrath, J. A.** (2007). Genetic diseases of junctions. *J Invest Dermatol* **127**, 2713-25.
- Lambert, M., Padilla, F. and Mege, R. M.** (2000). Immobilized dimers of N-cadherin-Fc chimera mimic cadherin-mediated cell contact formation: contribution of both outside-in and inside-out signals. *J Cell Sci* **113** (Pt 12), 2207-19.
- Lambert, M., Thoumine, O., Brevier, J., Choquet, D., Riveline, D. and Mege, R. M.** (2007). Nucleation and growth of cadherin adhesions. *Exp Cell Res* **313**, 4025-40.
- Lambert, O., Taveau, J. C., Him, J. L., Al Kurdi, R., Gulino-Debrac, D. and Brisson, A.** (2005). The basic framework of VE-cadherin junctions revealed by cryo-EM. *J Mol Biol* **346**, 1193-6.
- Lanza, A., Cirillo, N., Rossiello, R., Rienzo, M., Cutillo, L., Casamassimi, A., de Nigris, F., Schiano, C., Rossiello, L., Femiano, F. et al.** (2008). Evidence of key role of CDK-2 overexpression in pemphigus vulgaris. *J Biol Chem*.
- Leckband, D. and Sivasankar, S.** (2000). Mechanism of homophilic cadherin adhesion. *Curr Opin Cell Biol* **12**, 587-92.
- Lee, H. E., Berkowitz, P., Jolly, P. S., Diaz, L. A., Chua, M. P. and Rubenstein, D. S.** (2009). Biphasic activation of p38MAPK suggests that apoptosis is a downstream event in pemphigus acantholysis. *J Biol Chem* **284**, 12524-32.
- Legrand, P., Bibert, S., Jaquinod, M., Ebel, C., Hewat, E., Vincent, F., Vanbelle, C., Concord, E., Vernet, T. and Gulino, D.** (2001). Self-assembly of the vascular endothelial cadherin ectodomain in a Ca²⁺-dependent hexameric structure. *J Biol Chem* **276**, 3581-8.
- Levenberg, S., Katz, B. Z., Yamada, K. M. and Geiger, B.** (1998). Long-range and selective autoregulation of cell-cell or cell-matrix adhesions by cadherin or integrin ligands. *J Cell Sci* **111** (Pt 3), 347-57.
- Li, Y., Hofmann, M., Wang, Q., Teng, L., Chlewicki, L. K., Pircher, H. and Mariuzza, R. A.** (2009). Structure of natural killer cell receptor KLRG1 bound to E-cadherin reveals basis for MHC-independent missing self recognition. *Immunity* **31**, 35-46.
- Lickert, H., Bauer, A., Kemler, R. and Stappert, J.** (2000). Casein kinase II phosphorylation of E-cadherin increases E-cadherin/beta-catenin interaction and strengthens cell-cell adhesion. *J Biol Chem* **275**, 5090-5.
- Litjens, S. H., de Pereda, J. M. and Sonnenberg, A.** (2006). Current insights into the formation and breakdown of hemidesmosomes. *Trends Cell Biol* **16**, 376-83.
- Liwosz, A., Lei, T. and Kukuruzinska, M. A.** (2006). N-glycosylation affects the molecular organization and stability of E-cadherin junctions. *J Biol Chem* **281**, 23138-49.

- Luik, R. M., Wang, B., Prakriya, M., Wu, M. M. and Lewis, R. S.** (2008). Oligomerization of STIM1 couples ER calcium depletion to CRAC channel activation. *Nature* **454**, 538-42.
- Mahoney, M. G., Wang, Z., Rothenberger, K., Koch, P. J., Amagai, M. and Stanley, J. R.** (1999). Explanations for the clinical and microscopic localization of lesions in pemphigus foliaceus and vulgaris. *J. Clin. Invest.* **103**, 461-468.
- Mao, X., Choi, E. J. and Payne, A. S.** (2009). Disruption of desmosome assembly by monovalent human pemphigus vulgaris monoclonal antibodies. *J Invest Dermatol* **129**, 908-18.
- Marambaud, P., Shioi, J., Serban, G., Georgakopoulos, A., Sarnier, S., Nagy, V., Baki, L., Wen, P., Efthimiopoulos, S., Shao, Z. et al.** (2002). A presenilin-1/gamma-secretase cleavage releases the E-cadherin intracellular domain and regulates disassembly of adherens junctions. *EMBO J* **21**, 1948-56.
- Marquina, M., Espana, A., Fernandez-Galar, M. and Lopez-Zabalza, M. J.** (2008). The role of nitric oxide synthases in pemphigus vulgaris in a mouse model. *Br J Dermatol* **159**, 68-76.
- Marshall, B. T., Long, M., Piper, J. W., Yago, T., McEver, R. P. and Zhu, C.** (2003). Direct observation of catch bonds involving cell-adhesion molecules. *Nature* **423**, 190-3.
- Martinez-Rico, C., Pincet, F., Perez, E., Thiery, J. P., Shimizu, K., Takai, Y. and Dufour, S.** (2005). Separation force measurements reveal different types of modulation of E-cadherin-based adhesion by nectin-1 and -3. *J Biol Chem* **280**, 4753-60.
- May, C., Doody, J. F., Abdullah, R., Balderes, P., Xu, X., Chen, C. P., Zhu, Z., Shapiro, L., Kussie, P., Hicklin, D. J. et al.** (2005). Identification of a transiently exposed VE-cadherin epitope that allows for specific targeting of an antibody to the tumor neovasculature. *Blood* **105**, 4337-44.
- Meng, W., Mushika, Y., Ichii, T. and Takeichi, M.** (2008). Anchorage of microtubule minus ends to adherens junctions regulates epithelial cell-cell contacts. *Cell* **135**, 948-59.
- Meng, W. and Takeichi, M.** (2009). Adherens Junction: Molecular Architecture and Regulation. *Cold Spring Harbor Perspectives in Biology*, -.
- Mese, G., Richard, G. and White, T. W.** (2007). Gap junctions: basic structure and function. *J Invest Dermatol* **127**, 2516-24.
- Miloushev, V. Z., Bahna, F., Ciatto, C., Ahlsen, G., Honig, B., Shapiro, L. and Palmer, A. G., 3rd.** (2008). Dynamic properties of a type II cadherin adhesive domain: implications for the mechanism of strand-swapping of classical cadherins. *Structure* **16**, 1195-205.
- Miyaguchi, K.** (2000). Ultrastructure of the zonula adherens revealed by rapid-freeze deep-etching. *J Struct Biol* **132**, 169-78.
- Miyoshi, J. and Takai, Y.** (2008). Structural and functional associations of apical junctions with cytoskeleton. *Biochim Biophys Acta* **1778**, 670-91.
- Moll, T. and Vestweber, D.** (1999). Construction and purification of adhesion molecule immunoglobulin chimeric proteins. *Methods Mol Biol* **96**, 77-84.
- Morioka, S., Lazarus, G. S. and Jensen, P. J.** (1987). Involvement of Urokinase-Type Plasminogen Activator in Acantholysis Induced by Pemphigus IgG. *J Invest Dermatol* **89**, 474-477.
- Muller, E. J., Williamson, L., Kolly, C. and Suter, M. M.** (2008). Outside-in signaling through integrins and cadherins: a central mechanism to control epidermal growth and differentiation? *J Invest Dermatol* **128**, 501-16.

- Navaratna, D., Maestas, J., McGuire, P. G. and Das, A. (2008).** *Suppression of retinal neovascularization with an antagonist to vascular endothelial cadherin.* *Arch Ophthalmol* **126**, 1082-8.
- Nawroth, R., Poell, G., Ranft, A., Kloep, S., Samulowitz, U., Fachinger, G., Golding, M., Shima, D. T., Deutsch, U. and Vestweber, D. (2002).** *VE-PTP and VE-cadherin ectodomains interact to facilitate regulation of phosphorylation and cell contacts.* *EMBO J* **21**, 4885-95.
- Nelson, W. J. (2008).** *Regulation of cell-cell adhesion by the cadherin-catenin complex.* *Biochem Soc Trans* **36**, 149-55.
- Nguyen, V. T., Ndoye, A. and Grando, S. A. (2000a).** *Novel Human {alpha}9 Acetylcholine Receptor Regulating Keratinocyte Adhesion is Targeted by Pemphigus Vulgaris Autoimmunity.* *Am J Pathol* **157**, 1377-1391.
- Nguyen, V. T., Ndoye, A. and Grando, S. A. (2000b).** *Pemphigus Vulgaris Antibody Identifies Pemphaxin. A NOVEL KERATINOCYTE ANNEXIN-LIKE MOLECULE BINDING ACETYLCHOLINE.* *J. Biol. Chem.* **275**, 29466-29476.
- Nguyen, V. T., Ndoye, A., Shultz, L. D., Pittelkow, M. R. and Grando, S. A. (2000c).** *Antibodies against keratinocyte antigens other than desmogleins 1 and 3 can induce pemphigus vulgaris-like lesions.* *J Clin Invest* **106**, 1467-79.
- Niessen, C. M. and Gumbiner, B. M. (2002).** *Cadherin-mediated cell sorting not determined by binding or adhesion specificity.* *J Cell Biol* **156**, 389-399.
- Noe, V., Willems, J., Vandekerckhove, J., Roy, F. V., Bruyneel, E. and Mareel, M. (1999).** *Inhibition of adhesion and induction of epithelial cell invasion by HAV-containing E-cadherin-specific peptides.* *J Cell Sci* **112 (Pt 1)**, 127-35.
- Nollet, F., Kools, P. and van Roy, F. (2000).** *Phylogenetic analysis of the cadherin superfamily allows identification of six major subfamilies besides several solitary members.* *J Mol Biol* **299**, 551-72.
- Nose, A., Nagafuchi, A. and Takeichi, M. (1988).** *Expressed recombinant cadherins mediate cell sorting in model systems.* *Cell* **54**, 993-1001.
- Nose, A., Tsuji, K. and Takeichi, M. (1990).** *Localization of specificity determining sites in cadherin cell adhesion molecules.* *Cell* **61**, 147-55.
- Nwariaku, F. E., Liu, Z., Zhu, X., Turnage, R. H., Sarosi, G. A. and Terada, L. S. (2002).** *Tyrosine phosphorylation of vascular endothelial cadherin and the regulation of microvascular permeability.* *Surgery* **132**, 180-5.
- Overduin, M., Harvey, T. S., Bagby, S., Tong, K. I., Yau, P., Takeichi, M. and Ikura, M. (1995).** *Solution Structure of the Epithelial Cadherin Domain Responsible for Selective Cell-Adhesion.* *Science* **267**, 386-389.
- Ozawa, M. (2003).** *p120-independent modulation of E-cadherin adhesion activity by the membrane-proximal region of the cytoplasmic domain.* *J Biol Chem* **278**, 46014-20.
- Ozawa, M., Baribault, H. and Kemler, R. (1989).** *The cytoplasmic domain of the cell adhesion molecule uvomorulin associates with three independent proteins structurally related in different species.* *EMBO J* **8**, 1711-7.
- Ozawa, M., Engel, J. and Kemler, R. (1990a).** *Single amino acid substitutions in one Ca²⁺ binding site of uvomorulin abolish the adhesive function.* *Cell* **63**, 1033-8.
- Ozawa, M., Hoschutzky, H., Herrenknecht, K. and Kemler, R. (1990b).** *A possible new adhesive site in the cell-adhesion molecule uvomorulin.* *Mech Dev* **33**, 49-56.
- Ozawa, M. and Kemler, R. (1998).** *The membrane-proximal region of the E-cadherin cytoplasmic domain prevents dimerization and negatively regulates adhesion activity.* *J Cell Biol* **142**, 1605-13.

- Ozawa, M., Ringwald, M. and Kemler, R.** (1990c). Uvomorulin-catenin complex formation is regulated by a specific domain in the cytoplasmic region of the cell adhesion molecule. *Proc Natl Acad Sci U S A* **87**, 4246-50.
- Panorchan, P., George, J. P. and Wirtz, D.** (2006a). Probing intercellular interactions between vascular endothelial cadherin pairs at single-molecule resolution and in living cells. *J Mol Biol* **358**, 665-74.
- Panorchan, P., Thompson, M. S., Davis, K. J., Tseng, Y., Konstantopoulos, K. and Wirtz, D.** (2006b). Single-molecule analysis of cadherin-mediated cell-cell adhesion. *J Cell Sci* **119**, 66-74.
- Parisini, E., Higgins, J. M., Liu, J. H., Brenner, M. B. and Wang, J. H.** (2007). The crystal structure of human E-cadherin domains 1 and 2, and comparison with other cadherins in the context of adhesion mechanism. *J Mol Biol* **373**, 401-11.
- Patel, S. D., Ciatto, C., Chen, C. P., Bahna, F., Rajebhosale, M., Arkus, N., Schieren, I., Jessell, T. M., Honig, B., Price, S. R. et al.** (2006). Type II cadherin ectodomain structures: implications for classical cadherin specificity. *Cell* **124**, 1255-68.
- Perret, E., Benoliel, A. M., Nassoy, P., Pierres, A., Delmas, V., Thiery, J. P., Bongrand, P. and Feracci, H.** (2002). Fast dissociation kinetics between individual E-cadherin fragments revealed by flow chamber analysis. *EMBO J* **21**, 2537-46.
- Perret, E., Leung, A., Feracci, H. and Evans, E.** (2004). Trans-bonded pairs of E-cadherin exhibit a remarkable hierarchy of mechanical strengths. *Proc Natl Acad Sci U S A* **101**, 16472-7.
- Pertz, O., Bozic, D., Koch, A. W., Fauser, C., Brancaccio, A. and Engel, J.** (1999). A new crystal structure, Ca²⁺ dependence and mutational analysis reveal molecular details of E-cadherin homoassociation. *EMBO J* **18**, 1738-47.
- Peyrieras, N., Hyafil, F., Louvard, D., Ploegh, H. L. and Jacob, F.** (1983). Uvomorulin: a nonintegral membrane protein of early mouse embryo. *Proc Natl Acad Sci U S A* **80**, 6274-7.
- Pittet, P., Lee, K., Kulik, A. J., Meister, J. J. and Hinz, B.** (2008). Fibrogenic fibroblasts increase intercellular adhesion strength by reinforcing individual OB-cadherin bonds. *J Cell Sci* **121**, 877-86.
- Posthaus, H., Dubois, C. M. and Muller, E.** (2003). Novel insights into cadherin processing by subtilisin-like convertases. *FEBS Lett* **536**, 203-8.
- Posy, S., Shapiro, L. and Honig, B.** (2008). Sequence and structural determinants of strand swapping in cadherin domains: do all cadherins bind through the same adhesive interface? *J Mol Biol* **378**, 952-66.
- Prakasam, A. K., Maruthamuthu, V. and Leckband, D. E.** (2006). Similarities between heterophilic and homophilic cadherin adhesion. *Proc Natl Acad Sci U S A* **103**, 15434-9.
- Puviani, M., Marconi, A., Cozzani, E. and Pincelli, C.** (2003). Fas ligand in pemphigus sera induces keratinocyte apoptosis through the activation of caspase-8. *J Invest Dermatol* **120**, 164-7.
- Rabiet, M. J., Plantier, J. L. and Dejana, E.** (1994). Thrombin-induced endothelial cell dysfunction. *Br Med Bull* **50**, 936-45.
- Rabiet, M. J., Plantier, J. L., Rival, Y., Genoux, Y., Lampugnani, M. G. and Dejana, E.** (1996). Thrombin-induced increase in endothelial permeability is associated with changes in cell-to-cell junction organization. *Arterioscler Thromb Vasc Biol* **16**, 488-96.
- Ranheim, T. S., Edelman, G. M. and Cunningham, B. A.** (1996). Homophilic adhesion mediated by the neural cell adhesion molecule involves multiple immunoglobulin domains. *Proc Natl Acad Sci U S A* **93**, 4071-5.

Rayns, D. G., Simpson, F. O. and Ledingham, J. M. (1969). Ultrastructure of desmosomes in mammalian intercalated disc; appearances after lanthanum treatment. *J Cell Biol* **42**, 322-6.

Roux, A. F., Faugere, V., Le Guedard, S., Pallares-Ruiz, N., Vielle, A., Chambert, S., Marlin, S., Hamel, C., Gilbert, B., Malcolm, S. et al. (2006). Survey of the frequency of USH1 gene mutations in a cohort of Usher patients shows the importance of cadherin 23 and protocadherin 15 genes and establishes a detection rate of above 90%. *J Med Genet* **43**, 763-8.

Runswick, S. K., O'Hare, M. J., Jones, L., Streuli, C. H. and Garrod, D. R. (2001). Desmosomal adhesion regulates epithelial morphogenesis and cell positioning. *Nat Cell Biol* **3**, 823-30.

Sako, Y., Nagafuchi, A., Tsukita, S., Takeichi, M. and Kusumi, A. (1998). Cytoplasmic regulation of the movement of E-cadherin on the free cell surface as studied by optical tweezers and single particle tracking: corralling and tethering by the membrane skeleton. *J Cell Biol* **140**, 1227-40.

Sanchez-Carpintero, I., Espana, A., Pelacho, B., Lopez Moratalla, N., Rubenstein, D. S., Diaz, L. A. and Lopez-Zabalza, M. J. (2004). In vivo blockade of pemphigus vulgaris acantholysis by inhibition of intracellular signal transduction cascades. *Br J Dermatol* **151**, 565-70.

Schmidt, E. and Waschke, J. (2009). Apoptosis in pemphigus. *Autoimmun Rev* **8**, 533-7.

Schwander, M., Xiong, W., Tokita, J., Lelli, A., Elledge, H. M., Kazmierczak, P., Sczaniecka, A., Kolatkar, A., Wiltshire, T., Kuhn, P. et al. (2009). A mouse model for nonsyndromic deafness (DFNB12) links hearing loss to defects in tip links of mechanosensory hair cells. *Proc Natl Acad Sci U S A* **106**, 5252-7.

Sekiguchi, M., Futei, Y., Fujii, Y., Iwasaki, T., Nishikawa, T. and Amagai, M. (2001). Dominant Autoimmune Epitopes Recognized by Pemphigus Antibodies Map to the N-Terminal Adhesive Region of Desmogleins. *J Immunol* **167**, 5439-5448.

Shan, W., Yagita, Y., Wang, Z., Koch, A., Fex Svenningsen, A., Gruzglin, E., Pedraza, L. and Colman, D. R. (2004). The minimal essential unit for cadherin-mediated intercellular adhesion comprises extracellular domains 1 and 2. *J Biol Chem* **279**, 55914-23.

Shan, W. S., Tanaka, H., Phillips, G. R., Arndt, K., Yoshida, M., Colman, D. R. and Shapiro, L. (2000). Functional cis-heterodimers of N- and R-cadherins. *J Cell Biol* **148**, 579-90.

Shapiro, L., Fannon, A. M., Kwong, P. D., Thompson, A., Lehmann, M. S., Grubel, G., Legrand, J. F., Als-Nielsen, J., Colman, D. R. and Hendrickson, W. A. (1995). Structural basis of cell-cell adhesion by cadherins. *Nature* **374**, 327-37.

Shapiro, L. and Weis, W. I. (2009). Structure and Biochemistry of Cadherins and Catenins. *Cold Spring Harbor Perspectives in Biology* **1**, -.

Shi, Q., Chien, Y. H. and Leckband, D. (2008). Biophysical properties of cadherin bonds do not predict cell sorting. *J Biol Chem* **283**, 28454-63.

Shimoyama, Y., Takeda, H., Yoshihara, S., Kitajima, M. and Hirohashi, S. (1999). Biochemical characterization and functional analysis of two type II classic cadherins, cadherin-6 and -14, and comparison with E-cadherin. *J Biol Chem* **274**, 11987-94.

Sivasankar, S., Briehar, W., Lavrik, N., Gumbiner, B. and Leckband, D. (1999). Direct molecular force measurements of multiple adhesive interactions between cadherin ectodomains. *Proc Natl Acad Sci U S A* **96**, 11820-4.

Sivasankar, S., Gumbiner, B. and Leckband, D. (2001). Direct measurements of multiple adhesive alignments and unbinding trajectories between cadherin extracellular domains. *Biophys J* **80**, 1758-68.

- Sivasankar, S., Zhang, Y., Nelson, W. J. and Chu, S.** (2009). Characterizing the initial encounter complex in cadherin adhesion. *Structure* **17**, 1075-81.
- Sotomayor, M. and Schulten, K.** (2008). The allosteric role of the Ca²⁺ switch in adhesion and elasticity of C-cadherin. *Biophys J* **94**, 4621-33.
- Spencer, D. M., Wandless, T. J., Schreiber, S. L. and Crabtree, G. R.** (1993). Controlling signal transduction with synthetic ligands. *Science* **262**, 1019-24.
- Spindler, V., Drenckhahn, D., Zillikens, D. and Waschke, J.** (2007). Pemphigus IgG causes skin splitting in the presence of both desmoglein 1 and desmoglein 3. *Am J Pathol* **171**, 906-16.
- Spindler, V., Heupel, W. M., Efthymiadis, A., Schmidt, E., Eming, R., Rankl, C., Hinterdorfer, P., Mueller, T. D., Drenckhahn, D. and Waschke, J.** (2009). Desmocollin 3-mediated binding is crucial for keratinocyte cohesion and is impaired in pemphigus. *J Biol Chem*.
- Stanley, J. R. and Amagai, M.** (2006). Pemphigus, Bullous Impetigo, and the Staphylococcal Scalded-Skin Syndrome. *N Engl J Med* **355**, 1800-1810.
- Stanley, J. R., Koulu, L., Klaus-Kovtun, V. and Steinberg, M. S.** (1986). A monoclonal antibody to the desmosomal glycoprotein desmoglein I binds the same polypeptide as human autoantibodies in pemphigus foliaceus. *J Immunol* **136**, 1227-30.
- Steinberg, M. S.** (2007). Differential adhesion in morphogenesis: a modern view. *Curr Opin Genet Dev* **17**, 281-6.
- Stepniak, E., Radice, G. L. and Vasioukhin, V.** (2009). Adhesive and Signaling Functions of Cadherins and Catenins in Vertebrate Development. *Cold Spring Harbor Perspectives in Biology*, -.
- Takai, Y., Irie, K., Shimizu, K., Sakisaka, T. and Ikeda, W.** (2003). Nectins and nectin-like molecules: roles in cell adhesion, migration, and polarization. *Cancer Sci* **94**, 655-67.
- Takeichi, M.** (1988). The cadherins: cell-cell adhesion molecules controlling animal morphogenesis. *Development* **102**, 639-55.
- Tamura, K., Shan, W. S., Hendrickson, W. A., Colman, D. R. and Shapiro, L.** (1998). Structure-function analysis of cell adhesion by neural (N-) cadherin. *Neuron* **20**, 1153-63.
- Taubenberger, A., Cisneros, D. A., Friedrichs, J., Puech, P. H., Muller, D. J. and Franz, C. M.** (2007). Revealing early steps of alpha2beta1 integrin-mediated adhesion to collagen type I by using single-cell force spectroscopy. *Mol Biol Cell* **18**, 1634-44.
- Tiruppathi, C., Minshall, R. D., Paria, B. C., Vogel, S. M. and Malik, A. B.** (2002). Role of Ca²⁺ signaling in the regulation of endothelial permeability. *Vascul Pharmacol* **39**, 173-85.
- Tomschy, A., Fauser, C., Landwehr, R. and Engel, J.** (1996). Homophilic adhesion of E-cadherin occurs by a co-operative two-step interaction of N-terminal domains. *EMBO J* **15**, 3507-14.
- Tron, F., Gilbert, D., Mouquet, H., Joly, P., Drouot, L., Makni, S., Masmoudi, H., Charron, D., Zitouni, M., Loiseau, P. et al.** (2005). Genetic factors in pemphigus. *J Autoimmun* **24**, 319-28.
- Troyanovsky, R. B., Klingelhofer, J. and Troyanovsky, S.** (1999). Removal of calcium ions triggers a novel type of intercadherin interaction. *J Cell Sci* **112** (Pt 23), 4379-87.
- Troyanovsky, R. B., Laur, O. and Troyanovsky, S. M.** (2007). Stable and unstable cadherin dimers: mechanisms of formation and roles in cell adhesion. *Mol Biol Cell* **18**, 4343-52.

- Troyanovsky, R. B., Sokolov, E. and Troyanovsky, S. M.** (2003). Adhesive and lateral E-cadherin dimers are mediated by the same interface. *Mol Cell Biol* **23**, 7965-72.
- Troyanovsky, R. B., Sokolov, E. P. and Troyanovsky, S. M.** (2006). Endocytosis of cadherin from intracellular junctions is the driving force for cadherin adhesive dimer disassembly. *Mol Biol Cell* **17**, 3484-93.
- Troyanovsky, S.** (2005). Cadherin dimers in cell-cell adhesion. *Eur J Cell Biol* **84**, 225-33.
- Troyanovsky, S. M.** (1999). Mechanism of cell-cell adhesion complex assembly. *Curr Opin Cell Biol* **11**, 561-6.
- Tselepis, C., Chidgey, M., North, A. and Garrod, D.** (1998). Desmosomal adhesion inhibits invasive behavior. *Proc Natl Acad Sci U S A* **95**, 8064-9.
- Tsukasaki, Y., Kitamura, K., Shimizu, K., Iwane, A. H., Takai, Y. and Yanagida, T.** (2007). Role of multiple bonds between the single cell adhesion molecules, nectin and cadherin, revealed by high sensitive force measurements. *J Mol Biol* **367**, 996-1006.
- Tsunoda, K., Ota, T., Aoki, M., Yamada, T., Nagai, T., Nakagawa, T., Koyasu, S., Nishikawa, T. and Amagai, M.** (2003). Induction of Pemphigus Phenotype by a Mouse Monoclonal Antibody Against the Amino-Terminal Adhesive Interface of Desmoglein 3. *J Immunol* **170**, 2170-2178.
- Van Aken, E., De Wever, O., Correia da Rocha, A. S. and Mareel, M.** (2001). Defective E-cadherin/catenin complexes in human cancer. *Virchows Arch* **439**, 725-51.
- Vandenbroucke, E., Mehta, D., Minshall, R. and Malik, A. B.** (2008). Regulation of endothelial junctional permeability. *Ann N Y Acad Sci* **1123**, 134-45.
- Vaughn, D. E. and Bjorkman, P. J.** (1996). The (Greek) key to structures of neural adhesion molecules. *Neuron* **16**, 261-73.
- Vedula, S. R., Lim, T. S., Hui, S., Kausalya, P. J., Lane, E. B., Rajagopal, G., Hunziker, W. and Lim, C. T.** (2007). Molecular force spectroscopy of homophilic nectin-1 interactions. *Biochem Biophys Res Commun* **362**, 886-92.
- Vestal, D. J. and Ranscht, B.** (1992). Glycosyl phosphatidylinositol--anchored T-cadherin mediates calcium-dependent, homophilic cell adhesion. *J Cell Biol* **119**, 451-61.
- Wallez, Y., Cand, F., Cruzalegui, F., Wernstedt, C., Souchelnytskyi, S., Vilgrain, I. and Huber, P.** (2007). Src kinase phosphorylates vascular endothelial-cadherin in response to vascular endothelial growth factor: identification of tyrosine 685 as the unique target site. *Oncogene* **26**, 1067-77.
- Waschke, J.** (2008). The desmosome and pemphigus. *Histochem Cell Biol* **130**, 21-54.
- Waschke, J., Bruggeman, P., Baumgartner, W., Zillikens, D. and Drenckhahn, D.** (2005). Pemphigus foliaceus IgG causes dissociation of desmoglein 1-containing junctions without blocking desmoglein 1 transinteraction. *J Clin Invest* **115**, 3157-65.
- Waschke, J., Menendez-Castro, C., Bruggeman, P., Koob, R., Amagai, M., Gruber, H. J., Drenckhahn, D. and Baumgartner, W.** (2007). Imaging and force spectroscopy on desmoglein 1 using atomic force microscopy reveal multivalent Ca(2+)-dependent, low-affinity trans-interaction. *J Membr Biol* **216**, 83-92.
- Waschke, J., Spindler, V., Bruggeman, P., Zillikens, D., Schmidt, G. and Drenckhahn, D.** (2006). Inhibition of Rho A activity causes pemphigus skin blistering. *J Cell Biol* **175**, 721-7.
- Wendeler, M. W., Drenckhahn, D., Gessner, R. and Baumgartner, W.** (2007). Intestinal LI-cadherin acts as a Ca²⁺-dependent adhesion switch. *J Mol Biol* **370**, 220-30.

- Wilgram, G. F., Caulfield, J. B. and Lever, W. F.** (1961). An electron microscopic study of acantholysis in pemphigus vulgaris. *J Invest Dermatol* **36**, 373-82.
- Wilgram, G. F., Caulfield, J. B. and Madgic, E. B.** (1964). An Electron Microscopic Study of Acantholysis and Dyskeratosis in Pemphigus Foliaceus: With a Special Note on Peculiar Intracytoplasmic Bodies. *J Invest Dermatol* **43**, 287-99.
- Williams, G., Williams, E. J. and Doherty, P.** (2002). Dimeric versions of two short N-cadherin binding motifs (HAVDI and INPISG) function as N-cadherin agonists. *J Biol Chem* **277**, 4361-7.
- Williamson, L., Raess, N. A., Caldelari, R., Zakher, A., de Bruin, A., Posthaus, H., Bolli, R., Hunziker, T., Suter, M. M. and Miller, E. J.** (2006). Pemphigus vulgaris identifies plakoglobin as key suppressor of c-Myc in the skin. *EMBO J* **25**, 3298-309.
- Wojciak-Stothard, B. and Ridley, A. J.** (2002). Rho GTPases and the regulation of endothelial permeability. *Vascul Pharmacol* **39**, 187-99.
- Wu, H., Wang, Z. H., Yan, A., Lyle, S., Fakharzadeh, S., Wahl, J. K., Wheelock, M. J., Ishikawa, H., Uitto, J., Amagai, M. et al.** (2000). Protection against Pemphigus Foliaceus by Desmoglein 3 in Neonates. *N Engl J Med* **343**, 31-35.
- Xiong, J. P., Stehle, T., Zhang, R., Joachimiak, A., Frech, M., Goodman, S. L. and Arnaout, M. A.** (2002). Crystal structure of the extracellular segment of integrin alpha Vbeta3 in complex with an Arg-Gly-Asp ligand. *Science* **296**, 151-5.
- Yamada, S., Pokutta, S., Drees, F., Weis, W. I. and Nelson, W. J.** (2005). Deconstructing the cadherin-catenin-actin complex. *Cell* **123**, 889-901.
- Yap, A. S., Brieher, W. M., Pruschy, M. and Gumbiner, B. M.** (1997). Lateral clustering of the adhesive ectodomain: a fundamental determinant of cadherin function. *Curr Biol* **7**, 308-15.
- Yap, A. S., Crampton, M. S. and Hardin, J.** (2007). Making and breaking contacts: the cellular biology of cadherin regulation. *Curr Opin Cell Biol* **19**, 508-14.
- Yap, A. S., Niessen, C. M. and Gumbiner, B. M.** (1998). The juxtamembrane region of the cadherin cytoplasmic tail supports lateral clustering, adhesive strengthening, and interaction with p120ctn. *J Cell Biol* **141**, 779-89.
- Yin, H. L. and Stossel, T. P.** (1979). Control of cytoplasmic actin gel-sol transformation by gelsolin, a calcium-dependent regulatory protein. *Nature* **281**, 583-6.
- Yokouchi, M., Saleh, M. A., Kuroda, K., Hachiya, T., Stanley, J. R., Amagai, M. and Ishii, K.** (2009). Pathogenic Epitopes of Autoantibodies in Pemphigus Reside in the Amino-Terminal Adhesive Region of Desmogleins Which Are Unmasked by Proteolytic Processing of Prosequence. *J Invest Dermatol*.
- Yoshida, C. and Takeichi, M.** (1982). Teratocarcinoma cell adhesion: identification of a cell-surface protein involved in calcium-dependent cell aggregation. *Cell* **28**, 217-24.
- Zarnitsyna, V. I., Huang, J., Zhang, F., Chien, Y. H., Leckband, D. and Zhu, C.** (2007). Memory in receptor-ligand-mediated cell adhesion. *Proc Natl Acad Sci U S A* **104**, 18037-42.
- Zhang, Y., Sivasankar, S., Nelson, W. J. and Chu, S.** (2009). Resolving cadherin interactions and binding cooperativity at the single-molecule level. *Proc Natl Acad Sci U S A* **106**, 109-14.
- Zhu, B., Chappuis-Flament, S., Wong, E., Jensen, I. E., Gumbiner, B. M. and Leckband, D.** (2003). Functional analysis of the structural basis of homophilic cadherin adhesion. *Biophys J* **84**, 4033-42.
- Zhurinsky, J., Shtutman, M. and Ben-Ze'ev, A.** (2000). Plakoglobin and beta-catenin: protein interactions, regulation and biological roles. *J Cell Sci* **113** (Pt 18), 3127-39.

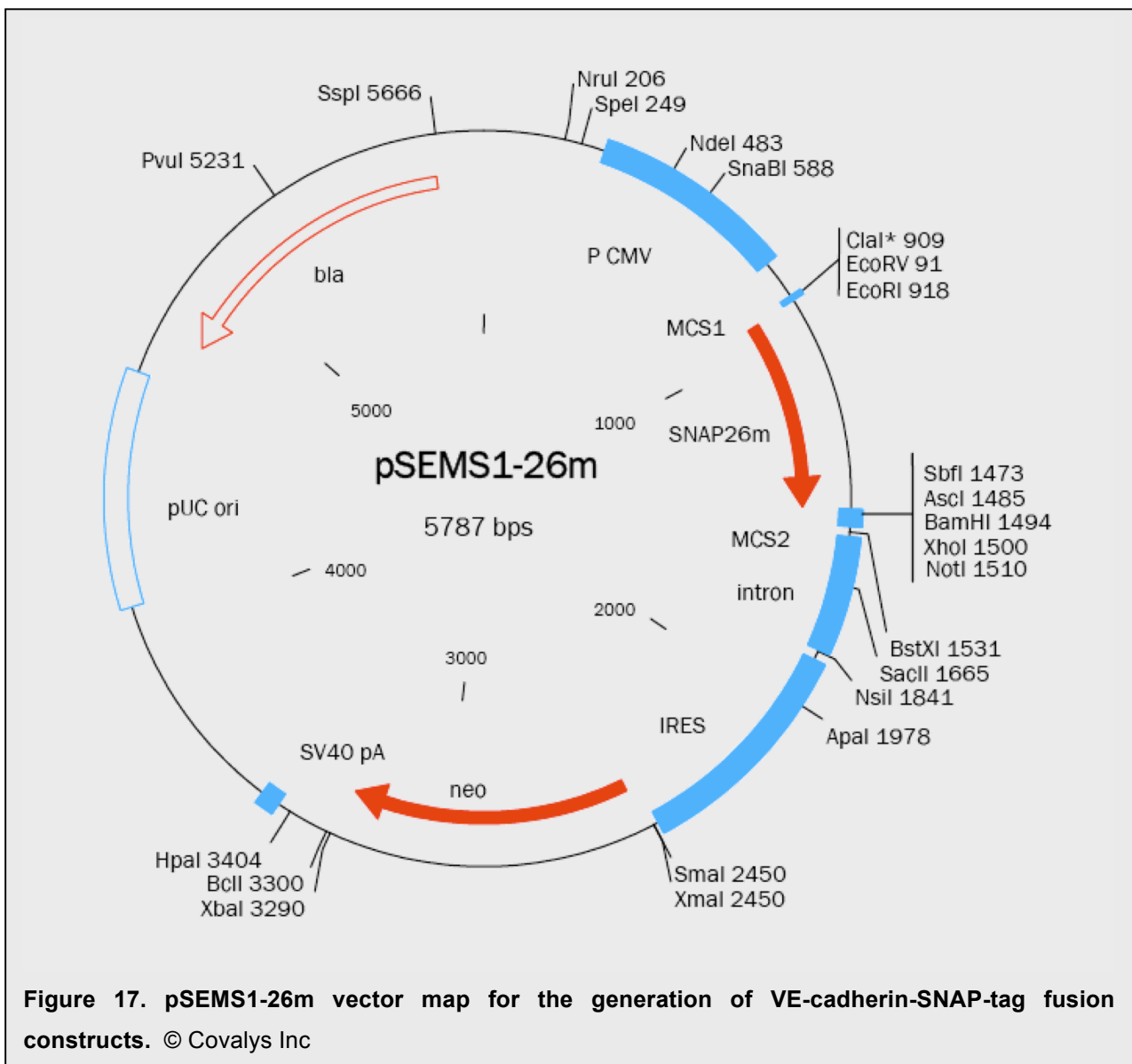
6 Appendix

6.1 Addendum

6.1.1 Vector construction of VE-cadherin-SNAP-his constructs

VE-EC15-SNAP-his

Addition of 3'-terminal poly-histidine tag including stop codon was achieved by oligo annealing of primers 5'- GATCCCATCATCATCATCATCATTA A GC -3' (forward) and 5'- GGCCGCTTAATGATGATGATGATGATGG-3' (reverse) into BamHI/NotI-digested SNAP-tag vector pSEMS1-26 (Covalys, Figure 16) to generate pSEMS1-26m_6xhis_STOP. Full-length mouse VE-cadherin EC domain was amplified via primers 5'- GGATATCGCCACCATGCAGAGGCTCACAGAGCT-3' and 5'- GGAATTCCTGGGCTGCCATCTCCTCAC-3' from template pIRES-VE-EC-1xFKBP-His6 (Gutberlet, 2006) and inserted into EcoRV/EcoRI – digested pSEMS1-26m-6xhis-STOP to yield VECad_pSEMS1-26m6xhis-STOP. Sequence integrity for all constructs was confirmed by sequencing.



VE-EC15-FKBP-SNAP-his

Vector VECad_FKBP_pSEMS1-26m6xhis-STOP was generated by cloning a VE-cadherin-FKBP fragment from template pIRES-VE-EC-1xFKBP-His6 (Gutberlet, 2006) via primers 5'-GGATATCGCCACCATGCAGAGGCTCACAGAGCT-3' and 5'-GGAATTCTTCCAGTTTTAGAAAGCTCCA-3' into EcoRV/EcoRI-digested pSEMS1-26m_6xhis_STOP.

VE-EC15-Fc-SNAP-his

Vector VECad_Fc_pSEMS1-26m_6xhis_STOP was cloned by inserting Fc fragment of human IgG 1 (including the hinge region and Ig domains CH2 and CH3) of pEGFP-Cad11-Fc (Heupel et al., 2008) via primers 5'-GGAATTCCTTACCCGGGGACAGGGAGA-3' and 5'-GGAATTCCTTACCCGGGGACAGGGAGA-3' into EcoRI-digested VE-EC15-SNAP-his. Correct orientation was verified by restriction enzyme digest with EcoNI.

6.1.2 List of abbreviations

3D three dimensional	HaCaT cells human adult low calcium elevated temperature cells
A adenosine	HAV “histidin-alanine-valine” motif of cadherin interaction
aa amino acid	HBSS Hank’s buffered salt solution
AFM atomic force microscopy	His (H) histidine
Ala (A) alanine	IC intracellular
Arg (R) arginine	Ig immunoglobulin
Asn (N) asparagine	Ile (I) isoleucine
Asp (D) aspartic acid	Leu (L) leucine
bp base pair	Lys (K) lysine
BSA bovine serum albumin	MAPK mitogen-activated protein kinase
C cytidine	Met (M) methionine
Ca²⁺ calcium	Ni²⁺-NTA nickel-nitrilotriacetic acid
CAR cell adhesion recognition	PAGE polyacrylamide gel electrophoresis
CHO cells Chinese hamster ovary cells	PBS phosphate buffered saline
CK cytokeratin	PDB protein data bank
Cys (C) cysteine	PF pemphigus foliaceus
Da dalton	Phe (F) phenylalanine
Dsc desmocollin	Pro (P) proline
Dsg desmoglein	PV pemphigus vulgaris
EC extracellular	PV-IgG pemphigus vulgaris autoantibodies
ECL enhanced chemoluminescence	SDS sodium dodecyl sulfate
EDTA ethylenediamine tetraacetic acid	Ser (S) serine
EGF epidermal growth factor	T thymidine
EGFR epidermal growth factor receptor	Thr (T) threonine
FCS fetal calf serum	Trp (W) tryptophan
FKBP FK506 binding protein	Tyr (Y) tyrosine
G guanosine	Val (V) valine
Gln (Q) glutamine	wt wild type
Glu (E) glutamic acid	
Gly (G) glycine	

6.2 Acknowledgement - Danksagung

Zuallererst und von ganzem Herzen möchte ich **Herrn Prof. Dr. Detlev Drenckhahn** für die Einführung in die Welt der Cadherine, seine Ideen und die Möglichkeiten während meiner Zeit an seinem Institut danken. Seine Betreuung und Unterstützung, die ich nun seit mehr als 6 Jahren erfahren durfte, war und ist weit über den immensen wissenschaftlichen Rat hinaus stets Wertevermittlung, Ansporn und Aufmunterung zugleich. Auch wenn meine zukünftigen Wege noch nicht abzusehen sind, bin ich mehr als dankbar, einen solchen Mentor zu haben, der mir einen der wahrsten inneren Werte der Wissenschaft, die Neugierde - auch fernab von Konventionen - mit auf den Weg gegeben hat.

Bei Prof. Dr. Jens Waschke bedanke ich mich für die professionelle Unterstützung und Zusammenarbeit in vielen Bereichen, die tolle Atmosphäre in der Arbeitsgruppe, die Anleitung zum effektiven wissenschaftlichen Arbeiten und das Vorantreiben von vielen Projekten, die meine Zeit in der Anatomie so erfolgreich gemacht haben.

PD Dr. Stefan Hübner gilt meine Verbundenheit und Dank als ein Kollege, den man sich nur wünschen kann: kompetent, hilfsbereit, und vor allem auch ein Freund, mit dem man vieles unternehmen kann, aber der sich in manchen Disziplinen (z.B. TT-Spielen, Joggen oder Liegestützen) ein bisschen mehr Mühe hätte geben können.

Mein herzlicher Dank gilt Lisa Bergauer, Nadja Niedermeier und Tanja Reimer, die mich bei Experimenten entweder sehr unterstützt oder aufgeheitert haben oder die Laborstunden teilweise zu einem Ereignis machten.

Während meiner Zeit am Institut hatte ich die Ehre wirklich jeden einzelnen Mitarbeiter des Hauses kennenzulernen und wertzuschätzen. So gilt mein Dank allen Mitarbeitern des Anatomischen Instituts: ich habe das gesamte Institut sehr in mein Herz geschlossen, immerhin war bzw. ist es während meiner wissenschaftlichen Laufbahn mein zweites Zuhause.

Prof. Dr. Georg Krohne bin ich für die Übernahme des Zweitgutachtens und die Diskussion und Ratschläge für diese Arbeit dankbar.

Prof. Gregory Harms und seinen Mitarbeitern danke ich für phasenweise Aufnahme in seine Arbeitsgruppe und die Einweisung in die vielfältigsten mikroskopischen Techniken.

Der DFG bzw. dem Sonderforschungsbereich 487 danke ich für die Finanzierung meiner Arbeiten und die Möglichkeit, an Forschungsreisen und Kongressen teilzunehmen.

Vielen wissenschaftlichen Kollegen bin ich zu Dank verpflichtet, da sie mich durch wertvolle Ratschläge, besondere Techniken und Reagenzien oder Kooperationen unterstützt haben:

- Dr. Nicolas Schlegel, Dr. Yvonne Baumer, Dr. Axel Steinke, Dr. Volker Spindler, Dr. Judith Gutberlet, Dr. Athina Hübner, Peter Engerer (Institut für Anatomie und Zellbiologie, Universität Würzburg)
- Prof. Dr. Hermann Schindelin, Bodo Sander (RVZ, Universität Würzburg)
- Prof. Dr. Detlef Zillikens, Dr. Dr. Enno Schmidt (Dermatologie, Universität Lübeck)
- Prof. Dr. Thomas Müller (Lehrstuhl für Botanik, Universität Würzburg)
- Prof. Dr. Peter Hinterdorfer, Prof. Dr. Hermann Gruber, Dr. Andreas Ebner, Dr. Linda Wildling (Institut für Biophysik, Universität Linz)
- Prof. Dr. Werner Baumgartner, Agnes Weth (Abteilung Zelluläre Neurobionik, RWTH Aachen)
- Prof. Dr. Klaus Groschner, Dr. Mike Poteser, Dr. Annarita Graziani (Institut für Pharmazeutische Wissenschaften, Universität Graz)
- Prof. Dr. Yasuo Kitajima (Dermatologie, Gifu University)
- Prof. Dr. Masayuki Amagai (Dermatologie, Keio University)
- Johannes Reithinger (Laboratory of Membrane Biology, Seoul National University)

Mein finaler und größter Dank gilt meiner Familie und besonders meiner Frau Julia, deren Liebe, Zusammenhalt und Unterstützung entscheidend zur Vollendung dieser Arbeit in für uns teilweise traurigen Zeiten beigetragen hat.

6.3 Ehrenwörtliche Erklärung

Erklärung gemäß §4 Absatz 3 der Promotionsordnung der Fakultät für Biologie der Bayerischen Julius-Maximilians-Universität Würzburg vom 15. März 1999

1. Hiermit erkläre ich ehrenwörtlich, dass ich die vorliegende und im Fachbereich Biologie der Julius-Maximilians-Universität Würzburg eingereichte Dissertation am Institut für Anatomie und Zellbiologie unter Leitung und Betreuung von Prof. Dr. Drenckhahn selbstständig angefertigt und keine anderen als die angegebenen Quellen und Hilfsmittel benutzt habe.
2. Ich erkläre, dass die vorliegende Dissertation weder in gleicher noch in ähnlicher Form bereits in einem anderen Prüfungsverfahren vorgelegen hat.
3. Ich erkläre, dass ich außer den mit dem Zulassungsantrag urkundlich vorgelegten Graden keine weiteren akademischen Grade erworben oder zu erwerben versucht habe.

Teile dieser kumulativen Dissertation wurden veröffentlicht. Die Verwendung der Arbeiten erfolgt mit Zustimmung der Verlage bzw. Journale.

Würzburg, den 01.06.2010



(Wolfgang-Moritz Heupel)

6.4 Curriculum vitae

Curriculum Vitae	Wolfgang-Moritz Heupel (M.Sc.)		
Adresse	Bergmeistergasse 6 97070 Würzburg Tel.: +49 179 901 6583 wolfgangmoritz.heupel@gmail.com		
Persönliche Daten	*09.07.1982 in Neuendettelsau, Bayern Nationalität: deutsch Familienstand: verheiratet		
Ausbildung	03/07 - 11/09	Naturwissenschaftliche Doktorarbeit am Institut für Anatomie und Zellbiologie Würzburg , Arbeitsgruppe Prof. Drenckhahn Thema: <i>Rolle und Modulation von Cadherinen in pathologischen Prozessen</i>	
	10/05 - 02/07	Studium der Biomedizin (M.Sc.) an der Julius-Maximilians-Universität Würzburg M.Sc. (mit Auszeichnung, Ø Note 1,0)	
	10/02 - 07/05	Studium der Biomedizin (B.Sc.) an der Julius-Maximilians-Universität Würzburg B.Sc. (mit Auszeichnung, Ø Note 1,2)	
	09/93 - 07/02	Johann-Sebastian-Bach-Gymnasium Windsbach Allgemeine Hochschulreife (Ø Note 1,0; Leistungskurse Mathematik, Wirtschaft&Recht)	
Praktika / wissenschaftliche Tätigkeiten	08/08 - 09/08	Forschungsaufenthalt am Institut für Biophysik, Universität Linz (Österreich) Arbeitsgruppe Prof. Hinterdorfer (Rasterkraftmikroskopie)	
	05/06 - 02/07	Masterthesis am Institut für Anatomie und Zellbiologie Würzburg Thema: <i>Analyse einer möglichen Interaktion zwischen VE-Cadherin und TRPC4</i> (Note 1,0)	
	03/06 - 05/06	Praktikum am Rudolf Virchow Zentrum für Experimentelle Biomedizin Würzburg Arbeitsgruppe Prof. Friedl (Molekulare Zelldynamik)	
	01/06 - 03/06	Praktikum am Rudolf Virchow Zentrum für Experimentelle Biomedizin Würzburg Arbeitsgruppe Prof. Harms (Molekulare Mikroskopie)	
	03/05 - 05/05	Bachelorthesis am Institut für Anatomie und Zellbiologie Würzburg Thema: <i>Charakterisierung der Bindungseigenschaften von Cadherin-11 im Hinblick synaptischer Plastizität</i> (Note 1,0)	
	03/04 - 07/05	Hilfswissenschaftler am Institut für Anatomie und Zellbiologie Würzburg	
Berufliche Stationen	01/10 -	Business Analyst, ZS Associates, Frankfurt (Unternehmensberatung)	
	03/07 - 11/09	Wissenschaftlicher Mitarbeiter am Institut für Anatomie und Zellbiologie Würzburg	
Publikationen (Auswahl)	Spindler V, Heupel WM, Efthymiadis A, Schmidt E, Eming R, Rankl C, Hinterdorfer P, Müller TD, Drenckhahn D, Waschke J (<i>Journal of Biological Chemistry</i> , 2009 Aug 28. [im Druck])		
	Busch A, Kiel T, Heupel WM, Wehnert M, Hübner S (<i>Experimental Cell Research</i> , 2009 Aug 15;315(14):2373-85. Epub 2009 May 12)		
	Heupel WM, Efthymiadis A, Schlegel N, Müller T, Baumer Y, Baumgartner W, Drenckhahn D, Waschke J (<i>Journal of Cell Science</i> , 2009 May 15;122(Pt 10):1616-25.)		
	Andresen V, Alexander S, Heupel WM, Hirschberg M, Friedl P (<i>Current Opinion in Biotechnology</i> , 2009 February;20(1):54-62)		
	Heupel WM Müller T, Efthymiadis A, Schmidt E, Drenckhahn D, Waschke J (<i>Journal of Biological Chemistry</i> , 2009 Mar 27;284(13):8589-95)		
	Heupel WM, Engerer P, Schmidt E, Waschke J (<i>American Journal of Pathology</i> , 2009 Feb;174(2):475-85)		
	Heupel WM, Zillikens D, Drenckhahn D, Waschke J (<i>Journal of Immunology</i> , 2008 Aug 1;181(3):1825-34)		
	Heupel WM, Baumgartner W, Laymann B, Drenckhahn D, Golenhofen N (<i>Molecular and Cellular Neuroscience</i> , 2008 Mar;37(3):548-58)		
Wissenschaftliche Kongresse	06/09	International Pemphigus Meeting, Bern, Schweiz	
	03/09	104 th International Meeting of the Anatomische Gesellschaft, Antwerpen, Belgien	
	05/08	2008 International Meeting on Autoimmune Bullous Diseases, Otsu, Japan	
	03/08	103 rd International Meeting of the Anatomische Gesellschaft, Innsbruck, Österreich	
	05/07	68 th Annual Meeting of the Society of Investigative Dermatology, Los Angeles, USA	
	04/07	102 nd International Meeting of the Anatomische Gesellschaft, Gießen, Deutschland	

Akademische Lehrtätigkeit	Kursus der mikroskopischen und makroskopischen Anatomie (SS 07; WS 08/09; SS 09) Seminar Neuroanatomie (WS 08/09)	
Gutachtertätigkeit	Gutachten für Artikel in <i>PLOS Biology</i> , <i>Journal of Cell Science</i> , <i>Histochemistry and Cell Biology</i> u. a.	
Stipendien und Auszeichnungen	09/08 07/07	Posterpreis beim Wettbewerb der Graduiertenschule der Lebenswissenschaften Ausgewählter Teilnehmer als „ Young Researcher “ am Lindauer Treffen der Nobelpreisträger
	10/02 - 04/10	e-fellows.net Stipendium & Mentoring (Betreuung durch <i>Roche Diagnostics GmbH</i>)
	10/02 - 02/07	Begabtenförderung durch das Bayerische Staatsministerium für Wissenschaft, Forschung und Kunst
	07/02	Karl von Frisch - Abiturientenpreis im Fach Biologie
	09/99 - 07/00	Oskar Karl Forster - Stipendium
Workshops und Schulungen	06/09 11/08 10/08 07/08 04/08 05/07 03/07	Viertätiges Seminar „ Erfolge schneiden 2009 “ Dreitägiges Training „ Leadership in Fach- und Führungspositionen “ Workshop „ Business etiquette and small talk “ Zweitätiges Rhetorikseminar „ English oral presentation “ Workshop „ Projektmanagement “ Dreitägiger Workshop „ Gründen - von der Idee zum Geschäftsplan “ Zweitägiger Workshop „ Effective scientific writing “
Sprachen	Deutsch:	Muttersprache
	Englisch:	fließend in Wort und Schrift (9 Jahre Schulunterricht; Schüleraustausch in Adelaide, Australien 02/00 - 05/00; zahlreiche englischsprachige Lehrveranstaltungen und Kongresse 10/02 - aktuell)
	Französisch:	Grundkenntnisse (3 Jahre Schulunterricht)
IT	MS Office:	sehr gute Kenntnisse
	Mathlab:	gute Kenntnisse
	Adobe Creative Suite:	gute Kenntnisse
		Grundkenntnisse in HTML und VBA
Weitere Aktivitäten und Engagement	03/07 - 05/09 10/06 - 04/07	Mitglied des studentischen Rats der Graduiertenschule der Lebenswissenschaften Projektarbeit in der studentischen Unternehmensberatung individual academic consulting Würzburg e.V.
	01/04 - 10/04	Mitgliedschaft in der biotechnologischen Studenteninitiative e.V.
	01/04 - 04/04	Musikprojekt „Gregorianik & Jazz“ ; Konzerttournee mit 40 jungen Musikern
	10/02 - 02/07	Jahrgangssprecher Biomediziner Universität Würzburg
	10/95 - 07/02	Schulisches Engagement als Schüler-, Jahrgangs- und Klassensprecher sowie Tutor für jüngere Mitschüler
Hobbys	Unternehmungen und Reisen (u.a. 4-wöchiger Aufenthalt in China 02/09), Musik (aktiv als Gitarrist / passiv), Fotografie und digitale Bildbearbeitung, Laufen	

(Würzburg, 01. Juni 2010)

6.5 Publikationsverzeichnis

Wolfgang-Moritz Heupel, geb. 09.07.1982 in Neuendettelsau

6.5.1 Originalarbeiten

Heupel WM, Baumgartner W, Laymann B, Drenckhahn D, Golenhofen N

Different Ca²⁺ affinities and functional implications of the two synaptic adhesion molecules cadherin-11 and N-cadherin.

Molecular & Cellular Neuroscience. 2008 Mar;37(3):548-58. Epub 2007 Dec 15.

Heupel WM, Zillikens D, Drenckhahn D, Waschke J

Pemphigus vulgaris IgG directly inhibit desmoglein 3-mediated transinteraction

Journal of Immunology. 2008;181:1825-1834.

Heupel WM[¶], Engerer P[¶], Schmidt E, Waschke J

Pemphigus vulgaris IgG cause loss of desmoglein-mediated adhesion and keratinocyte dissociation in HaCaT cells independent of epidermal growth factor receptor

American Journal of Pathology. 2009 Feb;174(2):475-85. Epub 2009 Jan 15.

Heupel WM[¶], Müller T[¶], Efthymiadis A, Schmidt E, Drenckhahn D, Waschke J

Peptides targeting the desmoglein 3 adhesive interface prevent pemphigus autoantibody-induced acantholysis in pemphigus

Journal of Biological Chemistry. 2009 Mar 27;284(13):8589-95. Epub 2009 Jan 21.

Heupel WM[¶], Efthymiadis A[¶], Schlegel N, Müller T, Baumer Y, Baumgartner W, Drenckhahn D, Waschke J

Endothelial barrier stabilization by a cyclic tandem peptide targeting VE-cadherin transinteraction in vitro and in vivo

Journal of Cell Science. 2009 May 15;122(Pt 10):1616-25.

Andresen V, Alexander S, **Heupel WM**, Hirschberg M, Friedl P

Infrared multiphoton microscopy: subcellular-resolved deep tissue imaging

Current Opinion in Biotechnology. 2009 February, 20(1):54–62

Busch A, Kiel T, **Heupel WM**, Wehnert M, Hübner S

Nuclear protein import is reduced in cells expressing nuclear envelopathy-causing lamin A mutants

Experimental Cell Research. 2009 Aug 15;315(14):2373-85. Epub 2009 May 12.

Spindler V, **Heupel WM**, Efthymiadis A, Schmidt E, Eming R, Rankl C, Hinterdorfer P, Müller TD, Drenckhahn D, Waschke J

Desmocollin 3-mediated binding is crucial for keratinocyte cohesion and is impaired in pemphigus

Journal of Biological Chemistry. 2009 Oct 30;284(44):30556-64. Epub 2009 Aug 28.

Heupel WM, Drenckhahn D

Extending the Knowledge in Histochemistry and Cell Biology

Histochemistry and Cell Biology. 2010 Jan;133(1):1-40. Epub 2009 Nov 28.

Cell-cell contact formation governs Ca²⁺ signaling by TRPC4 in the vascular endothelium – evidence for a regulatory TRPC4 - β-catenin interaction

Graziani A, Poteser M, **Heupel WM**, Schleifer H, Krenn M, Drenckhahn D, Romanin C, Baumgartner W, Groschner K

Journal of Biological Chemistry. 2010 Feb 5;285(6):4213-23. Epub 2009 Dec 8.

Desmoglein 2-mediated adhesion is required for intestinal epithelial barrier integrity

Schlegel N, Meir M, **Heupel WM**, Holthöfer B, Leube R, Waschke J

American Journal of Physiology - Gastrointestinal and Liver Physiology. 2010 Mar 11. (Epub ahead of print)

Actin reorganization contributes to loss of cell adhesion in pemphigus vulgaris

Gliem M [¶], **Heupel WM** [¶], Spindler V, Harms GS, Waschke J

American Journal of Physiology - Cell Physiology (June 16, 2010).

doi:10.1152/ajpcell.00075.2010

Cytokeratin retraction and loss of cell cohesion in pemphigus are mediated by p38MAPK and prevented by desmoglein 3 overexpression

Gliem M [¶], **Heupel WM** [¶], Harms GS, Hanakawa Y, Schmidt E, Hübner S, Waschke J

Journal of Cellular Physiology 2010 (to be re-submitted)

Anti-Desmoglein 3 autoantibodies result in plakoglobin-dependent p38MAPK activation

Heupel WM, Efthymiadis A, Harms GS, Drenckhahn D, Waschke J

2010 (in preparation)

([¶] authors contributed equally)

6.5.2 Kongressbeiträge

Heupel WM, Baumgartner W, Drenckhahn D, Golenhofen N

Characterization of cadherin-11 binding properties in the context of synaptic plasticity

Annual Workshop of the Anatomische Gesellschaft, Würzburg, Germany, 27.09.2006

Vortrag

Heupel WM, Drenckhahn D, Waschke J

Steric Hindrance of desmoglein 3 trans-interaction is involved in pemphigus vulgaris but not in pemphigus foliaceus

102nd International Meeting of the Anatomische Gesellschaft, Gießen, Germany, 02.04.2007

Vortrag

Heupel WM, Drenckhahn D, Waschke J

Steric hindrance of desmoglein 3 trans-interaction by pemphigus vulgaris IgG

68th Annual Meeting of the Society of Investigative Dermatology, Los Angeles, USA, 09. -

12.05.2007 Poster

Heupel WM, Zillikens D, Waschke J, Drenckhahn D

Pemphigus vulgaris IgG inhibit desmoglein 3- but not desmoglein 1-mediated binding by steric hindrance

International Symposium „Membrane Proteins and Diseases“ of the SFB487, Würzburg, Germany, 07. - 09.06.2007 Poster

Heupel WM

(Re)-Investing Pemphigus Pathogenesis: Role of Steric Hindrance vs. Cellular Signalling

3rd International Symposium of the Graduate School of Life Science, Würzburg, Germany,

08.10.2007 Vortrag

Heupel WM, Efthymiadis A, Drenckhahn D, Waschke J

Dissecting the role of steric hindrance in pemphigus pathogenesis with peptides targeting the desmoglein adhesive interface

103rd International Meeting of the Anatomische Gesellschaft, Innsbruck, Austria, 17.03.2008

Vortrag

Heupel WM, Efthymiadis A, Schmidt E, Müller T, Drenckhahn D, Waschke J

Peptides targeting the desmoglein adhesive interface prevent pemphigus autoantibody-induced direct inhibition of desmoglein binding

Post IID 2008 Satellite International Meeting on Autoimmune Bullous Diseases, Otsu, Japan, 17. - 19.05.2008 Poster

Heupel WM, Waschke J, Drenckhahn D

(Re-) Investigating Pemphigus Pathogenesis

GSLS poster contest, Würzburg, Germany, 05.09.2008 Poster

Heupel WM, Engerer P, Gutberlet J, Drenckhahn D, Waschke J

Pemphigus vulgaris IgG cause keratinocyte acantholysis independent of apoptosis and epidermal growth factor signalling

Annual Workshop of the Anatomische Gesellschaft, Würzburg, Germany, 26.09.2008

Vortrag

Efthymiadis A, **Heupel WM**, Schlegel N, Müller T, Baumer Y, Baumgartner W, Drenckhahn D, Waschke J

Cyclic tandem peptides targeting VE-cadherin trans-interaction stabilize endothelial barrier function

104th International Meeting of the Anatomische Gesellschaft, Antwerp, Belgium, 28.03.2009

Spindler V, **Heupel WM**, Khan S, Drenckhahn D and Waschke J

Desmocollin 3-mediated binding is crucial for keratinocyte cohesion and epidermal integrity

104th International Meeting of the Anatomische Gesellschaft, Antwerp, Belgium, 28.03.2009

Spindler V, **Heupel WM**, Khan S, Drenckhahn D and Waschke J

Desmocollin 3-mediated binding is crucial for keratinocyte cohesion: Contribution to pemphigus pathogenesis?

International Pemphigus Meeting, Berne, Switzerland, 27. – 29.06.2009

Heupel WM, Efthymiadis A, Drenckhahn D, Waschke J

Plakoglobin-mediated p38MAPK activation is involved in pemphigus autoantibody-induced acantholysis

International Pemphigus Meeting, Berne, Switzerland, 27.06.2009 Vortrag

Schlegel N, Meir M, **Heupel WM**, Holthöfer B, Leube R, Waschke J

Desmoglein 2-mediated adhesion is required for intestinal epithelial barrier integrity

Annual Workshop of the Anatomische Gesellschaft, Würzburg, Germany, 23.09.2009

Heupel WM, Efthymiadis A, Drenckhahn D, Waschke J

Pemphigus autoantibody-induced p38MAPK activation is dependent on plakoglobin

Annual Workshop of the Anatomische Gesellschaft, Würzburg, Germany, 24.09.2009

Vortrag

Gliem M, **Heupel WM**, Hübner S, Waschke J,

Role of cytokeratin retraction and actin reorganization in pemphigus acantholysis

105th International Meeting of the Anatomische Gesellschaft, Hamburg, Germany, 29.03.2010

Schlegel N, Meir M, **Heupel WM**, Waschke J, Germer CT

Die Desmoglein2(Dsg2)-vermittelte Adhäsion wird für die Aufrechterhaltung der Darmbarrierefunktion benötigt

127. Kongress der Deutschen Gesellschaft für Chirurgie, Berlin, Germany 20.-23.04.2010